An Examination of Heavy-duty Trucks Drivetrain Options to Reduce GHG Emissions in British Columbia

S. Mojtaba Lajevardi

B.Sc., K.N.Toosi University of Technology, 2005

M.Sc., Sharif University of Technology, 2008

A Dissertation Submitted in Partial Fulfillment of the
Requirements for the Degree of

DOCTOR OF PHILOSOPHY

in the Department of Mechanical Engineering

An Examination of Heavy-duty Trucks Drivetrain Options to Reduce GHG Emissions in British Columbia

S. Mojtaba Lajevardi

B.Sc., K.N.Toosi University of Technology, 2005

M.Sc., Sharif University of Technology, 2008

Supervisory Committee

Dr. C. Crawford, Supervisor
(Department of Mechanical Engineering, UVic)

Dr. Jonn Axsen, Co-Supervisor
(School of Resource and Environmental Management, SFU)

Dr. Andrew Rowe, Committee member
(Department of Mechanical Engineering, UVic)

Abstract

Heavy-duty trucks (HDTs) are vital in delivering products to the consumers around the world and help maintain the quality of life. However, they are heavily depending on fossil diesel use, which causing global climate change as well as local air pollutions. Although they represent a small percentage of vehicle population, they emit more than 30% of GHGs in road transportation or 5% of global greenhouse gas (GHG) emissions. Furthermore, GHG emissions from this sector are expected to steadily grow due to economic growth, globalization, industrialization, online shopping, and fast delivery expectations.

This study was focused on the Canadian province of British Columbia (BC) as a case study where HDTs are responsible for more than 4% of total provincial GHGs. BC, along with many regions around the world, has been committed to reduce its GHG emissions by 80% below 2007 levels by 2050. The goal of this study was to evaluate the potential of meeting this objective for BC HDTs using alternative drivetrain technologies. First, a component-level model was developed in Matlab to compute on-road energy consumption and CO_2 emissions of compressed natural gas and diesel HDTs based on their physical parameters (e.g. mass) over several selected drive cycles. Results of the first contribution indicated a compressed natural gas (CNG) drivetrain emits 13-15% fewer GHG than a comparable diesel. Road grades of several main BC routes were included in the drive cycle simulations, which is an important factor that can increase the fuel consumption and CO_2 emission by as much as 24% relative to a flat route assumption.

In the second contribution, the physical energy consumption model was extended to compare 16 diverse drivetrain technologies, including a pure battery electric. The comparison metrics were also extended to well-to-wheel GHG emissions, total ownership costs (TOC) (including infrastructure), and abatement costs (based on incremental TOC cost over GHG emissions reduction), and cargo capacity impacts. The 16 considered drivetrains were distinguished by their fuel types, combustion technology, drivetrain architecture, and connection to the electricity grid (e.g. catenary vs fast charging stations). Next, the activity data of 1,616 HDTs operating in BC with sparse recording intervals was used to select 6 representative freight routes with different ranges of 120-950 km split into short and long haul routes. A combination of filtering and interpolation techniques was used to develop 1-Hz drive cycles compatible with the

characteristic of HDTs categorized by the U.S. National Renewable Energy Laboratory. Results indicated a battery electric and battery electric catenary using hydroelectricity emits 95–99% lower GHGs than a baseline diesel. Furthermore, the parallel hybrid diesel was found to have both the lowest TOC and abatement costs for both short and long haul routes. Moreover, plug-in parallel hybrid fuel cell and conventional diesel drivetrains were found to have the highest cargo capacity on short and long haul routes respectively. Finally, a Monte Carlo analysis using 5000 simulations was performed for the longest freight routes to observe sensitivities to input parameters. Comparing median magnitudes, the uncertainty analysis indicated that the battery electric drivetrain has the lowest WTW GHG emissions, while the parallel hybrid diesel drivetrain has the lowest TOC.

In the third contribution, the energy consumption models that developed in chapter 2 and 3 were used to represent drivetrains (with a high technical resolution) in a dynamic vehicle adoption model to provide a realistic picture of emerging drivetrains under different scenarios up to 2050. Using the dynamic vehicle adoption model the diffusion rate of alternative drivetrains HDT was projected up to 2050 considering two zero emission vehicle (ZEV) mandates and various infrastructure roll-out scenarios. The HDT market was split into short and long haul segments. The vehicle adoption model was combined with a Monte Carlo analysis to evaluate the collective impact of input parameter variations on GHG emissions and market share projections. Both considered ZEV mandates included a linear adoption rate for ZEV drivetrains starting from 25% in 2025 and reaching 100% by 2040. They were also distinguished based on a constraint on the level of plug-in hybrid adoption. It was found infrastructure density increases the probability of meeting the 2050 target on both short and long haul HDTs. However, the increase in the probability is much higher for the short haul segment. Among various infrastructure roll-out scenarios, rapid deployment of hydrogen fueling stations was found to have the highest positive impact on GHG emissions reduction for both short and long haul markets. Both battery electric and hydrogen fuel cell drivetrains can succeed in the short haul market, depending on whether the infrastructure development is toward charging or H_2 station deployments. A similar result was found for the long haul market, except in all scenarios plug-in hybrid diesel captures market domination. Fuel cell was found as the second drivetrain option for long haul market that gains domination in most scenarios.

Contents

List of Tables

List of Figures

Nomenclature

F	Force (N)
V	Engine displacement (L)
a	Acceleration (m/s^2)
g	Gravitational Acceleration (9.81 m/s2)
t	Time (s)
C_D	Aerodynamic drag coefficient
A	Frontal Area (m^2)
K	Engine friction factor
K_0	Constant coefficient of engine friction factor
C_{r0}	Zero order of rolling friction coefficient
C_{r2}	Second order of rolling friction coefficient
N	Rotational speed
P_{br}	Engine braking power (kW)
P_{fr}	Engine friction power (kW)
P_{tr}	Tractive power (kW)
$\dot{m}_{FR}$	Mass Flow Rate of fuel consumption (g/s)
M_{CO2}	Total emitted CO_2 in a cycle (kg)
M	Gross mass of a vehicle (kg)
C_{fu}	Carbon content of fuel (%)
SR	Vehicle speed ratio (rpm/mph)
φ	Fuel–air equivalence ratio
d	Distance (m)
TD	Traveling Distance (km)
f_{burden}	Burden of battery pack
BS	Battery Size (kWh)
T	Torque (N.m)
SOC	State of charge
SE	Specific mass of energy conversion system (kg/kW or kg fuel/kg system)

R	Earth radius (km)

Greek letters

v	Vehicle speed (m/s)
ρ	Density (kg/L)
ε	Mass Correction Factor
Δ	Delta
θ	Road Grade Angle (degree)
η_i	Indicated thermal efficiency
η_T	Vehicle transmission efficiency
η_{reg}	Regenerative Braking efficiency
η_I	Inverter efficiency
η_M	Electric motor efficiency
η_{FC}	Fuel cell efficiency

Subscripts

fr	friction
tr	Tractive
br	Braking
FR	Flow rate
aux	Auxiliary
M	Motor
E	Engine
max	maximum
EC	Energy conversion
emi	emissions
inv	inverter
cat	catenary
ext	external

Acronyms

WOT	Wide Open Throttle

CNG	Compressed natural gas
DGE	Diesel Gallon Equivalent
FE	Fuel Economy (Liter/100 km)
GHG	Greenhouse Gas
LNG	Liquefied Natural Gas
LHV	Lower heating value (kJ/g)
TTW	Tank to wheel
LNG	Liquefied Natural Gas
DLE	Diesel Litter Equivalent
GHG	Greenhouse Gas
WECC	Western Electricity Coordinating Council
GWP	Global Warming Potential
HDT	Heavy-duty truck
WTP	Well to pump
BE	Battery electric
FC	Fuel cell
LCA	Life cycle assessment
WTW	Well to wheel
SI	Spark ignition
CI	Compression ignition
GPS	Global positioning system
ZEV	Zero emission vehicle
PHEV	Plug-in hybrid electric vehicle

Acknowledgements

This PhD research has been carried out in the Institute for Integrated Energy Systems and Mechanical Engineering department at the University of Victoria and in the School of Resource & Environmental Management at the Simon Fraser University. I would like to sincerely appreciate the primary funding received from the Pacific Institute for Climate Solution (PICS).

I would like to thank my both supervisors Dr. Curran Crawford from the University of Victoria and Dr. Jonn Axsen from Simon Fraser University who constantly have been providing me helpful advice to enhance the research. In particular, I would like to further thank Dr. Crawford for several reasons. First, he has been flexible in my physical location to conduct this PhD study. Second, he has given me out of box advices, which improved the overall output of this research. Finally, I appreciate him for facilitating several sideline projects including a summer internships, which are key in a successful career path after graduation. I express my deepest gratitude to my co-supervisor, Dr. Jonn Axsen for having me in his START group. Dr. Axsen provides me an opportunity to learn about social science research methods, which was added another color to this PhD dissertation.

I sincerely appreciate the love and support has received from my wife, Maryam, who is always beside me and has encouraged me during this PhD journey. Thank you, Maryam, for being extremely patient with me. I am also expressing my deepest gratitude toward my parent, Fateme and Mostafa, who shaped my personality to be an engineer and researcher. Hearing their comforting voices from a long distance conversations strengthen my ability to fulfill this PhD. Finally, I would like to thank all of my family members back in Iran for their love and support.

I would also thank all of my friends and colleagues in Sustainable Systems Design Laboratory (SSDL), Institute for Integrated Energy Systems (IESVic), Sustainable Transportation Action Research Team (START), and Energy and Materials Research Group (EMRG) groups for their positive and helpful comments toward fulfilling this PhD.

I am very grateful of the Vancouver Fraser Port Authority for providing the GPS activity data of the container trucks. Furthermore, I appreciate David C. Quiros from California Air Resources Board for providing several real-world drive cycles. I appreciate the insights received from

Michael Wolinetz from Navius Research regarding heavy-duty trucks market split. Finally, I thankful for explanations received from George Scora from University of Riverside regarding a diesel fuel consumption model for heavy-duty trucks.

S. Mojtaba Lajevardi

December 2019

Dedicated to my beloved wife Maryam
As well as my parents, Fateme and Mostafa for their support

Chapter 1

1 Introduction

1.1 Background and Motivation

Road transportation around the world contributes to more than 17% of the global greenhouse gas (GHG) emissions from fossil fuel use [1]. The share of heavy-duty trucks (HDTs) from the global road transportation GHG emissions is 30% (i.e. 5% of the total global GHG emissions) [2]. HDT refers to a class of trucks with a gross mass of 15 tonnes or more [2]. Annually, HDTs move 60% of the worldwide on-road freight demand, yet they represent only 7-9% of the global vehicle population [2], [3].

Beside their negative contribution to the global climate change due to their reliance on petroleum diesel use, HDTs are major source for cities air pollutions (e.g. oxides of nitrogen and particulate matter emissions), which are causing health problems [2], [4]. GHG emissions from this sector also is expected to grow around the world due to the economic growth, globalization, industrialization, increasing online shopping, and fast delivery expectations [2], [5]. Since there is limitation on fuel efficiency improvement for conventional diesel engine, moving toward alternative low carbon drivetrains seems inevitable [6]. However, there are challenges for shifting toward alternative drivetrains in this mode of transportation. For one thing, diesel engine considered as a reliable and flexible technology for HDTs that has developed continuously over the last 100 years [7]. Some other barriers for adopting alternative drivetrains HDTs (e.g. battery

electric and hydrogen fuel cell) are low energy density of battery and hydrogen, high capital cost of vehicle, high cost of renewable fuel production, and high capital cost of infrastructure [2], [8].

The British Columbia (BC) government, along with many regions around the world, has pledged to a GHG reduction target of 80% below 2007 levels by 2050 as part of global effort to avoid 2^{o} degree rise in average global temperature by 2100 [9]–[11]. This study explores the potential to achieve this target for BC HDTs, that contribute to 4% of the provincial emissions, through alternative low carbon drivetrain technologies and zero emissions mandates [12]. This study assumes all economic sectors including HDTs should equally attain this target. BC selected as a case study due to the province pioneering in adopting progressive climate policies such as carbon tax, low carbon fuel standard, and ZEV mandate for light-duty vehicles [13]–[15]. However, the method and results of this study could be potentially beneficial for other regions around the world.

Generally, the GHG emissions in freight transportation are the product of freight demand (tkm), specific energy consumption (MJ/t.km), and well-to-wheel GHG emissions of the fuel supply (g/MJ) [16]. A mitigation strategy in any of these components would result in total freight GHG emissions reduction. The objective of this study is to investigate the long term mitigation strategies via alternative and advanced drivetrain technology (for reducing specific energy consumption) and low carbon fuel supplies. The energy-economy models that used in previous studies mostly have the lack of detailed technical representation of alternative drivetrain technology [3], [9], [17]–[19]. Although a few studies have included battery and hydrogen into their analysis, they are lacking some details such as the size of battery or hydrogen tank considered as well as ignoring many combinations of hybrid technologies and fuel types [20]–[22]. The aim of this study is to fill this gap by developing a higher technical resolution of alternative drivetrain HDTs when modeling their future market-share projection in the case region of BC, which has not done before.

To achieve this goal, this study first developed a physical energy consumption model to compare the fuel efficiency and on-road CO_2 emissions of CNG and diesel conventional HDTs (see chapter 2). CNG was selected as a first low carbon option since there is abundant of natural gas supply in BC, which likely could help mitigate climate emissions in a near term [23]. There have been a number of physical energy consumption models such as CMEM [24], MOVES [25], Autonomie [26], Advisor [27] and PHEM [28]. These tools have been used in many studies for

examining, comparing, and designing alternative drivetrain HDTs [29]–[35]. Most of the commercial tools incorporate the input parameters and governing equations from their built-in libraries. Therefore, they usually have limited transparency in expressing details, which does not allow for future modifications such as including new technology. However, the present study aims to fill the gap by developing fuel efficiency models for several conventional drivetrains and then extend model to evaluate zero emission drivetrains such as battery electric and fuel cell.

Additionally, this study in chapter 3 developed a framework based on the physical energy consumption model to account well to wheel GHG emissions, total ownership cost, and abatement cost of GHG emissions of various alternative drivetrain HDTs. The well to wheel GHG emissions in this study refers to vehicle operation and fuel production stages. The well to wheel GHG emissions accounting in this study does not include embodied GHG emissions from vehicle manufacturing. The justification for excluding the manufacturing is due to negligible contribution of this source compare to the vehicle operation and fuel production emissions [36]. The considered GHGs in vehicle operation and fuel production stages are CO_2, CH_4 and N_2O emissions. There have been several studies on the well to wheel GHG emissions and total ownership cost for alternative drivetrain HDTs [32], [36]–[38]. These studies tend to account GHG emissions or cost based on averaged fuel consumption considering a typical energy storage (e.g. battery) size of an alternative drivetrain HDT without considering the linkage of energy storage size and the dominant freight route. However, the present study fills the gap in the literature by estimating the energy storage size of considered drivetrains based on realistic data for the freight routes in BC. Unlike a conventional diesel drivetrain that can serve both short and long haul routes, the size of energy storage is a critical factor for energy consumption and capital cost of alternative drivetrains. This is mostly due to the low energy density and high specific cost of battery and hydrogen systems. Short and long haul HDTs in this study is defined as an HDT with daily range of below and above 322 km respectively.

Finally, this study applied a dynamic vehicle adoption model (CIMS-HDT) in chapter 4 to explore GHG emissions projections in short and long haul markets of BC HDTs up to 2050 considering several infrastructure roll-out scenarios. While the aim of chapter 3 is creating a high resolution technical representations for 16 alternative drivetrain HDT options, the aim of chapter 4 is to forecast how a selected number of alternative options could compete over a longer term. Over the past few years, there have been a growing number of studies on adoption of low carbon

drivetrains in on-road freight [3], [16], [18], [21], [39]–[41]. However, there has been no study that considered the competition of multiple technology options, consumer behavior, and the role of refueling infrastructure in the adoption of zero emissions HDT drivetrains. This study incorporates energy consumption and total ownership cost characteristics of alternative drivetrains consistent with BC short and long freight routes using the developed in-house model, which has not done before. The aim is simulating adoption of alternative drivetrains as realistically as possible considering several consumer behavioral parameters such as market heterogeneity, discount rate, and non-financial or intangible cost. This intangible cost for each drivetrain is disaggregated into four category of risk, supply limitation of drivetrains, refueling inconveniences, and concern of cargo limitations.

1.2 Review of alternative drivetrains for HDTs

Generally, technology options to reduce specific fuel consumption (MJ/km) and well to wheel GHG emissions are a combination of drivetrain and fuel efficiency improvement technologies, which rely on at least one infrastructure technology for fuel supply. This study distinguishes drivetrain technology by: 1) fuel supply option (e.g. diesel or natural gas); 2) drivetrain architecture design (e.g. series or parallel hybrid); 3) energy conversion technology (e.g. fuel cell or micro gas turbine); and 4) connection to the electricity supply (fast charging station or catenary) (see Figure 1-1).

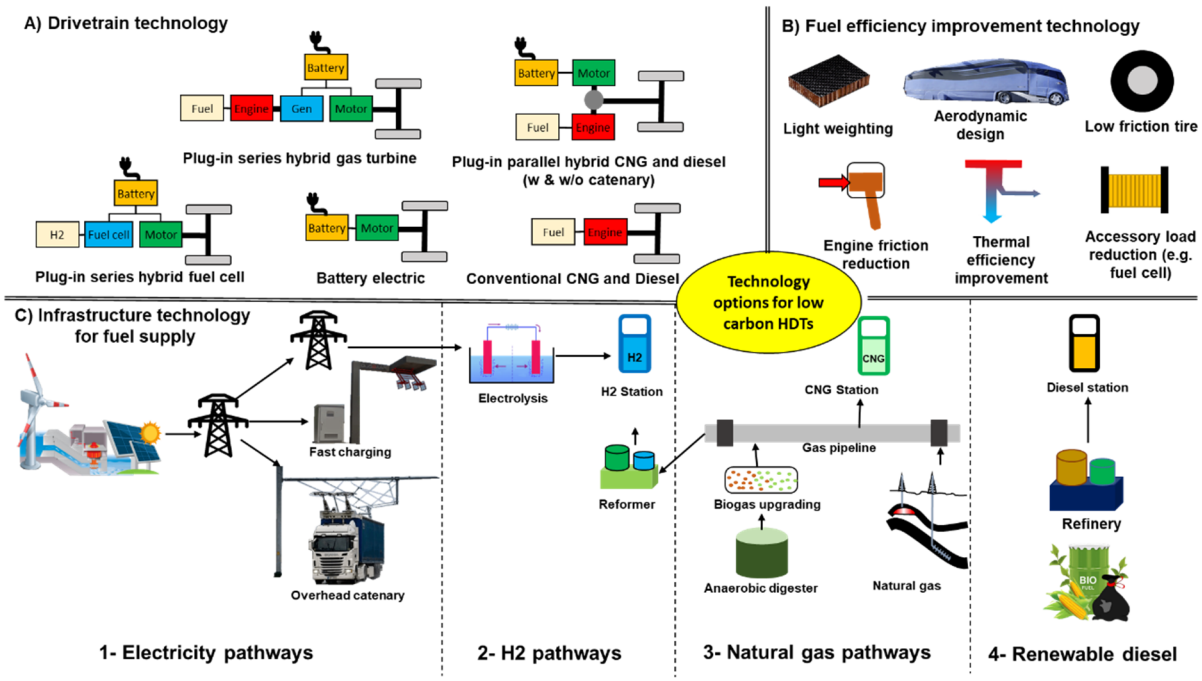

Figure 1-1. Technology options to support low carbon HDTs

The manufacturing of alternative drivetrain HDTs other than natural gas has started recently and intensified with Tesla Inc. announcement its battery electric truck with an 800 km range on a single charge [42]. Table 1-1 illustrates a list of HDTs with alternative drivetrains and their main specifications that have emerged recently for several niche markets such as freight movement in Ports [43]. This study simulates 15 drivetrains technology that are relatively consistent with the introduced options (see chapter 3).

Table 1-1: List of emerging alternative drivetrain HDTs

Technology	A view HDTs powered by the corresponding technology	Specifications	Source
1- Conventional CNG[1] (spark ignition)- Freightliner Cascadia		Westport-Cummins 11.9 L engine, 298 kW power	[44]
2- Conventional LNG[2] (compression ignition) - Volvo FH		Volvo 13 L engine, 343 kW power	[45]
3- Plug-in parallel hybrid diesel, Mack-Volvo		Mack MP7 (295 kW) hybridized with 150 kW PM Motor, 16 km zero emission range,	[43]
4- Plug-in parallel hybrid diesel catenary, Scania		9 L engine (268 kW) hybridized with a 130kW motor, 3 km + installed catenary distance zero emission range, 5 kWh battery	[46]
5- Plug-in parallel hybrid LNG[2], US-Hybrid and Peterbilt 384		8.9 L Cummins engine hybridized with 223 kW electric motor, 48 km zero emission, 80 kWh battery	[43]
6- Plug-in series hybrid CNG[1]-BAE/Kenworth		8.9 L Cummins engine hybridized with 400 kW electric motor, 64 km zero emission range, 100 kWh battery	[43]
7- Plug-in series hybrid CNG[1] & catenary- TransPower - International Prostar		3.7 L Ford engine hybridized with 300 kW electric motor, 64 km zero emission, 155 kWh battery	[43]
8- Plug-in Series hybrid with gas-turbine Peterbilt &Wal-Mart		65 kW capstone gas-turbine, 45.5 kWh battery	[47]

9- Battery electric-BYD		188 kWh lithium iron phosphate, 360 kW power, up to 148 km range	[48]
10- Battery electric Transpower		311 kWh lithium iron phosphate, 300kW power, up to 241 km range	[43]
11- Battery electric, US Hybrid		240 kWh battery, 320 kW power, up to 161 km range	[43], [49]
12- Battery electric, Daimler-Freightliner eCascadia		550 kWh battery, up to 400 km range	[50]
13- Battery electric, Thor Trucks (ET-One)		522 kW power, 480 km range	[51]
14- Battery electric, Tesla Inc		1000 kWh battery, 805 km range, 1.24 kWh/km	[42]
13- Battery electric, Nikola Tesla		500-1000 kWh battery, up to 640 km range	[52]
15- H2 fuel cell, Kenworth-Toyota		320kW power, 80 kW PEM fuel cell, 482 km range, 25 kg H2, 30 kWh battery	[53]
16- H2 fuel cell, US Hybrid		320kW power, 80 kW PEM fuel cell, 322 km range, 25 kg H2, 30 kWh battery,	[43], [49]
17- H2 fuel cell, Nikola Motor		745 kW power, 100 kg H2, up to 1,930 km range, 320 kWh battery pack	[52]

1- Compressed natural gas

2- Liquefied natural gas

1.3 Research contributions

The following items summarize the main contributions of this dissertation presented in three journal papers (chapter 2, 3, and 4):

1. **Developing a physical energy consumption model to compare alternative drivetrain HDTs:** There are several commercial life cycle emissions tools [54], [55] and physical energy consumption models [24], [26], [27] that widely have been used in the literature. Nonetheless, they are associated with several problems such as lack of considering a variety of technologies and lack of transparency and flexibility in their methodology and input parameters. To fill this gap, a physical energy consumption model was developed in Matlab that allows consistent analysis of all technology types and operating conditions.
2. **Incorporating road gradient into the energy consumption model:** Road gradient can have a significant impact on energy consumption that is usually missing in previous energy consumption analyses (e.g. [34], [56], [57]. Although some studies included grade into their analysis (e.g. [29], [33]), none considered steep grade with up to 8% slope associated with the BC freight routes [58].
3. **Evaluating the impact of advanced technologies on energy consumption and on-road emissions for conventional CNG and diesel HDTs:** The individual impact of advanced technologies (e.g. improving aerodynamics design) has been considered previously for diesel HDTs [59]–[64]. This study evaluates the individual as well as collective impact of adopting multiple technology options for both conventional diesel and CNG HDTs.
4. **Creating a simulation framework to compare 16 technologies for decarbonizing the HDTs of BC and around the world**: In the reviewed literature there have been only a few studies that considered 4 or more drivetrain options in one study (e.g. [31], [36], [38], [65]). Decision-making for a best low carbon option based on only a literature review could not reliable since each study considers a different set of assumptions. In contrast, the present study provides a consistent comparison across 16 drivetrains technologies (including battery electric and fuel cell) over a variety of short and long haul freight routes in BC. Well-to-wheel GHG emissions, total ownership cost (including infrastructure), abatement cost, and cargo capacity are metrics for comparison that have been considered altogether in this study. For each drivetrain technology, a low and high carbon content fuel is considered.

5. **Drive cycle development for HDTs in BC based on historical GPS activity data of heavy-duty container trucks** Historical GPS activity data of heavy-duty container trucks that are mostly operating around BC is used to create 6 realistic drive cycles. This dataset has a sparse nature and was collected by Vancouver Fraser Port Authority for around 1600 trucks during the month of November 2016. A technique is proposed to convert the sparse data to second-by-second format and combine it with associated grades profiles. This study uses 6 realistic drive cycles ranging from 120 to 950 km, instead of using the standard drive cycles, which are mostly applied in the reviewed literature.
6. **Determining minimum energy storage requirement for 16 different drivetrains operating across 6 different freight routes of BC:** Another contribution of this study is to determine the size of energy storage for 16 drivetrain technology in respect to each freight route before conducting well to wheel GHG and cost analysis, which has not been done before.
7. **Determining "winner" drivetrains in the short and long haul heavy-duty trucking sectors of BC:** Emergent dominant adopted drivetrains in the short and long haul HDT markets in BC for two ambitious zero-emissions vehicle (ZEV) mandates and various scenarios on refueling infrastructure deployment are determined. The key contribution is developing a vehicle adoption model (CIMS-HDT) combine with a Monte Carlo analysis to consider a wide variety of options, realistic consumer behavior, refueling infrastructure density, and vehicle technical parameters consistent with BC freight routes that have not been done before. Winner drivetrains are defined as those capturing 80% of the average of new market share in 2050 which is consistent with Pareto's Law [66]. Considering the Monte Carlo analysis by 2050, a dominant drivetrain in each scenario is also distinguished by a percentage of domination over other competitors.
8. **Disaggregating the non-financial cost of drivetrains**: In addition to the financial costs of technology, the CIMS-HDT model captures non-financial costs and disaggregates them into 4 different categories of refueling inconveniences, lack of model availability, risk, and cargo capacity limitation, that rarely has been considered [21].
9. **Estimating the chance of meeting the 80% GHG emissions target for 2050 in the short and long haul heavy-duty trucking sectors:** Using Monte Carlo analysis the

chance of meeting 2050 targets for both short and long haul market is estimated considering the uncertainty of input parameters, which has not done been for the specific case of BC.

1.4 Dissertation outline

Figure 1-2 illustrates briefly the main contents of this dissertation and relations between the papers. The ultimate goal of the work is to explore the possibility and market share of zero emissions drivetrains in BC HDTs and their impact on GHG emissions reduction considering various ZEV mandates and infrastructure roll out scenarios. Each chapter from 2 to 4 is framed into a journal paper and is a step toward achieving the ultimate target. Therefore, chapters 2 to 4 as journal papers have their own abstract, introduction, results, and conclusion. Chapter 2 and 3 as two journal papers already have been published in the peer-reviewed Elsevier journal, Transportation Research Part D: Transport and Environment. Chapter 4 as the third journal paper will be submitted in the same journal of Transportation Research Part D: Transport and Environment.

Chapter 2 formulates the foundation of the physical energy consumption and emissions model. The model is used to compare the fuel efficiency and on-road CO_2 emissions of diesel and compressed natural gas (CNG) HDTs. Section 2.2 explains the methodology including drive cycle development, CO_2 emissions model, and diesel and CNG vehicular parameters. The drive cycles are based on a second-by-second speed profile of HDTs on California routes paired with road grade profiles of selected BC freight routes. Vehicular parameters represent factors that contribute to the energy consumptions such as mass and aerodynamic drag coefficient. These parameters are categorized into a baseline and a sensitivity range and are determined through carefully scrutinizing scientific and technical literature, manufacturer catalogs, and other online sources. The result section first discusses the validation of the methodology compared with the literature and then discusses the comparison of diesel and CNG with baseline parameters. The result section continues by expressing a sensitivity analysis for several key model parameters, ending by comparing diesel and CNG energy consumption improvement when adopting several advanced drivetrain technologies. The conclusion section 2.4 highlights the key results and areas for future studies.

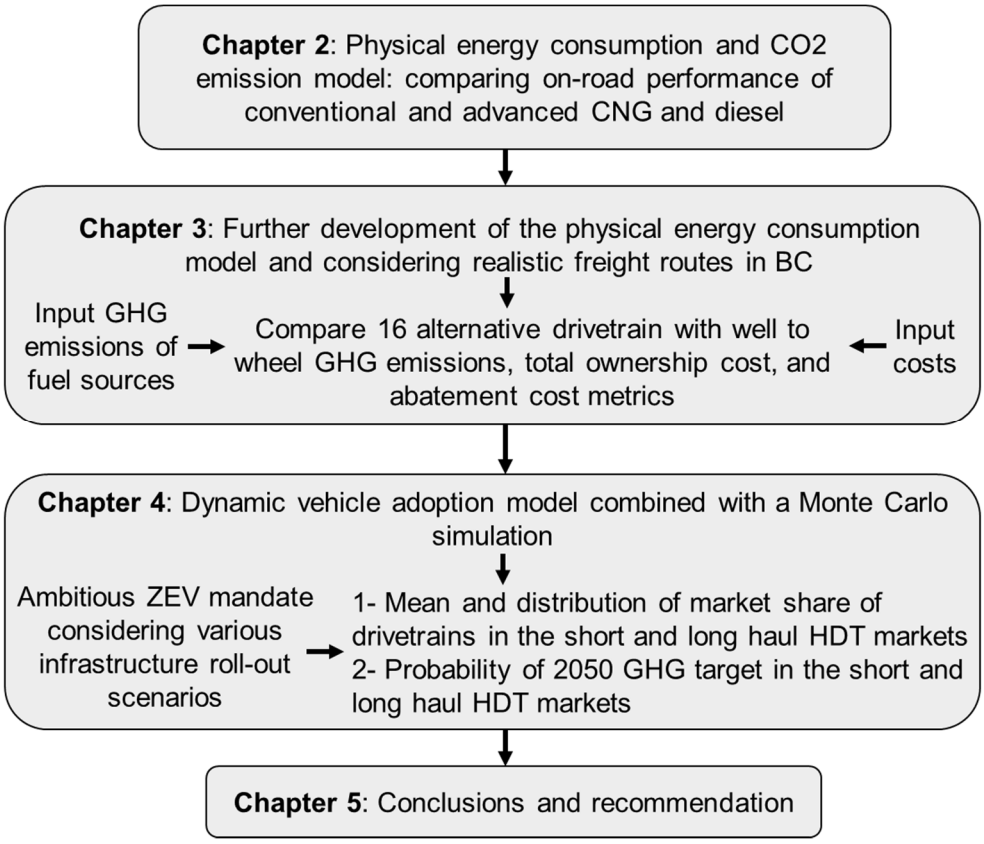

Figure 1-2. A summary for approach and contents of each chapter

Chapter 3 deals with comparing 16 alternative drivetrain technologies including battery electric and hydrogen fuel cell in terms of life cycle cost and GHG emissions. Section 3.2 reviews the subcomponents and technologies associated with alternative drivetrains including battery electric, hydrogen fuel cell, and hybrid options. Section 3.3 describes the methodology including the drive cycle development procedures based on historical activity data of 1600 heavy-duty trucks operating in BC. Additionally, it describes how the physical energy consumption model developed in chapter 2 is extended to incorporate 14 more drivetrains technology. Additionally, the methodology section presents input vehicular parameters, input cost, and GHG emissions intensity of fuel supplies and their uncertainty ranges. The GHGenius and GREET models are used for obtaining well-to-pump GHG emissions as well as on-road CH_4 and N_2O emissions. The results section 3.4 illustrates fuel efficiency, well to wheel GHG emissions, total ownership cost, abatement cost, and cargo capacity comparison across 16 drivetrains on short and long haul routes.

Chapter 4 presents projections for market share, GHG emissions, and energy demand from various fuel type in the short and long haul markets of BC considering several zero emissions mandate and infrastructure roll out scenarios. Section 4.1 describes the novelties related to the market share projection compared to the previous study. Section 4.2 reviews the related literature and modeling approaches that were used for on-road freight energy and economic analysis. Section 4.3 presents the governing equations for a dynamic vehicle adoption model (called CIMS-HDT), modeling parameters, and policy scenarios. This section also presents financial and non-financial costs for each alternative drivetrain HDTs, as well as a method for quantifying these costs. Section 4.3 indicates the results of market share and GHG emissions projections under several infrastructure deployment and two ambitious zero emissions mandate scenarios for both short and long haul markets.Chapter 5 summarizes the key finding of this work. Additionally, this chapter reviews the limitation of this work and then recommends several potential pathways for future studies and practical implementation steps.

Chapter 2

2 Examining the role of natural gas and advanced vehicle technologies in mitigating CO_2 emissions of heavy-duty trucks: Modeling prototypical British Columbia routes with road grades

This paper was co-authored with Jonn Axsen and Curran Crawford and published in the volume 62 of Transportation Research Part D: Transport and Environment journal in July, 2018.

S. M. Lajevardi, J. Axsen, and C. Crawford, "Examining the role of natural gas and advanced vehicle technologies in mitigating CO_2 emissions of heavy-duty trucks: Modeling prototypical British Columbia routes with road grades," *Transp. Res. Part D Transp. Environ.*, vol. 62, pp. 186–211, Jul. 2018.Available online at: https://doi.org/10.1016/j.trd.2018.02.011

This chapter presents a physical energy consumption and emission model to compare on-road performance of diesel and compressed natural gas (CNG) HDTs. This model is a foundation to compare further 14 different drivetrain technologies presented in chapter 3. The focus is to quantify and comapre the imact of various parameters such as mass and operating conditions (e.g. drive cycle) on fuel consumption and CO_2 emissions for diesel and CNG drivetrains. Additionally, this chapter discuses the role of advanced technologies to improve energy consumption of diesel and CNGs HDTs.

Abstract: This study presents a simulation framework for estimating on-road CO_2 emissions of compressed natural gas (CNG) and diesel tractor-trailer heavy-duty trucks under various operational conditions. A second-by-second component-level model was developed and then used to simulate seven distinct drive cycles. This paper specifically considers road grade, and develops a novel technique to pair road grade profiles with given speed vs. time data when gradient data are not available. Six routes around the Canadian province of British Columbia were used as case study drive cycles, including an extreme hill climb route. Results showed that omission of road grade under-estimates CO_2 emissions by as much as 24% for both CNG and diesel drivetrains. Simulations indicated that CNG trucks emit 13–15% less CO_2 than comparable diesel trucks, depending on weight class and drive cycle. Sensitivity analyses highlighted the importance of aerodynamic drag, rolling friction, and engine efficiency for all cycles. An assessment of advanced vehicle technology options for CNG trucks showed achievable CO_2 reductions of 28–35% in the near-term and 41–51% over the longer term, compared to current diesel technology. The same advanced technology options would reduce diesel drivetrain CO_2 emissions by 17–23% and 31–42% over the near and long-term respectively. It is worthwhile to emphasize that with commensurate technology developments, CNG drivetrains offer the same 13–15% CO_2 reductions compared to diesels over the near and long term. The results demonstrate that CO_2 reductions in heavy-duty trucks depend primarily on drivetrain technology, while operational conditions play a less significant role.

Keywords: Heavy-duty truck, CNG, Diesel, road grade, emission model, drive cycle

2.1 Introduction

Worldwide, freight transport by trucks has been steadily growing as a result of globalization of trade and supply chain changes, and now constitutes a major source of greenhouse gas (GHG) emissions [67]. In the United States and Canada, more than 70% of domestic freight volume is moved via trucks [68], [69]. Trucks also carry 75% of the total freight volume in the European Union (EU) and account for 30% of total EU on-road GHG emissions [70]. By 2030, their contribution to EU on-road emissions is projected to increase to 40% without any additional policy [70]. In 2015, Canadian freight trucks emitted 37% of on-road GHG emissions (63.2 Mt CO_2eq) and 9% of the total GHG emissions respectively. In contrast, in 2005, the GHG emissions from Canadian freight trucks were 30% of on-road emissions (49.5 Mt CO_2eq), a 28% decadal increase in GHG emissions from this sector [71]. Heavy-duty[1] trucks are the most significant contributor to on-road freight volume in the United States and Canada [72] and are employed for a broad range of applications such as long-haul, short-haul[2] and port drayage[3].

This research focuses on the Canadian province of British Columbia as a case study, which also aligns with Canada, the United States, and EU trends in terms of GHG emissions from freight trucks. Heavy-duty trucks contribute to 33% and 8% of on-road and total provincial GHG emissions, respectively [73]. The fleet of 42,000 heavy-duty trucks in British Columbia plays important role in the economy and moves $3 billion of commodities every year [74]. In recent years, the increased economic feasibility of extracting natural gas resources has brought this fuel to the attention of decision makers and industries globally, due to the potential for lower costs and less carbon intensity for heavy-duty vehicles [68], [75], [76]. For example, FortisBC, a natural gas utility company in British Columbia, has started to pay an incentive in 2012 for the adoption of natural gas vehicles, which can cover up to 90% of the incremental cost over a diesel vehicle [77]. On the other hand, many governments around the world including British Columbia have set an ambitious GHG reduction target of 33% below 2007 levels by 2020, and 80% below 2007 levels by 2050 [11]. Meeting these targets will require aggressively adopting low and zero

[1] Heavy-duty refers to the Class 8 category of trucks with gross weight of 15,000 kg or more.
[2] By British Columbia government definition any trip for heavy-duty Class 8 truck exceed 160 km from home terminal then it consider as long-haul trip and below this limit consider as short-haul trip [299].
[3] Drayage refer to a short trip that is a part of longer trip such as delivery of goods from a seaport into a warehouse [300].

emission technologies for this sector. Many people have proposed natural gas as a transitional fuel because hydrogen fuel cell and battery electric trucks may not be available in this market for several decades [78], [79].

Natural gas combustion produces approximately 32% fewer CO_2 emissions than the combustion of diesel fuel per heating unit [80]. Since the major GHG intensive stage in the life cycle of a vehicle with a combustion engine is the tailpipe CO_2 emissions, the focus of the present study is on the vehicle on-road stage. In the literature available to date, there has been no consensus with regard to the absolute CO_2 benefits of natural gas vehicles over comparable diesel ones, in part due to difference in lifecycle modeling assumptions, assumed drive cycles and technology characteristics, as well as whether one uses a lifecycle emissions model or measures emissions in the field.

For example, Rose et al. [81] and Shahraeeni et al. [82] assessed the potential of natural gas for refuse and light-duty trucks, respectively, in British Columbia (the city of Surrey), Canada and applied the GHGenius model as a life cycle analysis tool. Although Shahraeeni et al. [82] demonstrated that light-duty CNG trucks produce 34% fewer on-road GHG emissions compared to the baseline diesel, Rose et al. [81] used the same methodology and found a 15% on-road GHG reduction for a heavy duty CNG refuse truck compared to the baseline diesel. Shahraeeni et al. [82] clarified that the discrepancy was due to a difference in fuel efficiency assumptions in the GHGenius tool for light and heavy duty vehicles. The default setup of the GREET.net model [83], on the other hand, predicts a 19% reduction in CO_2 emissions for a long-haul CNG heavy-duty truck during the operation stage. The GHGenius life cycle model [55] indicates a 28% reduction in CO_2 emissions for a heavy- duty LNG truck over a comparable diesel during the in-use stage.

Real-time measurement of emissions for a heavy-duty tractor-trailer truck has revealed that the CO_2 mitigation benefit of a CNG truck in fact depends on the traveled routes and vehicle technologies, such as whether one assumes a drayage route or a hill climb route. For example, a CNG truck with 11.9 L engine produces 29% less CO_2 in a local drayage route compared to a diesel truck with 12.8 L engine. In addition, the same CNG truck produces 11% more CO_2 in a hill climb route compared to a 15 L diesel engine [84]. However, the excessive CO_2 emissions can be explained by the 11.9 L CNG engine being under-powered for the hill climb cycle, causing the engine to work at a low efficiency operating point to meet the demanded speed. This

problem can be alleviated with a suitable engine size, such as the 15 L Westport LNG engine that is not currently on the market (as of the writing of this paper) but expected to be available in the near future [80], [85].

A challenge is that real-time emissions measurements are an expensive endeavor. Although the life cycle assessment models are simple, their aggregated nature makes them inadequate to fully quantify the CO_2 mitigation benefit of a CNG truck. Furthermore, both methods have a lack of flexibility for examining technological change or modeling various operational conditions. To address these difficulties, a second-by-second microscopic CO_2 emission model was developed in Matlab for studying various operational conditions and drivetrain technologies.

There are many physical emission models, such as VECTO [86], CMEM [24], GEM [87], MOVES [25]; Autonomie (and PSAT which is the former version of Autonomie) [26], AVL Cruise [88], Advisor [27] and PHEM [28]. These tools have been used for heavy-duty vehicle performance analysis in a number of studies [29], [30], [93], [33], [34], [57], [64], [89]–[92]. Autonomie has been used most frequently among these tools. Zhao et al. [57] for example, used PSAT to explore the fuel consumption savings potential of diesel heavy-duty trucks (Class 8) with conventional and hybrid powertrains under four duty cycles, without considering road gradient. In addition, Gao et al. [31] applied Autonomie and compared conventional and hybrid CNG heavy-duty trucks (Class 8) with conventional and hybrid diesel powertrains in terms of cost saving and CO_2 mitigation benefits under several operating cycles in which they included grade profiles. In an inclusive technical report, Delgado and Lutsey [64] investigated the role of technological change beyond 2020 with the conventional and hybrid diesel powertrain within the Autonomie model. Kast et al. [34] used Autonomie to explore the applicability of fuel cell powertrains and appropriate hydrogen tank sizes for all vocational classes, including long-haul heavy-duty trucks (Class 8).

These previous studies mainly showed that simulation tools are reliable and insightful for the decision making process but require an extensive set of input parameters. Although road gradients were considered in a number of previous studies [29], [31], [33], [64], [90], [91], none considered the kind of steep road conditions found in British Columbia topography. Road transportation in British Columbia usually includes passing over elevated summits with steep grades of up to 8% [58], while previous literature tends not to simulate grades exceeding 6%

[29], [33], [90], [93]. Additionally, regression and neural network methods have been applied to investigate road grade impacts on energy consumption for a combination of light duty electric vehicles [94], [95] and a mining truck [96]. However, these methods are not physical emission models since they are developed based on experimental data for a particular drivetrain. Therefore, they are not applicable for examining various alternative or futuristic drivetrain technologies.

Besides steep road grades simulations, the other novel contribution of this study is to develop a technique to attach grade data to a speed vs. time profile. This study proposes a method to extract elevation profiles from the freely available Google Earth tool [97] which can be translated into grade profiles. Additionally, determining the vehicular parameters is another important aspect of the present study that is rarely fully presented in previous studies. The overall objective of this study is to compare the on-road CO_2 emissions from conventional CNG and diesel tractor-trailer truck operating on British Columbia roads as case studies. The in-house physical CO_2 emissions model provides accessibility to all details and parameters of the code while some of the aforementioned tools such as Autonomie, VECTO, AVL Cruise, and Moves use built-in libraries and several parameters and variables are not observable to a user. Furthermore, modeling in a code environment allows inclusion of other advanced powertrain technologies such as hybrid, hydrogen, and battery electric in future studies.

Finally, this study is exploring the impact of technologies to reduce CO_2 emission for both conventional diesel and CNG trucks. The U.S. National Research Council (NRC) [59]–[61] and the U.S. Environmental Protection Agency (EPA) with the National Highway Traffic Safety Administration (NHTSA) [62], [63] have extensively reviewed numerous technologies and their associated costs to reduce fuel consumption for heavy-duty Class 8 trucks. These technologies were mainly divided into rolling friction, aerodynamics, weight, and engine efficiency groups; for each category various technologies were presented and their impact on fuel consumption analyzed. The EPA and NHTSA [63] also used the GREET analysis tool and demonstrated the tailpipe CO_2 reduction benefits of natural gas over diesel drivetrain for heavy-duty trucks are 13% and 22% assuming 15% and 5% thermal efficiency gaps respectively. The present study, in addition to sensitivity analysis of individual vehicular parameters on CO_2 emissions similar to that done previously [59]–[63] aims to examine the collective impact of improvements in several parameters on CO_2 emissions.

This paper is organized into the following sections. Section 2.2 outlines the methodology comprising input drive cycles with a detailed description of road gradient calculations, CO_2 emissions model, and vehicle parameters. Section 2.3 presents results and discussion of the comparative analysis of CNG and diesel tractor-trailer trucks, in terms of fuel consumption and CO_2 emissions. Additionally, this section considers sensitivity analyses and the future technological change assessments for CNG and diesel drive- trains. Section 2.4 provides a conclusion and proposes directions for future research.

2.2 Methodology

Two modeling approaches were used in previous studies to assess vehicle performance, termed backward facing and forward facing models. The backward facing model is an explicit model in which it is assumed the vehicle speed trace (see Figure 2-4 containing various speed profiles) is met and the goal is to find the energy use of the vehicle. In contrast, the forward facing model has an implicit nature in which the throttle or braking commands are given parameters and the goal is to find how the vehicle could meet the desired speed trace dynamically. Therefore, depending on the control signal the target speed might be overshot, undershot, or achieved. Modeling with the forward facing approach is more useful for analyzing the transient performance of a vehicle's components during the design process but requires more inputs and runtime cost [27], [91]. For this study, a backward approach was chosen since it is faster and requires limited information compared to the forward-looking simulation.

Figure 2-1 presents the main components of this model. The core element of this approach is the power demand model. The power demand is the result of the vehicle interaction with its environmental surroundings. Four basic elements of friction, aerodynamics, acceleration, and gravitational forces contribute to the power demand [98]. Vehicle parameters are frontal area of vehicle, rolling resistance factor, aerodynamic drag coefficient, and weight. Drive cycles are defined by vehicle speed and road grade profiles. The input of the engine model is the power demand and transmission efficiency to calculate the fuel consumption rate as a function of engine parameters. If the estimated braking torque (T_b) of the engine at any engine speed is beyond the engine wide open throttle torque (T_{WOT}), then speed is re-calculated according to this maximum limit. Engine manufacturers normally provide the WOT torque performance in their catalogues. The instantaneous rate of fuel consumption as a function of braking power, engine speed, and

other vehicle parameters is integrated over the whole drive cycle to obtain the total fuel consumption and then translated to CO_2 emissions based on the carbon content of the fuel. The next sub-sections describe more details of this methodology.

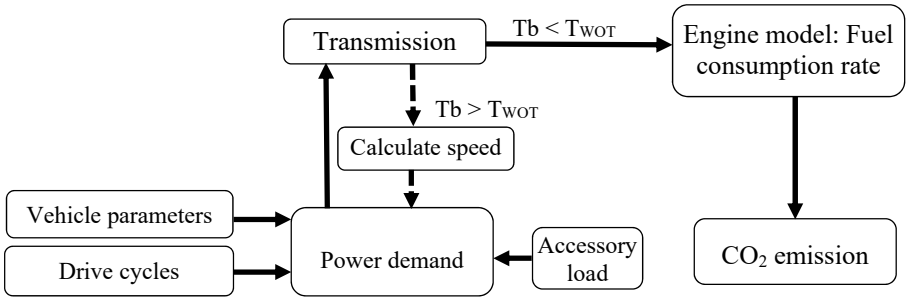

Figure 2-1: Basic principle of CO_2 emission model

2.2.1 Input drive cycles

Standard dynamometer driving cycles [99] normally do not fully represent real world driving patterns which are influenced by variable traffic congestion and road grades. However, these cycles can be useful for the purpose of verification and calibration, as they have been used in a few similar studies [31], [98]. Therefore, in this study a standard test cycle called the "Heavy Duty Urban Dynamometer Driving Schedule (HD-UDDS)" [100] was used to benchmark the model. In addition, six real world speed profiles were applied from a recent California Air Resources Board study [84].

These six drive cycles are representative of driving patterns for a tractor-trailer heavy-duty truck (Class 8) on several routes across the state of California, US. It was justifiable to use California-based data as representative for British Columbia since there are some similarities between these two territories in terms of the port drayage, urban, and highway freight networks. Due to the lack of grade profiles in the supplied California speed data, the following method was employed to pair gradient profiles to the speed data for several selected routes around British Columbia. Although to some extend speed and grade are correlated, it was rational to attach British Columbia grades to California speed profiles, as in reality vehicle speeds are more dependent on traffic flow while grades link to road topography. This means that in the absence of drivetrain power limitations and traffic congestion a vehicle can go at any high speed, even on steep grades. Furthermore, in the model implementation, if an input torque demand (see Figure 2-1) is beyond the maximum available engine torque, then speed is re-calculated to

determine a lower vehicle speed limited by available power at the given steep positive grade angle and acceleration.

Representative freight routes for British Columbia were selected according to a study done by Port Metro Vancouver, which provided trucking routes in the Lower Mainland (Pittman and Stanevicius) [101]. Figure 2-2 displays these selected routes created in the Google- Earth tool [97]. This tool was used to build the elevation profile for these six representative routes. The total distance of each route was selected to be compatible with the trip distance of each drive cycle. Four routes were labeled similar to the original study (Quiros et al., 2016) [84] as "Near Dock Drayage" (NDD), "Local Drayage" (LD), "Regional Highway" (RH), and "Urban Arterial" (UA); the "Hill Climbing" and "Interstate highway" were re-named to Hill Climb Provincial Highway (HCPH) and Flat Provincial Highway (FPH), respectively. A round trip was assumed for LD and FPH routes, to account for the shorter distance of these British Columbia routes relative to the original data.

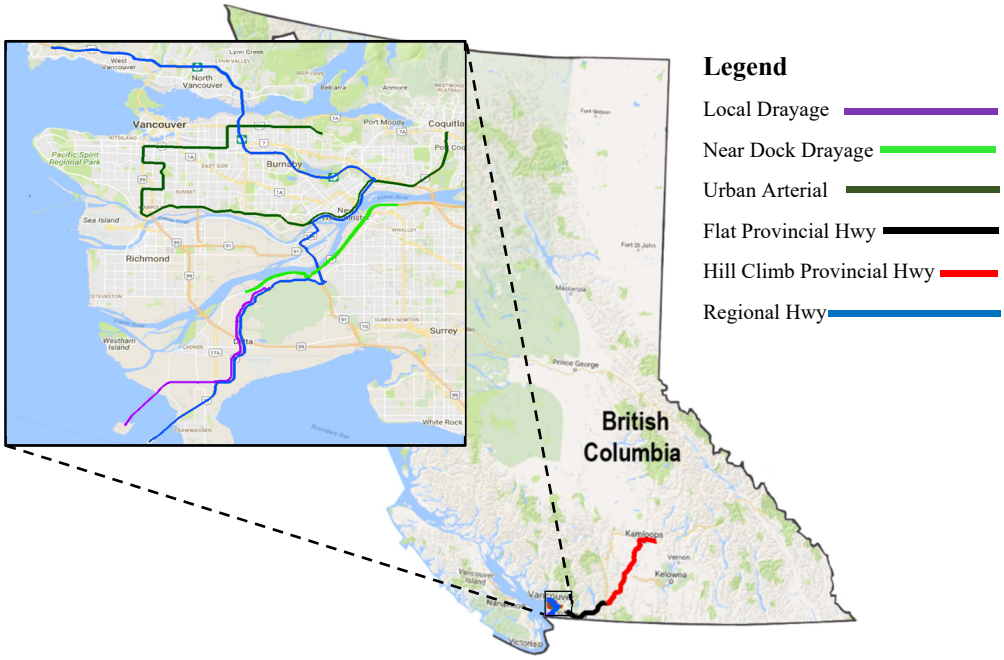

Figure 2-2: Selected fright transportation routes in British Columbia [97]

Next, .kml files created in Google-Earth were exported to the TCX Converter tool (TCX Converter) [102] where their numerical magnitudes of distance versus elevation can be extracted. In order to pair the speed and gradient profiles, the speed trace was first converted from time-velocity basis to distance-velocity basis. Eq. (2-1) was used to calculate the traveled distance (x_i) from start until time (t_i). Then, the traveled distance (x_i) was interpolated on the

distance-elevation trace extracted from Google-Earth yielding matched cycle speed and grade profiles.

$$x_i = \int_0^{t_i} v(t)dt \qquad 2\text{-}1$$

Raw interpolated elevation profiles consisted of many non-physical changes in elevation, since passing over bridges was neglected by the Google Earth tool (Figure 2-3). To remove the erroneous elevations the raw interpolated data was smoothed using the Savitzky-Golay filter in Matlab, as proposed by NREL [103]. Figure 2-3 presents the smoothed and raw elevation profiles for all adapted cycles. The grade θ_i (deg) at each time step was calculated using the following equation:

$$\theta_i = \left(\tan^{-1}\frac{\Delta h_i}{\Delta x_i}\right)\frac{180}{\pi} \qquad 2\text{-}2$$

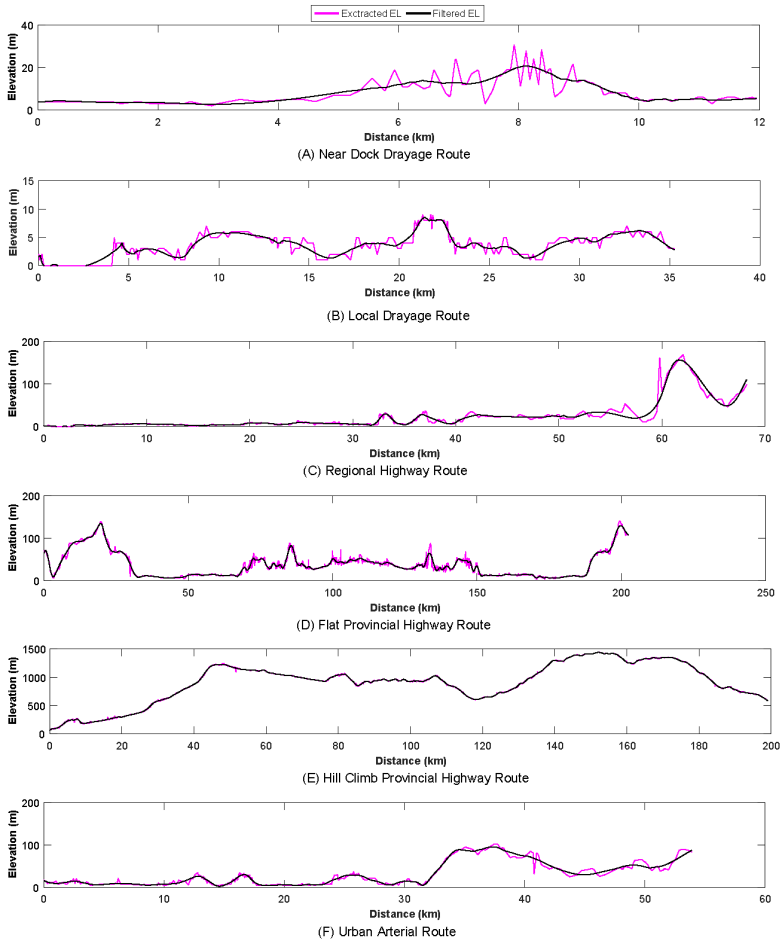

Figure 2-3: Modifying elevation profile using Savitzky-Golay smoothing filter

where Δh_i and Δx_i indicate the difference in elevation and traveled distance between adjacent points. Figure 2-4 displays all selected drive cycles along with their British Columbia grade profiles; Table 2-1 summarizes the main characteristics of all cycles. Near Dock Drayage and Local Drayage routes have a higher amount of idling time, while the Hill Climb Provincial Highway, Flat Provincial Highway and Regional Highway routes have the lowest. The trip distance presented in Table 2-1 can be calculated by integration of the speed profile over the entire of drive cycle.

$$TD = \frac{\int_0^T v(t)dt}{3600} \qquad 2\text{-}3$$

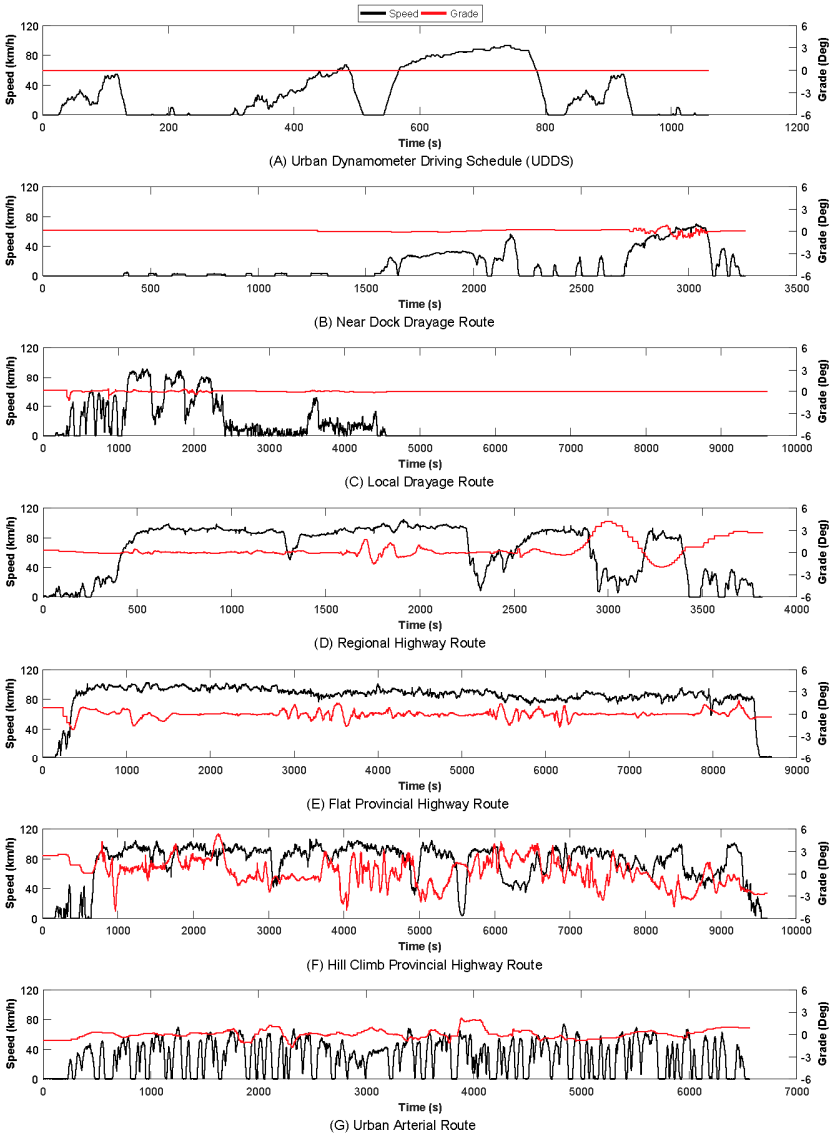

Figure 2-4: Selected drive cycles each comprising of speed and grade profiles

where TD is the total trip distance of a given cycle (km), v (t) is the vehicle speed (km/h) at time t, and T (s) is the total elapsed time of the cycle. The characteristic acceleration metric indicates the amount of inertial work per unit mass and distance to accelerate or elevate a vehicle, computed using Eq. (2-4) from [104].

$$\tilde{a} = \frac{\sum_{i=1}^{N-1} positive\left(\frac{1}{2}(v_{i+1}^2 - v_i^2) + g(h_{i+1} - h_i)\right)}{TD} \quad 2\text{-}4$$

The significance of aerodynamics loads on fuel consumption can be captured by the square of the aerodynamic speed and is defined by Eq. (2-5) [104].

$$v_{aero}^2 = \frac{\int_0^T v^3 dt}{TD} \quad 2\text{-}5$$

The kinetic intensity determines how much advantage a hybrid drivetrain has over a conventional one considering the characteristics of the cycle. Generally, higher kinetic intensity is the result of more aggressive stop and go conditions in which a hybrid drivetrain would be preferable [105]. It is defined as the ratio of the characteristic acceleration over the square of aerodynamic speed, computed as in Eq. (2-6) from O'Keefe et al. [104] for each cycle.

$$KI = \frac{\sum_{i=1}^{N-1} positive\left(\frac{1}{2}(v_{i+1}^2 - v_i^2) + g(h_{i+1} - h_i)\right)}{\int_0^T v^3 dt} \quad 2\text{-}6$$

Table 2-1: Summary of main characteristics of drive cycles used in this study

Driving cycles	Urban Dynamometer Driving Schedule	Hill Climb Provincial Highway	Flat Provincial Highway	Local Drayage	Near Dock Drayage	Regional Highway	Urban Arterial
Average speed (km/h)	30.3	74.5	83.8	13.2	13.2	64.3	29.5
Traveled distance: TD (km)	8.9	199	202.5	35.2	12	68.2	53.8
Idling percent%	35%	5%	3%	59%	49%	6%	24%
Elevation change (m)	0	1377	129	9	18	156	93
Characteristic acceleration (m/s^2)	0.14	0.16	0.06	0.12	0.09	0.1	0.2
Aerodynamic speed (km/h)	68.4	86	88.9	62.2	44.9	84.3	47.9
Kinetic intensity (1/km)	0.38	0.29	0.1	0.41	0.58	0.18	1.1
Number of stops	14	6	15	42	17	13	49

2.2.2 CO_2 emissions model

In order to determine the tailpipe CO_2 emissions for a given vehicle, the first step was to calculate the road tractive power. The vehicle tractive load was calculated by accounting for rolling friction force, gravity force due to road grade angle, aerodynamic force, as well as vehicle acceleration (see Figure 2-5). Applying Newton's second law of motion in the longitudinal direction yields the required tractive force to propel the vehicle (see Eq. (2-7)).

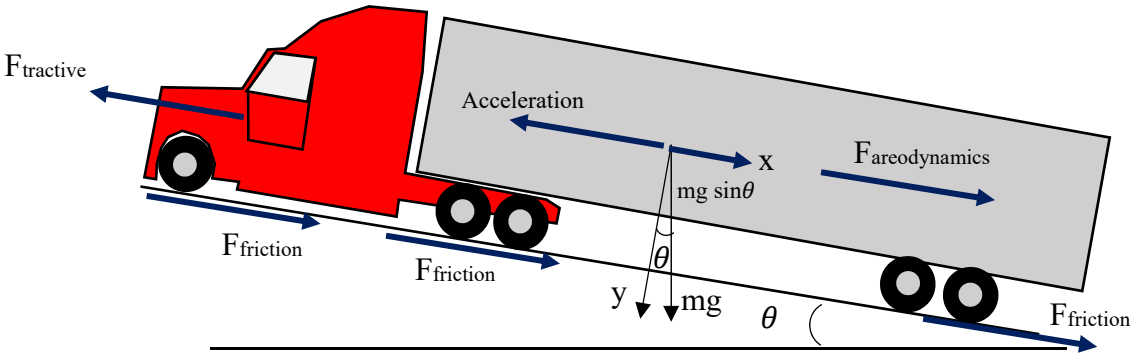

Figure 2-5: A schematic for a heavy-duty tractor-trailer truck

$$F_{tr} = F_{friction} + F_{areodynamics} + Ma + Mg\ \sin\theta \qquad 2\text{-}7$$

where F_{tr} is the tractive force (N), M is the vehicle mass (kg), g is the gravitational acceleration (9.81 m/s^2), θ is the road grade angle (deg), and a is the acceleration (m/s^2). By substituting the tire rolling friction and aerodynamic forces into Eq. (2-7) from Giannelli et al. [106], the tractive force was determined as follows:

$$F_{tr} = Mg(C_{r0} + C_{r2}v^2)\cos\theta + \frac{C_D A_f \rho_a}{2}v^2 + Ma + Mg\ \sin\theta \qquad 2\text{-}8$$

where C_{r0} and C_{r2} are the zero and second order coefficients for the tire rolling friction force, θ is the road grade angle (deg), C_D is the aerodynamic drag coefficient, A_f is the frontal area of vehicle (m^2), and ρ is the air density (kg/m^3). Then, the product of tractive force and vehicle speed gives the tractive power. In order to account for the effect of rotational and reciprocating parts of the powertrain (e.g., wheels, gears, and shafts) a mass correction factor (ε) was used from [107]. This factor depends on gear number and normally varies between 0.075 and 0.25 [107]. Applying this factor in Eq. (2-8), the tractive power (P_{tr} (kW)) equation becomes:

$$P_{tr} = \frac{W_{tr}}{\Delta t} = F_{tr} \cdot v$$
$$= \left[Mg(C_{r0} + C_{r2}v^2)\cos\theta + \frac{C_D A_f \rho_{air}}{2} v^2 + M(a(1+\varepsilon) + g\ \sin\theta) \right] v \quad \text{2-9}$$

After rearranging Eq. (2-5), the tractive power demand is determined as follows:

$$P_{tr} = Mgv C_{r0}\cos\theta + \left[MgC_{r2}\cos\theta + \frac{C_D A_f \rho_{air}}{2} \right] v^3 + Mv[a(1+\varepsilon) + g\ \sin\theta] \quad \text{2-10}$$

One should note that the road tractive power might become negative in the case of vehicle deceleration or driving on a road with downgrade angle. The braking system or an electric motor (in the case of hybrid powertrain) absorbs the negative power. To translate the tractive power to engine braking power one needs to know the transmission efficiency and accessory loads. The following equation from Barth et al. [98] was used to estimate the engine braking power.

$$P_{br} = \frac{P_{tr}}{\eta_T} + P_{acc} \quad \text{2-11}$$

where P_{br} is the braking power output of the engine (kW), η_T is vehicle transmission efficiency, and P_{acc} is the accessory loads (kW) related to vehicle operation from devices such as: lighting, air-conditioning, air compressor, alternator, steering pump, and engine cooling fan [64]. The mass flow rate of fuel was estimated using the basic definition for indicated thermal efficiency; after rearranging, the mass flow rate, $\dot{m}_{FR}$ (g/s), can be computed as:

$$\dot{m}_{FR} = \frac{P_{fr} + P_{br}}{\eta_i\, LHV} = \frac{1}{LHV}\left(\frac{P_{fr}}{\eta_i} + \frac{P_{br}}{\eta_i} \right) \quad \text{2-12}$$

where P_{fr} is the engine friction power (kW), η_i is the indicated thermal efficiency, and the LHV is the lower heating value of input fuel (kJ/g). One should note that indicated thermal efficiency is different from maximum braking efficiency or total maximum efficiency that engine OEMs typically quote in their catalogues. The indicated thermal efficiency contains a lot of engine characteristics like compression ratio, fuel mixing, valve timing, and combustion chamber geometry. This should be interpreted as the overall thermodynamic efficiency limit of the powertrain, rather than the efficiency at a specific point of operations. Nam and Giannelli [108] underscored that over a period of 30 years friction losses of powertrains have been reduced by 30%, yet the indicated thermal efficiency has not been much improved [108]. The engine or braking efficiency can be determined by following equation:

$$\eta_b = \frac{P_{br}}{\dot{m}_{FR} \times \text{LHV}} \quad 2\text{-}13$$

Ross and An [109] used dynamometer test data of 25 spark ignition and 5 compression ignition engines. They demonstrated that for load levels less than two-thirds of maximum engine power, the rate of input energy of fuel ($\dot{m}_{FR} \times LHV$) per engine speed has a linear relationship with braking power output, P_{br}, per engine speed. They proposed the following equation for the engine friction power calculation as:

$$\frac{P_{fr}}{\eta_i} = K\ N\ V \quad 2\text{-}14$$

where K is the engine friction factor normally as a function of engine speed and required to be determined via dynamometer test data, N is the engine speed (revolution per second (rps)) which is a function of vehicle speed, and V is the engine displacement (L). After rearranging Eq. (2-12) and multiplying it by fuel-air equivalence ratio (φ) [108], the general form of the instantaneous fuel consumption (gram/s) can be obtained which is applicable for both gasoline and diesel engines.

$$\dot{m}_{FR} = \frac{\varphi}{\text{LHV}}\left[K.N.V + \frac{P_{br}}{\eta_i}\right] \quad 2\text{-}15$$

A more detailed form of instantaneous fuel consumption was applied from Barth et al. [98], which was calibrated exclusively for heavy-duty diesel vehicles (see Eq. (2-16)). Due to the lack of an engine efficiency map for CNG, some parameters in Eq. (2-16) were tuned in order to make it applicable for a CNG drivetrain; these drivetrain parameters include: maximum braking power, the constant coefficient of friction factor (K_0), LHV, indicated thermal efficiency, and engine displacement volume. The next sub-section provides more details about these five parameters.

$$\dot{m}_{FR} = \frac{1}{\text{LHV}}\left(K.N.V + \frac{P_{br}}{\eta_i}\right)[1 + b_1(N - N_o)^2] \quad 2\text{-}16$$

$$K = K_o[1 + C(N - N_o)]$$

$$N_o \approx 30\sqrt{\frac{3}{V}}$$

where $C = 0.00125$ and $b_1 = 10{-}4$ are also constant coefficients, No is the engine idle speed (revolutions per second (rps)), and N (rps) is the engine speed corresponding to the vehicle

speed. The engine speed was determined by applying the following equation from Barth et al. [98]:

$$N = SR\frac{R(G)}{R(G_t)}v \qquad 2\text{-}17$$

where N is in revolutions per minute (rpm), SR (rpm/kph) is the engine speed over vehicle speed in top gear (G_t), R(G) is the gear ratio in the designated gear, and ν is the vehicle speed. The transmission was assumed to be an Eaton Fuller system (FR-15210B) [110] which is the typical transmission system for both CNG and Diesel heavy-duty trucks. Table 2-2 presents the typical gear ratio and logic of shifting points for this transmission system of 10 gears, with top gear speed ratio (SR) of 1550 rpm/100 kph. After obtaining engine speed, the engine braking torque (T_{br}) can be specified by using the following equation [98]:

$$T_{br}(N.m) = \frac{P_{br}\ (kW) \times 9549}{N\ (rpm)} \qquad 2\text{-}18$$

Table 2-2: Gear ratio based on Eaton Fuller (FR-15210B) Transmissions [110]

Gear no	Gear ratio	Speed range (kph)
Gear 1	14.8	1 - 3.7
Gear 2	10.95	3.7 - 7.3
Gear 3	8.09	7.3 - 11.2
Gear 4	5.97	11.2 - 16.2
Gear 5	4.46	16.2 - 22.9
Gear 6	3.32	22.9 - 33.3
Gear 7	2.45	33.3 - 46.6
Gear 8	1.81	46.6 - 63.2
Gear 9	1.34	63.2 - 83
Gear 10	1.00	83 - 120

Considering Eq. (2-16) as the baseline model for both diesel and CNG technology, the fuel consumption (kg/100 km) for a given cycle was determined by integrating mass flow rate over the driving period and then considering the total trip distance (TD) obtained from Eq. (2-3):

$$FC = \frac{\int_0^t \frac{1}{\mathrm{LHV}}\left(K.N.V + \frac{P_{tr}}{\eta_i\eta_t} + \frac{P_{acc}}{\eta_i}\right)[1 + b_1(N - N_o)^2]dt}{10 \times TD} \qquad 2\text{-}19$$

where FC can be used for both diesel and CNG powertrain. The multiplier of 1/10 (100/1000) is the result of converting the numerator to kilo-gram unit and then accounting for the specific distance of 100 km. In order to obtain the fuel consumption for diesel powertrain in L/100 km, the FC was divided by diesel density, ρ_f (kg/L). Similarly, the equivalent diesel fuel consumption for the CNG powertrain was calculated by multiplying Eq. (2-19) by a $LHV_{CNG}/(\rho_f \times LHV_{Diesel})$ factor. Finally, the tailpipe CO_2 emissions of the vehicle in kg/100 km is the product of the FC and the carbon content of fuel, C_{fu}, followed by a conversion factor of 44/12 to account the molecular mass of CO_2 over molecular mass of carbon.

$$M_{CO2} = \frac{44}{12} \times C_{fu} \times FC \qquad 2\text{-}20$$

2.2.3 Vehicle parameters

The input parameters were chosen via scrutinizing relevant literature including manufacturing catalogues, scientific papers, and technical reports. Table 2-3 presents a summary of considered parameters for both CNG and diesel tractor-trailer trucks. In order to conduct a sensitivity analysis, a possible range of improvements or changes were assumed for key parameters. These parameters consisted of: indicated thermal efficiency, constant coefficient of friction (K_0), accessory load, aerodynamic drag coefficient, frontal area, and loaded mass of trucks. The last column of the table also provides data sources for these parameters.

CO_2 reduction potential per heating unit for natural gas compared to diesel depends on the assumptions for the chemistry and heating values of diesel and natural gas, for which various sources report slightly different values. This study used values from the U.S. Energy Information Administration [111] to obtain the theoretical CO_2 content of fuels; the CO_2 content of natural gas according to this source is 53.1 kg /MMBTU [111]. Comparing natural gas and diesel using this data source, the theoretical CO_2 emission reduction per heating unit is 27.5%. However, that source considered diesel to have a LHV of 139,000 BTU/Gallon. In contrast, in the current work it was assumed that on a volume unit "low sulfur diesel" with a LHV of 129,488 BTU/Gallon [112] and "home heating and diesel fuel" [111] have equal CO_2 contents of 10.16 kg/Gallon. Therefore, the CO_2 content of the low-sulfur diesel becomes 78.5 kg/MMBTU. Applying the conversion ratio of 1055.05 (1 MMBTU equal to 1055.05 MJ [113]), the CO_2 content of the low-sulfur diesel and natural gas becomes 74.4 g/MJ and 50.3 g/MJ respectively. Hence, the CO_2 reduction potential of natural gas over diesel becomes 32.3%. Finally, considering the LHV of

low-sulfur diesel (42.6 MJ/kg) and natural gas (47.1 MJ/kg) and conversion factor of CO_2 to carbon (12/44), the carbon content of diesel and natural gas becomes 86.4% (kg carbon/kg fuel) and 64.7% (kg carbon/kg fuel) respectively.

The Cummins Westport ISX 11.9 CNG [114] and Mack-MP7-395C [115] engines were considered to be the representative technologies for CNG and diesel powertrains, respectively. The ISX 11.9 CNG engine with rated power of 400 HP (298 kW) and 11.9-liter displacement is a stoichiometric spark ignition system that entered to the market in 2013. The Mack-MP7-395C engine with rated power of 395 HP (295 kW) and 11-liter displacement is a compression ignition diesel engine. These two powertrain technologies were selected because they have relatively similar rated power and engine displacement. The range of indicated thermal efficiency for diesel heavy-duty trucks ranges from 45% to 50% according to the comprehensive investigation done by Giannelli et al. [106]. Therefore, the baseline indicated thermal efficiency of diesel engine was assumed to be 47% [98].

The CNG engine has a lower compression ratio than a diesel engine; however, no specific source on the indicated thermal efficiency of a spark ignition NG engine has been found. The indicated thermal efficiency was considered to be 38.5% after several executions of the model to inspect if the same final maximum efficiency as reported in Zhao et al. [38] is obtainable. Unlike a diesel engine that relies on fuel injectors for managing engine power, the spark ignition engine uses a throttle valve to control the air fuel ratio. It is expected that a CNG engine with spark ignition technology has 25% higher friction factor than compression ignition diesel due to the use of throttling valve [109], [116]. Manual transmission efficiency is in the range of 87–99% which depends on the gear number [108]. The transmission efficiency was considered 96% and constant for all gears.

The CNG truck was assumed to have a 45 Diesel Gallon Equivalent (DGE) fuel tank. The dry mass of the ISX 12G engine is 1247 kg including the mass of an after-treatment system [44]. Neglecting the mass of an emission control system, the diesel engine has a mass of 1037 kg [115]. The mass of the diesel fuel tank with 45 gallons of volume is around 204 kg [44]. On the other hand, the CNG fuel tank weighs 860 kg. As a result, the combined mass of engine and fuel systems is approximately 866 kg heavier than the comparable diesel ones. In this study, two weight categories were considered to account for various applications like highway and urban cycles. In the medium weight class, the CNG and diesel trucks had a loaded mass of 22,866 kg

and 22,000 kg, respectively. In the heavy weight class, loaded mass of 31,866 kg and 31,000 kg were considered for the CNG and diesel trucks respectively. Aerodynamic drag coefficient depends on many parameters like vehicle speed and the body shape of trucks. A value of 0.99 was suggested for a flat top tractor and 0.6 for a sleeper tractor with high roof [117]. In this study, the aerodynamic drag coefficient and vehicle frontal area for the baseline simulation were assumed to be 0.6 and 10 m^2 respectively [57], [118], [119].

Table 2-3: Summary of parameters used to for simulation

Parameter	Baseline parameters		Sensitivity range	Sources
	CNG	Diesel		
Engine model	Cummins ISX 11.9	MP7 395C		[114], [115]
LHV of fuel (kJ/g)	47.14	42.6		[112]
Engine displacement (L)	11.9	11		[44], [115]
Indicated thermal efficiency	38.5%	47%	0-24% improvement	[98], [108], [120]
K_o	0.25	0.2	0-32% improvement	[98][106][121]
Engine max power	298	295		
Transmission	10 Speed Manual (14.8-1)			[110]
Transmission Efficiency	96% for all gears			[63], [108]
Engine rpm to speed ratio in top gear (rpm/kph), SR	15.5			[108]
Accessory load (kW)	3.5		3.5-11.2	[57], [63]
Carbon content of fuel (kgC/kgfuel)	64.7%	86.4%		[111], [112]
Vehicle loaded weight (kg)	22,866-31,866	22,000-31,000	0-12% weight reduction	[64], [122]
Vehicle curb weight (kg)	15,606	14,740		[64]
Vehicle payload weight (kg)	7,260-16,260	7,260-16,260		[64]
Rolling friction coefficient, C_{r0}	0.007 (0.003 to 0.007 range)		0-28 % improvement	[31], [57], [106]
Rolling friction coefficient, C_{r2}	0 (0 to 0.00012 range)			[31], [57], [106]
Drag Coefficient, C_D	0.6		0-50% improvement	[57], [118]
Frontal area A (m^2)	10			[57], [119]
Air density (kg/m3)	1.225			
Mass Correction Factor	0.1			[107]
Fuel density (kg/m3)	188	850		

2.3 Results and discussion

2.3.1 Validation

The validity of the developed model was appraised relative to previous simulations of CNG and diesel drivetrains [31] and field measurement data for a CNG truck [84]. First, the following specific input parameters were taken from [31]: loaded mass of the diesel truck: 18700 kg; the loaded mass of CNG truck: 19150 kg; engine volume: 15 L; engine max power: 354 kW; C_D: 0.58; C_{r0}: 0.007; C_{r2}: 0; A_f: 10 m^2; 10-speed manual transmission with gear ratio of 14.8–1.

There were some additional parameters to capture the CNG and diesel powertrain as follows: indicated thermal efficiency of diesel 50% and 45% for CNG engines; constant coefficient of engine friction factor 0.15 for diesel and 0.18 for CNG; transmission efficiency: 87%, accessory Load: 10 kW; mass correction factor (ε): 0.10.

Figure 2-6 illustrates validation results for the assumed diesel powertrain. The model is in agreement with both engine power energy as well as fuel consumption. Figure 2-7 demonstrates validation results for the CNG powertrain with respect to Autonomie simulations [31]. The scatter plot of engine efficiency versus engine power shows a reasonable agreement with the Autonomie simulation. Table 2-4 shows a summary of comparative results between current model and the simulation results of Autonomie [31] for the standard Urban Dynamometer Driving Schedule cycle. The predictive outcome of the current model was found to be very consistent with Gao et al.'s [31] results; however, the current model displays the CO_2 content for CNG as 20.8 kg lower than the Autonomie simulation (16% difference from Gao et al. [31]). The reason for this discrepancy can be explained by the assumption of the carbon content of NG, in which it was estimated as 64.7% while Gao et al. apparently considered it to be 76%.

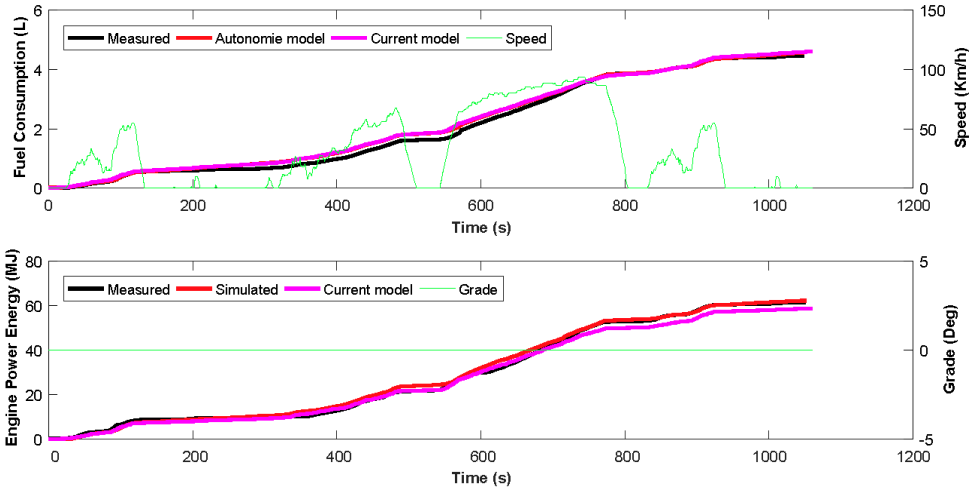

Figure 2-6: Validating current model of diesel powertrain under UDDS cycle with Autonomie model and field measurement which were adapted from [31]

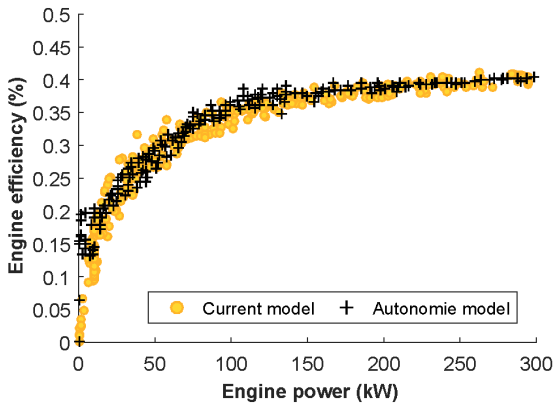

Figure 2-7: Validating current model of CNG powertrain under UDDS cycle with Autonomie model adapted from [31]

Table 2-4: Comparative result used for validation

Method	Current model		Gao et al used Autonomie tool [31]	
Powertrain	**CNG**	**Diesel**	**CNG**	**Diesel**
CO_2 (kg/100 km)	108	138.9	128.6	136.7
Fuel consumption L/100 km	59.3	51.6	59[a]	51.4

a: Diesel equivalent fuel consumption

Table 2-5: Comparative result with field measurement for a CNG tractor-trailer truck

Method	Hill Climb Provincial Highway	Flat Provincial Highway	Local Drayage	Near Dock Drayage	Regional Highway
Current model: CO_2 (kg/100 km)	105.3	83.3	165.0	150.1	97.4
Field measurement: CO_2 (kg/100 km) [84]	131.0	82.5	164.7	150	96.75
Discrepancy %	19.6%	-1.0%	-0.2%	-0.1%	-0.7%

CO_2 emissions data from another study [84] were also used for benchmarking the current model. Table 2-5 displays this comparison for a CNG tractor-trailer truck with total mass of 30844 kg for the Hill Climb Provincial Highway (HCPH), Flat Provincial Highway, Local Drayage, Near Dock Drayage, and Regional Highway drive cycles. Beside total mass, other input parameters were implemented according to the CNG baseline parameters in Table 2-3. The result of benchmarking with field experiment data was found satisfactory for all routes except for the HCPH route where the model indicates 19.6% less CO_2 emissions.

The discrepancy for the HCPH route could originate from three sources. First, as it was pointed out in the introduction the 11.9 L stoichiometric CNG engine (with φ ratio equal to 1) is not an appropriate engine size for the hill climb cycle and therefore the engine operates most of the time close to the wide open throttle (WOT) points. At these operating conditions the engine burns rich where φ ratio is much higher than 1 [123]. Rich combustion circumstances are equivalent to excessive fuel consumption and CO_2 emission which cannot be captured by Eq. (2-16). Obtaining an appropriate model for φ requires an extensive amount of field measurements which is beyond the scope of current study. Second, the road grade profiles between the selected British Columbia route and the location of the experiment in California is slightly different. Third, as was reported in Quiros et al. [84], the total loaded mass of truck is different from one measurement to another by ± 453 kg, which makes it difficult to compare simulations with field measurements. Overall, the consistent benchmarking results with previous literature gives confidence that the current model is adequate for the current study.

2.3.2 Baseline comparative results

The input parameters for the baseline simulation are described in Table 2-3 under "Baseline parameters" column. Figure 2-8 shows the performance of the diesel and CNG engines in terms of the braking efficiency (overall engine efficiency) versus engine power over all drive cycles. The total loaded mass associated with these simulations were 31,000 kg and 31,866 kg respectively. The differences between average braking efficiency for diesel and CNG engines are in the range of 2.9–6.1% where the lowest corresponds to Local Drayage route and the highest corresponds to Flat Provincial Highway route. Therefore, one can expect a higher CO_2 reduction on the Flat Provincial Highway route that has the highest average speed; there is lower gap in average braking efficiency between diesel and CNG for this route.

Figure 2-9 presents comparative assessments of CNG and diesel tractor-trailer heavy-duty trucks under all drive cycles in terms of cumulative CO_2 emissions and cumulative energy consumption. These analyses were performed for the heavy weight class. The figure indicates how cumulative energy consumption and CO_2 emissions vary by alterations in vehicle speed and road grade profile. It is noticeable that in all drive cycles energy consumption for the CNG engine is higher than the diesel one, while the CO_2 emissions for CNG engine is less than diesel. This is because natural gas has 32% less carbon than diesel fuel per heating unit; however, due to the efficiency gap, the natural gas drivetrain consumes more energy than the diesel one.

Comparing the simulation speed profile with initial input speed profile (Figure 2-10 - Hill Climb Provincial Highway), one can discern that the time to complete the route is extended by more than 400 s. This time extension occurs when the engine torque is beyond maximum torque limit of the vehicle. Therefore, vehicle speed is re-calculated and the time to complete the trip is re-estimated. These additional times are found to be 445 s and 485 s for diesel and CNG drivetrains respectively. For other routes, these time delays are determined to be less than 10 s. The difference between time delays of diesel and CNG drivetrains is coming from the fact that CNG has a heavier drivetrain than diesel, and corresponds to an increase in truck energy demand.

Table 2-6 presents a summary of baseline simulation results in terms of fuel consumption, CO_2 emissions, and re-generable energy for both heavy and medium weight category under all drive cycles. It is evident that the heavy weight class can gain slightly more climate benefit by switching to natural gas compared to the medium weight class. The re-generable energy is the amount of wasted energy produced through braking or deceleration events. The re-generable energy is slightly higher for a CNG drivetrain as it is heavier than diesel. The Urban Arterial cycle has the most re-generable energy since the cycle has more kinetic intensities due to the many acceleration and deceleration events.

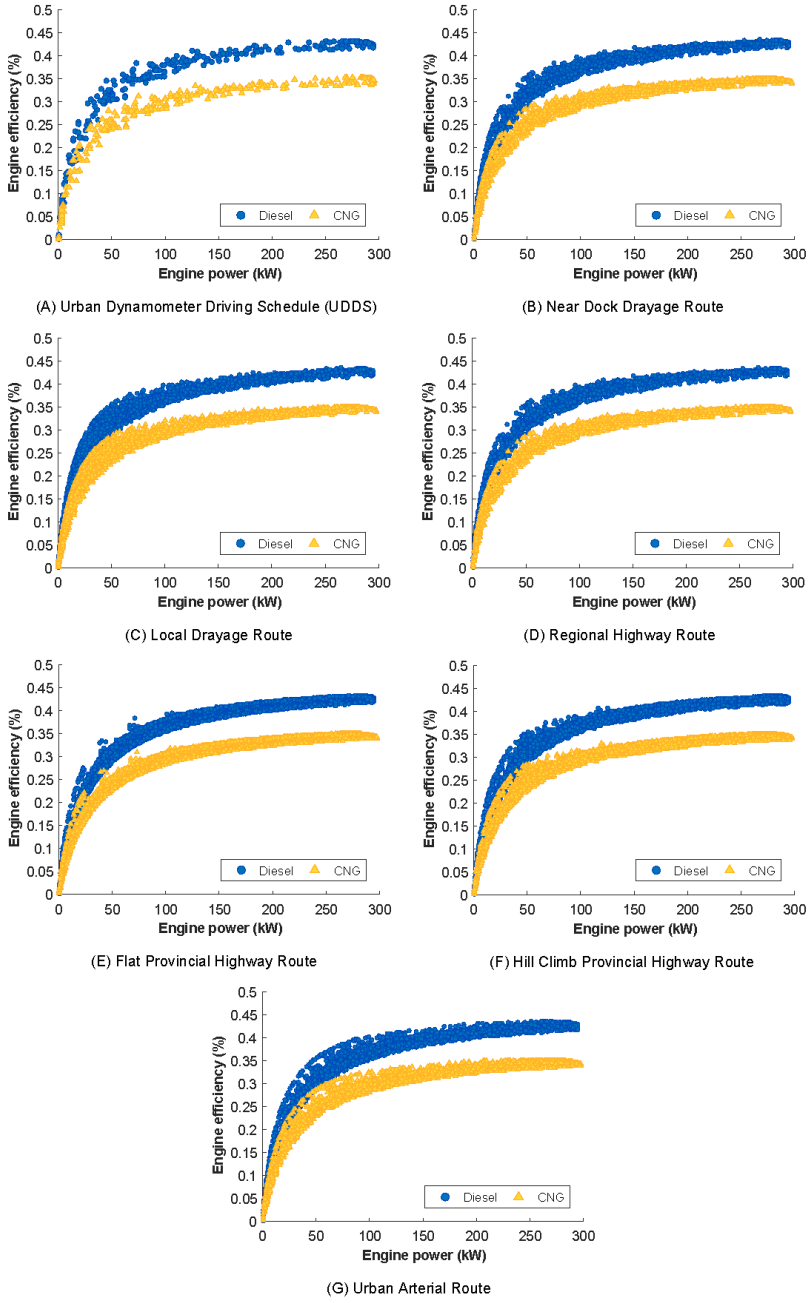

Figure 2-8: Comparison of engine operating points for diesel and CNG engines over all drive cycles

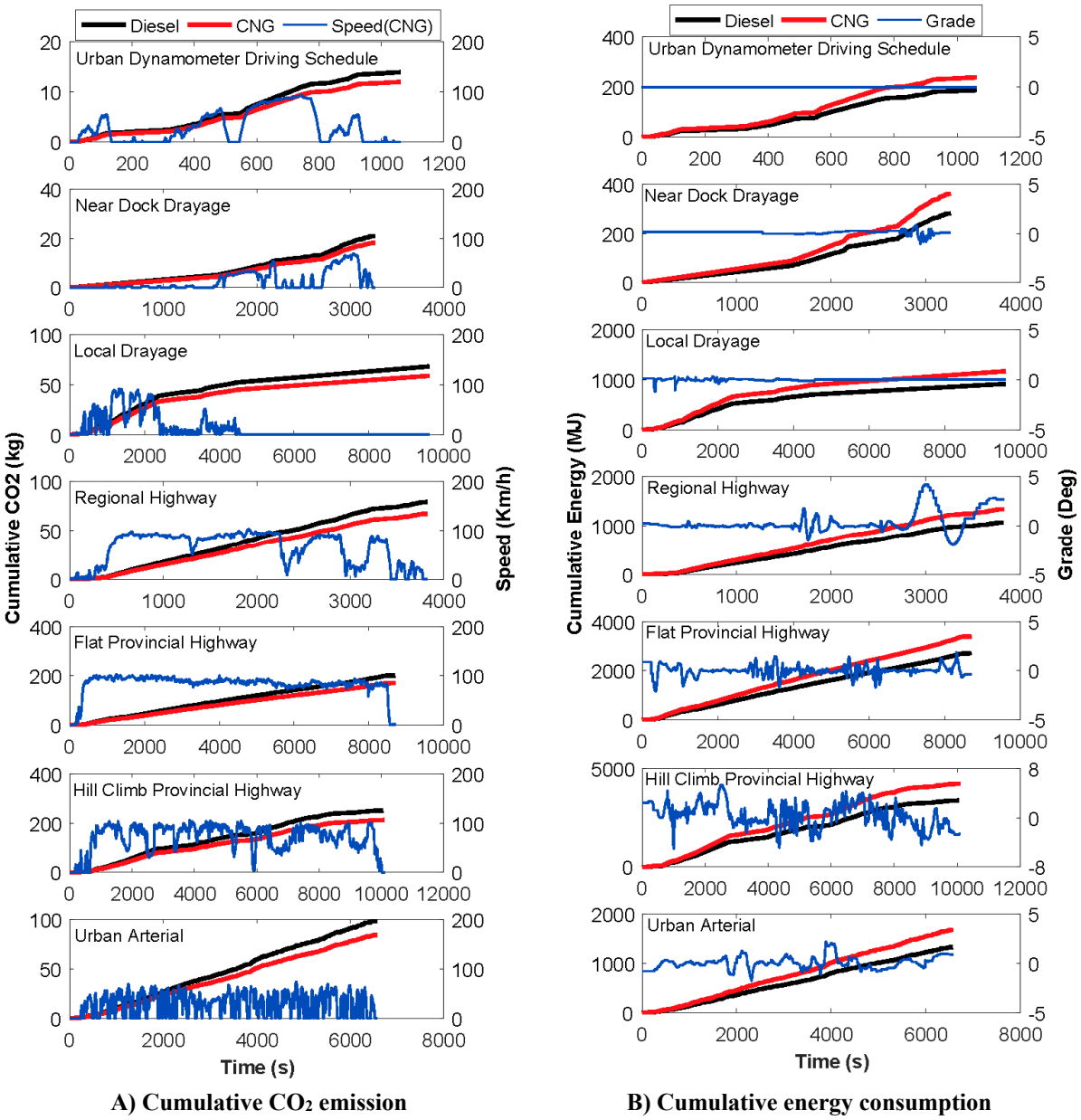

Figure 2-9: Comparison the performance of heavy weight class diesel and CNG trucks over all drive cycles

Since most of the roads in British Columbia are associated with steep road grades, it is important to understand the impact of road grade profiles on the fuel consumption and CO_2 emissions. Therefore, a set of experiments were conducted for the heavy weight baseline simulation: 1-drive cycles with grade profile (w/) and 2-drive cycles without grade profile (w/o). Figure 2-10 demonstrates the result of this experiment. The graph indicates the importance of considering grade factor into simulation that can increase the fuel consumption and CO_2

emissions by up to 24% for both CNG and diesel drivetrains. As expected, a significant difference was found for the Hill Climb Provincial Highway route that includes many steep gradients. The lowest impacts are from Local Drayage and Near Dock Drayage that are associated with relatively flat terrain.

Table 2-6: Summary result of fuel efficiency and CO_2 emission for each cycle based on two weight classes of diesel and CNG heavy-duty trucks

Fuel	Driving cycles	Urban Dynamometer Driving Schedule (UDDS)	Hill Climb Provincial Highway (HCPH)	Flat Provincial Highway (FPH)	Local Drayage (LD)	Near Dock Drayage (NDD)	Regional Highway (RH)	Urban Arterial (UA)
Diesel 31,000 kg	Fuel consumption (L/100km)	58.0	46.8	37.0	71.8	65.0	43.2	68.1
	CO_2 (kg/100km)	156.2	125.9	99.5	193.5	175.0	116.3	183.5
	Regenerable energy (kWh/100km)	103.7	60.2	71.9	80.4	51.2	40.8	134.2
CNG 31,866 kg	Fuel consumption [a] (L/100km)	73.8	58.6	46.3	91.6	83.4	54.2	86.1
	CO_2 (kg/100 km)	134.3	106.7	84.3	166.8	151.9	98.8	156.7
	Regenerable energy (kWh/100km)	106.8	62.4	74.9	83.0	52.8	42.3	138.2
	L/100km increase compared to diesel%	27.2%	25.4%	25.3%	27.5%	28.4%	25.6%	26.3%
	CO_2 reduction compared to diesel%	14.0%	15.2%	15.3%	13.8%	13.2%	15.1%	14.6%
Diesel 22,000 kg	Fuel consumption (L/100km)	50.5	40.0	32.5	63.9	57.9	37.4	56.6
	CO_2 (kg/100km)	136.1	107.8	87.5	172.0	155.8	100.8	152.3
	Regenerable energy (kWh/100km)	71.1	37.9	42.0	54.0	34.3	26.4	92.3
CNG 22,866 kg	Fuel consumption [a] (L/100km)	64.7	50.5	41.0	82.1	74.8	47.4	72.6
	CO_2 (kg/100 km)	117.9	92.0	74.7	149.5	136.2	86.3	132.3
	Regenerable energy (kWh/100km)	74.2	40.0	44.7	56.5	35.9	27.7	96.3
	L/100km increase compared to diesel %	28.0%	26.2%	26.4%	28.5%	29.3%	26.7%	28.4%
	CO_2 reduction compared to diesel %	13.4%	14.7%	14.6%	13.1%	12.6%	14.3%	13.1%

a: Diesel equivalent fuel consumption

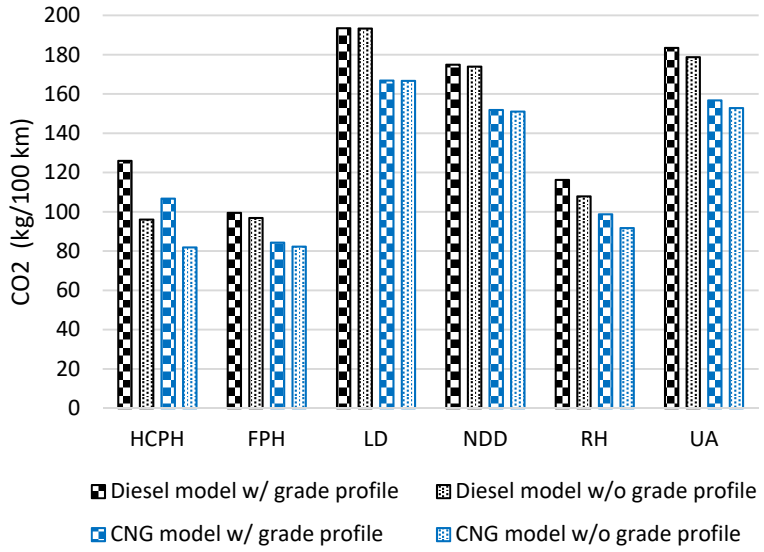

Figure 2-10: Impact of grade profile on CO_2 emissions for various drive cycle

2.3.3 Sensitivity analysis

A sensitivity analysis was used to assess the impact of key simulation parameters on CO_2 emissions predictions for every drive cycle, to account for model and input data uncertainties. These key input parameters are aerodynamic drag-area factor ($C_D \times A_f$), rolling friction coefficient (C_{r0}), constant coefficient of engine friction factor (K_0), loaded mass of the vehicle (M), indicated thermal efficiency (η_i), and vehicle accessory power (P_{acc}). Note that all of the key parameters were varied to improve performance and decreased CO_2 emissions, except for accessory loads which were increased to ascertain the associated increased emissions.

The DOE SuperTruck program demonstrated a 40–50% reduction in drag coefficient is possible in respect to the baseline estimate of 2010 [64]. Changing the location of the engine from the front to the rear of the tractor and bringing the windshield and driver forward allow enhancement of the vehicle body aerodynamics. Removing mirrors, reducing the gap between tractor and trailer, adding a steep slope-windscreen, roof fairing, a low ride height bumper, drive wheel skirt, trailer skirt, and trailer boat tail are also further aerodynamic enhancement technologies [64], [120].

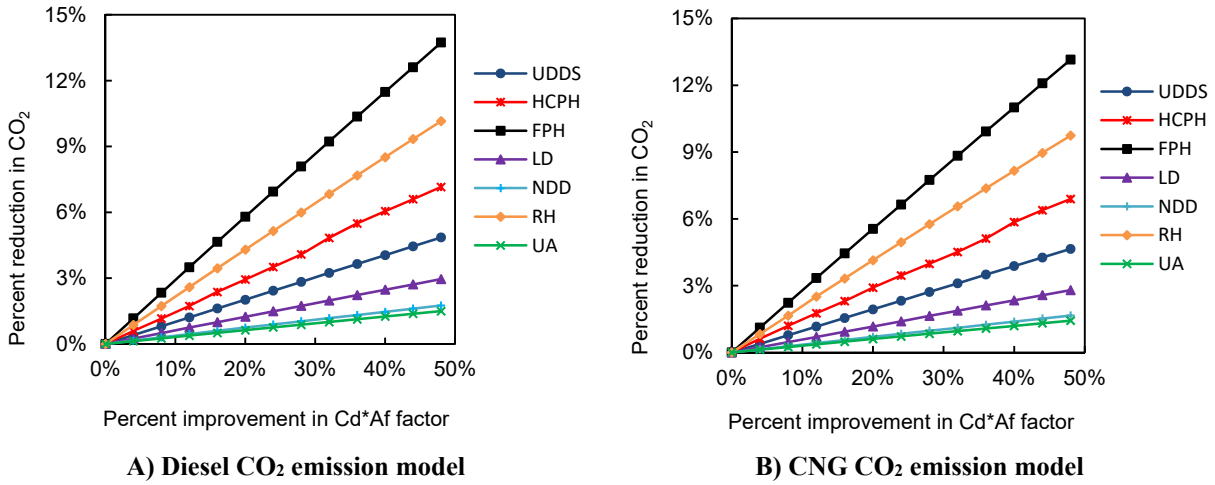

Figure 2-11: Sensitivity of CO_2 emission model on each driving cycle to the variation of aerodynamic factor, $C_D \times A_f$, for Diesel and CNG heavy-duty trucks

Figure 2-11 demonstrates how the improvement in aerodynamic drag-area factor ($C_D \times A_f$) can reduce CO_2 emissions of diesel and CNG powertrains for all driving cycles. These graphs indicate that aerodynamic improvements strategies seem more promising for FPH and RH routes because they are associated with higher vehicle speeds. On the other hand, adopting aerodynamic improvement strategies does not seem to be significant for UA, NDD, and LD routes since they are associated with slow average speeds. In addition, aerodynamic improvement strategies is slightly more important for diesel powertrains as they are lighter with lower tractive power, which leads to further CO_2 reductions compared to the CNG powertrain.

Tire friction can be reduced by using low resistance tires, single wide tires, and applying tire monitoring devices. It is possible to reduce the tire rolling friction coefficient from 0.007 to 0.005 (28% reduction) [57]. Figure 2-12 displays the sensitivity of the CO_2 emission model to the reduction of zero order rolling friction coefficient, Cr0, for diesel and CNG powertrains under all drive cycles. Similar to the aerodynamic factor, applying low resistance technologies brings a great impact on FPH and RH routes, which are associated with higher average speeds. However, unlike the drag-area factor, tire technology improvements have a lower impact on CO_2 reduction for all cycles and they are less divergent. This can be explained by the fact that rolling friction load is not as significant as aerodynamic load.

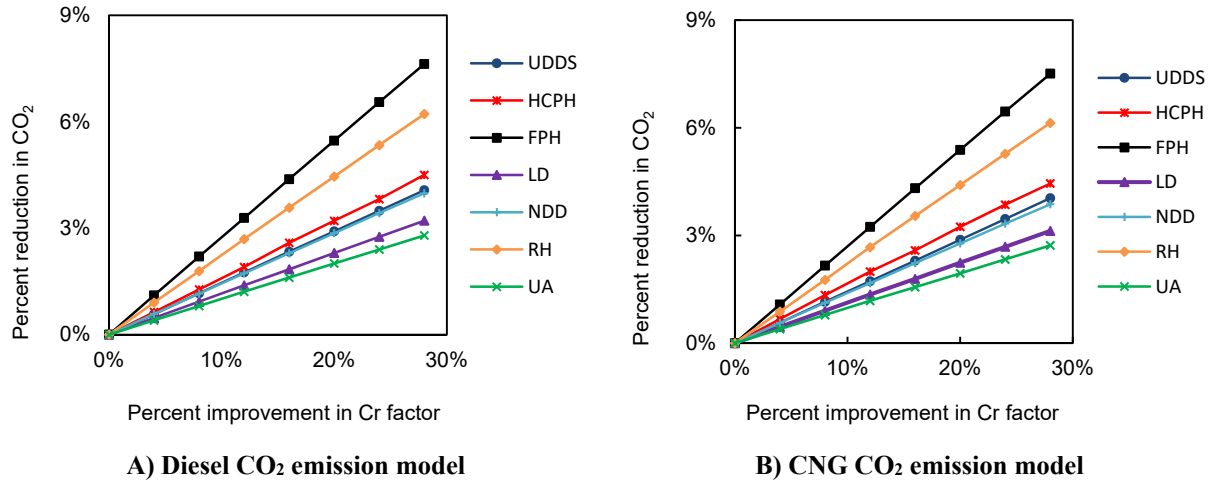

A) Diesel CO_2 emission model **B) CNG CO_2 emission model**

Figure 2-12: Sensitivity of CO_2 emission model on each driving cycle to the variation of rolling friction coefficient, Cr, for Diesel and CNG heavy-duty trucks

In general, low viscosity lubricant offers a fuel saving of 3–5% [121]. Applying low friction coatings on cylinder surfaces and using variable speed water and oil pumps can also bring further positive fuel saving effects [64]. Furthermore, Cummins has proposed several strategies such as reducing shaft seal friction, a variable- flow lubrication pump, reducing the power of coolant and fuel pump, and finally reducing the gear train friction will result in 30% reduction of engine friction wasted energy. Therefore, a 32% reduction of engine friction was considered to be attainable in the near future. Figure 2-13 shows the sensitivity of the constant coefficient of engine friction factor K_0 on CO_2 emissions for diesel and CNG powertrains under all driving cycles. As can be seen from this figure, NDD and LD are best-suited routes for reducing CO_2 emissions by improving engine friction factor. On the other hand, FPH and HCPH are the least important routes in terms of the engine friction improvement. Overall, the reduction benefits for CO_2 emissions because of the improvement in engine friction are slightly higher for CNG engine than diesel. This could be justifiable from the fact that CNG engine has 25% higher friction than diesel and thus the model is more sensitive to reduction of engine friction for this drivetrain.

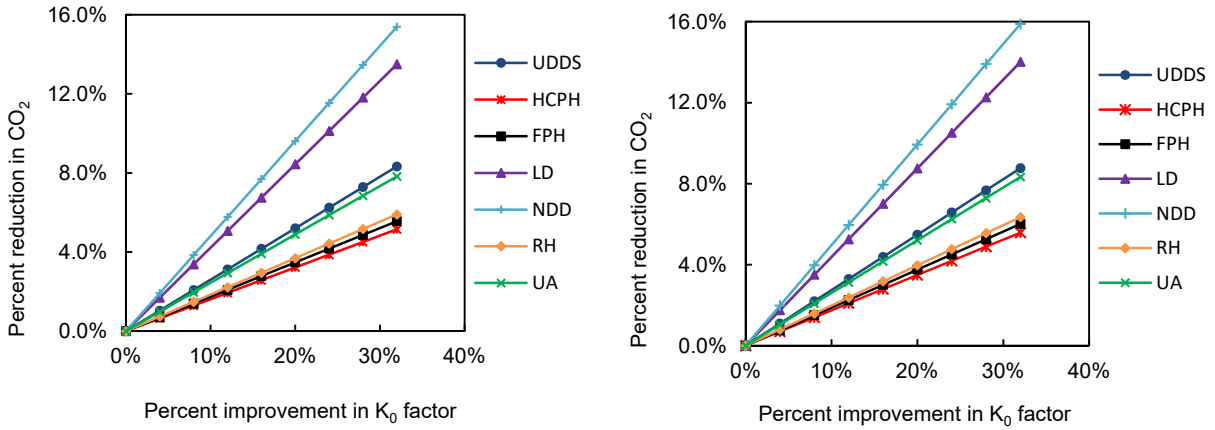

A) Diesel CO_2 emission model **B) CNG CO_2 emission model**

Figure 2-13: Sensitivity of CO_2 emission model in each driving cycle to the variation of engine friction coefficient, K_0, for Diesel and CNG heavy-duty trucks

Mass (weight) reduction is another CO_2 emissions reduction strategy that has two physical impacts including decreasing rolling friction and acceleration loads. A total mass reduction of around 1400 kg (4.5% of 31,000 kg) is possible in the near future through applying low weight materials like aluminum alloys in the tractor-trailer structure [122]. This amount of mass reduction translates to an approximately 2% reduction in CO_2 emissions for all driving cycles and powertrain options. Generally, a total mass reduction of 3700 kg (12% of 31,000 kg) is achievable in 2040 compared to the 2010 baseline through using advanced low weight materials like aluminum alloys, carbon fiber, and polymer composites in the structure of tractor-trailer [124].

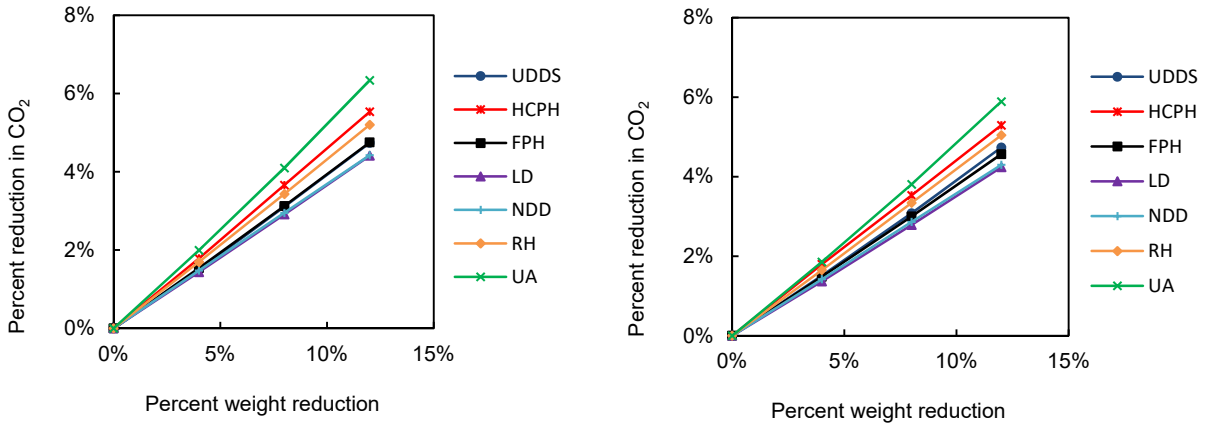

A) Diesel CO_2 emission model **B) CNG CO_2 emission model**

Figure 2-14: Sensitivity of CO_2 emission model in each driving cycle to the variation of total loaded weight of vehicle for Diesel and CNG heavy-duty trucks

Figure 2-14(A) indicates CO_2 emissions reduction in the range of 4.4–6.3% can be reached if the loaded mass of diesel tractor-trailer truck is dropped from 31,000 kg to 27,280 kg (12% reduction, assuming the payload remains constant). Likewise, Figure 2-14(B) shows that if the loaded mass of a CNG tractor-trailer truck is decreased from 31,866 kg to 28,042 kg (12% reduction), CO_2 emissions reduction in the range of 4.2–5.9% is available. NDD and LD gain the smallest amount of benefit for mass reduction, since these cycles are associated with creeping at slow speed. Furthermore, a drive cycle with higher acceleration events (kinetic intensities) like UA can take more advantage of mass reduction strategies than other cycles.

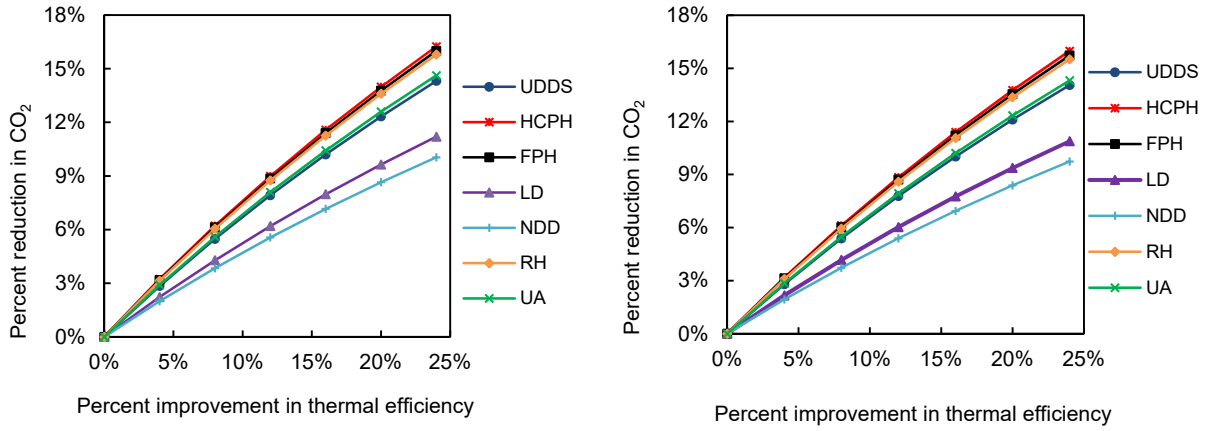

Figure 2-15: Sensitivity of CO_2 emission model in each driving cycle to the engine thermal efficiency for Diesel and CNG heavy-duty trucks

Cummins in the SuperTruck program demonstrated that a 22% increase in maximum braking efficiency (overall engine efficiency) is realistic with respect to the baseline year through improvement of engine waste heat recovery, combustion, after-treatment, pumping, and friction reductions [120]. Therefore, it was assumed a 24% increase in the indicated thermal efficiency is attainable through energy recovery and combustion improvements as well as increase in compression ratio. Figure 2-15(A) shows that if indicated thermal efficiency of the diesel powertrain is increased from 47% to 58.3%, a CO_2 emissions reduction in the range of 10–16.2% is achievable. The lowest benefit is for the NDD route and the highest is for HCPH route. Figure 2-15(B) illustrates a similar trend where CO_2 emissions reductions in the range of 9.7–16% is attainable by enhancing CNG powertrain efficiency from 38.5% to 47%. For both CNG and diesel powertrains, LD and NDD are the least sensitive to increasing indicated thermal

efficiency. This result is related to the fact that these cycles are associated with lower average speed and increased idling time.

The accessory loads can be varied depending on the driving cycle. In this study, a constant magnitude for the accessory loads was assumed. However, the aim was to demonstrate how CO_2 emissions could be affected by increase in accessory load. Figure 2-16 shows how sensitive diesel and CNG drivetrains on each route are to an increase in accessory loads by as much as 190%. Among all cycles, NDD and LD are more affected by increase in accessory load due to the higher amount of idling time linked to these cycles.

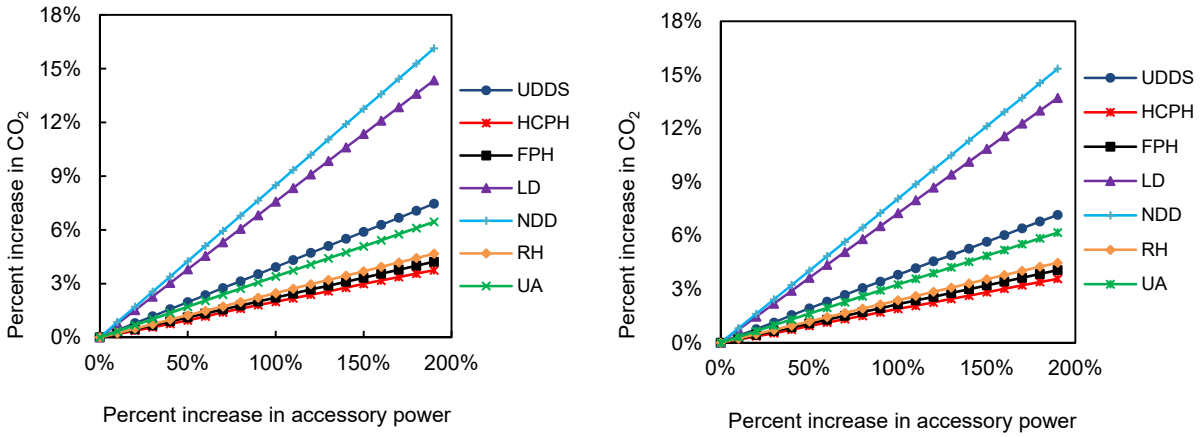

A) Diesel CO_2 emission model **B) CNG CO_2 emission model**

Figure 2-16: Sensitivity of CO_2 emission model in each driving cycle to the accessory power for Diesel and CNG heavy-duty trucks

The baseline results were found very consistent with previous investigations [31], [84]. However, it was difficult to benchmark the results of the sensitivity analysis, as there are not any similar studies that incorporated all the parameters and drive cycles used in this study for both CNG and diesel drivetrains. Nonetheless, the sensitivity analyses for diesel drivetrains are quite comparable with sensitivity results in Zhao et al. [57]. For example, they showed a 22% improvement in aerodynamic drag coefficient is equivalent to 1–9% fuel savings for a diesel drivetrain depending whether the cycle is port, day, or highway, while this study demonstrates a 24% improvement of the coefficient leads to 0.8–7% reduction in CO_2 emissions. Comparing aerodynamic drag and other parameters such as rolling friction, weight, and engine efficiency between two studies, one can notice that Zhao et al. [57] found slightly higher fuel saving potential compared to this study. One explanation for this discrepancy is that the road gradient

was neglected in Zhao et al. [57]. Therefore, the total tractive powers per unit distance was lower, making the energy consumption more sensitive to vehicular parameter improvements.

Although cost was not in the scope of this study, it is worthwhile to mention the incremental costs related to the technology improvements. Table 2-7 presents an estimation of cost and expected improvements in fuel efficiency for various advanced technologies discussed in this section, taken from [125]. It is evident from this table that those strategies related to weight reduction and engine efficiency improvements are more expensive than other technologies as they require a significant amount of research and development. Furthermore, the least expensive one is the low friction lubricant that emphasizes the advantage of these strategies for cycles with slower average speeds such as NDD and LD.

Table 2-7: Incremental cost and fuel efficiency improvement by various advanced technologies [125]

Vehicular parameters	Technology Details	Incremental capital cost (2009 US $)	Improvement in fuel economy
Aerodynamics drag	I: Conventional features	1000	4.6%
	II: SmartWay features	1506	4.2%
	III: Under body airflow, down exhaust, lowered ride height	2675	5.8%
	IV: Skirts, boat tails, nose cone, vortex stabilizer, pneumatic blowing	5500	13.0%
Rolling friction	I: Low rolling resistance tires	194	2.0%
	II: Super single tires	150	5.3%
	III: Single wide tires on trailer	800	3.1%
Weight reduction	I: Aluminum dual tires or super singles	650	1.0%
	II: Weight reduction 15%	6200	3.0%
	III: Weight reduction 20%	11000	3.5%
Engine friction	I: Low friction lubricants	4	0.5%
	II: Variable valve actuation	300	1.0%
	III: Engine friction reduction, improved bearings to allow lower viscosity Oil	250	1.0%
	IV: Improved water, oil, fuel pump; pistons; valve train friction reduction	18	1.5%
Thermal efficiency	I: Improved turbo efficiency	186	1.3%
	II: Improved cylinder head, fuel rail and injector, EGR cooler	31	4.7%
	III: Sequential downsizing/turbocharging	1200	2.5%
	IV: Turbo mechanical compounding	1000	3.9%
	VI: Waste heat recovery, Organic Rankine Cycle (bottoming cycle)	10000	8.0%
	VII: Electric turbo compounding	8000	7.6%
Accessories	Auxiliary power unit	5400	5.8%

2.3.4 Energy efficiency technologies

This section focuses on the cumulative impact of near-term (1–3 years) and long-term (5–15 years) efficiency improvement technologies to reduce CO_2 emissions for CNG and diesel tractor-trailer trucks. These technology improvements are grouped into three separate classes called road load (tractive power) reduction, engine improvement, and engine and road load

improvement together. The presumed amount of advancement for the near-term and the long-term were selected in such a way as to be consistent with achieving the 50% and 100% SuperTruck program targets respectively [120].

Table 2-8 summarizes the near-term efficiency improvement strategies. The near-term road load technologies include supposing aerodynamic improvement by 24%, weight reduction by 6%, reducing tire friction by 14%, and using a 300 W (8% of accessory load) flexible solar photovoltaic system to cover accessory load partly. The near-term engine technologies comprise improvement in indicated efficiency by 12% and reduction of engine friction by 15%.

There are a number of ways to compare technology enhancements for CNG and diesel drivetrains. One way is to compare advanced CNG with advanced diesel. However, since the CNG and diesel engines are considered to be improved alike, it yields a CO_2 emission reduction margin of 13%-15% for CNG over diesel drivetrain, analogous to the trends observed for the baseline technologies (see Table 2-6). An alternative approach is to compare both advanced CNG and diesel technologies to the baseline diesel. This approach seems justifiable as diesel heavy-duty trucks currently are the dominant technology in the market and this study aims to examine how much advanced drivetrains contribute toward the 80% GHG emissions reduction targets of British Columbia. Therefore, the research aims to show with all the engine and road load advantages for CNG and diesel how much CO_2 emissions can be reduced with respect to the currently dominant diesel technology.

Table 2-8: Summary for near-term fuel efficiency strategies

Group	Technology strategy	Powertrains	Urban Dynamometer Driving Schedule (UDDS)	Hill Climb Provincial Highway (HCPH)	Flat Provincial Highway (FPH)	Local Drayage (LD)	Near Dock Drayage (NDD)	Regional Highway (RH)	Urban Arterial (UA)
	Baseline diesel	Baseline Diesel CO_2 (kg/100km)	156.2	125.9	99.5	193.5	175	116.3	183.5
Road loads	1- Aerodynamics 24% 2- Weight reduction 6% 3- Low traction tire 14% 4- Photovoltaic solar power 8% of accessory power	Diesel CO_2 (kg/100km)	145.2	114.9	86.4	182.2	165.1	103.6	173.5
		CO_2 % reduction in respect to baseline Diesel	7.0%	8.8%	13.2%	5.8%	5.7%	10.9%	5.5%
		CNG CO_2 (kg/100km)	125.1	97.7	73.5	157.5	143.6	88.3	148.7
		CO_2 % reduction in respect to baseline Diesel	19.9%	22.5%	26.1%	18.6%	17.9%	24.1%	19.0%
Engine	1- Engine efficiency improvement 12% 2- Engine friction factor 15%	Diesel CO_2 (kg/100km)	137.7	111.6	88.1	169.3	152.6	102.9	161.9
		CO_2 % reduction in respect to baseline Diesel	11.80%	11.40%	11.50%	12.50%	12.80%	11.50%	11.80%
		CNG CO_2 (kg/100km)	118.4	94.5	74.6	145.8	132.4	87.3	138.2
		CO_2 % reduction in respect to baseline Diesel	24.2%	25.0%	25.0%	24.6%	24.3%	24.9%	24.7%
Engine and road loads	1- Engine efficiency improvement 12% 2- Engine friction factor 15% 3-Aerodynamics 24% 4- Weight reduction 6% 5- Low traction tire 14% 6- Photovoltaic solar power 8% of accessory power	Diesel CO_2 (kg/100km)	127.9	101.7	76.4	159.2	143.8	91.5	153
		CO_2 % reduction in respect to baseline Diesel	18.1%	19.2%	23.3%	17.7%	17.8%	21.3%	16.6%
		CNG CO_2 (kg/100km)	110.1	86.4	65	137.5	125	78	131
		CO_2 % reduction in respect to baseline Diesel	29.5%	31.4%	34.7%	28.9%	28.6%	32.9%	28.6%

The near-term road load technologies offer 5.5–13.2% CO_2 reductions for diesel truck and 18–26% CO_2 reductions for CNG truck in respect to the baseline diesel truck. For both powertrains, the most advantages are for Flat Provincial Highway and Regional Highway cycles associated with higher average speeds. Engine technologies have a relatively flat improvement impact of about 12% for diesel truck and around 25% for CNG truck under all drive cycles. When engine technologies and road load technologies are combined together, they can provide further benefit of 16.6–23.3% for diesel powertrain. Interestingly, if road load and engine technologies are combined together with a CNG drivetrain, the CO_2 reduction benefit of the CNG drivetrain in respect to the baseline diesel can surpass the 33% theoretical limit comparing the two input fuel characteristics.

Table 2-9 gives a summary of the comparative assessment for CNG and diesel powertrains for long-term technology improvement strategies. Again, in this table the reduction of CO_2 emissions were evaluated in respect to the baseline diesel. Long-term road load technologies for diesel powertrains suggest 11–26.1% CO_2 reduction while the most advantage

in this class again are related to Flat Provincial Highway and Regional Highway cycles. On the other hand, road load technologies offer 22.4–36.7% CO_2 reductions for the CNG truck. Similarly, a 50.6% reduction in CO_2 emissions is anticipated when engine technologies and road load technologies are combined in a CNG powertrain. Overall, Flat Provincial Highway and Regional Highway cycles seem the most promising in terms of adopting combined engine and road load technologies.

Table 2-9: Summary for long-term fuel efficiency strategies

Group	Technology strategy	Powertrains	Urban Dynamometer Driving Schedule (UDDS)	Hill Climb Provincial Highway (HCPH)	Flat Provincial Highway (FPH)	Local Drayage (LD)	Near Dock Drayage (NDD)	Regional Highway (RH)	Urban Arterial (UA)
	Baseline diesel	Baseline Diesel CO_2 (kg/100km)	156.2	125.9	99.5	193.5	175	116.3	183.5
Road loads	1- Aerodynamics 48% 2- Weight reduction 12% 3- Low traction tire 28% 4- Photovoltaic solar power 16% of accessory power	Diesel CO_2 (kg/100km)	134.1	103.6	73.6	171.1	155.7	91.2	163
		CO_2 % reduction in respect to baseline Diesel	14.1%	17.8%	26.1%	11.6%	11.0%	21.6%	11.2%
		CNG CO_2 (kg/100km)	115.8	88.4	63	148.3	135.8	78.1	140.2
		CO_2 % reduction in respect to baseline Diesel	25.9%	29.8%	36.7%	23.4%	22.4%	32.9%	23.6%
Engine	1- Engine efficiency improvement 24% 2- Engine friction factor 30%	Diesel CO_2 (kg/100km)	121.6	99.4	78.4	147.4	132.1	91.5	143.2
		CO_2 % reduction in respect to baseline Diesel	22.1%	21.1%	21.2%	23.8%	24.5%	21.3%	22.0%
		CNG CO_2 (kg/100km)	104.4	84.1	66.3	126.8	114.5	77.6	122.1
		CO_2 % reduction in respect to baseline Diesel	33.1%	33.2%	33.4%	34.5%	34.6%	33.3%	33.5%
Engine and road loads	1- Engine efficiency improvement 24% 2- Engine friction factor 30% 3-Aerodynamics 48% 4- Weight reduction 12% 5- Low traction tire 28% 6- Photovoltaic solar power 16% of accessory power	Diesel CO_2 (kg/100km)	103.8	81.4	57.5	129.3	116.6	71.2	126.7
		CO_2 % reduction in respect to baseline Diesel	33.5%	35.4%	42.2%	33.2%	33.4%	38.7%	31.0%
		CNG CO_2 (kg/100km)	89.5	69.4	49.2	111.8	101.5	60.9	108.7
		CO_2 % reduction in respect to baseline Diesel	42.7%	44.9%	50.6%	42.2%	42.0%	47.6%	40.7%

2.4 Conclusion

A physical emissions model was developed to understand the on-road CO_2 mitigation benefit of CNG tractor-trailer trucks over diesels. This study simulated six realistic drive cycles based on the grade profile extracted from six selected routes in British Columbia, Canada as case studies. In this regard, a technique was proposed to extract and include grade profile into a speed vs. time cycle when gradient data are not available in a given drive cycle. The applied technique presented in this study is also applicable for other locations around the world. Additionally, the

important role of considering grade profiles into CO_2 emission models was highlighted, an omitted factor in a number of previous drivetrain analysis [27], [34], [57], [93] which include only speed profiles. In particular, it was found that if the elevation profiles of the cycles are omitted from the simulation, the predicted emissions were underestimated by up to the 24% for both CNG and diesel drivetrains. This magnitude for British Columbia with steep grade conditions is almost two times that of the 12.7% that Scora et al. [29] found for some selected route of California, US. Although the grade impacts CNG and diesel drivetrains in a similar way, considering its effect is important for accounting climate emission of road transportation. Therefore, further study requires exploration of the impact of grade on the rest of British Columbia roads.

The difficulty associated with physical emission models is that they rely mainly on input vehicular parameters, which typically have not been fully provided in previous published studies. The other key contribution that can be insightful for future studies was a summary of CNG and diesel heavy-duty trucks specification parameters (see Table 2-3) by carefully scrutinizing relevant sources. Using a realistic set of input parameters, the developed CO_2 emission model of the CNG engine was shown to be reasonable and consistent with previous studies [31], [84]. Theoretically, the CO_2 footprint of burning natural gas per heating unit is around 32% less than diesel fuel [80]. However, on-road CO_2 emissions reductions of CNG trucks were shown to be in the range of 13.2–15.3% for heavy weight class and 12.6–14.7% for medium weight class vehicles. This potential loss is due to the assumption of an 18% indicated thermal efficiency gap between spark ignition CNG and compression ignition diesel technologies. In addition, the higher engine friction factor and heavier weight of CNG versus diesel drivetrains were found be additional weak- nesses of current natural gas drivetrain technology. Still, further investigation of the model parameters and real-time fuel consumption data are required to increase the model certainty under all operating conditions. Specifically, future modeling could explore if the CNG and diesel drivetrains might actually be impacted by grades in different ways, since a 20% discrepancy was found [84] for CNG drivetrains on the Hill Climb Provincial Highway cycle (see Table 2-5).

The sensitivity analysis of every key input parameter revealed the influence of each parameter on CO_2 mitigation over each drive cycle. It was found that improvement in aerodynamic drag-area coefficient, tire rolling resistance coefficient, and indicated thermal

efficiency is highly favorable for all highway cycles (FPH, HCPH, and RH). Moreover, the model was shown to be more sensitive to the weight improvement for cycles with higher amounts of acceleration events or kinetic intensity, like the Urban Arterial cycle. Lastly, engine friction factor and accessory load were found to be more critical for cycles with significant amount of idling time, like Near Dock Drayage and Local Drayage cycles.

Additionally, the results of the sensitivity analyses were found to be consistent with Zhao et al. [57] and NRC investigations [59], [61]. For example, it was shown that a 20% improvement in aerodynamic drag and rolling friction leads to reduction in CO_2 emissions of diesel drivetrains by as much as 5.8% and 5.5% respectively. In contrast, NRC [59], [61] showed similar improvements in aerodynamic drag and rolling friction resulted to fuel consumption reduction of 10% and 4.5% respectively. Results of reduction potential for these two parameters were found to be slightly lower in this study compared Zhao et al. [57]. Overall, the slightly different CO_2 reduction potential can be due to the assumptions of drive cycles and whether they considered the grade into the tractive power estimations.

It was found that when technological improvements are implemented on a future-concept CNG truck, natural gas offers up to 35% and 51% less CO_2 footprint in the near-term and the long-term, respectively, compared to the baseline ("present day") diesel truck. In contrast, the CO_2 reduction benefit of a future-concept diesel truck was found to be as much as 23% and 42% less than baseline diesel in the near-term and the long-term, respectively. Viewed from another perspective, an advanced technology CNG truck would reduce emissions by 13–15% compared to an advanced technology diesel truck. Although some of these technologies, such as thermal efficiency improvements, require an extensive amount of research and development, these results are insightful to inform climate policy and technical development.

Although the on-road CO_2 emissions are the major GHG footprint in the life cycle of a vehicle, further studies into fugitive methane emissions are necessary to expand understanding about the climate benefits (or negative impacts) of CNG truck, since methane is such a potent greenhouse gas. In addition, the accessible re-generative power from each drive cycle that could be captured through an electric motor in a hybrid drivetrain should be assessed. Future studies are focused on extending the model to include alternative drivetrains beyond diesel and natural gas including hybrid, hydrogen fuel cell, and battery electric drivetrains.

Chapter 3

3 Comparing Alternative Heavy-duty Drivetrains based on GHG Emissions, Ownership and Abatement costs: Simulations of Freight Routes in British Columbia

This paper was co-authored with Jonn Axsen and Curran Crawford and published in the volume 76 of Transportation Research Part D: Transport and Environment journal in November, 2019.

S. M. Lajevardi, J. Axsen, and C. Crawford, "Comparing alternative heavy-duty drivetrains based on GHG emissions, ownership and abatement costs: Simulations of freight routes in British Columbia," *Transp. Res. Part D Transp. Environ.*, vol. 76, pp. 19-55, Nov. 2019. Available online at: https://doi.org/10.1016/j.trd.2019.08.031

This chapter presents a comprehensive methodology expanded from chapter 2 to compare 16 different drivetrain technologies for HDTs in terms of well to wheel GHG emissions, ownership cost, and abatement cost. The methodology includes drive cycle development based on several selected route in BC. The technical representations of each technology are used in a vehicle adoption model presented in chapter 4 to simulate the adoption of various zero emissions HDTs under various infrastructure roll out scenarios and zero emissions vehicle (ZEV) mandates.

Abstract: This study quantified the well-to-wheel GHG emissions, total ownership costs and abatement cost for 16 different heavy-duty truck (HDT) drivetrains, including those powered by natural gas, electricity, and hydrogen. Using the case of British Columbia, Canada, we employed GPS activity data for almost 1600 container tractor-trailer trucks to extract six distinct drive cycles. Monte Carlo simulation was used to evaluate the range of uncertainties in several critical model parameters. Results vary widely across drivetrains and across drive cycles. Using hydroelectricity, the battery electric catenary and pure battery electric drivetrains emit the lowest GHG per tonne km on short and long haul cycles respectively. On average over the variety of drive cycles, the plug-in parallel-hybrid diesel has the lowest total ownership cost (including infrastructure costs) for both short and long haul operations. We divided ownership costs by GHG reductions to calculate abatement costs ($/tonne). Plug-in parallel hybrid diesels have the lowest abatement cost, with negative costs on most drive cycles either using diesel or bio-diesel. Comparing drivetrains with their maximum cargo loads, plug-in parallel hybrid fuel cell and conventional diesel have the highest capacity on short and long haul routes respectively. Our analyses can help policymakers, industry and other stakeholders to compare different pathways to reduce GHG emissions in freight, including tradeoffs between the magnitude and cost of emissions reduction. Our conclusion highlights the implications and challenges of drivetrain choice, as well as recommending some areas for further improving the analysis.

Keywords: Heavy-duty truck, alternative drivetrains, well to wheel GHG emissions, total ownership cost, GHG abatement cost, energy consumption

3.1 Introduction

Heavy duty trucks (HDTs) are responsible for about 20% of the transportation-related GHGs emissions in the United States (US) and Canada [12], [126], yet they represent only a minor fraction of on-road vehicles (1% in the US and 1.7% in Canada [12], [127]). HDTs in the European Union (EU) emit more than 30% of the on-road GHG emissions [70]. Freight transportation by HDTs is expected to continue to grow due to population increase, economic growth, change in global supply chain and international manufacturing, increases in online shopping, and the fast delivery expectations of consumers [5]. For example, travel demand by trucks in the US is expected to grow by 80% between 2010 and 2050 [34]. Although efficiency improvements are mandated for future diesel HDTs in the US, EU, and several countries around the world [128]–[130], they appears insufficient for deep GHG emissions reduction. Therefore, substantial changes are needed for decarbonizing HDTs, though to date little progress has been made, in part due to their long distance operation with heavy payloads [2]. There have been some examples of progress; the requirement for cleaner HDTs in container shipping ports near urban areas (e.g. Port of Los Angeles) has initiated a niche market for developing zero and near-zero emissions alternatives for short-haul applications [131], [132].

Promisingly, attention to alternative drivetrains for HDTs has increased in recent years, with Tesla Inc. announcing its futuristic battery-electric truck with an 800 km range on a single charge [42]. Hydrogen fuel cells (FC) have also attracted some attention with Toyota & Kenworth [133], Nikola Motor [52], and US-Hybrid [49] each releasing prototypes of a FC-based HDT with various ranges. Other manufacturers such as Volvo and Scania have invested heavily in hybrid drivetrains and overhead catenary solutions [46], [134]–[136]. Besides switching to alternative drivetrains, lower carbon intensity fuels (e.g. biodiesel) can be effective, as implemented in several locations (e.g. California, British Columbia) as one way to comply with low carbon fuel standards [16].

Considering the wide variety of proposed HDT options, this paper aims to compare the well to wheel (WTW) GHG emissions and total ownership cost (TOC) associated with two conventional HDT drivetrains and 14 alternative drivetrains, each powered by fuel or energy with high and low levels of carbon intensities. WTW GHG emissions refers to upstream fuel production and vehicle operation emissions and as such represent a sub-set of the full life cycle impact, absent vehicle manufacture and recycling [137]. In this study, total ownership cost accounts for costs to

the operator (initial capital purchase and ongoing energy and maintenance costs) as well as costs borne by other businesses (infrastructure costs). Ultimately, this paper aims to quantify the abatement cost of mitigating GHG emissions for various drivetrain options compared to a baseline diesel vehicles during both short and long haul HDTs operations.

There have been many previous studies comparing alternative drivetrains for light duty vehicle and buses using different lenses of energy efficiency, total ownership cost, and WTW GHG emissions (e.g. [138]–[147]). However, there has not been such an effort made on HDTs, which the present study targets. Table 3-1 presents a summary of 14 previous studies related to the GHG reduction potential and associated costs of alternative drivetrains for medium and heavy duty trucks. In the reviewed studies, only Zhao et al. [38] considered 8 drivetrains technologies, while the rest tend not to simulate more than 4 drivetrains at once [31], [36], [65]. In contrast, the present study provides a consistent comparison across 16 drivetrains technologies and a variety of routes.

Table 3-1: A summary of previous study focusing on alterative drivetrains for medium and heavy-duty trucks

Reference	Method (specific model)	Grade	Technologies	Key findings
Sen et al. [36]	Life cycle emission and cost	No	1-Diesel (including biodiesel), 2- BE 3-CNG, and 4-hybrid diesel HDTs	• CNG emits 33% more WTW GHG than conventional diesel. • Life cycle cost of CNG and diesel $1.5 and diesel $1.51 million respectively. • On average the WTW impact of battery electric, diesel, biodiesel, CNG, mild hybrid, full hybrid are 3,900, 4,600, 4,200, 6,100, 4,000, 4,100 ton CO_2 eq, respectively.
Gao et al.[31], [148]	Simulation (Autonomie)	Yes	1- Diesel, 2- SI-CNG, , 3-hybrid SI-CNG, and 4-hybrid diesel HDTs	• CNG emits 5.9-14.6% fewer on-road CO_2 emissions than the baseline diesel. • Hybrid CNG and hybrid diesel emit 20.1-32.4% and 6.8-28.6% respectively fewer on-road CO_2 compared to the baseline diesel. • Payback period for CNG, hybrid diesel, and hybrid CNG in city driving condition are less than 5 years if they are being used for more than 96,000 km a year. • The integration of energy efficiency and parallel hybrid configuration can improve fuel economy of diesel by 60%.
Camuzeaux et al.[80]	LCA (GREET)	No	1- Diesel, 2- CI-LNG, and 3- SI-CNG (including LNG) HDTs	• The negative climate impact of switching to CNG-LNG today (due to methane emissions) remains for 50-90 years before generating a positive climate outcome.
Lajunen [92]	Simulation (Autonomie)	Yes	1- Diesel 2- Hybrid diesel HDTs	• A parallel hybrid with 3.8-25 kWh battery pack can improve fuel consumption by 6%.
Zhao et al.[38], [57]	Simulation (PSAT)	No	1- Diesel (including advanced) an 2- hybrid diesel Zhao et al. , [57]. 1- Diesel, 2- hybrid diesel, 3- SI-LNG, 4-SI-LNG hybrid, 5-CI-LNG, 6- CI-LNG hybrid, 7- BE, and 8-FC HDTs Zhao et al. , [38]	• A parallel hybrid drivetrain can reduce energy consumption by 16% compared to a baseline diesel. • 28-50% fuel consumption reduction is expectable by combination of efficiency improvement technologies and hybrid drivetrain. • CNG, LNG, hybrid, battery electric and fuel cell drivetrains can reduced the well to wheel CO_2 emissions by 12-39% considering natural gas as a primary supply.
Quiros et al. [126]	Field measurement	Yes	1- Diesel, 2- hybrid diesel, and 3- SI-CNG HDTs	• CNG emits up to 15% fewer on-road CO_2 on flat grade routes, while emits up to 12% more emissions on hill climb routes. • Hybrid emits 11-22% fewer GHGs than diesel on route with lower speed; however, it has 20-27% higher GHG emissions on routes with higher average speeds.
Zhou et al.[149]	LCA (GHGenius) and simulation (Autonomie)	No	1- Diesel and 2-BE MDT	• BE emits 85% fewer WTW GHGs than diesel. • BE emits 15% higher GHGs in hot climate and fully loaded conditions. • Life cycle cost of BE including infrastructure cost is $153,000, while it is $144,000 for diesel.
Tong et al.* [65]	LCA (GREET and literature)	No	1- Diesel, 2- hybrid diesel, 3- CI-LNG, and 4- SI-CNG (including LNG) HDTs	• A CNG HDT emits up to 3% more WTW GHGs than a comparable diesel.
Lee et al. [32], [150]	LCA (FASTSim and recorded data)**	No**	1-Diesel and 2-BE MDT Lee et al. , [150]. 1- Diesel and 2- FC MDT and HDT Lee et al. , [32]	• On low average speed cycle, BE emits 42−61% less WTW GHGs than a diesel while the total cost of its ownership becomes 22% less than the diesel. • On high average speed cycle, BE emit 19-43% less GHGs than a diesel while its total cost of ownership is 1% higher than a diesel. • A tractor-trailer FC can improve WTW GHG emissions by 20% and 90% if compressed hydrogen via steam methane reformer of natural gas and solar powered electrolysis respectively are being used.
Zirn et al.[151]	Simulation	Yes	1- Diesel and 2- hybrid diesel HDTs	• Fuel saving of parallel hybrid HDT trucks with 10 kWh battery is up to 15% and specifically is higher on mountain routes. • The fuel saving over the life time is around €25,000 considering diesel price of 1.1 euro/liter.
Lajevardi et al. (2018)	Simulation	Yes	1- Diesel and 2-SI-CNG	• The CNG technology emits 13-15% less on-road CO_2 than baseline diesel. • Applying advanced technologies, a future-concept CNG trucks offers 41-51% less on-road CO_2 emissions compared to a current diesel technology
Present study	Simulation	Yes	**Technologies**: 1- Diesel, 2-SI-CNG, 3-plug-in parallel hybrid diesel, 4-plug-in series hybrid diesel, 5- plug-in parallel hybrid diesel catenary, 6-plug-in series hybrid diesel catenary, 7-plug-in parallel hybrid SI-CNG, 8- plug-in series hybrid SI-CNG, 9- plug-in parallel hybrid SI-CNG catenary, 10- plug-in series hybrid CNG catenary, 11- plug-in series hybrid gas turbine, 12- BE, 13- plug-in series hybrid FC, 14- plug-in parallel hybrid FC HDTs, 15- parallel hybrid FC HDTs (without plug-in), 16- battery electric catenary for short hauls.	

* Tong et al. [65] also considered BE and FC drivetrains for buses and BE for delivery trucks

** Lee et al [32] recently used a combination of Autonomie simulation (with grade) and GREET tool for the LCA analysis

The reviewed literature held no consensus with regard to the GHG emissions reductions and cost benefits of CNG drivetrains. Although the Zhao et al. [38] study found up to a 10% reduction in WTW of long-haul spark-ignition (SI) LNG over a baseline diesel, Tong et al. [65] and Sen et al. [36] indicated 3% and 33% (respectively) higher WTW GHG emissions for the CNG drivetrain compared to the baseline diesel. Camuzeaux et al. [80] estimated that the negative impact of switching to CNG drivetrains today could remain for 90 years before generating a positive impact. Sen et al. [36] also showed that the life cycle cost of CNG is only slightly better than the baseline diesel. On the other hand, Gao et al. [31] and Quiros et al. [126] found on-road CO_2 emissions reductions up to 15% for CNG, but Quiros et al. [126] found that on hilly mountain routes CNG emits 12% more than a comparable diesel. Further, in contrast to Sen et al. [36], Gao et al. [31] found that CNG had cost savings up to $200,000 over its life time, considering 96,000 km per year usage and city driving conditions.

The reviewed studies on HDTs often focused on one or two aspects of alternative drivetrains such as fuel economy [148], energy storage sizing [34], [56], [151], [152], life cycle GHG emissions [65], [80], or sometimes both life cycle cost and emissions [36]. In comparison, the novelty of the present study is to combine energy storage sizing and fuel economy simulation together with life cycle GHG and cost analysis. Several realistic drive cycles (with grade) were used for computing appropriate energy storage sizes for all 16 drivetrains, which is rarely considered in component sizing studies [151]. This study also employed the GPS activity data from 1616 container trucks operating mainly in Metro Vancouver [153] to develop several representative drive cycles for HDTs in BC.

Another uniqueness of the present study is the focus on the Canadian province of British Columbia (BC) as a case study, which along with many regions around the world is targeting 80% GHG emissions reduction for 2050 (below the 2007 levels) and more than 4% of the its overall provincial GHGs arises from HDTs [154]. In the context of BC, Talebian et al. [155] calculated the energy demand for the entire BC freight vehicles to be electrified, considering average fuel economy obtained from a literature review. However, they did not include the impact of energy consumption under real driving conditions and various drivetrains configurations that are the focus of the present study. The authors of the present study [156] previously examined the role of natural gas and advanced diesel in reducing on-road CO_2 emissions of heavy-duty trucks. The objective of the current study is expand that study to explore

and examine additional low-carbon technologies beyond natural gas and advanced diesel drivetrains for heavy-duty trucks to help BC achieving the 2050 GHG targets.

The rest of the paper is presented as follows. Section 3.2 first introduces 16 simulated drivetrains for HDTs and then overviews the various alternative drivetrain technologies in four main groups: natural gas, battery electric, hybrid, and fuel cell. Section 3.3 presents the applied method for drive-cycle development, on-road performance analysis, input parameters, cost estimation, and total GHG emissions accounting. Section 3.4 presents the results including validation, baseline analysis, feasibility discussions, and uncertainty analysis for a long distance trip using a Monte Carlo method. Section 3.5 offers conclusion and proposes several areas for future research.

3.2 Alternative drivetrains for heavy-duty trucks

This section first presents 16 simulated drivetrains that were considered in this study and then reviews natural gas, battery electric, hybrid, and hydrogen fuel cell technologies as the main categories of alternative options for HDTs. Generally, alternative drivetrains can be categorized by fuel type, combustion/energy conversion technology, drivetrain topology (e.g. series, parallel), and connection to the electricity grid (e.g. overhead conductive catenary wires, on-road inductive charging, and DC fast-charging stations). Corresponding to each fuel type (diesel, natural gas, hydrogen, biofuel) and electricity source, there is at least one conversion system for propelling the vehicle. Conversion systems can be conventional combustion engines and hybrid drivetrains, the latter configured into parallel, series, and parallel-series topologies. Currently, available combustion technologies for heavy-duty tractor- trailer trucks are the diesel piston engine with compression ignition technology, (compressed or liquefied) natural gas piston engine with spark ignition, and gas turbines, though the latter due to a lack of required torque only can be used as a range extender unit.

3.2.1 Simulated drivetrains

Figure 3-1 presents various topologies and the main propulsion-related components for all 16 simulated drivetrains. Since the conventional, plug-in parallel hybrid (with and without catenary), and plug-in series hybrid (with and without catenary) drivetrains can be differentiated by whether they use CNG or diesel, the 16 drivetrains were summarized to 10 distinct topologies. Except for the battery electric catenary that was considered only for short haul operation, other drivetrains were considered for both short and long haul operations. The 13 L

Mack diesel engine [157] was used for the conventional diesel, plug-in parallel hybrid diesel, and plug-in parallel hybrid diesel catenary. Likewise, the 11.9 L Cummins Westport CNG engine [114] was considered for the conventional CNG, plug-in parallel hybrid CNG, and plug-in parallel hybrid CNG catenary.

A 10-speed Eaton transmission [110] was assumed for the configurations above, and in the case of parallel hybrids, a 220 kW UQM [158] was used. It was assumed that both the plug-in series hybrid CNG and diesel drivetrains (with and without catenary) have four 220 kWh UQM [158] electric drive systems (on every driver wheel) respectively with a 3.7 L gasoline Ford engine and a 3.2 L diesel Ford engine [159], [160]. Moreover, it was assumed that the plug-in series hybrid gas turbines have a maximum power of 80 kW. Plug-in series and parallel fuel cells as well as battery electric drivetrains were used four 220 kW UQM electric drive motors. Furthermore, the plug-in parallel and series fuel cell drivetrains were assumed to use two and four 60 kW Loop Energy [161] fuel cell systems respectively.

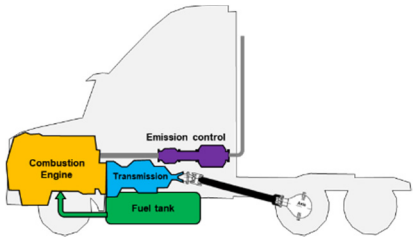

Diesel engine: 13 L Mack MP8 (332 kW) [157] **CNG engine**: 11.9 L Cummins Westport (298 kW) [114], **Transmission**: Eaton 10 speed (gear ratio of 14.8-1) [110]

A) Conventional diesel and CNG

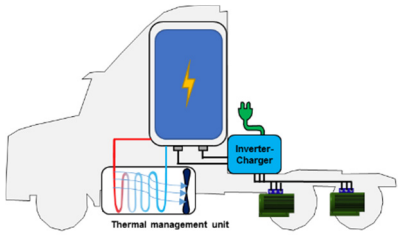

Electric motor: 4*220 kW UQM 3-speeds electric drive system [158]

B) Battery electric drivetrains

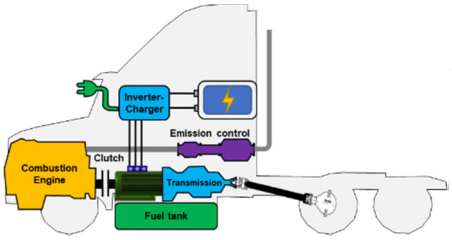

Diesel engine: 13 L Mack MP8 (332 kW) [157] **CNG engine**: 11.9 L Cummins Westport (298 kW) [114], **Transmission**: Eaton 10 speed (gear ratio of 14.8-1) [110], **Electric motor** 220 kW UQM [158]

C) Plug-in parallel hybrid diesel and CNG

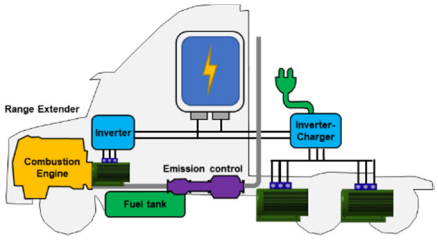

Diesel engine: 3.2 L Ford engine (138 kW), **CNG engine**: 3.7L Ford engine (82 kW) [160], **Gas turbine**: 80 kW, **Electric motor**: 5*220 kW UQM 3-speeds system [158]

D) Plug-in series hybrid diesel, CNG, gas turbine

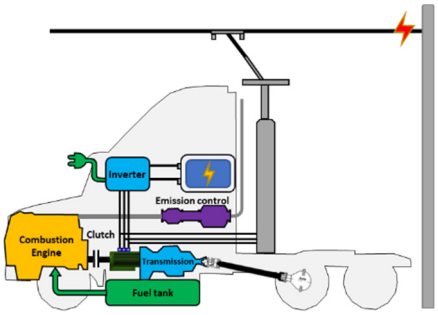

Diesel engine: 13 L Mack MP8 (332 kW) [157] **CNG engine**: 11.9 L Cummins Westport (298 kW) [114], **Transmission**: Eaton 10 speed (gear ratio of 14.8-1) [110], **Electric motor:** 220 kW UQM [158], catenary components

E) Plug-in parallel hybrid Catenary diesel and CNG

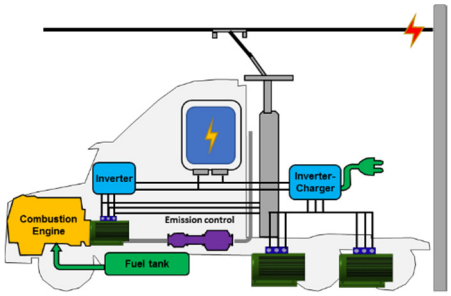

Diesel engine: 3.2 L Ford engine (138 kW), **CNG engine**: 3.7L Ford engine (82 kW) [160], **Electric motor**: 5*220 kW UQM 3-speeds system [158], catenary components

F) Plug-in series hybrid Catenary diesel and CNG

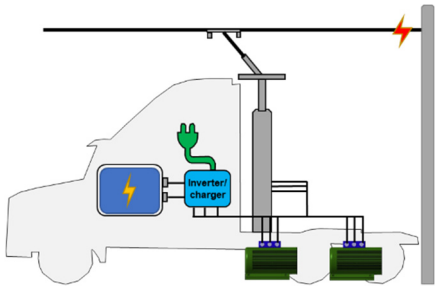

4*220 kW UQM 3-speeds system [158] plus catenary components

G) Battery electric catenary

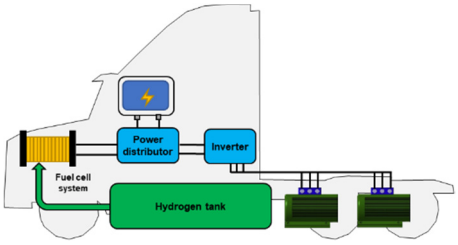

Fuel cell: 6*60 kW Loop Energy [161], **Electric motor**: 4*220 kW UQM 3-speeds system [158]

H) Parallel hybrid fuel cell (without plug-in)

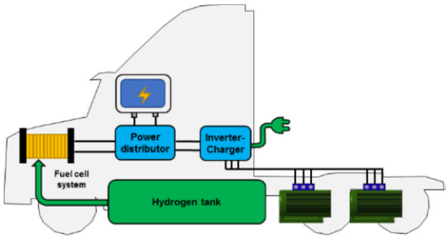

Fuel cell: 4*60 kW Loop Energy [161], **Electric motor**: 4*220 kW UQM 3-speeds system [158]

I) Plug-in parallel hybrid fuel cell

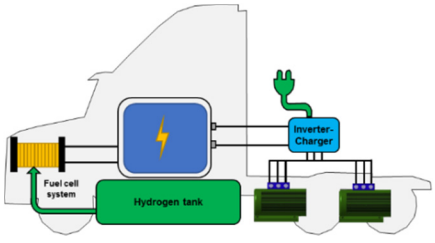

Fuel cell: 2*60 kW Loop Energy [161], **Electric motor**: 4*220 kW UQM 3-speeds system [158]

J) Plug-in series hybrid fuel cell

Figure 3-1: Various drivetrain topology and the main propulsion sub-systems assumed for the on-road performance analysis

3.2.2 Natural gas drivetrains

Natural gas engines are a mature technology and today more than 40% of new refuse trucks and 25% of new transit buses in the U.S. operate on natural gas [162]. Combustion technologies compatible with natural gas include the compression ignition (CI) engine, spark ignition (SI) engine, and micro gas turbine [163], [164]. The CI technology uses 5‑10% diesel per unit of energy input to start a pilot ignition and then natural gas is directly injected into the engine cylinder. This technology, called high-pressure direct-injection (HPDI), can be integrated into an existing diesel engine with minimal modification [165]. The Westport & Cummins 15 ISX G natural gas engine was developed based on this technology [166]. The production of this engine has ceased since 2013 due to market disinterest [167]. However, recently Volvo Group announced the production of a new HPDI engine technology in the near future [45]. This new 13 L engine with a maximum power of 343 kW (460 hp) has similar performance to the retired 15 L Westport and Cummins engine [45]. Currently, the 11.9 L Westport & Cummins SI engine is the only commercially natural gas engine available for tractor-trailer HDTs [114].

3.2.3 Battery electric drivetrains

Various manufacturers have been developing prototype battery electric HDTs suitable for short haul applications (see Table A1 in Appendix A). The main components of a battery electric drivetrain are the battery pack, which consists of individual battery cells, connectors, battery jackets, and thermal management units. The main challenge of battery electric drivetrains is the low energy density of today's battery packs (compared to diesel fuel), which entails a heavy and bulky battery pack for longer travel ranges. Currently, the best lithium-ion battery cell has a power density of 243 Wh kg^{-1}[152]. These battery cells are developed by Panasonic (NCR18650B [168]) and are being used by the Tesla Inc. in their electric vehicles [169].

Another key component of battery electric drivetrains are electric motors to generate propulsive power. There are three types of AC motors that have been considered for electric vehicles including induction, permanent magnet, and switched reluctance machines. Permanent magnet motors are attractive for battery electric vehicles since they offer high power density, high reliability, and high efficiency [170]; BYD and US-hybrid use permanent magnet motors [49], [171].

Other important drivetrain components for battery electric HDTs are the battery management system (BMS), thermal management unit, reduction gears, and an integrated

inverter-charger unit (ICU). The ICU is responsible for converting the DC power to AC to drive electric motors, convert AC grid power to DC during charging, and control charging balance in battery cells to avoid over-charging [172]. The efficiency of an inverter is normally around 95% to 98% [170]. Electric motors have high electrical to mechanical efficiency ranging from 70% to 95% [170] compared to today's diesel engines with maximum motive efficiency of 42% [120]. They can also work as generators during braking events.

3.2.4 Hybrid drivetrains

Several manufactures, including Volvo and Scania, are currently developing hybrid drivetrains for HDTs (see Table A1 in Appendix A). The hybrid technology can be categorized based on various factors including the hybridization degree, topology, and alternative power source [173]. Most commonly, they are classified as series, parallel, and series-parallel. In the parallel configuration, the combustion engine and electric motor are independently connected to the wheels through the transmission system. The combustion engine in a series configuration is only responsible for charging the batteries via a coupled generator, and the electric motor is the sole propulsion source [173]. The parallel hybrid drivetrain has been widely used for hybrid HDTs; it allows the vehicle to use electricity from the battery at lower speeds, while at higher speed the internal combustion engine propels the vehicle through a direct mechanical path. Therefore, the combustion engine works at higher loads where it has a better fuel efficiency. In addition, it enables electrifying the accessory loads and regenerative braking for fuel savings.

The size of the electric motor and battery in parallel designs can be much smaller than for series since the supply of power is shared by two sources and most of the energy demand is fulfilled by the combustion engine. These two factors could reduce significantly the cost and weight of the parallel drivetrain. The fuel efficiency of a series drivetrain is highly dependent on the drive cycle. If the majority of a cycle is occurring on the highway, then double energy conversion from mechanical to electrical and then from electrical to mechanical degrades the overall efficiency. The added weight and cost of the drivetrain due to the larger battery and motor is the important drawback of the series design compared to a parallel. However, the potential for removing heavy components of the powertrain, such as engine, transmission, differential, and drive shaft, could partially offset the added weight of battery and electric motors [57], [173].

Overhead catenaries are a solution pursued by Volvo and Scania in collaboration with Siemens for HDTs to be connected via a conductive system to overhead wires [7], [134]. The catenary solution can be compatible with parallel and series configuration as well as diesel and natural gas engines. This system appears to be a practical near-term option as it is already widely used by trolley buses and trains around the world. However, key actors in transportation sector believe transformation to a catenary option is a 10‑50 year process due to the fact that truck manufacturers would have to change their business model [7]. This requires an intense collaboration between drivetrain manufacturer, power utility company, and road authority. Despite the challenges of a new business model and significant infrastructure costs, road freight transportation using a conductive electrified road system has a chance of success relative to simply increasing battery pack size [174]. Therefore, the technology shift could be slow, starting with niche market such as drayage trucks for hauling cargo from port to local warehouses and then gradually expanded to highway networks [2], [7].

Micro-turbine technology has been proposed as a range extender for battery electric HDTs by the Wrightspeed Company [175] in a series hybrid configuration. Micro-turbines have the advantage of not being sensitive to fuel type and are best suited to generate electricity at constant speed. Other advantages are lighter weight and lower volume than internal combustion engines [173].

3.2.5 Hydrogen fuel cell drivetrains

Hydrogen fuel cells can overcome the low specific energy density of today's lithium-ion batteries that limit the travel range of battery electric HDTs. There are two structures for PEM fuel cell stacks: dead-ended and flow-through anodes. Dry hydrogen supplies the dead-ended structure, but the system needs to be purged more frequently than traditional flow-through anodes to remove the accumulated water and nitrogen [176]. The purging process is an online control strategy dependent on voltage drop and the amount of water accumulated on the anode side, which creates an efficiency loss. Dead-ended anode configurations help to save cost, reduce volume and weight compared to flow-through systems, since they have fewer components [176].

Two possible locations for storing hydrogen (similar to CNG) on-board are the side rail of the tractor and behind the cab. Kast et al., 2017a [56] considered a relatively conservative estimate and found using 350 bar pressure tanks, there is enough space for 78

kg on the rail side and 62 kg behind the cab. Furthermore, they showed in total there is adequate space for 151 kg and 257 kg of hydrogen using 350 bar and 700 bar pressure tanks respectively [56].

There are several obstacles toward deployment of hydrogen for fuel cell HDTs including scarce refueling infrastructure. Furthermore, hydrogen technically is not an alternative fuel since similar to electricity, it is a secondary form of energy. Hydrogen can be generated from various energy sources. Currently, the least expensive way to produce hydrogen is via reforming of fossil natural gas. However, using fossil fuels for generating hydrogen will not mitigate climate emissions. Therefore, hydrogen production with fossil fuel should be combined with carbon capture technology, or alternatively using renewable energy via electrolysis but both increase production costs [177].

3.3 Methodology

Figure 3-2 provides an overall description of the method implemented in this study. First, the GPS data from 1616 HDTs (Input 1) was used to develop 6 distinct drive cycles to represent major freight routes in BC. The elevation data for calculating road grades was paired with GPS data from the U.S. Geological Survey (USGS) database (Input 2).

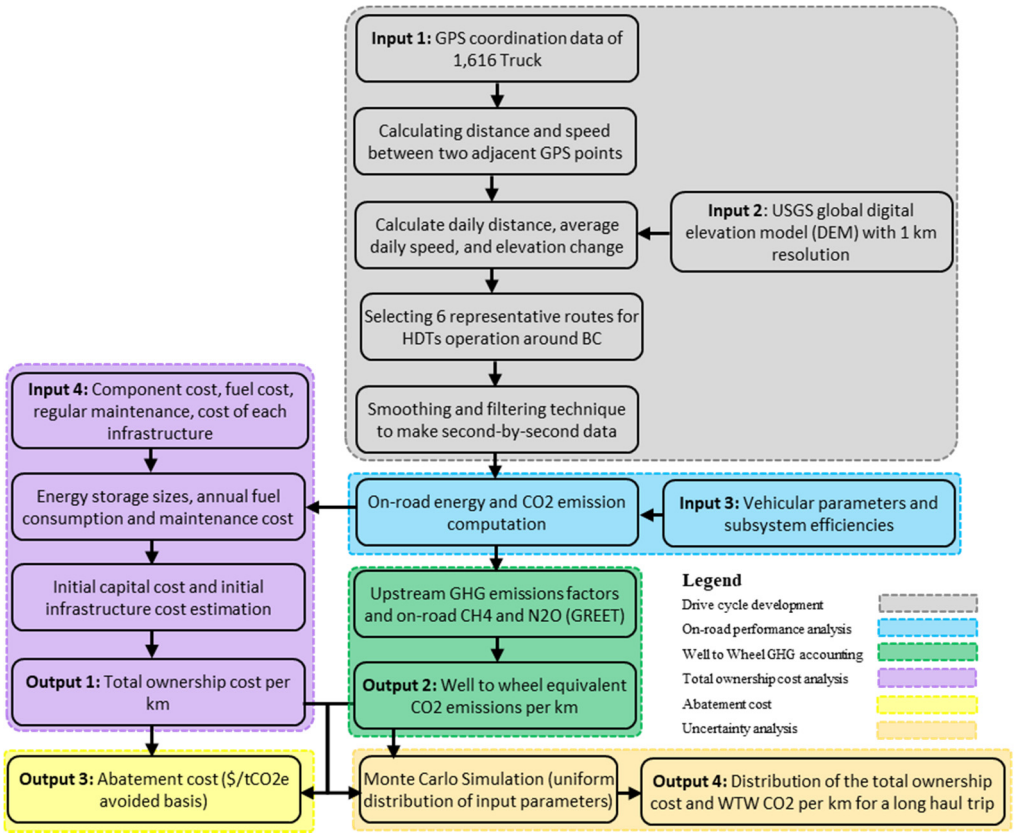

Figure 3-2: Summary of drivetrain study methodology

Next, on-road energy consumption and CO_2 emissions were simulated for 16 drivetrains on the developed cycles considering vehicular parameters (Input 3). Then, based on fuel cost, drivetrain component cost, maintenance cost, infrastructure cost (Input 4), and considering on-road energy consumption, the total ownership cost (Output 1) for all 16 drivetrains on the developed cycles was computed. The WTW GHG emissions (Output 2) are comprised of on-road CO_2, on-road methane (CH_4), on-road nitrous oxide (N_2O), upstream CO_2, upstream CH_4, and upstream N_2O. Furthermore, besides simulated on-road CO_2 emissions, other on-road and up- stream GHGs were estimated using GREET and GHGenius [54], [55]. Finally, a Monte Carlo simulation was conducted for the longest route to determine a projected range of well-to-wheel GHG emissions and costs over the range of uncertainties in several critical model parameters. Although it would be ideal to perform Monte Carlo analysis for all cycles, this study only looked at sensitivity for long haul operation since the main technical barrier of today's battery electric and hydrogen fuel cell drivetrains are long haul operations [34], [56], [152].

Therefore, battery electric catenary drivetrain was not included in Monte Carlo and sensitivity analyses.

3.3.1 Drive cycle development

In our previous study [156], the speed profiles from California HDT data and grade profiles from BC were paired together to generate several prototypical BC drive cycles. The drive cycles in the current study (see Figure 3-6) were developed based on GPS data from November 2016 for an entire fleet of 1,616 drayage[1] container trucks received from Vancouver Fraser Port Authority (VFPA) [153]. VFPA uses the GPS data predominantly to manage truck waiting times at the terminal gates and optimize overall logistical operations. This study utilizes the activity data to account for the energy requirements and on-road CO_2 emissions of tractor-trailer HDTs with conventional and alternative drivetrains.

The goal was to draw 6 samples from the one-month activity data of 1616 trucks that is representative of both short-haul and long-haul operations of HDTs in BC. The main limitation of the GPS data is that it was not recorded at 1 Hz and needed some processing to be converted to a second-by-second format suitable for drivetrain analysis input. Only 5% of the recorded data was at 1 Hz. 71% of the data was recorded at 1 s to one minute intervals. Finally, 24% of the data was recorded at more than one-minute intervals. Since the majority of data was recorded sparsely, the trip trajectories did not exactly match the actual road profiles. Therefore, the actual traveled distances are higher than the estimated distances. This means the actual vehicle speed between any consecutive data points can be higher than the interpolated magnitudes used in this study. Still, these underestimations in the development of cycles does not mean inaccuracy in the study outcomes as the goal was to estimate and compare GHGs emission for various distinct drive cycles on the unit of distance basis. However, the underestimation can be important when the aim is to find the exact amount of fuel consumption between an origin and a destination using these data.

One of the key performance criteria for HD tractor-trailer trucks is the daily range requirement which directly impacts the size of the energy storage on-board the vehicle and associated drivetrain costs. According to the National Renewable Energy Laboratory (NREL)

[1] In the logistic industry drayage refers to the transport of goods for a short distance that is part of a longer distance haul such as transportation of containers from port terminals to local warehouses or intermodal facilities (https://en.wikipedia.org/wiki/Drayage)

that collected 8577 days of data for a total of 287 HDTs all around the US, 90% of daily trip ranges are up to 1000 km [178]. However, only considering the maximum distance each of the 287 trucks traveled during the collection period, the 90% threshold would increase to 1450 km (see Figure 3-3 (A)). Figure 3-3 (B) presents the frequency of maximum daily travel distance for the BC fleet drayage truck data during one month period. It is noticeable that the US fleet is associated with higher travel distances than the drayage fleet in BC, since the US fleet contains trucks from all vocations.

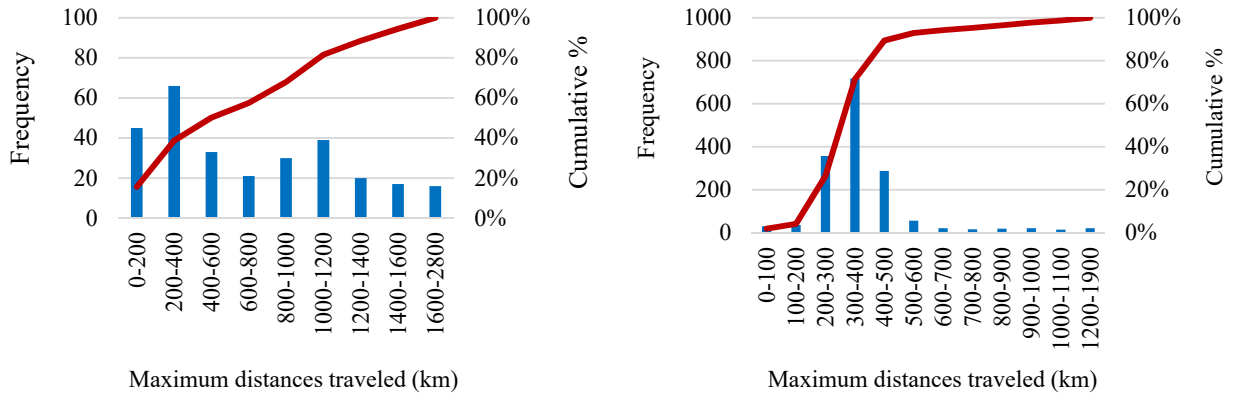

A) 287 HDTs across US (all vocations) **B)** 1598 HDTs BC (Drayage fleet)

Figure 3-3: Frequency of maximum daily distances traveled by 287 HDTs on US roads and 1598 HDTs on BC roads

In order to determine the daily travel distance for the BC truck data, the first step was to calculate the distance between two adjacent GPS coordinate points (d_i) [179]:

$$d_i = 2 \times R \times sin^{-1}\left(\sin^2\left(\frac{\lambda_i - \lambda_{i-1}}{2}\right) + \cos\lambda_i \cos\lambda_{i-1} \sin^2\left(\frac{\phi_i - \phi_{i-1}}{2}\right)\right)^{0.5} \qquad 3\text{-}1$$

where R is the radius of the earth equal to 6378 km, λ is the latitude angle, ϕ is the longitude angle, and index i and i-1 denote two consecutive coordinate points. The sum of all calculated segments gives the total trip distances per day for a truck.

There are other drive cycle related criteria that impact the energy storage size of a vehicle, including road gradient and average speed. Since the gravitational component of the tractive power demand is proportional to the elevation difference in each segment, the sum of the positive elevation differences between two consecutive coordinate points per km was selected as representation of overall gradient. Additionally, average speed is representative of road

congestion, with higher vehicle speeds associated with highway driving and lower speeds associated with congestion and stop and go conditions.

Truck daily activities were categorized by daily travel distance, average speed, and the sum of the positive elevation changes per km (as metrics for grade). The global digital elevation model (DEM) from the U.S. Geological Survey (USGS) [180] with 30" (approximately 1 km) resolution was used to extract elevations of all coordinate data points. Figure 3-4 presents the main characteristic of the drayage fleet in terms of the sum of the positive elevation changes per km, daily travel distances, and average speed. The graph shows how the sum of positive elevation changes, travel range, and average speeds are related. For example, higher daily travel distances are associated with higher average speeds and higher positive elevation changes per km. The average speed based on almost 33,000 daily recorded data was 18.7 km/h with a maximum average speed of 87 km/h. The red line fitted through the scatter data represents the mean value of the data and the red dots are the selected routes for the drive cycle development based on representative characteristics.

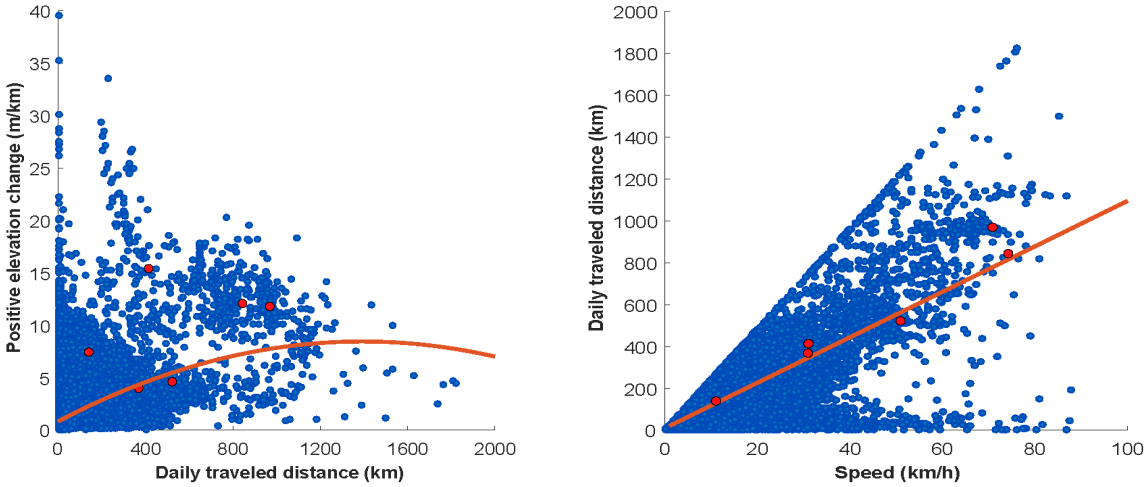

Positive elevation change vs daily travel distance

Daily travel distance vs average speed

Figure 3-4: Relationship of average daily speed, daily travel range, and positive elevation change

A combination of linear interpolation and a smoothing process using a Savitzky-Golay filter were applied in Matlab to create 1 Hz drive cycles and remove unrealistic accelerations and deceleration in the raw data. Table 3-2 demonstrates some of the main characteristics for the generated drive cycles including distance, average speed, kinetic intensity, aerodynamic speed, characteristic acceleration, average acceleration, average deceleration, maximum acceleration,

and maximum deceleration. Methods for calculating kinetic intensity, aerodynamic speed, and characteristic acceleration are provided in [104].

Table 3-2: Main characteristics of the created drive cycles

Drive cycle	Distance (km)	Average speed (km/h)	Kinetic intensity (1/km)	Aerodynamic speed (km/h)	Characteristic acceleration (m/s^2)	Average acceleration (m/s^2)	Average deceleration (m/s^2)	Maximum acceleration (m/s^2)	Maximum deceleration (m/s^2)
Short distance drayage (SDD)	120	10	0.73	33.4	0.06	0.022	-0.028	0.234	-0.286
Long distance drayage (LDD)	349	29.9	0.11	68.1	0.04	0.041	-0.046	0.359	-0.376
Regional Hwy (RH)	394	30	0.17	66.2	0.06	0.038	-0.04	0.295	-0.352
Flat Hwy (FH)	502	49.9	0.05	87.4	0.03	0.023	-0.031	0.321	-0.367
Hill Climb Hwy 1 (HCH1)	824	69.8	0.08	99.2	0.06	0.033	-0.028	0.301	-0.406
Hill Climb Hwy 2 (HCH2)	950	73.2	0.08	90.9	0.05	0.032	-0.034	0.401	-0.36

By comparison, characteristic accelerations from NREL FleetDNA [178] range from 5.02E−05 to 0.87 (m/s^2) with a mean value of 0.03 m/s^2. Additionally, the NREL kinetic intensities vary from 1.19E−04 to 19.06 1/km with a mean value of 0.13 1/km. Comparing the two key parameters from Table 3-2 to FleetDNA calculations [178], it is noticeable that the kinetic intensity and characteristic accelerations obtained in this process are close to the mean values reported in FleetDNA [178]. Therefore, it appears that our generated 1 Hz cycles are appropriate for performance analysis of HDTs, as their magnitudes are consistent with the NREL data.

Figure 3-5 illustrates the GPS track of the 6 selected representative routes of BC and neighboring provinces. The figure also includes several imaginary routes for overhead catenary systems around BC. Two drayage cycles were considered, one with a short distance of 120 km and the other a long distance of 350 km. The flat highway consist of a round trip from Vancouver, Canada to Seattle, US. The two hill climb highway cycles consist of a round trip from Vancouver to Tappen, BC and the other a one-way trip from Calgary to Vancouver. Additionally, the black line in Figure 3-5 depicts the hypothetical Catenary route on the BC Lower Mainland. Finally, the Short Distance Drayage (SDD), Long Distance Drayage (LDD), and Regional Hwy (RH) routes with daily travel ranges below 400 km were assumed representative for short haul freight transportation; Flat Hwy (FH), Hill Climb Hwy 1 (HCH1), and Hill Climb Hwy 2 (HCH2) were long haul trips with daily travel ranges above 500 km.

Figure 3-6 illustrates the speed and grade profiles of the selected routes after conversion to 1-Hz format.

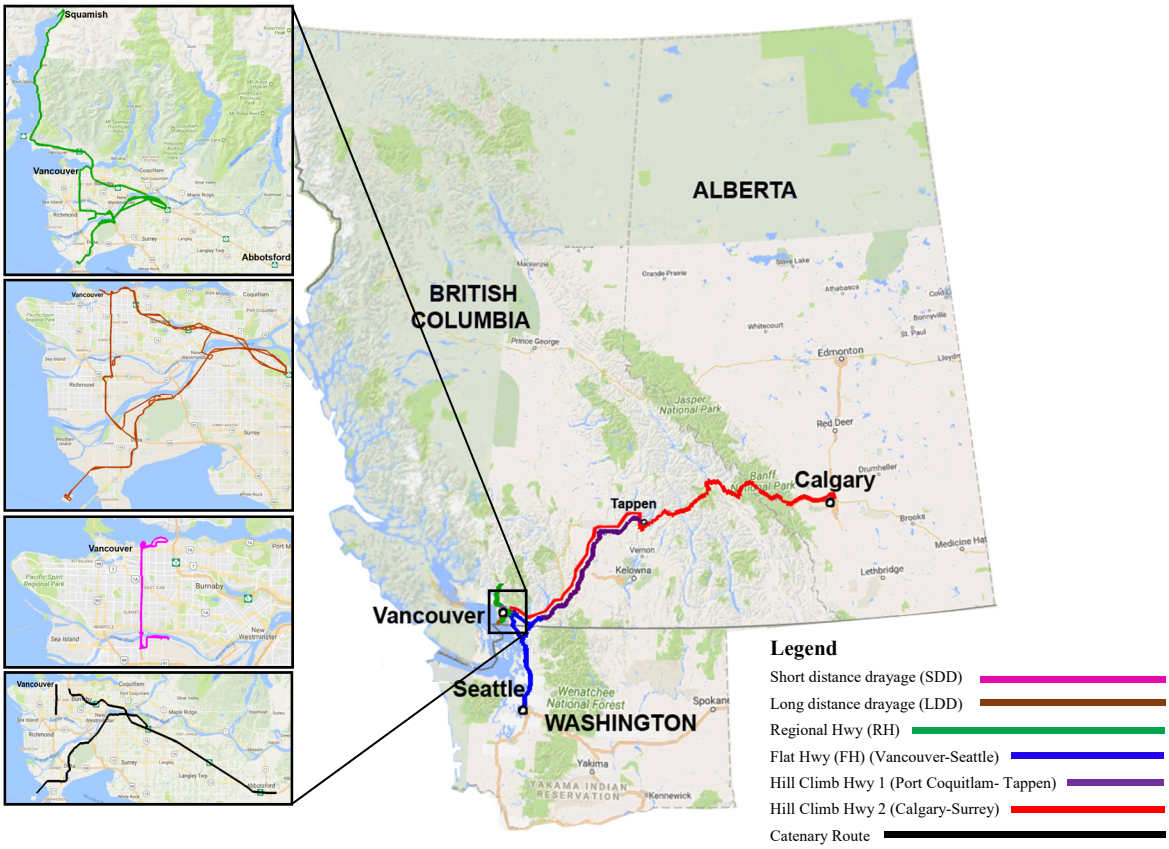

Figure 3-5: Selected routes for HDTs around BC and nearby provinces

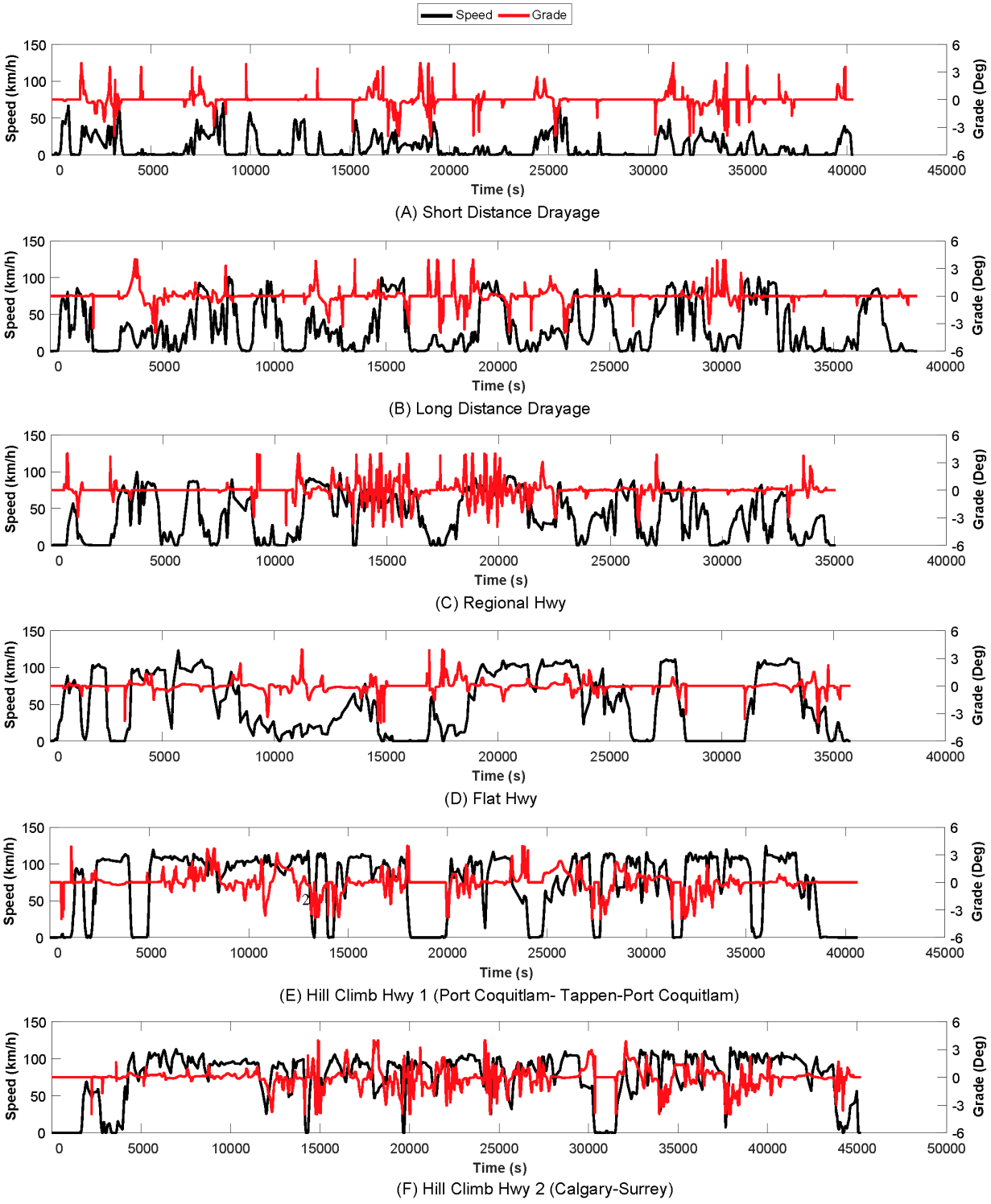

Figure 3-6: Processed speed profiles for the 6 selected routes around BC and nearby provinces

3.3.2 Fuel efficiency and on-road CO_2 emissions analysis

A backward-looking energy consumption model that was developed for vehicle performance analysis of CNG and diesel trucks [156] was extended for this study to include 14 more alternative drivetrains. Additionally, the energy consumption model was improved by estimating the energy storage size for all drivetrains with respect to the associated drive cycle. Figure 3-7 explains the general assessment method for on-road performance analysis.

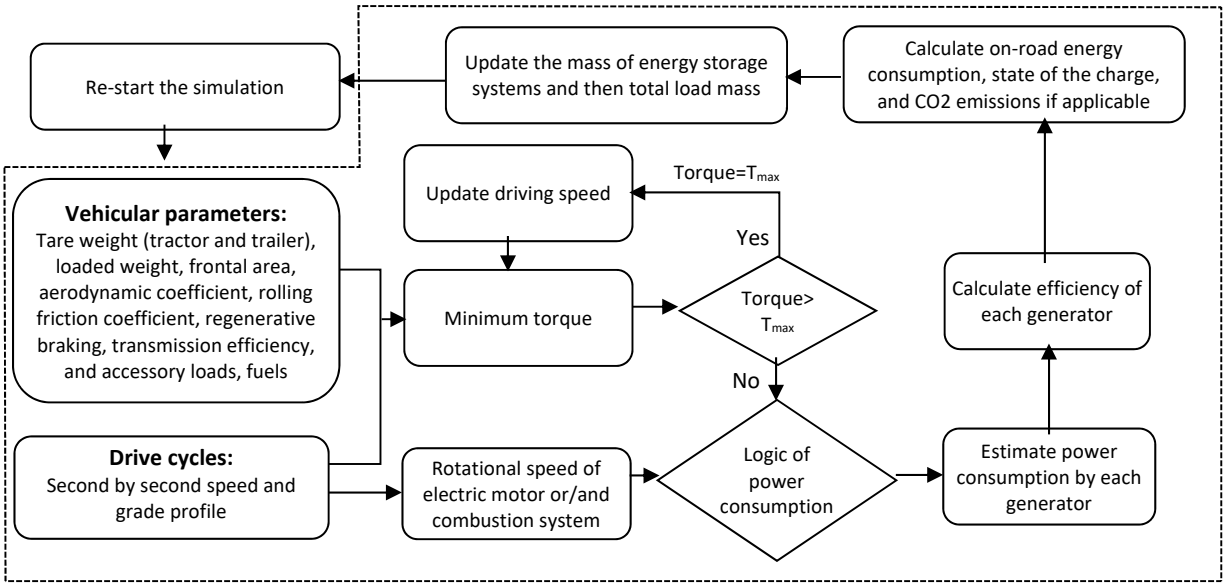

Figure 3-7: General simulation model for HDTs with alternative drivetrains

The tractive force demand (F_{tr}) of the vehicle is the fundamental component for the energy consumption and considers the physical balance of acceleration, gravity, aerodynamics, and rolling friction. The following equation from [156] was used:

$$F_{tr} = \frac{C_D A_f \rho_{air}}{2} v^2 + C_{r0} M g \cos\theta + M[a(1+\varepsilon) + g \sin\theta] \quad 3\text{-}2$$

where M is the total loaded mass (kg) of the vehicle, g is the gravitational acceleration (m/s^2), C_{r0} is the zero order of rolling friction coefficients, is the road grade angle, C_D is the aerodynamic coefficient, A_f is the vehicle frontal area, ρ_{air} is the air density, v is the vehicle speed, ε is a mass correction factor for moving rotary components of the vehicle. The engine power, torque, speed, and fuel consumption for drivetrains with conventional diesel and CNG engines were calculated using the detailed method provided in [156]. The goal of the study was to determine the impact

of drivetrain masses on HDT performance if they all can carry the same mass of 16,050 as an average of cargo mass for HDTs [59]. Although the masses of cargo and trailer were constant for all drivetrains, the total loaded mass varied with drivetrain-related components; Table 3-3 summarizes the equations for total loaded mass. Furthermore, the mass of tractor was assumed 700 kg heavier in long haul operations than short haul (see Table 3-5). Finally, after sizing the energy storage of drivetrains the available cargo mass on each route was determined with considering the gross HDT mass of 62,500 kg consistent with the Canadian limit [181].

Table 3-3: A summary of calculating loaded mass for different drivetrains

Drivetrains	Equation	Equation number
Conventional CNG and diesel	$M = M_{Cargo} + M_{Tractor} + M_{Trailer} + M_{tank} + M_{EC} + M_{emi} + M_{other}$	3-3
Battery electric	$M = M_{Cargo} + M_{Tractor} + M_{Trailer} + M_{battery} + M_{motor} + M_{inv}$	3-4
Plug-in parallel hybrid diesel and CNG	$M = M_{Cargo} + M_{Tractor} + M_{Trailer} + M_{tank} + M_{EC} + M_{emi} + M_{other} + M_{battery} + M_{motor} + M_{inv}$	3-5
Plug-in parallel hybrid diesel and CNG with catenary system	$M = M_{Cargo} + M_{Tractor} + M_{Trailer} + M_{tank} + M_{EC} + M_{emi} + M_{other} + M_{battery} + M_{motor} + M_{inv} + M_{Cat}$	3-6
Plug-in series hybrid diesel and CNG with catenary system	$M = M_{Cargo} + M_{Tractor} + M_{Trailer} + M_{tank} + M_{EC} + M_{battery} + M_{motor} + M_{inv} + M_{Cat}$	3-7
Plug-in parallel and series hybrid fuel cell, series diesel and CNG	$M = M_{Cargo} + M_{Tractor} + M_{Trailer} + M_{tank} + M_{EC} + M_{battery} + M_{motor} + M_{inv}$	3-8

where M_{Cargo}, $M_{Tractor}$, $M_{Trailer}$, M_{tank}, M_{EC}, $M_{battery}$, M_{motor}, M_{emi}, M_{inv}, M_{cat}, M_{other} refer to the mass of cargo, tractor, trailer, fuel tank, combustion engine or fuel cell system, battery, electric motor, emission control system, inverter, catenary component on-board, and other drivetrain related components (such as transmission, drive shaft, and differentials), respectively.

As mentioned, compared to our previous study, the model was improved to account for increased fuel consumption due to the larger fuel storage requirement on-board for longer haul trips. To achieve this, the size of the fuel storage on-board was initially assumed. The fuel consumption and CO_2 emissions were then re-calculated according to the modified mass of the energy storage system. The mass of the fuel tank (M_{tank}) was calculated according to the Eq. (3-9). Furthermore, Eq. (3-10) was used to calculate the mass of the battery pack ($M_{battery}$) from [152].

$$M_{tank} = \frac{M_f}{SM_{tank}} \quad (3\text{-}9)$$

$$M_{battery} = \frac{BS_n}{SM_{battery} \times f_{burden}} \quad (3\text{-}10)$$

where M_f is the mass of consumed CNG, diesel, or hydrogen, SM_{tank} is the specific mass of the fuel system (kg fuel/kg system), BS_n is the updated battery size (see Eq. (3-15)), $SM_{battery}$ is the specific mass of battery cell (Wh/kg), and f_{burden} is the burden of battery pack related to the non-cell component of the battery pack [152].

3.3.2.1 Battery electric and series hybrid

These drivetrains were simulated in a similar way since the electric motor is the main propulsion system. The torque demand (T_M) of the electric motor for battery electric as well as series hybrid drivetrains was calculated as:

$$T_M = \frac{F_{tr} \times R_w}{\eta_T \times G_R} \quad (3\text{-}11)$$

where R_w is the wheel radius (m), η_T is the transmission efficiency, and G_R is the gear ratio. Furthermore, the electric motor rotational speed (N_M) in rpm was calculated as:

$$N_M = \frac{v \times G_R}{R_w}\left(\frac{60}{2\pi}\right)$$
$$G_R = G_F \times G_{R_j} \quad (3\text{-}12)$$

where G_F is the final gear ratio equal to 5, G_{Rj} can be 1 (if $v > 20$ m/s), 1.86 (if 10 m/s $< v <$ 20 m/s), or 3.58 (if $v < 10$ m/s). The required power (P_M) to obtain this amount of torque then obtained from:

$$P_M = \frac{T_M \times N_M}{\eta_M \times \eta_I}\left(\frac{2\pi}{60}\right) \quad (3\text{-}13)$$

where η_M and η_I are the efficiency of the electric motor and the DC-AC inverter respectively. Moreover, the re-generative power (P_{reg}) extractable for negative T_M (stored in battery pack) was determined from:

$$P_{reg} = \frac{F_{tr} \times R_w}{G_R} \times N_M \left(\frac{2\pi}{60}\right) \times \eta_{reg} \times \eta_T \times \eta_M \times \eta_I \quad (3\text{-}14)$$

where η_{reg} is the regenerative efficiency. In respect to all series hybrid drivetrains, a simple logic of energy supply from a corresponding range extender unit was used on each cycle based on

several trial and error simulations, in order to ensure that the state of charge was above 20% during the associated cycles (or only 80% of battery remain usable). Table 3-4 presents normalized time span intervals (on a percentage basis) that each range extender unit is in operation. For example, the 43‑50% interval for the plug-in series hybrid gas turbine on the short distance drayage (SDD) means the gas turbine is in operation during the 7% of the cycle time span before its mid-point.

Table 3-4: Operation intervals for all drivetrains with series hybrid configuration

Drivetrains	SDD	LDD	RH	FH	HCH1	HCH2
Plug-in series hybrid CNG, diesel, gas turbine, fuel cell	95.2-100%	90.9-100%	83.3-100%	50-100%	33.3-100%	33.3-100%
Plug-in series hybrid diesel and diesel Catenary	6.4-7.5%	32.3-37.7% & 51.8-53.3%	62.1-70% & 79.2-87.4%	39.9-61.4%	12.3-71.7%	24.4-53.7% & 63.3-92.2%

The battery pack and fuel tank were sized on each cycle with respect to the energy consumption of the cycle. Eqs. (3-15) and (3-16) were used for estimating the battery and the total fuel consumption; the latter is applicable to series hybrids. The mass of the fuel tank and battery pack systems were calculated according to Eqs. (3-9) and (3-10) respectively. Finally, the simulation were repeated one more time, for each drivetrain and cycle, based on the updated battery and fuel tank sizes.

$$BS_n = BS_o\left(1 - SOC_f\right) \times MF_b \qquad 3\text{-}15$$

$$M_f = \frac{1}{1000}\int_0^T \dot{FR}dt \qquad 3\text{-}16$$

where BS_n is the updated battery size, BS_o is the initial guess for battery size, MF_b is a sizing factor for battery to account for the fact that usable battery capacity is 80% and set 1.25 for all battery electric and series hybrid drivetrains, $\dot{FR}$ in g/s is the flow rate of fuel consumption for conventional CNG and diesel engines as well as gas turbine and fuel cell system, T is the total time span of the cycle, and 1/1000 is the conversion factor to obtain M_f in kg. Furthermore, the following equation were used for simulating the state of charge (SOC) and the total energy consumption of the cycle (EC):

$$SOC(t) = SOC\ (t0) - \frac{1}{3600 \times BS_o}\int_0^t \left(P_M + P_{acc} - P_{reg} - P_{ext}\right)dt \qquad 3\text{-}17$$

$$EC\ (kWh) = \frac{1}{3600}\int_0^T \left(\dot{FR} \times LHV + P_{cat}\right)dt + BS_n\left(SOC\ (t_0) - SOC(T)\right) \qquad 3\text{-}18$$

where $SOC\ (t_0)$ is the initial state of charge and is set to 1 for all battery and series hybrid drivetrains, P_M is the motor power that was supplied by battery, P_{acc} is the accessory power, P_{ext} is the external power from a range extender unit and is zero for battery electric drivetrain, P_{cat} is the power from catenary system and is zero for drivetrains without catenary system, t is time, and (1/3600) conversion factor to obtain EC in kWh.

For fuel cell drivetrains, P_{ext} was obtained as the difference between rated and auxiliary power of the fuel cell system ($P_{max} - P_{aux}$). For the gas turbine drivetrain, P_{ext} was estimated as the product of generator and inverter efficiency ($P_{max} \times \eta_I$). Furthermore, in the series configuration it was assumed the continuous power and torque for both diesel and CNG engines are 10% lower than their maximum rated power. Therefore, P_{ext} was found as a product of engine rated power, electric motor efficiency, transmission efficiency, and inverter efficiency ($0.9 \times P_{max} \times \eta_M \times \eta_T \times \eta_I$). For SOC calculation of series hybrid catenary drivetrain, PM, P_{acc}, and P_{ext} were assumed zero when the truck connected to an overhead grid. Furthermore no battery charging was considered for series hybrid and battery electric catenary drivetrains, which means battery and catenary independently supply power.

3.3.2.2 Parallel hybrid

For all parallel hybrid drivetrains (except for fuel cell) it was assumed the battery supplies power if the braking power requirement is below 20% of the maximum engine braking power limit. Furthermore, if the torque requirement is beyond the maximum engine torque capacity, the battery via the electric motor provides the supplementary torque. For drivetrains with a catenary system, this 20% threshold was applied outside the catenary supply domains that were specified in Figure 3-5. However, it was assumed that when a parallel hybrid diesel or CNG is on a road with catenary system, one electric motor continuously provides a portion of tractive power. If the available catenary power is more than required power, it was assumed the extra power is stored inside the battery pack. Furthermore, if tractive power demand during connection to the catenary system is not enough, the combustion engine provides the supplementary power.

Additional logic for all parallel hybrid drivetrains ensured that when the state of the charge (SOC) goes below 10%, the electric motor turns off and the liquid or gaseous fuels via conversion systems propel the vehicle. Furthermore, if the state of charge exceeds 90%, regenerative braking is not used and the conventional braking system absorbs the energy. The 10% and 90% thresholds was assumed to ensure the usable battery capacity remains 80%. It was assumed that the fuel cell system in the parallel configuration follows the vehicle power demand. Since the fuel cell system has low efficiency at partial loads, it was assumed for power requirements below 4.5% of fuel cell maximum system power, the battery pack supply power to increase efficiency. Furthermore, if the power demand is beyond the fuel cell system rated power, the battery pack was assumed to generate the make-up power. For parallel hybrid fuel cell without plug-in it was assumed the battery are fully charged in its initial status, which was a similar assumption for all plug-in drivetrains. However, it was assumed the fuel cell system in this configuration is responsible to recharge the battery to its initial state (SOC equal to 0.9) at the end of each trip.

Additionally, it was assumed 10% of the nominal fuel cell power was used to supply the auxiliary power of fuel cell system. The battery size, fuel tank size, state of charge (SOC), and total energy consumption (*EC*) for drivetrains with parallel hybrid configuration were estimated using Eqs. (3-15), (3-16), (3-17), and (3-18) respectively. In Eq. (3-17) for parallel hybrid catenary drivetrains, the P_{ext} is the difference between maximum continuous power of electric motor (P_{max}) and tractive power when tractive power is lower than the electric motor power ($P_{max} - P_M$). Additionally, in Eq. (3-18), the *SOC* (t_0) was set to 0.9. Moreover, P_{ext} is zero for parallel hybrid drivetrains without catenary, The MF_b was set to 1 for all parallel drivetrains as the usable capacity of 80% was already accounted in SOC calculation by considering the SOC is changing between 90% and 10%.

3.3.2.3 Electric motor model

A parametric equation was used to estimate the efficiency of the electric motor (η_M) under various loads. This equation was extracted from the UQM 220 HD catalogue that represents a map of the electric motor efficiency as a function of torque and rotational speed [158]. Matlab's curve-fitting tool was used to obtain a simple equation that represents the UQM 220 HD electric motor behavior:

$$\eta_M(N_M, T_M) = a_1 {N_M}^{b_1} {T_M}^{c_1} \quad \text{3-19}$$

$$If\ \frac{N_M}{N_{max}} > 0.25\ \Rightarrow\ \frac{T_M}{T_{max}} = 1.18 - \frac{N_M}{N_{max}} \times 0.75\ \ else\ \ \frac{T_M}{T_{max}} = 1$$

where η_M is in percentage, N_M is the normal electric motor speed that was normalized by maximum speed of 6000 rpm (N_{max}), T_M is the electric motor torque that normalized by the maximum torque of 700 N.m (T_{max}), a_1 is 100, b_1 is 0.07, and c_1 is 0.03. The root mean square error (RMSE) and R-square value for this Matlab fitting were 9.6 and 0.46 respectively. Furthermore, a constraint was added to account for the limitations on electric motor operation.

3.3.2.4 Fuel cell model

The efficiency of the fuel cell system was formulated from the experimental test data of the Ballard MK9 PEM technology used in a 12-m Mercedes-Benz Citaro bus [182]. Eq. (3-20) was fit to the efficiency data of the fuel cell system at part-load operation:

$$\eta_{FC}(system) = a_2\ exp\left(b_2 \frac{P_{FC}}{P_{max}}\right) + c_2\ exp\left(d_2 \frac{P_{FC}}{P_{max}}\right) \quad 3\text{-}20$$

where η_{FC} (system) is the fuel cell system efficiency, P_{FC} is the fuel cell system power output, P_{max} is the maximum power of the fuel cell stacks, and a_2, b_2, c_2, and d_2 are fitting coefficients obtained from Matlab, which are 53, −0.179, −1.21e+04, −53 respectively. The a_2 parameters then was adjusted to 67 with regard to the recent trend in fuel cell system advancements to achieve peak efficiency of 64% [183] (US DOE, 2017b). In the series configuration, it was assumed the fuel cell operates at maximum rated power with the efficiency of 55% obtained from Eq. (3-20). The rate of hydrogen consumption ($\dot{FR}$) was estimated using Eq. (3-21):

$$\dot{FR}_{FC} = \frac{P_{FC}}{\eta_{FC}(system)\ LHV_{H_2}} \quad 3\text{-}21$$

3.3.2.5 On-road CO_2 emissions

For all drivetrains with combustion engines, the on-road CO_2 emissions (tank to wheel (TTW)) was obtained by translating the fuel consumption into CO_2 emissions based on the carbon content of the fuel [156]. The following equation was used to account for the amount of CO_2 emissions in g/tkm:

$$TTW_{CO2\_Use} = \frac{M_f \times C_{fu} \times (44/12)}{TD \times M_{Cargo}} \quad 3\text{-}22$$

where C_{fu} is the carbon content of fuel in (g C/g fuel), which was assumed 0.86 and 0.65 for diesel and natural gas respectively, M_f is fuel consumption in gram, TD is the travel distance in km, and M_{Cargo} is the cargo mass in tonne, 44/12 is a factor to convert carbon into CO_2 emissions.

3.3.3 Input parameters

Table 3-5 summarizes all the specific parameters that were used to obtain energy performance. Moreover, an uncertainty range was considered for these parameters, which was used for Monte Carlo simulation to highlight the possible WTW GHG emissions and total ownership cost ranges for the longest (i.e. most demanding) route of Hill Climb Hwy 2 (HCH2). There were some additional parameters for modeling alternative drivetrain HDT that are provided in Table A2 in Appendix A.

Table 3-5: Summary of input parameters for modeling alternative drivetrain HDT

Main	Component	Unit	Baseline	Uncertainty bound[1]	Source
Mass	Tractor base for short haul (glider)	kg	5,900	±10%	[91]
	Tractor base for long haul (glider)	kg	6,600	±10%	[91]
	Trailer chassis and container	kg	6,100	±10%	[91]
	Payload weight	kg	16,050	-	[184]
	13 L MP8 Mack diesel engine	kg	1,217	±5%	[157]
	11.9 L Cummins CNG engine	kg	1,202	±5%	[44]
	10 speed Transmission, drive shaft, differential, and engine oil and coolant masses	kg	600	500-700	
	Catenary	kg	250	200-300	
Efficiency of energy conversion systems	Efficiency of transmission	%	96%	90%-99%	[156]
	Gas turbine power to electricity efficiency	%	30%	28%-33%	[185]
	Indicated thermal efficiency of CNG engine	%	38.5	35%-50%	[156]
	Indicated thermal efficiency of diesel engine	%	47%	45%-55%	[156]
	Electric generator efficiency	%	95%	90%-99%	
	Regenerator efficiency	%	85%	60%-95%	
	Inverter efficiency	%	97%	95%-99%	
	Electric motor maximum efficiency	%	95%	90%-99%	
	Fuel cell maximum system efficiency	%	64%	60%-70%	[183]
	Usable capacity of battery	%	80%	-	[186]
	Inverter-charger specific mass	kW/kg	14	13.5-14.5	[187]
	Integrated electric motor and transmission specific mass	kW/kg	0.9	0.6-1	[188], [189]
	Electric motor specific mass	kW/kg	1.45	1.15-1.75	[190], [191]
	Fuel cell system	kW/kg	0.55	0.24-0.65	[192]
	Gas turbine power density	kW/kg	0.62	0.48-0.75	[193]
	Battery cell specific mass	Wh/kg	243	220-700	[152]
	Diesel tank specific mass	kg diesel/kg System	0.72	0.7-0.8	[194]
	Hydrogen tank specific mass	kg H_2/kg System	0.05	0.045-0.065	[195]
	CNG tank specific mass	kg CNG/kg System	0.28	0.25-0.35	[194]
	a1 coefficient in equation (3-20)	-	100	94-103	
	a2 fitting coefficient in equation (3-203-21)	-	67	63-73	
Vehicular parameters	Battery pack burden factor	-	0.48	0.4-0.6	[152]
	Constant coefficient of engine friction factor for CNG engine (K_o)	-	0.25	0.2-0.3	[156]
	Constant coefficient of engine friction factor for diesel engine (K_o)	-	0.2	0.15-0.25	[156]
	Aerodynamic drag coefficient, C_D	-	0.6	0.36-0.7	[42], [57]
	Zero order of rolling friction coefficient, C_{r0}	-	0.007	0.0045-0.009	[156]
	Accessory load for hybrid and electric drivetrains	kW	4.8	4-8	[92]
	Accessory load for conventional drivetrains	kW	6	5-10	[92]
	Mass Correction Factor	-	0.1	0.075-0.25	[156]
	Frontal area	m^2	10	9.5-10.5	[57]
Efficiency of refueling at stations	CNG	%	99	98-100	[75]
	Hydrogen	%	96	92-100	[196]
	Catenary	%	98	95-99	[8], [197]
	60 kW charging	%	95	88-98	[198]
	500 kW charging	%	86	71-98	[199]

1- Assuming uniform distribution of the uncertainties for the Monte Carlo analysis

3.3.4 Cost estimation

This study evaluates the total ownership cost (TOC) per unit of distance including capital, infrastructure, energy, and maintenance costs. The capital cost for each drivetrain on each route is based on the estimated energy storage capacity and other drivetrain related components. Table 3-6 presents a summary of the assumed specific and absolute costs for different components of the drivetrains. The availability of drivetrains were assumed to be in 2020. Therefore, the component and fuel costs were mostly selected in accordance to this availability year. A comprehensive study by Nykvist and Nilsson [200] found that the cost of Li-ion batteries should be around 300$/kWh with a possible range of 140‑620 $/kWh. However, in their most recent study they showed the battery pack price with current cost declining trend could reach 150 $/kWh by 2020 [201]. Additionally, the DOE [202] has targeted a cost of 125 $/kWh for Li-ion batteries in order to be competitive with conventional drivetrains. Therefore, it was assumed the baseline price and the uncertainty bounds of the battery pack to be 150 $/kWh and 50‑250 $/kWh respectively.

Table 3-6: Various component costs for alternative drivetrains

Component	Cost (U.S. $)	Uncertainty bound[1]	Source
Tractor base for short haul (glider)	108,000[2]	-	-
Tractor base for long haul (glider)	120,000[3]	95,000-145,000	[8], [203]
Battery $/kWh	150	50-250	[201]
H2 tank $/kg	400	300-500	[8], [204]
CNG tank $/kg	110	90-120	[203]
Diesel tank $/kg	6	4-7	[194]
Fuel cell system $/kW	70	30-90	[205]
Electric motor $/kW	13	8-19	[8], [206]
Gas turbine $/kW	400	300-500	[185]
Diesel engine $/Liter	700	650-750	[203]
CNG engine $/Liter	840	800-900	[203]
Transmission (combustion)	8,550[4]	8,000-9,000	[8]
Transmission (electric)	2,000[5]	1,800-2,200	[8]
Diesel after-treatment system per liter of engine	450	425-475	[194]
CNG after-treatment system per liter of engine	225	200-250	[194]
Catenary components	6,500	6,000-7,000	[8]

1- Assuming uniform distribution of the uncertainties for the Monte Carlo analysis
2- Assuming a short haul glider with a day cab is 10% less expensive than the long [203]
3- Averaging between two studies
4- For all drivetrains with combustion engine as the main propulsion system
5- For all drivetrains with electric motor as the main propulsion system

Table 3-7 illustrates the cost of various fuels that were assumed in this study. This study considered fuel costs based on their retail prices, which mostly obtained from Fulton and Miller's study [203]. For each drivetrain the calculated energy consumptions were divided by the refueling efficiencies (provided in Table 3-5) and included into the annual fuel cost calculations.

Table 3-7: Price of fuels from various source (2020 timeframe)

Fuel	Cost (U.S. $)	Uncertainty bound[1]	Description
Fossil CNG ($/kg)	0.74[2]	0.78-1.74	[203]
Renewable CNG ($/kg)	1.66		Assuming the production cost of landfill gas is 2.25 times higher than fossil CNG [207]
Electricity ($/kwh)	0.13[3]	0.08-0.18[3]	[208]
Diesel ($/kg)	1.15[3]	1.15-1.25	Based on average retail price of diesel in Vancouver, Canada for 2019 [209]
Diesel (B20) ($/kg)	1.25		B20 is 20% biodiesel blended with 80% regular diesel. The assumed price for B20 is consistent with [203]
Hydrogen ($/kg)	4.7[2]	4.7-8.35	Natural gas reformer process [203]
Hydrogen ($/kg)	8.35[2]		Electrolysis [203]

1- Assuming uniform distribution of the uncertainties for the Monte Carlo analysis
2- Costs are linearly interpolated for 2020 based on the reported data for 2014 and 2030 [203].
3- The Canadian dollar was converted to the US dollar at the rate of 1.34

Table 3-8 summarizes the estimated cost of maintenance and repair for alternative drivetrains considering ± 10% uncertainty range. Note that beside these maintenance regular costs, battery pack and fuel cell stack replacement costs were discounted and added to the total ownership cost calculation. The fuel cell stack contributes to almost 75% of total fuel cell systems costs [210]. The typical lifetime for PEM fuel cells for operation in heavy-duty vehicles is around 19,000 h [211]. This can be translated into almost 3 years of operation if a HDT is being used for 16 h per day and with 90% of operation on a yearly basis. However, a more recent study indicated a life expectancy of 3‑6 years for a fuel cell stack [8]. Therefore, every 5 years a replacement cost was considered for fuel cell drivetrains. Lithium ion batteries have a life time of 2000‑5000 cycles [210]. This study assumed a lithium battery can last 2000 cycles, translating into more than 5 years of operation considering a similar service operational tempo. In the case of Monte Carlo analysis 3‑7.5 years uncertainty were assumed for replacement period of both battery and fuel cell stack. The expected life time for a tractor- trailer truck is assumed to be 15 years [119]. The baseline discount rate was assumed as 15% [212], [213] with an uncertainty

range of 10‑30% [16], [214]. Finally, it was assumed that the operational uptime percentage for all simulated HDTs during a year is 90%.

Table 3-8: Maintenance and repair cost for various alternative drivetrains

Drivetrain	Cost (US $/km)	Uncertainty bound[1]	Description
Diesel	0.045	±10%	Based on [215] estimation
CNG	0.051	±10%	Based on [215] estimation
Parallel and series hybrid fuel cell (including no plug-in option)	0.054	±10%	Regular maintenance was assumed 20% more costly than diesel due to the hydrogen tanks based on [210] estimation
Battery electric	0.022	±10%	50% less costly than diesel based on [150]
Plug-in parallel hybrid diesel	0.049	±10%	10% more costly than diesel based on [216]
Plug-in parallel hybrid CNG	0.056	±10%	10% more costly than conventional CNG
Plug-in series hybrid diesel	0.029	±10%	Assumed 30% more costly than battery electric due to the existence of diesel engine
Plug-in series hybrid CNG	0.031	±10%	Assumed 40% more costly than battery electric due to the existence of diesel engine
Plug-in parallel hybrid diesel catenary	0.054	±10%	Assumed 10% more costly than parallel hybrid diesel due to the existence of Catenary component
Plug-in parallel hybrid CNG catenary	0.062	±10%	Assumed 10% more costly than parallel hybrid CNG due to the existence of Catenary component
Plug-in series hybrid diesel Catenary	0.032	±10%	Assumed 10% more costly than series hybrid diesel due to the existence of Catenary component
Plug-in series hybrid CNG Catenary	0.034	±10%	Assumed 10% more costly than series hybrid CNG due to the existence of Catenary component
Plug-in series hybrid gas turbine	0.04	±10%	Assumed 80% more costly than battery electric due to the gas turbine
Battery electric with catenary	0.024	-	Assumed 10% more costly than battery electric due to combination of battery and catenary systems

1- Assuming uniform distribution of the uncertainties for the Monte Carlo analysis

Table 3-9 demonstrates various components that contribute to the total infrastructure cost of each alternative drivetrain. It was assumed that series hybrid and battery electric drivetrains recharge by fast charging station at 500 kW level, while parallel hybrid and battery electric catenary configurations with much smaller battery pack recharge by a 60 kW charger. The catenary cost was found by assuming a specific cost of $3.5 M/km [217], a fleet size of 2000 trucks, and total catenary distance of 119.2 km. The cost of CNG and hydrogen stations with capacities of 14,081 kg/d and 1500 kg/d were assumed $6 M and $5.05 M respectively [218]. The infrastructure cost for CNG or hydrogen station were calculated based on average daily fuel consumption of corresponding CNG or hydrogen drivetrain on all cycles with baseline parameters. For example, for conventional CNG the average of CNG consumption was found to be 211 kg/day leading to the cost of CNG station per drivetrain to be $89,986. The uncertainty range for each alternative drivetrain was assumed to be 10% higher and lower than the baseline magnitude. The equipment and installation costs of charging stations at 60 kW and 500 kW were

assumed $105,000 and $500,000 respectively [218]. The cost of charging station for each plug-in drivetrains then was estimated based on the average of charging time over different cycles considering 12 h for charging operation.

Table 3-9: The infrastructure cost for all alternative drivetrains

Drivetrain	Hydrogen station ($)	Charging station, 500 kW level ($)	Charging station, 60 kW level ($)	Catenary ($)	CNG station ($)	Total ($)	Uncertainty range[1]
Diesel	-	-	-	-	-	-	-
CNG	-	-	-	-	$89,986	$89,986	±10%
Battery electric	-	$150,000	-	-	-	$150,000	±10%
Battery electric catenary	-	-	$35,000	$208,705	-	$243,705	-
Plug-in series hybrid fuel cell	$79,237	$60,000	-	-	-	$139,237	±10%
Plug-in parallel hybrid fuel cell	$160,057	-	$15,000	-	-	$175,057	±10%
Parallel hybrid fuel cell (no-plug)	$180,908	-	-	-	-	$180,908	±10%
Plug-in parallel hybrid Diesel	-	-	$8,750	-	-	$8,750	±10%
Plug-in series hybrid diesel	-	$60,000	-	-	-	$60,000	±10%
Plug-in parallel hybrid diesel Catenary	-	-	$4,038	$208,705	-	$212,743	±10%
Plug-in series hybrid diesel Catenary	-	$54,545	-	$208,705	-	$263,250	±10%
Plug-in series hybrid gas turbine	-	$85,714	-	-	$34,153	$119,867	±10%
Plug-in parallel hybrid CNG	-	-	$9,545	-	$72,793	$82,338	±10%
Plug-in parallel hybrid CNG Catenary	-	-	$4,375	$208,705	$61,650	$274,730	±10%
Plug-in series hybrid CNG	-	$100,000	-	-	$36,450	$136,450	±10%
Plug-in series hybrid CNG Catenary	-	$75,000	-	$208,705	$26,062	$309,767	±10%

1- Assuming uniform distribution of the uncertainties for the Monte Carlo analysis

3.3.5 GHG emissions

Table 3-10 summarizes the well to pump emissions intensities of the fuel sources considered in this study. It was assumed natural gas engines are operable on 100% renewable natural gas, compared to most of today's diesel engines that have a technical barrier of 20% for biodiesel blending [219]. Renewable diesel is different than biodiesel and has the exact characteristic of fossil diesel, which can be used in diesel engines at 100% purity [220]. The present study does not consider this fuel since it is relatively new and has not been widely available in BC. Currently 6.3% biodiesel is blended into diesel refinery processing in BC [221]. Therefore, 6.3% biodiesel blended into low sulfur diesel was assumed an upper limit of carbon intensity and diesel blended with 20% bio-diesel (B20) was assumed as lower limit of carbon intensity. Low carbon diesel was assumed that is a mixture of 10% Canola oil, 10% Yellow Grease, and 80% low sulfur diesel per unit mass [55]. Additionally, it was assumed that the

lower heating value is the same for all the constituents of low carbon diesel. High carbon diesel was assumed to be a mixture of 3% Canola oil, 3% Yellow Grease, and 94% of low sulfur diesel.

Table 3-10: Well to pump GHG emissions of considered fuels [54], [55]

GHGs	Hydrogen (g/MJ)		Natural gas (g/MJ)		Diesel (g/MJ)		Electricity (g/MJ)	
	Low carbon: Electrolysis (BC electricity mix)	High carbon: Reformer (Natural gas)	Low carbon: RCNG (Landfill)	High carbon: CNG (Fossil)	Low carbon: 20% biodiesel + 80% low sulfur diesel	High carbon: Low sulfur diesel + 6% biodiesel	Low carbon: BC electricity mix	High carbon: WECC electricity mix
CO_2	10.25	100	-50	8.85	10.76	12.68	6.1	100
CH_4	0.03	0.35	0.37	0.25	0.14	0.16	0.018	0.2
N_2O	0.14×10^{-3}	2.33×10^{-3}	1.08×10^{-3}	1.52×10^{-3}	2.85×10^{-3}	1.02×10^{-3}	8.5×10^{-5}	1.62×10^{-3}
GHG-100	11.2	111.1	-38.6	16.8	15.8	17.8	6.7	106

The upper limit of carbon intensity for CNG was assumed to be via fossil natural gas, which is compatible with current natural gas resources in BC. The fugitive and leakage of CH_4 in the natural gas production pathways is accounted for and regularly updated into the GREET model. GREET assumes the methane leakage from conventional and shale gas wells during well-to-pump stages to be 1.32% and 1.38% of produced natural gas respectively according to the 2016 update [222]. These percentages are translated to methane emissions of 0.28 g/MJ and 0.29 g/MJ respectively for conventional and shale gas wells. In the well to wheel analysis for drivetrains that powered by CNG, the methane leakage from refueling station also included into the analysis since GREET does not consider anything beyond crank case and tailpipe of vehicle for the pump to wheel stage [223].

The low carbon intensity CNG was assumed sourced from landfill which GREET considers a negative intensity; this negative credit for bio-methane is attributed to the avoidance of methane flaring. Hydrogen was assumed to be generated via the BC electricity mix or via the higher carbon intensity feedstock of natural gas via a reforming process. The BC electricity mix is assumed 95% hydro-electricity and 5% natural gas, which was considered the low carbon intensity electricity source. An electricity mix from the Western Electricity Coordinating Council2 (WECC) with 32% natural gas, 26% coal, 21% hydroelectric, 9% wind & solar, 8% nuclear, and 4% others fuel sources was assumed as the high carbon electricity [54].

100-year global warming potential (GWP) factors were selected according to the Fifth assessment report of the IPCC to convert fossil methane (CH_4) and nitrous oxide (N_2O) to equivalent CO_2, which are 30 and 265 for CH_4 and N_2O respectively [224]. The well-to-pump

CO_2, CH_4, and N_2O emissions ($WTP_{CO2,\ CH4,\ N2O}$) in g/t.km for those drivetrains that have two energy storage systems can be estimated:

$$WTP_{CO2,CH4,N2O} = \frac{CE_1 \times SE_1 + CE_2 \times SE_2}{TD \times M_{Cargo}} \quad 3\text{-}23$$

where CE_1 and CE_2 are the amount of energy in MJ consumed by source one and two respectively, SE_1 and SE_2 can be either the specific CO_2, CH_4 or N_2O emissions (g/MJ) of source one and two respectively, TD is the travel distance in km, and M_{cargo} is the mass of cargo in tonne. Finally, the on-road (TTW) CH_4 and N_2O emissions ($TTW_{CH4,\ N2O}$ *(Current)*) for drivetrains with CNG or diesel source were estimated by multiplying the amount of CH_4 or N_2O ($TTW_{CH4,N2O}$ *(GREET)*) emissions reported in the GREET to the fraction of on- road CO_2 emissions obtained from current simulation (TTW_{CO2} *(Current)*) over on-road CO_2 emissions reported in GREET (see Eq. 3-24(3-24)):

$$TTW_{CH4,N2O}\ (Current) = \frac{TTW_{CO2}\ (Current)}{TTW_{CO2}\ (GREET)} \times TTW_{CH4,N2O\ (GREET)} \quad 3\text{-}24$$

For each drivetrain the estimated upstream emissions were divided by its corresponding refueling efficiency provided in Table 3-5 to account the impact of refueling losses. Beside the increase in upstream emissions as the result of refueling losses, the impact of refueling loss for CNG drivetrains is direct methane emissions that were included into the analysis. The abatement cost (AC) of GHG emissions compared to the baseline diesel was calculated as follows:

$$AC_{i,j,k}\left(\frac{\$}{tonne}\right) = \frac{TOC_{i,j,k} - TOC_{D,j,R}}{WTW_{i,j,k} - WTW_{D,j,R}} \frac{10^6}{M_{Cargo}} \quad 3\text{-}25$$

where the indices i, j, and k refer to drivetrain type, drive cycle, and the fuel type respectively. $TOC_{D,j,R}$ refers to the total ownership cost of the baseline diesel powered by regular diesel fuel on a given cycle j. WTW GHG emission is in g/tkm unit and $10^6/M_{cargo}$ is conversion factor to obtain abatement cost in US dollar per tonne of GHG emission reduction.

3.4 Results and discussion

This section details the findings of the study. Section 3.4.1 first expresses the validation method of on-road fuel consumption. Next, Sections 3.4.2 and 3.4.3 presents and discusses the main results across drivetrains: on-road fuel consumption, well to wheel GHG emissions, total ownership costs, and abatement cost of GHG emissions. Section 3.4.4 provides a practical feasibility discussion with regard to a number of technologies including battery electric,

hydrogen fuel cell, and catenary drivetrains. Finally, Section 3.4.5 presents the results of the Monte Carlo analysis for the key long haul HCH2 route.

3.4.1 Validation

The on-road energy consumption for battery electric, series hybrid fuel cell, parallel hybrid CNG, and parallel hybrid diesels were examined and validated against available literature [31], [43], [56]. Table 3-11 summarizes the benchmarking results for these drivetrains with the obtained quantities from the literature, which appear to be satisfactory and in a reasonable range. In the reviewed literature, no such relevant information was found for validation of series hybrid diesel or CNG, with and without catenary, or series hybrid gas turbine, parallel hybrid diesel or CNG with catenary. However, since the validated drivetrains have similarities with the non-validated drivetrains in terms of configurations and fuel sources, overall the comparison gives confidence that the model for non-validated drivetrains is adequate.

Table 3-11: Validation metrics for battery electric, series hybrid fuel cell, parallel hybrid CNG and diesel drivetrains

Drivetrains	Used parameters for simulation	Drive Cycle	Current model	Reported quantity	Source
Battery electric	RF[1] 0.007, RB[2] %85, AL[3] 4 kW, FA[4] 10 m^2, AD[5] 0.6, LM[6] 31,751, TE[7] %95	UDDS[8]	1.84 kWh/km	1.86 kWh/km	[43]
Series hybrid fuel cell	RF[1] 0.007, RB[2] %85, AL[3] 4 kW, FA[4] 10 m^2, AD[5] 0.58, LM[6] 24,040 kg, TE[7] %95	CARB[9] transient	8.5 kg/100 km	8.3 kg/100 km	[56][12]
Parallel hybrid CNG	RF[1] 0.007, RB[2] %85, AL[3] 6 kW, FA[4] 10 m^2, AD[5] 0.58, LM[6] 19,150 kg, TE[7] %95, ITE[10] %45, BET[11] below 53 kW (of power demand)	UDDS[8]	30.5 kg/100 km	30 kg/100 km	[31]
Parallel hybrid diesel	RF[1] 0.007, RB[2] %85, AL[3] 6 kW, FA[4] 10 m^2, AD[5] 0.58, LM[6] 19,150 kg, TE[7] %95, ITE[10] %50, BET[11] below 53 kW (of power demand)	UDDS[8]	36.1 L/100 km	36.6 L/100 km	[31]

1- RF: Rolling friction coefficient
2- RB: Regenerative braking efficiency
3- AL: Accessory load
4- FA: Frontal area
5- AD: Aerodynamic drag coefficient
6- LM: Loaded mass
7- TE: Transmission efficiency
8- UDDS: Urban Dynamometer Driving Schedule [225]
9- CARB: California Air Resources Board [225]
10- Indicated thermal efficiency
11- Battery electric operation threshold
12- The configuration of the fuel cell drivetrain is not mentioned in this study

3.4.2 Energy consumption results

Figure 3-8 demonstrates the specific energy consumption of all drivetrains on the six drive cycles from Section 3.3.1, applying baseline parameters from Table 3-5 and Table A2 in Appendix A. The energy consumption metrics are divided into short (A) and long haul (B) categories, and sorted by average energy consumption in short haul operation. Drivetrains in

long haul category are matched up with their short haul counterparts. The dashed lines (in orange) are showing the average of energy consumption of drivetrains on corresponding short and long haul cycles. The obtained rank of each drivetrain in terms of energy consumption in short and long haul categories are presented beside each drivetrain label on the vertical axes. The highest calculated specific energy consumption was 9 kWh/km for the conventional CNG drivetrain on the SDD cycle. The lowest calculated energy consumption was 1.3 kWh/km for the battery electric catenary on the LDD and RH cycles, slightly lower than the pure battery electric mainly due to their smaller battery packs. Battery electric catenary and battery electric have the best performance on these cycles due to a lower average speed, which reduces aerodynamic forces while having more efficient conditions for electric motor operation. Besides the battery electric catenary that is only available for short haul, battery electric has the lowest specific energy consumption in both short and long haul categories, despite a significant incremental mass of up to 18.6 tonnes (on HCH2 route) compared to the baseline diesel. Table S3 in supplementary section in supplementary section presents the incremental mass of drivetrains on various cycles.

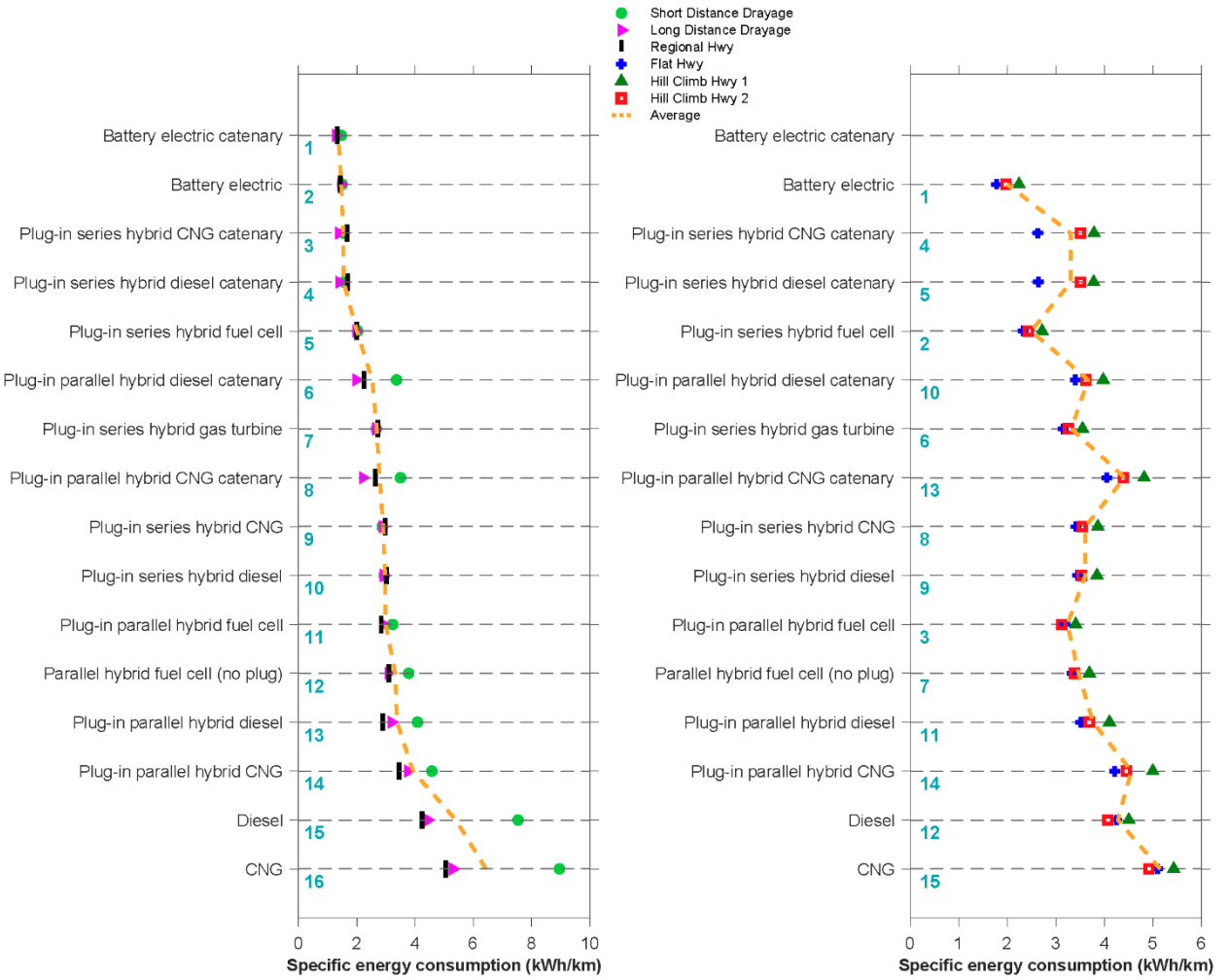

Figure 3-8: Specific energy consumption (kWh/km) of alternative drivetrains on short (A) and long (B) haul cycles

The present study predicts a 9-46% reduction in fuel consumption of the parallel hybrid diesel compared to the baseline diesel. This range of improvement is higher than 6-8% found in the Gao et al. [148] study and 10-15% from Zirn et al. [151] for a parallel hybrid diesel HDT. However, the range in the present study is lower than the 81% found by Zhao et al. [57] for a parallel hybrid diesel HDT on a drayage cycle.

On both short and long haul routes, conventional CNG is the most energy intensive drivetrain since the combustion engine is the main power source with a thermal efficiency lower than diesel. On both short and long haul cycles the series hybrid CNG consumes 28-68% less fuel than the conventional CNG, which is relatively consistent with the 30% reduction found by Yun et al. [226] for a series hybrid CNG bus. Series hybrid CNG in both short and long haul is

slightly more efficient than series hybrid diesel since it was assumed to be powered by an engine with lower maximum power.

Unlike Karvountzis-Kontakiotis et al. [227] who found a 34% increase in energy consumption for a gas turbine range extender (for a light-duty vehicle) compared to a baseline diesel, the present study predicts a 20‑65% improvement in energy consumption of the gas turbine drivetrain compared to the baseline diesel. The discrepancy is mainly due to the thermal efficiency assumptions: 30% [185] for a gas turbine in the present study, compared to 26% in Karvountzis-Kontakiotis et al. [227] study. Different assumptions related to drive cycle and battery size are additional reasons for the discrepancy. However, the result for the gas turbine drivetrain is in agreement with Chaim et al.'s [228] study that found hybridization with a gas turbine resulted in a 13% improvement in fuel consumption compared to a hybrid diesel light-duty vehicle. In fact, the present study indicates a gas turbine range extender unit consumes less energy than many parallel and series hybrid CNG on both short and long haul cycles. The highest improvement is about 42% when comparing series hybrid gas turbine with parallel hybrid CNG on the SDD mainly due to the dominance of battery operation on this cycle.

The series hybrid fuel cell was found to have up to a 73% reduction in energy consumption compared to the baseline diesel, which is in agreement with Vliet et al. [229]; they found a 66% reduction for a series hybrid fuel cell in a light duty vehicle. The parallel hybrid fuel cell drivetrains (with and without plug-ins) have lower performance than series hybrid fuel cell. The reason for the lower performance of the parallel hybrid fuel cell is reduction in overall conversion efficiency as a result of following the tractive load during the entire vehicle operation. The series hybrid fuel cell has higher overall conversion efficiency compared to the parallel hybrid fuel cell drivetrain because battery with higher conversion efficiency is the dominant power supplier in this drivetrain. Furthermore, fuel cell system in the series hybrid operates only over a segment of routes that significantly improves the overall efficiency compared to the parallel hybrid.

Generally, drivetrains that have catenary systems consume less energy than comparable drivetrains without catenary systems, due to smaller battery pack requirements that reduce the total mass of the truck. Furthermore, catenary drivetrains use grid electricity when connected, leading to higher conversion efficiency than drivetrains relying on fuel combustion. However, the reduction impact varies by drivetrain technology and catenary distance in each drive cycle.

The parallel and series hybrid CNG catenary lead to up to 41% and 52% reductions in energy consumption when compared with parallel and series hybrid CNG without catenary systems. The parallel and series hybrid diesel catenaries indicate relatively similar reduction potentials of up to 38% and 52% compared to the parallel and series hybrid diesel.

3.4.3 GHG and cost results

Figure 3-9 illustrates the well to wheel GHG emissions for all drivetrains on short haul (A) and long haul (B) cycles considering low and high carbon intensity energy sources for each drivetrain. All drivetrains in the short haul group are sorted by their average of well to wheel GHG emissions when powered by low carbon fuel supplies (see Table 3-10). Next, drivetrains in long haul category are matched up with their short haul counterparts. The rank of each drivetrain is presented on the vertical axes. For both short haul and long haul groups, the dashed line in orange demonstrates the average of well to wheel GHG emissions when drivetrains are powered by low carbon fuel supplies. Although there are some exceptions with regard to a specific cycle and fuel type, drivetrains from bottom to top of the figure tend to emit less GHGs. Furthermore, neglecting drivetrains with catenary system, in the short haul category drivetrains on SDD cycle emit more WTW GHG emissions due to the high kinetic intensity of the cycle that requires more tractive energy. In the long haul category, HCH1 have higher WTW GHG emissions due to its higher characteristic accelerations and more aggressive grades.

Consistent with the energy consumption performance, the battery electric catenary emits the least GHGs compared to other drivetrains in the short haul category when hydroelectricity (low carbon energy supply) is available. In the long haul and absent a battery electric catenary, the battery electric drivetrain emits the least amount of GHGs using hydroelectricity. In short haul, when drivetrains run on high carbon intensity fuels, the battery electric catenary emits the least amount of GHG emissions. In long haul comparing high intensity fuels, battery electric is associated with the least amount of GHG emissions. Moreover, besides the battery electric catenary, averaging the GHG emissions of drivetrains on all cycles with both low and high carbon intensities, the battery electric has the lowest overall GHG emission footprint.

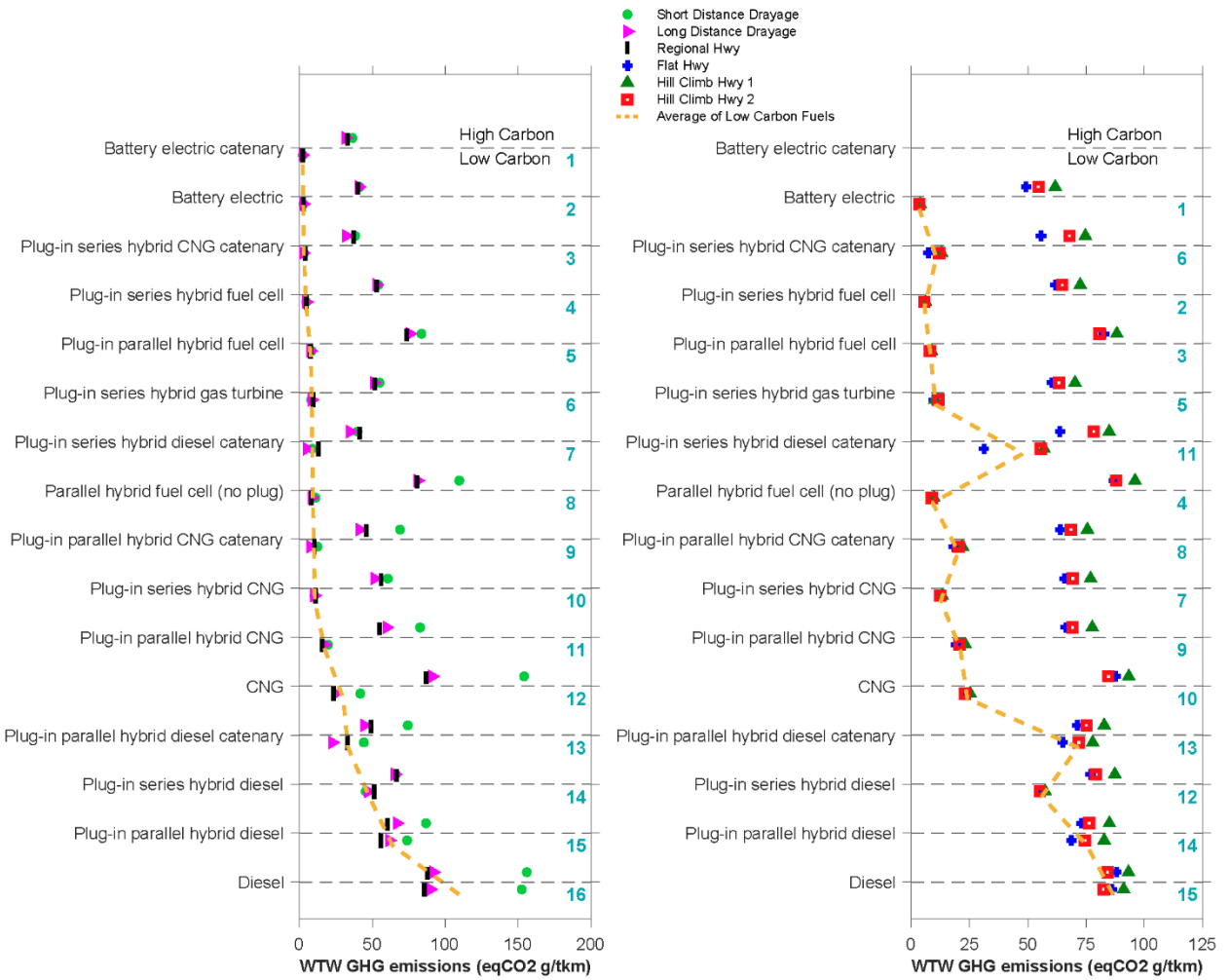

A) Short haul (SDD, LDD, and RH) **B) Long haul (FH, HCH1, and HCH2)**

Figure 3-9: Well to wheel GHG ($eqCO_2$ g/tkm) emissions of all alternative drivetrains with low and high carbon energy fuel supply on short (A) and long (B) haul cycles. Below the grey dashed line presents well to wheel GHGs of drivetrain with low carbon fuels and above that are corresponding to the GHG results with high carbon fuels.

Furthermore, averaging the low and high carbon intensities for the short haul routes, battery electric is in the third rank after battery electric catenary and series hybrid CNG catenary. Overall, the battery electric catenary drivetrain emits 62‑99% less GHGs than conventional diesel depending on the cycle and electricity source. Additionally, comparing all short and long haul cycles battery electric emits 34‑98% fewer GHG emissions than the comparable diesel. The result of the present study is relatively consistent with Sen et al.'s [36] study in term of the GHG reduction potential of battery electric HDT with WECC electricity source compared to the baseline diesel. However, unlike Sen et al. [36] who found a ~20% reduction for battery electric compared to the baseline diesel, the present study found a 34‑74% reduction. The discrepancy is the result of two factors. First, the drive cycle based simulation used in the present study leads to

energy consumptions for diesel and battery electric drivetrains that can be very different than assumed values in Sen et al. [36]. Second, Sen et al. [36] accounted the GHG emissions associated with lithium-ion battery manufacturing and battery electric recharging station, which were not considered in the present study.

After battery electric, series hybrid CNG catenary lies in third place for GHG emissions in the short haul group using bio CNG from landfill. On the long haul routes, the series and parallel hybrid fuel cell drivetrains stand in second and third places respectively when hydrogen via electrolysis pathway is being used. Despite consideration of methane leakage of 1% during CNG refueling, other drivetrains powered by landfill CNG have a relatively better GHG footprint than most biodiesel based drivetrains for both short and long haul cycles. The low GHG emissions of drivetrains operating on landfill CNG owes to the negative carbon credit received by avoiding GHG emissions from landfills. Therefore, these landfill gas based CNG drivetrains could be considered as serious alternatives to battery electric and hydrogen fuel cell, especially for long haul operation since their GHG footprints are quite comparable to these zero emission (tailpipe) options.

The present study confirms Lee et al. [32] and Zhao et al. [38] results regarding the role of hydrogen produced via reforming natural gas in reducing WTW GHG of HDTs. However, unlike Lee et al. [32] that found an 18‑35% reduction, the present study demonstrated a wider range for change including an increase of 4% or reduction of up to 65% depending on the drive cycle and drivetrain technology. Additionally, the present study indicates fuel cell drivetrains depending on their architecture and drive cycles can reduce WTW GHG emissions by 89‑97% compared to the baseline diesel. This is also consistent with Lee et al. [32] that found a 90% reduction from fuel cell HDT using hydrogen generated by solar energy.

Comparing the high carbon intensity ranges, the series hybrid gas turbine appears to be less GHG intensive than parallel and series hybrid CNG. Moreover, unlike Sen et al. [36] that found the WTW GHG of CNG is 33% higher than the diesel, the present study indicates a marginal 1% reduction for CNG drivetrain on all short haul cycles and almost equal GHG emissions on all long haul cycles. However, the present result for the short haul CNG is relatively consistent with Zhao et al. [38] who found up to a 5% reduction in WTW GHG of LNG-SI over a baseline diesel for a short haul cycle. The present study indicates 73% reduction of WTW GHG emissions for

the CNG drivetrain powered by landfill gas compared to the baseline diesel. This reduction is in agreement with Mintz et al. [162] who found an 81‑110% reduction in WTW GHG emissions of bio-methane fuel pathways in CNG light-duty vehicle compared to a baseline gasoline.

Generally, beside the carbon intensity of input fuels, the ranges of GHG emissions for each drivetrain rely on the drivetrain energy efficiency (see Figure 3-8) and how various energy supplies are being allocated; the latter is applicable for hybrid drivetrains. Table A4 in Appendix A provides the detail of the WTW GHG emissions analysis by gas type and emissions stage for each drivetrains on all cycles with low and high carbon intensity energy sources. The table also provides the percentage of GHG emissions reduction in respect to a comparable baseline diesel to identify potential drivetrains and corresponding cycles that can reduce GHG emissions by 80%.

Figure 3-10 displays the total ownership cost (TOC) of each alternative drivetrain on all short haul and long haul cycles applying conventional and renewable fuel prices from Table 3-7. The conventional (low cost) fuels are equivalent to the fuels with high carbon intensities specified in Table 3-10; similarly, the renewable fuels or high cost fuels correspond to the fuels with low carbon intensities provided in Table 3-10. Electricity is an exception in which only one rate for electricity was assumed. Similar to Figure 3-9, drivetrains in both short and long haul categories are sorted by their average TOC per km when they are powered by low carbon intensity fuels (high cost). Then, drivetrains in long haul category (B) are matched up with their short haul counterparts. The ranks of drivetrains in both short and long haul categories are provided beside their vertical axes. Additionally, the orange dashed lines demonstrate the average of each drivetrain TOCs on the corresponding cycles using high cost fuels.

Parallel hybrid diesel for both short and long haul trips appears to have the lowest total ownership cost, since the drivetrain is associated with a less expensive, 60 kW charging station and they can benefit from up to 46% in saving for fuel consumption. Over various cycles and comparing conventional fuels the parallel hybrid diesel is associated with 4‑13% reduction in TOC compared to the diesel. This range of reduction is in agreement with Sen et al. [36] who found a 12% reduction in life cycle cost for a hybrid HDT. The present study indicates CNG has up to 15% higher TOC on short haul cycles while having up to 8% lower TOC on long haul cycles than diesel considering conventional fuels. This variation seems relatively comparable

with Sen et al. [36] that found almost similar life cycle cost for conventional diesel and CNG HDTs. Comparing high carbon intensity fuel, except for the SDD cycle, parallel hybrid CNG appears to have 4-12% lower TOC than conventional diesel mainly due to its efficient operation and low cost fossil CNG supply.

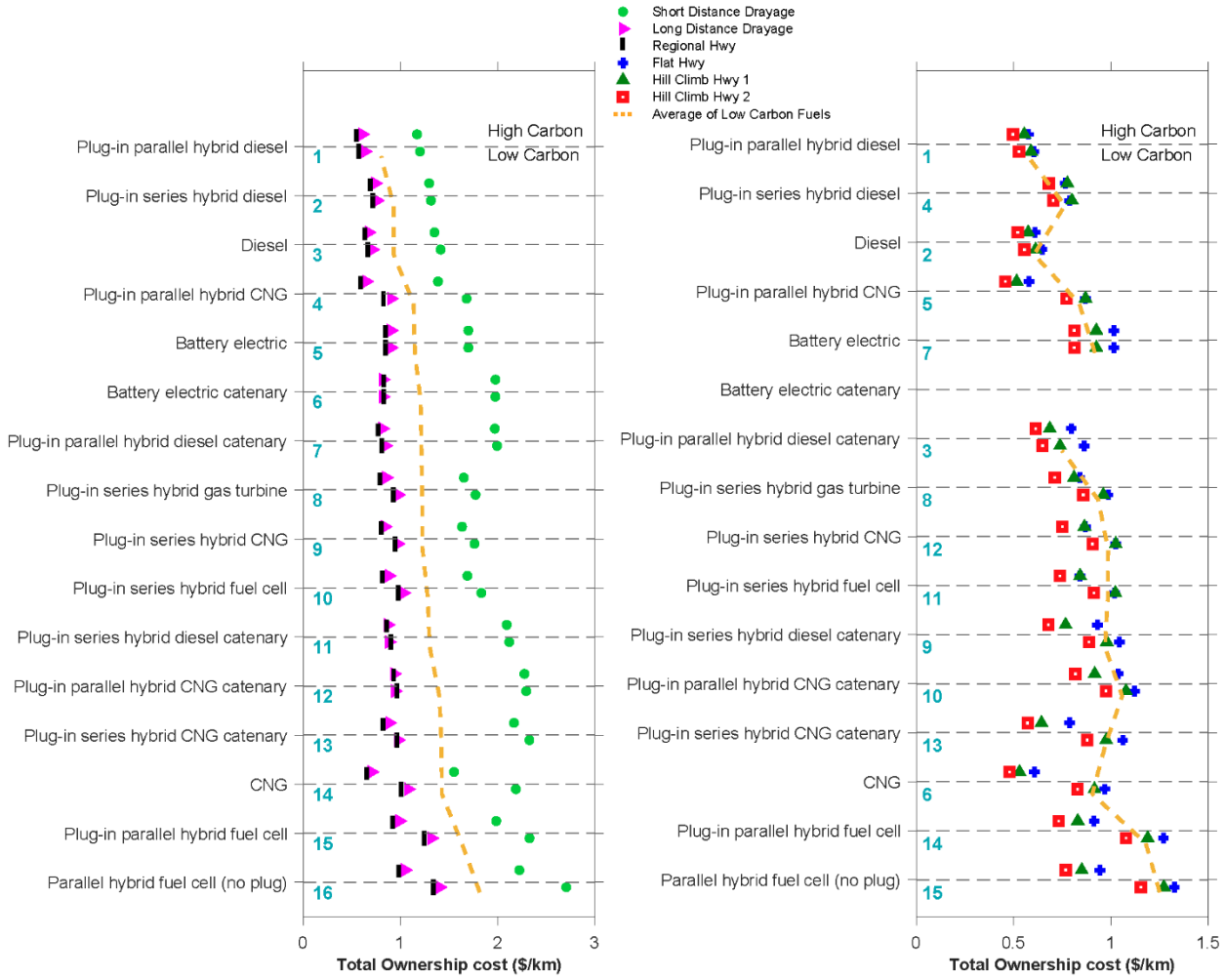

Figure 3-10: Total ownership cost (TOC) (in US dollar per km) for all drivetrains on short and long haul cycles considering high cost fuel (renewable or blended with renewable) and low cost conventional fuels. Below the grey dashed line are related to the TOCs with more expensive low carbon fuels and above that are corresponding to the TOCs with less expensive low carbon fuels.

Furthermore, on average, the battery electric drivetrain appears to be unable to compete with many conventional and hybrid drivetrains that have combustion engines due to the high cost of the battery pack and fast charging stations. This is different to Sen et al. [36] who found 16-27% lower life cycle cost for battery electric HDT compared to a diesel HDT. The main discrepancy in TOC estimation between the present study and Sen et al. [36] relates to the different battery

pack size and more expensive charging station cost assumptions in the present study. Still, battery electric seems to be a less expensive option compared to the most series drivetrains since it is the most efficient drivetrain, which requires only a fast charging station. However, most series hybrid drivetrains require additional infrastructures such as CNG or hydrogen station (see Table 3-9), which subsequently increases cost.

Overall, it can be seen that the TOCs have a wider range of $/km for short haul cycles than long haul routes. This is partly due to a wider fuel efficiency range for short haul cycles compared to long haul (see Figure 3-8), and to more extent related to the infrastructure cost calculation method. The infrastructure cost of each drivetrain was assumed similar for all cycles and then the total ownership cost per km was calculated over a smaller denominator value (shorter routes), which increases the sensitivity for short haul cycles. Table A5 in Appendix A demonstrates the detail of the total ownership cost analysis with and without infrastructure cost for all considered cycles and drivetrains.

Figure 3-11 present the abatement cost of GHG emissions from alternative drivetrains on various short and long haul cycles. This figure is a combination of WTW GHG and TOC results using Eq. (25). In each category, drivetrains are sorted by the average of abatement cost using low carbon intensity fuels and then drivetrain in long haul category are matched up with their short haul counterparts. The dashed lines in orange present these averaged quantities. The rank of each drivetrain are presented on each plot. Except for HCH1 and HCH2 with abatement costs of 38-86 ($/tonne CO_2e) using bio fuel, the abatement costs are negative for parallel hybrid diesel on other cycles. Parallel hybrid CNG, CNG, and series hybrid diesel have negative abatement costs on several drive cycles due to their lower TOC costs.

Series hybrid diesel and parallel hybrid CNG are found as the second cost effective option in short and long haul respectively. Battery electric despite of its high TOC cost place third in both short and long hauls mostly due to its much higher potential for reducing GHG emissions. Overall catenary drivetrains are found to be a less cost effective drivetrain than battery electric. This is due to the higher infrastructure cost for catenary drivetrains and assumption about the availability of the catenary network (see Figure 3-5) that was considered to be limited around the Metro Vancouver area, BC (higher traffic volume areas).

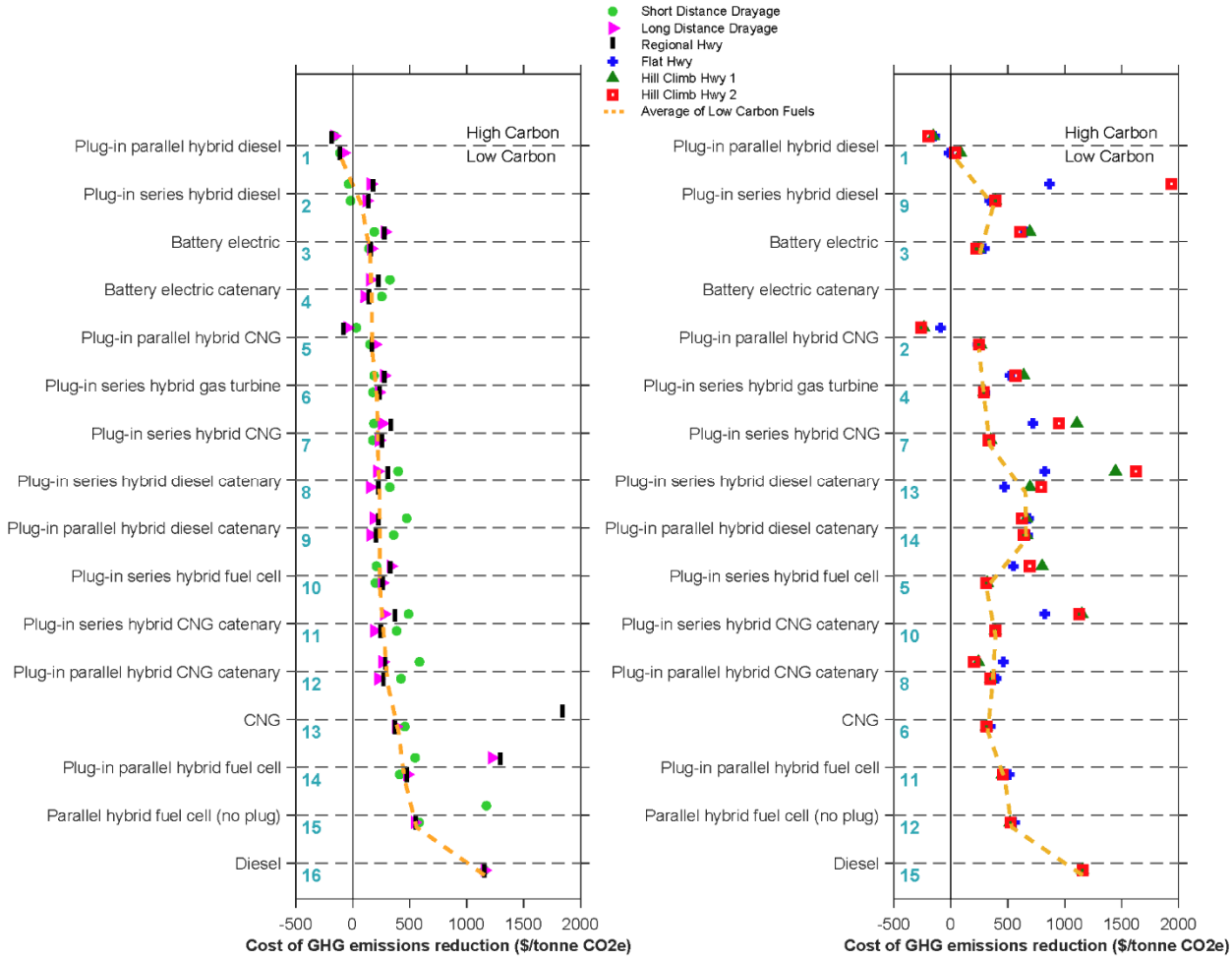

Figure 3-11: Abatement cost (in US dollar) of CO_2 emissions for alternative drivetrains on various (A) short and (B) long haul cycles compared to the baseline diesel powered by regular diesel. Below the grey dashed line demonstrates abatement costs with more expensive low carbon fuels and above that are corresponding to the abatement costs with less expensive low carbon fuels. (These plots do not show data points beyond -500-2000 $/tonne. see Table S6 for the complete list of abatement costs)

3.4.4 Discussion of drivetrain challenges

This study focused on the total ownership cost and GHG emissions aspects without considering their limitations in real world conditions. Although the feasibility assessment is beyond the scope of this paper, this section highlights briefly the limitations and technical challenges of the considered drivetrains. First, the maximum cargo capacity of considered alternative drivetrain HDTs are compared with diesel (see Figure 3-12). Then, a number of technical challenges of the battery electric, catenary, and fuel cell drivetrains as well as their related infrastructures are discussed.

The bulk of this study estimated how much the gross vehicle weight and performance are impacted if all drivetrains can carry the same cargo mass of 16,050 kg; in reality each drivetrain has a specific limit for cargo mass. For the worst-case scenario, this assumption leads to the gross HDT mass of 49,880 kg in the case of battery electric (on HCH2 cycle), which is still lower than the maximum Canadian limit of 62,500 kg [181]. The maximum cargo capacities on each route was estimated and normalized with the corresponding diesel considering an equal maximum gross HDT mass of 62,500 kg. The drivetrains were then ranked on each route in regard to their maximum cargo capacity, assuming the unchanged masses of the drivetrains sized previously (see Table A3 in Appendix A).

Figure 3-12 demonstrates the cargo capacity on various short and long haul routes at the maximum gross mass of 62,500 kg. Overall, parallel hybrid fuel cell and conventional diesel have the highest cargo capacity on short and long haul respectively. On the SDD cycle, parallel hybrid fuel cell and CNG have higher cargo capacity (more than 100%) due to their smaller energy storage and lighter drivetrain components (e.g. lighter after-treatment system for CNG). This figure further confirms that all routes with larger battery pack requirements are associated with smaller cargo capacities. Therefore, the lowest cargo capacity is associated with the battery electric on the HCH1 and HCH2 cycles. It is noteworthy to mention that the range of these drivetrains could be reduced significantly when they loaded up to this maximum capacity. However, the impact is different across various drivetrains technologies. Furthermore, these drivetrains could be under-powered if they operate at a gross mass of 62,500 kg. For example, the Cummins & Westport manufacturer of the ISX12 G engine does not recommend using their engine for gross mass more than 36,000 kg [114].

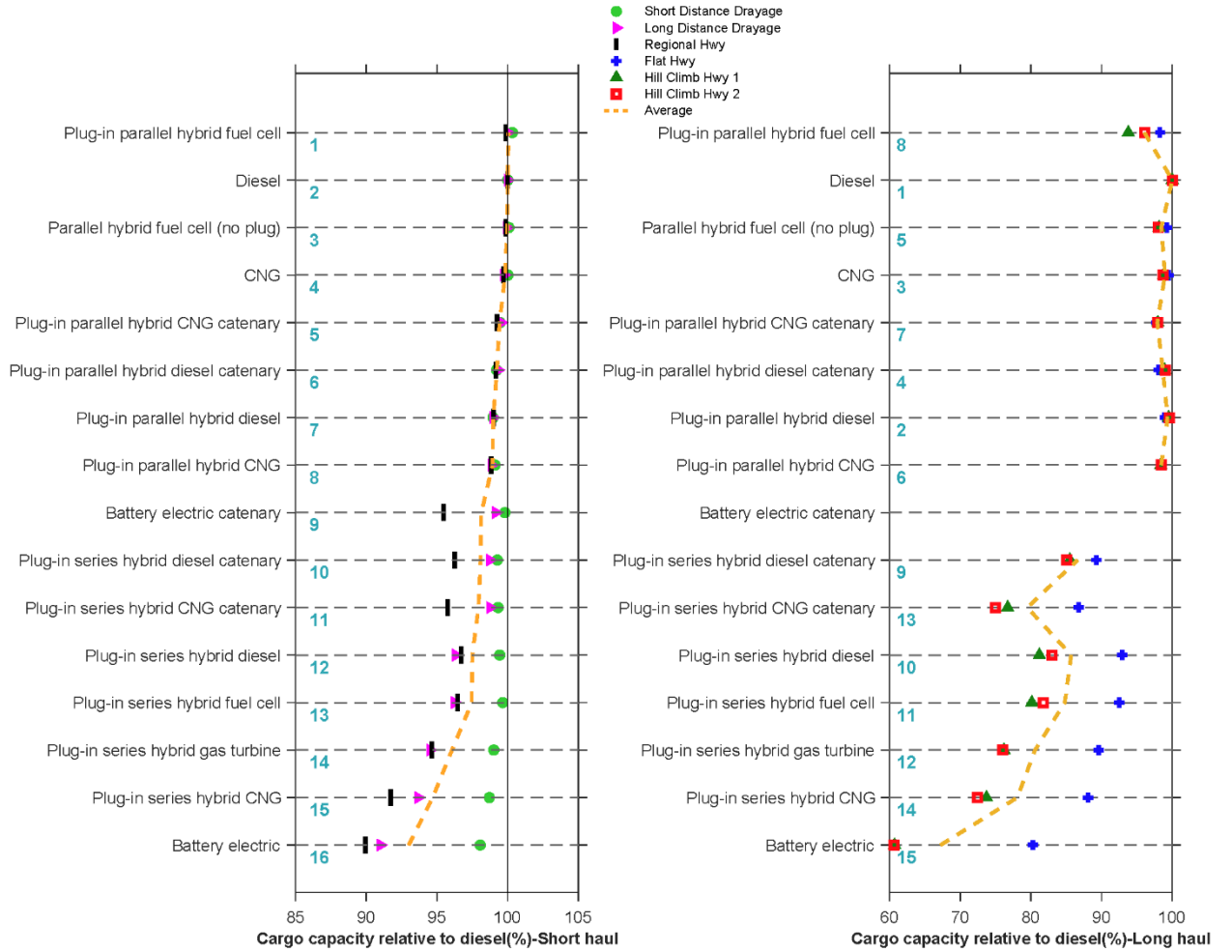

A) Cargo capacity relative to diesel on the same route for short haul cycles (%)

B) Cargo capacity relative to diesel on the same route for long haul cycles (%)

Figure 3-12: Relative cargo capacity for alternative drivetrains on various routes with respect to comparable diesel at maximum gross mass of 62,500 kg.

Bulky battery pack requirement leading to reduced cargo capacity is another technical challenge of pure battery electric drivetrains for long haul operation. For example, with today's battery pack volumetric factor of 295 Wh/l [230], the battery pack for the longest routes of HCH2 would be 8 cubic meters. Therefore, the feasibility of long haul battery electric drivetrains with today's battery technology considering the added mass and volume for packaging is still a challenge to be resolved. Extreme climate conditions including very cold and hot weather negatively impact battery performance. The charging capacity reduces to 60% below -10oC and only 22% of battery capacity is dischargeable below -40oC. Therefore, a thermal management system is required to minimize the negative impact of low temperatures Lei et al [231]. Cold climate also expedites the battery degradation process due to high polarization of the anode

below 0ºC Jaguemont et al. , [232]. Additionally, grid upgrading is another challenge for battery electric and series drivetrains relying on 500 kW fast charging stations. Grid modification could involve upgrading distribution line, transformer, and other power equipment [233]. Finally, long charging times of more than 4 hrs for the longest route is another limitation of battery electric drivetrains for long haul operation.

Although the catenary drivetrains eliminate the need for a larger and heavier battery packs, their general drawback is the lack of flexibility with respect to different travel routes. The catenary wire needs to be sized for supplying power under extreme traffic conditions that may increase the costs. Additionally, HDTs should be able to connect or disconnect to catenary lines at varying speeds. Finally, passing catenary lines over bridges and tunnels may require increasing height, which simultaneously increases the installation complexity and cost [8]. The selection of catenary drivetrains in this study was mostly in-line with a demonstration project in California [43]. However, the feasibility of catenary HDTs could be challenging when they use multiple fuels such as plug-in, catenary, and combustion fuel which would increase system complexity. Finally, using micro gas turbines as range extenders could also be challenging as they have a 2-5 minutes delay in their startup [234].

A hydrogen fuel cell system could satisfy the HDT application from a durability perspective [8]. However, hydrogen fuel systems for HDTs are still bulky, though not as critical as for pure battery electric drivetrains. A 70 kg hydrogen system needs a volume of 3 cubic meters [8]. As pointed out earlier there is enough space for around 151-257 kg of hydrogen on the rail side and behind the cab of HDTs [34]. Furthermore, there are several challenges in producing, delivery, and storing of hydrogen through economic and carbon-free pathways, as currently most hydrogen demand is satisfied via reforming of natural gas [235].

3.4.5 Monte Carlo Analysis

To address the uncertainty of the baseline analysis presented in Section 3.4.3 a Monte Carlo simulation was performed on the longest drive cycle (HCH2). This route was selected since as stated before, it is the most challenging route for alternative drivetrains such as battery electric. The aim was to demonstrate the impact of uncertainty in input parameters on WTW GHG emissions and TOCs for all drivetrain variants. Figure 3-13 demonstrates the range of WTW GHG emissions (A) and the total ownership costs (B) using a uniform distribution of parameters in Tables 3.5‑3.10 with 5000 simulations. For simplicity, it was assumed the fuel

cost and the upstream fuel GHG intensities are changing between their low and high values. For each alternative, the box indicates the 25th, 50th, and 75th percentiles of WTW GHG emissions and TOCs. Additionally, the whiskers demonstrate the 5th and 95th percentile of WTW GHG emissions and TOCs. In this figure, drivetrains are sorted by their median quantities of the WTW GHG emissions and the TOC.

Overall, comparing the median quantities, the battery electric has the lowest WTW GHG emissions and the parallel hybrid diesel is associated with the lowest TOC. The uncertainty range for several drivetrains, such as parallel hybrid fuel cell, are much higher than the rest mainly due to a wider range of changing in upstream GHG emissions for the fuel supply. A sensitivity analysis was performed to determine the importance of each input parameter to the WTW GHG emissions and TOC estimations of all drivetrains on the HCH2 cycle. Figures A1 and A2 in Appendix A demonstrate the results of the sensitivity analysis for each drivetrain in a tornado presentation. Results indicates that the WTW GHG emissions from the upstream fuel emissions and rolling friction coefficients are the top most important factors. Additionally, discount rate, fuel price, battery cost, and rolling friction coefficient are the most important parameters contributing to the drivetrains TOCs.

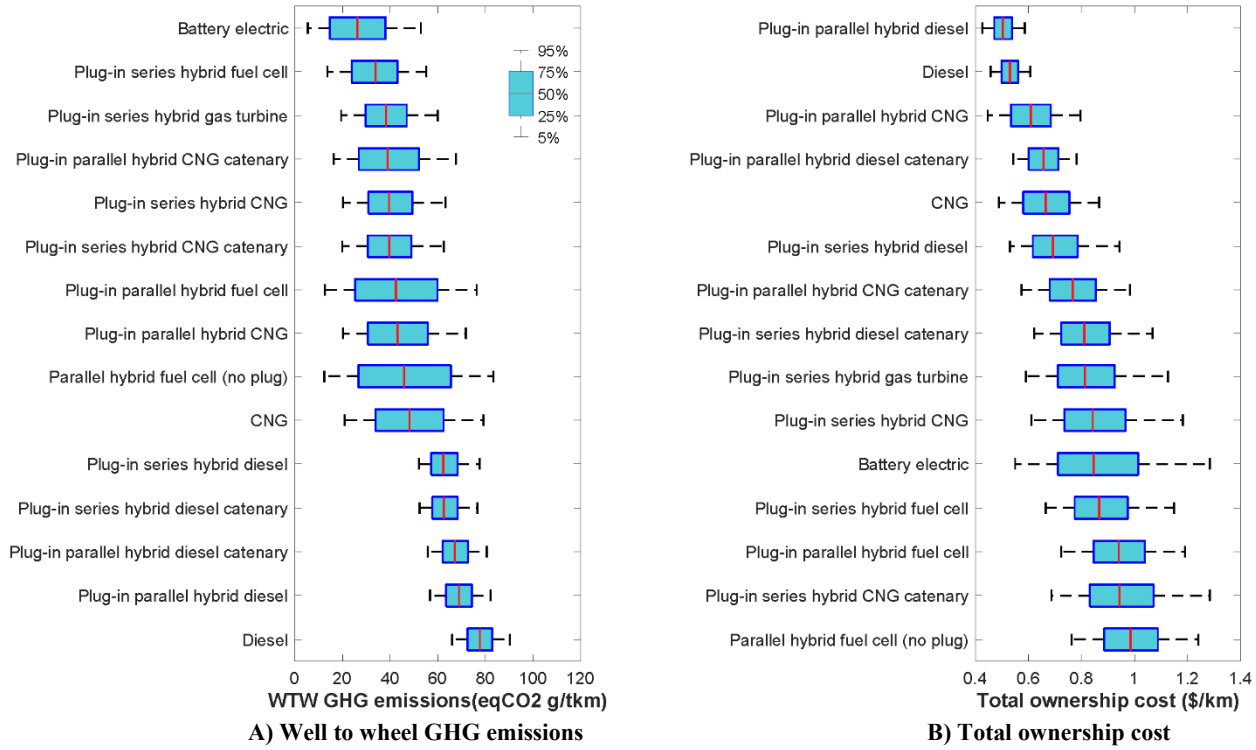

Figure 3-13: Monte Carlo uncertainty analysis for (A) well to wheel GHG emissions and (B) total ownership costs for all drivetrains on the HCH2 cycle

3.5 Conclusion

This study provided comprehensive insights into the suitability of alternative drivetrains for heavy-duty tractor-trailers in terms of technology overview, energy consumption, well-to-wheel GHG emissions, total ownership cost, and GHG abatement cost. This study calculated the size of the on-board energy storage systems with respect to their power demand for each drivetrain and every travel route ranging from 120 km to 950 km. Due to the high density of diesel fuel, conventional diesel trucks can accommodate both short and long haul cycles with just minor upgrading in their fuel storage. However, due to the low density of alternative fuels, particularly battery and hydrogen, they are inefficient to use a purposed-design long haul alternative drivetrain in a short haul application, as the energy storage systems of alternative drivetrain should be designed for the intended route.

Overall, the input parameters for this study were obtained through careful examination of the literature. Various drive cycles were considered in the baseline analysis. Then the sensitivity and Monte Carlo analyses were performed on the longest cycle to show the degree of uncertainty in results with changing the input parameters. The focus of this research was BC, Canada as a case study. Therefore, the results of this study serve as an initial local assessment. The relative ranking of drivetrains could change by considering different input parameters, especially energy and component costs, upstream emissions intensities, and conversion efficiencies. However, the presented method in this study could be exploited in the future. A number of technical challenges of the considered drivetrains were highlighted in the results section, which could be a potential area for future studies. Additionally, several other avenues for future research to address the limitations of this study are proposed here.

To evaluate and compare alternative drivetrains, six distinct routes in BC were selected from the raw activity data of around 1616 heavy-duty trucks that are operating mainly in Metro Vancouver [153]. The selection criteria was based on average speed, elevation difference, daily travel distance, and location. Next, the speed profiles of selected routes were converted to second-by-second intervals and then combined with road gradients. These developed cycles represented the real world drive cycles and operation routes of HDTs in BC.

This study demonstrated how activity data for a fleet of 1616 trucks that was initially collected for freight management can be useful for other applications such as estimating energy consumption, GHG emissions, and cost estimation of heavy-duty trucks with alternative

drivetrains. Hence, this approach can be extended to analysis of other commercial fleets with data from electronic tracking devices, increasingly being collected all around the world especially in US and Canada for the sake of road safety [236]–[238].

Generally, it was shown that the GHG emissions of all drivetrains are a function of fuel type, drivetrain sub system efficiencies, drive cycle, and the rational of fuel use for hybrid configurations. The study found battery electric catenary the lowest GHG emitter for short haul. In the absence of battery electric catenary for long haul, pure battery electric drivetrains are the least GHG emitter, with 96‑98% fewer WTW GHGs than the baseline diesel when low carbon hydroelectricity is available. Considering the total ownership cost, the parallel hybrid diesel was found to be the least expensive drivetrain for both short and long haul cycles. The study also indicated the parallel hybrid diesel to be the most cost effective (i.e. the least abatement cost) option for both short and long haul operations with negative costs on several cycles. The reason for obtaining negative costs is because the non-monetary factors (e.g. risk) were not considered into the drivetrains ownership cost calculations.

This study confirms the findings in the literature [36], [38], [149], [150] on the significance of battery electric drivetrains in reducing GHG emissions of HDTs. The study was also consistent with Zhao et al. [38] and Lee et al. [32] on the WTW GHG emissions reduction potential of the series hybrid fuel cell HDT using hydrogen from natural gas reformation and electrolysis production pathways. Furthermore, the study found battery electric has a 26‑66% higher total ownership cost than the baseline diesel. Despite the deep GHG emissions reduction potential, the result highlighted the challenges of long haul battery electric operation such as limited cargo capacity and performance in cold climate. The low energy density of today's lithium-ion batteries significantly increases the mass of the battery electric drivetrain (see Table A3 in Appendix A), making long-haul operation challenging. Battery electric drivetrains are therefore likely better suited to serve short distance routes (up to 400 km) to avoid a massive battery pack.

This study highlights the importance of renewable natural gas (RNG), hydroelectricity, renewable hydrogen (electrolysis pathway), and biodiesel in achieving the 80% GHG emissions reduction target for BC. It was found that using low or high carbon fuels leads to a considerable difference in overall well-to-wheel GHG emissions, though the difference is not even. In particular, due to the negative emissions credit for avoided landfill gas direct methane emissions,

the difference between using low and high carbon natural gas for CNG-powered drivetrains was quite significant. In contrast, biodiesel (B20) with only a 20% renewable content, was found to have much lower GHG reduction potential. Therefore, the use of renewable energy sources such as RNG (bio-methane) should be considered as a serious short term option for HDTs, especially when combined with the cost effective parallel hybrid drivetrains on long haul routes where the required infrastructure is not readily available to use fast charging and hydrogen refueling stations.

However, the lack of production scale-up is a common challenge with most biofuel sources [239], [240]. Renewable natural gas in this regard seems promising, as preliminary estimation shows its resources in BC are 94‑400 PJ [241], [242], enough to fulfill the energy demand of the heavy-duty trucking sector in BC that is 36.7 PJ [154]. A caveat is that most of the renewable CNG resources was estimated to be from gasification of woody biomass, a technology that is still under development [242]. Future studies can focus further on the role of biofuels, including renewable CNG and diesel, but also synthetic fuels from electrolysis with methanation, in decarbonizing HDTs in BC.

Despite the life cycle emissions reduction benefit of biofuels, the criteria pollutants from HDT tailpipes will be challenging going forward, especially in urban regions. Therefore, climate policies might focus on battery electric (with and without catenary charging) and fuel cell drivetrains as they are the only current options for zero tailpipe emissions. There are other co-benefits with regard to battery and fuel cell drivetrains including the advantage of using domestic and renewable energy sources, and the potential for increased employment opportunities (Clean Energy Canada, 2019). Although there are few CNG stations in BC offering CNG for medium and heavy-duty vehicles [243], there are almost no fueling stations to support electrified and hydrogen powered HDTs. Future studies could focus on the level of infrastructures readiness that would be required to support extensive deployment of these HDT drivetrains.

This study established a method to compare alternative drivetrains based on a physical fuel consumption model. However, in the future, the model can be improved by applying more refined operational rules to determine the energy consumption for the series hybrid drivetrains. Furthermore, energy consumption calculations and battery sizing in parallel hybrid drivetrains requires further improvement by considering more refined power split and energy management strategies between various sources. A combination of a refined power splitting strategy together

with a global optimization method (e.g. genetic algorithm) could be useful in searching for more absolute optimized designs in respect to energy and cost objectives. Furthermore, vehicle component sizing (e.g. electric motor and fuel cell system) can be extended for optimizing further drivetrain sub-systems on each route, and between multiple routes for vehicles operating variably on both short and long haul routes. Beside the low energy density of lithium-ion batteries, cold climates as well as battery performance degradation over time [231], [244] are factors that negatively impact energy consumption, which results in even a larger battery pack requirement.

Moreover, the sensitivity of well to wheel GHG emissions and total ownership cost using Monte Carlo simulation was conducted only for HCH2 cycles; this could be expanded to other cycles. Additionally, the infrastructure costs were assumed identical for both short and long haul cycles, which in future studies can be broken down into different costs. Finally, it would be beneficial to quantify non-monetary factors such as risk, technology readiness, refueling time, and refueling station availability to further explore the economic competitiveness of the drivetrain options relative to each other.

Chapter 4

4 Which Heavy-Duty ZEV Drivetrains Are "Winners"? Simulating Competition and Adoption of Short- and Long-Haul Trucks in British Columbia, Canada

This paper co-authored with Jonn Axsen and Curran Crawford will be submitted to Transportation Research Part D: Transport and Environment journal.

This chapter evaluates the mix of "winner" zero emissions drivetrains for short and long haul HDT markets in BC, considering various infrastructure roll-out scenarios in combination with a 100% ZEV requirement for 2040. The chapter also estimates the probability of meeting the 2050 GHG target in the short and long haul markets. The focus is on exploring the competitiveness of zero emissions drivetrains (introduced in chapter 3) from a market perspective using a vehicle adoption model that takes into account both financial and non-financial costs. The adoption model estimates financial costs using the energy consumption models developed in chapter 3.

Abstract: There is a great deal of uncertainty regarding which low-carbon fuels and drivetrains might be most suitable for the heavy-duty truck (HDT) sector. While an increasing number of studies evaluate different drivetrains according to performance and cost, there is little exploration of how these technologies might compete with one another in the long-term. To help fill this gap, this study simulates adoption of various drivetrains in the short and long haul HDT sectors – including those fueled by electricity and hydrogen. Using the case of British Columbia, Canada, we used a dynamic vehicle adoption model coupled with a Monte Carlo uncertainty analysis, representing technology, cost, and behavioral parameters. Scenarios included two ambitious zero-emissions vehicle (ZEV) mandates and various levels of refueling infrastructure deployment. We found the "winning" drivetrains (those that capture more than 80% of 2050 market share) varied between the infrastructure roll-out scenarios and between the short and long haul markets. We found battery electric and hydrogen fuel cell as the top winners of short haul and plug-in hybrid diesel and hydrogen fuel cell as the top winners of long haul, depending on whether the infrastructure development was toward charging or H_2 station deployments. The highest GHGs reduction impact for both short and long haul was related to scenarios with rapid hydrogen station deployment. This study implies the necessity for strategies to encourage the rapid deployment of infrastructure to increase the adoption of ZEV drivetrains HDTs and increase the chance of GHG emissions reduction in transportation.

***Keywords**:* Simulation model, ZEV mandate, heavy-duty trucks, alternative drivetrains, market share, GHG emissions

4.1 Introduction

Globally, freight transportation by heavy-duty trucks (HDTs) is one of the major and steadily growing sectors for fossil fuel use and greenhouse gas (GHG) emissions [3], [245]. The estimated contribution of HDTs to global GHG emissions from the transportation sector is 22-30% (in 2010) and expected to grow to 25-34% by 2050 [3]. This growth is driven by sustained economic development in emerging economies, globalization, and industrialization, as well as increases in online shopping and fast delivery expectations of consumers [5], [245].

In the face of such growth, decarbonization of the HDT sector will inevitably require a transition to low-carbon fuels and drivetrains. The current CO_2 reduction potential of diesel engine by increasing engine efficiency is less than 15% [6]. This reduction could be obtained via improvement in engine heat recovery system, reduction of friction losses, auxiliary power improvement, exhaust gas after-treatment, and down-speeding [6]. There are potentially many fuels and drivetrain options for deep GHG reduction of HDTs, but there exists little consensus on which options are more realistic for a transition to a low-carbon transportation system [2], [5], [246]. For example, while several studies imply fuel cell is a more practical option for HDTs especially for long haul operations [2], [203], others are more in favor of battery electric and catenary electric options mostly due to their higher fuel efficiency and lower ownership cost advantages [8], [9], [247]. Renewable natural gas (RNG) also is evaluated in a number of studies as a deep GHG emissions reduction option for transportation sector [248], [249], others disagree over its long term feasibility, mainly due to the lack of sufficient economically viable resources [250].

The study focuses on the case of British Columbia (BC), Canada, which along with many regions aims to reduce its 2050 GHG emissions by 80% below 2007 levels [251]. The BC government has recently announced an ambitious ZEV mandate for light-duty vehicles and trucks requiring 100% ZEV sales by 2040 – but has no such policy for HDTs.

The research objective of this study is to first explore if any specific infrastructure roll-out scenario leads to domination of a particular ZEV drivetrain in the short and long haul market of BC. The second objective is to quantify domination percentage for a particular ZEV drivetrain using Monte Carlo analysis. The third objectives is to quantify the GHG emissions reduction implications of the adopted ZEVs scenarios for the short and long haul HDT market of BC. We

aim to examine the implementation of a similarly ambitious ZEV mandate for the HDT sector. Policy makers often face a dilemma between whether to pick a winner technology and support its required infrastructure or to remain technology-neutral [252]. We defined "winning" drivetrains consistent with [66] as those that obtain more than 80% of 2050 mean market shares. ZEV drivetrains usually are considered as those that partially or fully powered by grid electricity or hydrogen. We distinguish the short and long haul HDT markets based on the U.S. EPA [253] definition, in which less than a 322 km daily range is assumed to be short haul and above that is considered long haul.

The on-road freight transport modeling literature is more focused toward comparison of multiple options for HDTs based on financial cost, GHG emissions reduction, and other performance criteria (e.g. cargo capacity) [8], [18], [257], [258], [22], [152], [155], [203], [245], [254]–[256]. There are a few studies that consider consumer behavior when capturing the long term competition of multiple ZEV drivetrains HDTs [3], [20], [21], [40], [41]. In particular, fewer studies explicitly capture infrastructure role in relation to consumer behavior [20], [21], [41]. To fill the gap in the literature we developed a method to capture consumer behavior and quantify explicitly how refueling infrastructure density affects the market share competition of various alternative HDT drivetrains.

Additionally, the previous freight-related literature tends to simulate fuel cell [16], [203] or battery electric options [40], [245]. In fact, no study has been found that considers battery electric, plug-in hybrids, catenary, and fuel cell drivetrains altogether in the simulation. The present study fills the gap by simulating a wider range of technology options, covering 10 and 8 HDT drivetrains options in the short and long haul markets, respectively. The vehicle adoption simulation includes behavioral factors including market heterogeneity, discount rate, and non-financial costs rather than only comparing financial costs, or assuming pure "optimization" behavior [259]. Furthermore, the competition of HDTs are split into short and long haul markets, and few studies consider the split [21], [203]. Finally, drivetrain technical parameters (i.e., capital costs, energy consumption, etc.) and energy storage sizes of drivetrains are based on a novel in-house model that considers several representative trucking routes in the case region of BC [260].

The rest of the study organizes as follows. The next sub-section 4.1.1 introduces the considered drivetrains in the short and long haul market. Section 4.2 summarizes several insights

obtained from an extensive literature review. Section 4.3 explains the method including an overview of the CIMS-HDT, modeling parameters, and implemented scenarios. Section 4 presents results including the probability of meeting 80% GHG emissions target, new market share, and the sum of energy consumptions from short and long haul markets. Section 4.5 discusses the results comparing with previous findings, offers implications of the study, and highlight limitation of the study including several directions for future research.

4.1.1 Considered drivetrain technologies

Figure 4-1 illustrates the alternative drivetrain technologies considered in this study. We assumed 10 and 8 HDT drivetrains technologies respectively for the short and long haul markets. We considered conventional diesel and CNG (compressed natural gas), plug-in parallel hybrid diesel and CNG, battery electric (BE), and parallel hybrid fuel cell (FC) without plug, and plug-in series hybrid fuel cell drivetrains in both short and long haul markets. We did not include catenary options for the long haul market as we assumed that the low traffic density of long haul routes in BC does not justify a significant catenary installation in its freight corridors. The plug-in series hybrid gas turbine only considered for long haul market. The parallel architecture for plug-in hybrid diesel and plug-in hybrid CNG with and without catenary means both combustion engine and electric motor can separately propel HDTs. The plug-in hybrid gas turbine and plug-in hybrid fuel cell have a series architecture in which the fuel cell and gas turbine works as a range extender, while the battery and electric motors provide the main propulsions. The full explanations of architecture design for each drivetrain options are provided in [260].

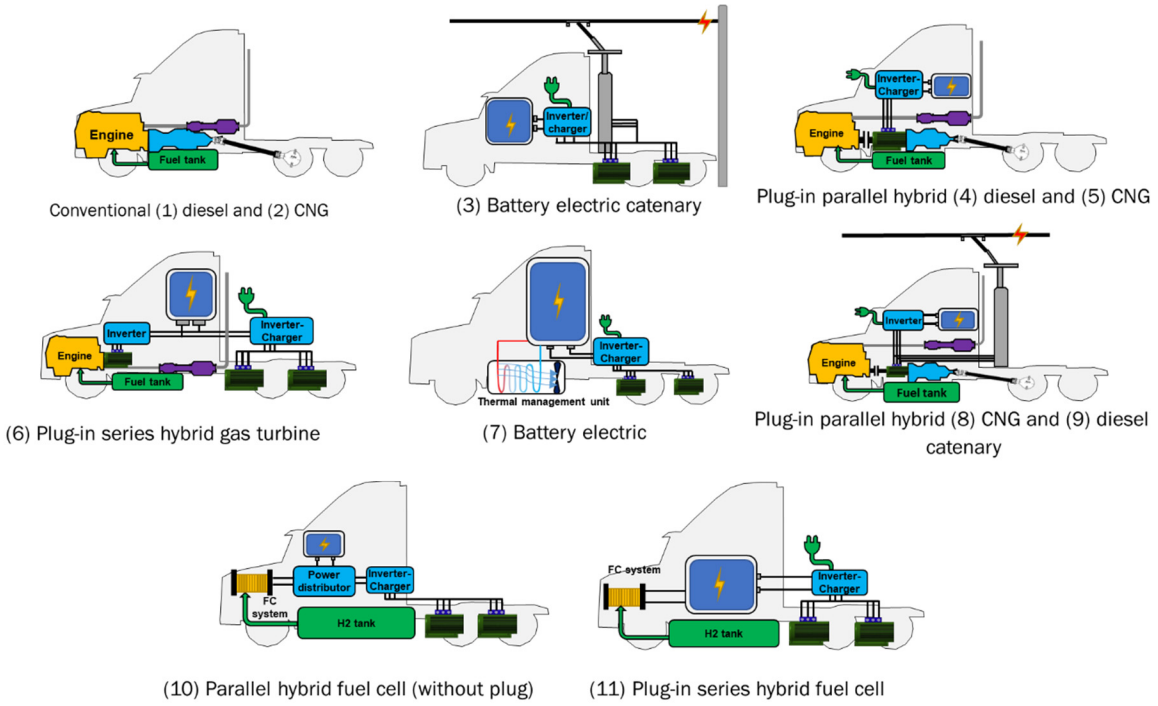

Figure 4-1: Alternative drivetrains simulated in the present study [260]

4.2 Literature review

While low-carbon HDTs received little attention in the past, in recent years more studies have been focused exclusively on alternative drivetrain for the HDT market. A number of these studies have been focused more on technology and cost attributes (e.g. [36], [56]), which is not the attention of the current study. We aimed to review those on-road freight related studies that have macro-economic approach and explicit technology representation. Based on a comprehensive review by Kluschke et al. [6], we divide these studies by their applied method into three categories: simulations, optimization, and accounting. Simulation models are trying to capture technology and economic interaction as realistically as possible, as opposed to optimization models that aims to find an optimal cost solution [261]. It is worthwhile to mention that simulation models are not necessarily capture the "non-financial" drivers for drivetrain adoption. The accounting models are seeking to estimate the requirement for meeting a climate target or potential for technology change considering a set of constrains [6]. We provide literature insights of dominate drivetrains considering their modeling category mostly associated

with their ambitious scenarios. We also present literature insights on the role of infrastructure on the vehicle adoption rate of zero-emissions HDTs.

Accounting models have been used in several studies mostly to evaluate freight electrification potential [256], [257] and necessity to meet future climate targets [19], [155]. Çabukoglu et al. [256] found 12-100% of Switzerland HDTs are electrifiable with battery electric drivetrain. Liimatainen et al. [257] found 18-93% electrification potential in Switzerland compared to 6-82% in Finland. Both of these studies considered various factors such as battery and charging technology, battery swap, cargo weight, daily travel, and cargo volumes. In respect to electrification necessity studies, Talebian et al [155] found 70% of BC HDTs should be battery electric by 2040 HDTs to meet the BC climate target in freight sector. Mai et al. [19] estimated by 2050, 31% of the US HDTs can be battery electric under an optimistic scenario.

Optimization models have been used to determine minimal cots pathways for decarbonizing freight [17], [18], [258], [262]. These studies showed different optimal path depending on their assumed technology and scenarios. Keller et al. [17] showed the hydrogen from the electrolysis process of electricity with more 50% renewable content has the lowest abatement cost and the highest GHG emissions reduction impact. Plötz et al. [18] found 40-50% total market share for catenary HDTs in 2040 if one-third of EU highways be electrified with catenary installation. Gambhir et al. [258] found that mild hybrid diesel is an optimal path in terms of both GHG emissions reduction and abatement cost. Bahn et al. [262] predicted bio-fuels as a winner option with 50-80% market share, while plug-in hybrids and battery electric HDTs have up to 12% and 2% uptake respectively [262].

The view of literature with simulation approach on future dominant ZEV drivetrains greatly varied depending on technology and policy scenarios included in their analyses. Table 4-1 summarizes the method, scope, technology, and the dominant ZEV drivetrains in the previous studies with simulation approach. The dominant ZEV findings in this table are associated with the ambitious scenarios considered in each study. There have been only a few studies that considered the competition of battery electric and fuel cell altogether for HDTs [20]–[22]. The simulation models are different in terms of method for adopting alternative options, technical details, geographical focus, and energy system domain. While Palencia et al. [254], Fulton and Miller [203], Mulholland et al. [245], and International Energy Agency [9] applied

exogenous market share allocations for alternative drivetrains HDTs to examine several "what if" scenarios, others employed endogenous competition models [3], [16], [20]–[22], [40], [41].

Among reviewed studies there is no consensus on which ZEV technology can be superior or the degree of superiority. Although most of these reviewed studies suggest fuel cell as dominated ZEV technology, they indicate a wide degree of market share findings. Furthermore, there are example for dominance of battery electric, plug-in hybrid, catenary, and biofuel options. Hammond et al. [20], Siskos and Moysoglou [22], Lepitzki and Axsen [16], Yeh et al. [3], Shafiei et al. [41] found dominance of fuel cell with various degree of superiority ranging from 1.32% to 100% of new market share in 2030-2050. Plug-in hybrid diesel and catenary are dominated ZEVs in Mulholland et al. [245] and International Energy Agency [9] with 36% to 70% market penetration. Carrara and Longden [40] found battery electric dominance by 2100 with 69-74% penetration while Miller et al. [21] estimated 25% penetration for battery electric by 2050 in short-haul market. Those studies that were captured competition of fuel cell with battery electric or plug hybrid diesel are showing contrasting results. While Miller et al. [21] estimated equal market share for both battery electric and fuel cell in short haul market, Siskos and Moysoglou [22], Hammond et al. [20],and Shafiei et al. [41] found dominance of fuel cell over battery electric or plug-in hybrid diesel.

The reference scenarios in these studies mostly indicate domination of conventional diesel with a small market share for ZEV drivetrains by 2050 (0-10%). Ambitious climate policies indicate the necessity of 100% adoption of zero-emissions HDTs. The 2 ºC scenario considered in these studies is examining the pathway of keeping the average global temperature increase below 2 ºC by 2100. Likewise, the 1.75 ºC scenario explores technology advancement to go beyond 2 ºC and keep the average global temperature increase below 1.75 ºC [9].

Table 4-1: The summary of previous simulation studies with simulation approach

Studies	Simulation model	Drivetrains/fuels	Country /region	Time horizon	Policy scenarios	Dominate ZEV drivetrains
Hammond et al. [20]	CIMS (endogenous market share with disaggregation of intangible cost)	Standard diesel, medium efficiency diesel, high efficiency diesel, hybrid diesel, LNG/CNG, biodiesel, FC, BE	Canada	2005-2050	3 policy packages of fuel efficiency standards, carbon tax, LCFS, ZEV mandate, and subsidy with three levels of weak, moderate, ambitious stringencies	**FC** dominates with 68% median market share in the most stringent policy package. In this scenario **BE** obtains 23% median market share.
Lepitzki and Axsen [16]	CIMS (endogenous market share with consumer behavior but without disaggregation of intangible cost)	Diesel, CNG/LNG, hybrid, PHEV, FC	British Columbia, Canada	2015-2050	12 scenarios including three stringency levels of fuel efficiency standards, carbon tax, LCFS, and ZEV mandate policies in combinations with 4 four stringencies of LCFS	**FC** dominates with 74% market share in moderate stringency of LCFS and ambitious policies
Shafiei et al [41]	Multinomial logit (endogenous market share with intangible cost attributes of refueling service availability and range)	Diesel, hybrid, PHEV, FC	New Zealand	2015-2050	6 scenarios including reference, supply-push, subsidy, banned-ICE, banned-ICE&HEV, banned-petroleum	**FC** dominates with 100% market share in Banned-Petroleum and 50% market share for each **FC** and **PHEV** in Banned-ICE&HEV
Palencia et al [254]	Logistic function (exogenous market share and lack of consumer behavior)	ICEV, hybrid, BE, FC	Japan	2012-2050	4 “silver bullet” scenarios of 100% ZEV sale of either hybrid, BE, FC, and both BE and FC	All **hybrid**, **BE** and **FC** depending on the “silver bullet” scenarios
Mulholland et al [245]	MoMo (exogenous market share informed by cost attributes and lack of consumer behavior)	Diesel, catenary, hybrids, BE	Global	2015-2050	2 scenarios including reference technology and modern truck scenarios	**Catenary** dominates with 36% penetration in global HDT stock under the modern technology scenario
Carrara and Longden [40]	WITCH (producer perspective, endogenous market share with constrains on rapid shift to new technology)	Diesel, hybrid, PHEV, BE,	Global	2005-2100	9 scenarios including three economic growth levels in combination with baseline, 2.5 ºC, and 2 ºC scenarios	**BE** dominates with 69-74% penetration in 2 ºC scenarios. In the 2 ºC scenarios **PHEV** obtains 7-15% penetration.
International Energy Agency [9]	MoMo (exogenous market share informed by cost attributes and lack of consumer behavior)	diesel, CNG, hybrid, BE, plug-in or catenary, FC,	Global	2015-2060	Baseline, 2 ºC, 1.75 ºC scenario	**Plug-in hybrid or catenary** dominates with 70% market penetration for 2060
Yeh et al [3]	4 bottom-up models including GCAM (endogenous logit), MESSAGE-Transport (endogenous optimization), MoMo and Roadmap (exogenous expert) (all lack of consumer behavior)	Coal, liquid fuels, natural gas, electricity, hydrogen	Global	2010-2050	Baseline and 2 ºC scenario	**Hydrogen** dominates with up to 7.5% of HDT energy demand. Electricity meets up to 3% of HDTs demand.
Siskos and Moysoglou [22]	PRIMES-TREMOVE (endogenous market share with consumer behavior factors of acceptance and technology readiness)	Diesel, hybrid, LNG, BE, FC	European Union countries	2015-2030	4 scenarios of baseline, 20%,30%, and 35% CO2 reduction for 2030 HDTs	**FC** dominates with 1.32% new market share in 2030. **BE** reaches 0.26% new market share in 2030.
Fulton and Miller [203]	TOP-HDV (exogenous market share and lack of consumer behavior)	Diesel, hybrid, CNG, FC	California and the U.S.	2015-2050	3 scenarios including baseline and 2 ºC scenario with 60% biofuel blends and w/o biofuel	**FC** dominates with 90% penetration for both short and long hauls (no BE considered).
Miller et al. [21]	Multinomial logit (consumer behavior with disaggregation of intangible cost)	Diesel, hybrid, CNG, FC, BE (short haul only)	California	2010-2050	4 scenarios including baseline, 25% ZEV requirement by 2050,25% ZEV requirement by 2050 w/o refueling inconveniences, 50% ZEV requirement by 2050	**FC** dominates in long haul market with 50% penetration. **BE** and **FC** dominate in short haul each with 25% penetration.

Most of the previous studies acknowledged the importance of infrastructure and recommended its deployment to increase the adoption rate for alternative drivetrains [9], [203], but only a few quantified its impact [21], [41]. Miller et al. [21] found that the penetration of battery electric and fuel cell short haul HDTs increases from 12.5% to 17% respectively, by comparing two scenarios with low and high refueling infrastructure intensities. Shafiei et al. [41] found by 2050 the sale of fuel cell HDTs increases from 0 to 35% without a tangible impact on plug-in hybrids comparing reference and a build-out of hydrogen and charging stations scenarios. In a qualitative study, Tongur and Engwall [252] evaluated the causalities associated with setting up a catenary infrastructure project in Ports of California and implementing a ZEV mandate for HDTs in this region. They found infrastructure projects could create a social environment for transitioning a niche technology option (e.g catenary) to a radical ZEV penetration with active engagement of government and other stakeholders [252].

4.3 Method

This section explains our simulation modeling approach including all assumed parameters and their uncertainty ranges for the Monte Carlo simulation.

4.3.1 Overview of the CIMS-HDT model

We used a simulation-based vehicle adoption model called CIMS-HDT, a subset of the full CIMS model [263]. The full CIMS model is a partial equilibrium simulation model with explicit technology and behavior representations and has linkages to all energy sectors of the Canadian economy [263], [264]. We used Matlab to develop the current version of CIMS-HDT, covering only the HDTs market of BC. Figure 4-2 demonstrates the overall procedure and connection of different elements of the CIMS-HDT model in a flow chart diagram.

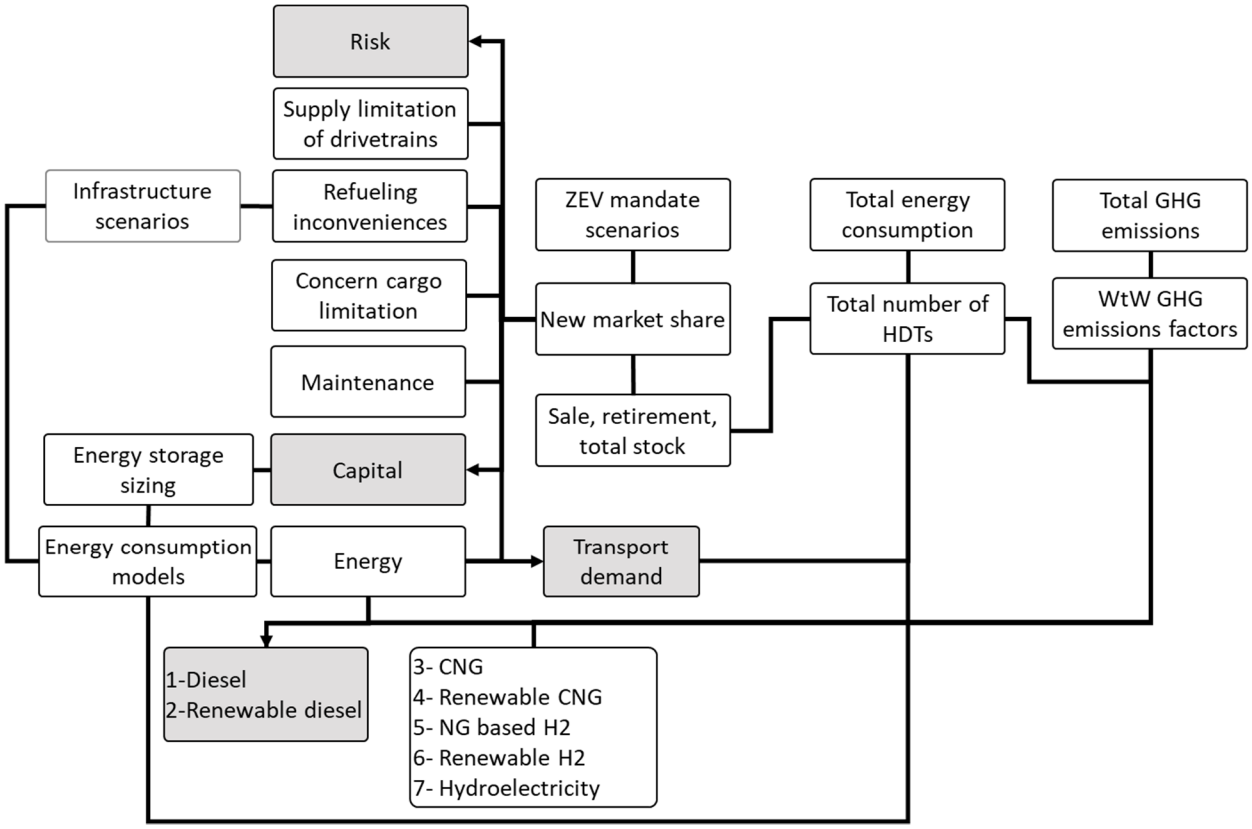

Figure 4-2: Flow chart diagram for CIMS-HDT model (the grey boxes demonstrate endogenous features)

We used Eq. (4-1) from [263], [265] for the projection of new market share of alternative drivetrain HDTs. The new market share function ($MS_j(t)$) captures both financial and non-financial costs of alternative drivetrains during the technology's lifetime (n_j) from a freight operator perspective.

$$MS_j(t) = \frac{\left[CC_j(t)\frac{r}{1-(1+r)^{-n_j}} + MC_j + EC_j(t) + i_j(t)\right]^{-v}}{\sum_{k=1}^{K}\left\{\left[CC_k(t)\frac{r}{1-(1+r)^{-n_k}} + MC_k + EC_k(t) + i_k(t)\right]^{-v}\right\}} \quad 4\text{-}1$$

In Eq. (4-1), $CC_j(t)$, $i_j(t)$, $MC_j(t)$, and $EC_j(t)$ refer to capital cost, intangible cost, maintenance cost, and energy cost of technology, j, in simulation time t, respectively. v is the market heterogeneity parameter, which captures the heterogeneity in consumer preferences towards different technology options emerging in the market. Furthermore, r refers to the private discount rate. The intangible cost refers to the non-financial costs such as risk perception of adopting a given technology.

We assumed that the HDTs sale, retirement, total stock, and cargo mass remain constant during the simulation period (2020-2050). This means transport demand growth only occurs via annual travel distance increase. We applied the transport demand growth for the reference scenario exogenously using Eq. (4-2):

$$D_{REF}(t) = D_{REF}(t_0) \times (1 + GR)^{(t-t_0)} \quad 4\text{-}2$$

$D_{REF}(t)$ is the demand in tkm at any simulation year, t, $D_{REF}(t_0)$ is the assumed demand at the base year of 2015, and GR is the annual growth ratio.

We employed four endogenous dynamic features in CIMS-HDT. The grey boxes in Figure 4-2 shows the relationship of these features with the rest of the CIMS-HDT. First, capital costs decline endogenously based on the accumulation of drivetrain sub-systems (e.g., battery pack). Eq. (4-3) from [263] is used to estimate the endogenous cost decline:

$$CC_k(t) = CC_k(t_0)\left(\frac{N_k(t)}{N_k(t_0)}\right)^{\log_2 PR_k} \quad 4\text{-}3$$

PR_k is the progress ratio for drivetrain sub-system k and $N_k(t_0)$ is the base stock of drivetrain sub-system k at the base year of 2020 (see Table 4-4 in section 2.2.2). Additionally, we model key vehicular components costs (e.g. battery) declining exogenously, consistent with a global trend on their cost reduction. We applied the exogenous and endogenous decline factors for the following drivetrain sub-systems:1) lithium-ion battery, 2) fuel cell stack, 3) hydrogen tank, 4) CNG tank, 5) gas turbine range extender, and 6) electric motors. The overall cost decline is the product of the exogenous and endogenous components. Section 2.2.1 describes the estimation of capital cost for each drivetrain option. The second endogenous feature of CIMS-HDT is applied for a segment of intangible costs called perception of risk (see section 2.2.3 for further details).

The third endogenous feature of CIMS-HDT is used for the transport demand calculation in policy scenarios relative to the baseline scenario. We used Eq. (4-4) from [266] to account for the change in transport demand as the result of price change in the policy scenarios.

$$D_{POL}(t) = D_{REF}(t) \times \left(\frac{\sum\left(LC_j(t) \times St_j(t)\right)_{POL}}{\sum\left(LC_j(t) \times St_j(t)\right)_{REF}}\right)^e \quad 4\text{-}4$$

$D(t)$ is the travel demand (in tkm) at time t, LC_j is the life cycle cost of technology j, St_j(t) is the total stock of technology j at time t, and e is the "own-price" elasticity of demand for tonne

kilometer (TKT). *POL* and *REF* indexes symbolize policy and reference cases, respectively. The fourth dynamic feature of CIMS-HDT is used for calculating the blending percentage of renewable diesel (see section 2.2.4). Overall, we aimed to capture the decision of a freight operator in BC as realistically as possible, which lead us to choose these four endogenous features.

4.3.2 Transport demand in short and long haul market of BC

The Natural Resources Canada (NRCan) database [12] contains recorded freight parameters such as energy and freight demands for the entire HDT sector of BC. We used the Canadian Freight Analysis Framework (CFAF) assumptions to split the NRCan-based HDT data into short and long haul markets [267]. In the CFAF, we considered truck shipments as a proxy for the number of trucks to estimate how many trucks and how much transport demand are associated with short and long haul trucks, using the criteria of 322 km daily range. A shipment was defined as the transport of a single commodity between an origin and a destination [267]. Averaging between groups of trucks and transport volumes originating from BC and those destined for BC, we found around 62.5% and 37.5% of BC HDTs are short and long haul, respectively. Using a similar approach, we found that around 28% and 72% of transport demand is associated with short and long haul, respectively (see Table 4-2).

4.3.3 Model parameters

Table 4-2 summarizes the assumed transport demand, market, and characteristic parameters for the short and long haul diesel-powered HDTs of BC. We selected the average of cargo masses in short and long haul using an iterative trial- and-error method, such that the daily travel distance of long haul double the amount of the short haul to be consistent with the Canadian average [246]. We used an in-house model developed for our previous studies to estimate the energy consumption of all drivetrain options. The model estimates energy consumption by considering several HDT parameters (e.g., aerodynamic drag), drive cycles (that are based on several representative routes of BC), and logic of energy consumption for different technology options [156], [260]. We adjusted the magnitude of the HDT parameters to match with the energy demand of BC's HDTs [12].

Table 4-2: The transport demand, market parameters, and characteristic related assumptions for diesel-powered HDTs in the short and long haul markets of BC.

Items		Short-haul	Long-haul	Source
Demand	HDT Population of BC in 2015	28,125	16,875	[12], [267]
	Annual sale and retirement	1/15 of BC HDTs	1/15 of BC HDTs	[12]
	Transport demand (millions Tonne km)	4,756	12,230	[12], [267]
	Energy demand (PJ) in 2015	16.09	18.35	[12]
Market	Private discount rate	8-28.5%	8-28.5%	[214], [268]
	Annual growth rate	1.3-1.59%	1.3-1.59%	[12], [16], [269]
	Market heterogeneity	7.5-12.51	7.5-12.51	[270]
	Transport Demand elasticity	-0.47 to -0.51	-0.47 to -0.51	[16], [266]
Characteristic	Average daily travel distance (km/d)	103	198.5	
	Average HDT life time	15	15	[119]
	Aerodynamic drag coefficient	0.7	0.6	[57]
	Tractor mass (kg)	5,900	6,600	[260]
	Cargo mass (kg)	4,500	10,000	
	Average of fuel consumption (MJ/km)	15.22	14.2	

We used a Monte Carlo Simulation with a uniform distribution of input parameters to evaluate the impact of uncertainty in results. We considered uncertainty ranges for most of the input parameters. The uncertainty ranges of input parameters are indicated in section 2.2 (see Table 4-2-Table 4-9). We programmed the Matlab code to pick a different set of input parameters for every simulation of market share and GHG emissions. Overall, we applied 20,000 simulations in the Matlab code for the Monte Carlo analysis.

4.3.3.1 Specifications of drivetrain technologies

Table 4-3 summarizes the main specifications of alternative drivetrains considered in this study. The energy consumption and energy storage capacities of drivetrains were estimated using our in-house model [260]. We selected these drivetrains based on our previous findings on their cost effectiveness, GHG emissions reduction, and practicality (i.e., cargo capacity) criteria [260]. For drivetrains with dual fuel consumption (e.g., diesel and electricity), the specific energy consumptions are presented from each source. Additionally, for each drivetrain the energy consumption is presented in separate columns called “Slow” and “Rapid”, which refers to infrastructure scenarios that will be defined in section 2.3.1.

Table 4-3: Specifications of drivetrains for short and long haul market of BC.

Drivetrain	Propulsion system for both Short and Long hauls	Short haul				Long haul				Maintenance ($/km)[C]
		Storage size	Year[A]	Energy (MJ/km)[B]		Storage size	Year[A]	Energy (MJ/km)[B]		
				Slow	Rapid			Slow	Rapid	
Diesel	13 L diesel engine	125 kg diesel	2015	15.22 diesel	15.22 diesel	300 kg diesel	2015	14.2 diesel	14.2 diesel	0.045
CNG	13 L CNG engine	135 kg CNG tank	2020	18.1 CNG	18.1 CNG	330 kg CNG	2020	17.1 CNG	17.1 CNG	0.051
Plug-in hybrid diesel	13 L diesel engine plus 220 kW electric motor	85 kg diesel plus 60 kWh battery	2020	10.1 diesel plus 0.6 electricity (e)	7.3 diesel plus 1.3 e	265 kg diesel plus 60 kWh battery	2020	12.3 diesel and 0.1 e	12.1 diesel and 0.2 e	0.049
Plug-in hybrid CNG	13 L CNG engine plus 220 kW electric motor	95 kg CNG plus 60 kWh battery	2020	12.0 CNG plus 0.6 e	8.6 CNG plus 1.3 e	295 kg CNG plus 60 kWh battery	2020	15.07 CNG and 0.13 e	14.8 CNG and 0.24 e	0.056
Plug-in hybrid diesel catenary	13 L diesel engine plus one 220 kW electric motor	80 kg diesel plus 60 kWh battery	2025	6.78 diesel plus 1.52 e	2.21 diesel plus 3.23 e	-	-	-	-	0.054
Plug-in hybrid CNG catenary	13 L CNG engine plus one 220 kW electric motor	85 kg CNG plus 60 kWh battery	2025	8.20 CNG plus 1.45 e	2.82 CNG plus 3.19 e	-	-	-	-	0.062
Battery electric catenary	4*220 kW electric motors	575 kWh battery	2025	4.4 e	4.4 e	-	-	-	-	0.024
Battery electric	4*220 kW electric motors	600 kWh battery	2025	4.4 e	4.4 e	600 kWh battery	2030	5.9 E	5.9 E	0.022
Fuel cell	4*220 kW electric motors	22 kg H_2 plus 20 kWh battery	2025	6.6 H_2	6.6 H_2	73 kg H_2 20 kWh battery	2030	9.5 H_2	9.5 H_2	0.054
Plug-in hybrid fuel cell	60 kW fuel cell system plus 4*220 kW electric motors	15 kg H_2 200 kWh battery	2025	3.92 H_2 1.99 e	1.55 H_2 3.32 e	34 kg H_2 plus 1000 kWh battery	2030	3.52 H_2 and 3.72 e	0.05 H_2 and 5.66 e	0.054
Plug-in hybrid gas-turbine	80 kW micro gas turbine plus 4*220 kW electric motors	-	-	-	-	162 kg CNG plus 1000 kWh battery	2030	6.63 CNG and 3.7 e	0.1 CNG and 5.66 e	0.04

[A] Adoption year of drivetrain

[B] For Monte Carlo simulation with uniform distribution we assumed 10% uncertainty range for 2020-2030 and then increase to 20% for 2035-2050 period

[C] 40% uncertainty range was assumed for maintenance costs

4.3.3.2 Financial costs

We estimated the capital cost for each technology based on their sub-systems, such as the propulsion system and energy storage sizes, presented in Table 4-3. We used Eq. (4-5) to estimate the capital costs for all HDT options:

$$CC_j(t) = CC_{Base_j}(t_0) + CC_{Engine_j}(t_0) + CC_{Range\_Extender_j}(t) + CC_{Battery_j}(t) + CC_{Transmission_j}(t_0) + CC_{After\_Treatment_j}(t_0) + CC_{Electric\_Motor_j}(t) + CC_{Cattery_j}(t_0) \quad 4\text{-}5$$

We assumed that the costs of the base (tractor glider), engine, and catenary system are constant over the modelling period. However, the range extender (i.e., fuel cell and gas turbine), battery, and electric motors decline both endogenously and exogenously during the simulation period.

Table 4-4 and Table 4-5 display the cost-related parameters used to estimate the capital cost of drivetrain options using Eq.s (4-3) and (4-5). Most parameters in these tables are associated with a lower and upper limit, representing their uncertainty ranges. To calculate the sub-system costs, we considered their initial stock, their price range for the adoption year (2020-2030), as well as their progress ratios, based upon [203], [260], [270]–[274]. Table 4-6 specifies assumed energy costs and their uncertainty ranges during the simulation period. The maintenance cost of each drivetrain is the sum of the specific cost per km provided in Table 4-3 plus a cost related to battery and fuel cell replacement. We assumed a 3 to 10 years uncertainty range for the lifetime of fuel cell and battery packs.

Table 4-4: Assumed dynamic cost-related parameters for capital cost estimations (price in USD$).

Drivetrain	Price range in 2020	Initial stock	Progress ratio (PR)	Exogenous annual decline rate %
Lithium-ion battery	200-300 $/kWh	70,000 MWh	0.91-0.94	3-6%
Electric motor	16-24 $/kW	125,000 MW	0.88-0.92	0.9-1.8%
Hydrogen tank	300-500 $/kg	43,110 kg	0.88-0.92	0.5-1%
Fuel cell system	170-260 $/kW	290 MW	0.75-0.95	2-4%
CNG tank	110-130 $/kg	2.64×108	0.88-0.92	0.5-1%
Micro gas turbine	600-800 $/kW	465 MW	0.75-0.95	0.9-1.8%

Table 4-5: Assumed static cost-related parameters for capital cost estimations (price in USD$) [260]

Component	Price range in 2020
Base (Short-haul)	$75,000-$125,000
Base (Long haul)	$95,000-$145,000
11.9 L NG engine	$8,000-$12,000
13 L diesel engine	$7,000-$11,000
Transmissions for drivetrains with combustion engine	$8,000-$9,000
Transmissions for drivetrains with electric motor as the main driver	$1,500-$2,500
After-treatment for diesel	$4,500-$7,000
After-treatment for CNG	$2,000-$3,000
Catenary system on-board an HDT	$6,000-$7,000
Diesel tank	4-7 $/kg

Table 4-6: The assumed energy costs (in 2020 USD$ per GJ) and their uncertainty ranges.

Fuels	2020		2025		2030		2035		2040		2045		2050		Source
	Low	High	Low	High	Low	High	Low	High	Low	High	Low	High	Low	High	
Diesel	28.7	41.0	24.6	36.3	23.4	34.4	22.5	33.5	21.7	32.6	20.9	33.4	20.3	34.6	[275]
CNG	13.3	16.5	13.3	17.0	13.3	17.4	13.3	17.6	13.1	17.9	13.2	18.0	13.2	18.1	[275]
Renewable CNG	20.8	28.3	25.5	41.5	29.4	54.5	32.9	67.3	36.0	79.9	38.9	92.5	41.6	104.9	[203], [276]
H_2 (NG Reformer)	31.6	47.4	28.8	43.1	25.9	38.9	25.6	38.4	24.7	37.0	23.9	35.9	23.3	35.0	[203]
H_2 (Electrolysis)	56.3	84.4	48.7	73.0	41.1	61.6	40.4	60.6	38.2	57.3	36.4	54.7	35.0	52.5	[203]
Electricity	20.5	29.2	21.0	30.2	21.4	31.2	21.5	31.4	21.7	31.8	21.9	32.2	22.0	32.5	[275]
Renewable diesel	29.7	44.5	26.3	39.4	22.9	34.4	22.5	33.8	21.5	32.2	20.7	31.0	20.0	30.0	[203]

4.3.3.3 Non-financial (intangible) costs

Intangible costs account for the non-financial costs perceived by a freight operator when making decision to purchase a HDT with new drivetrain technology. Based on the reviewed studies we disaggregate this cost into four categories: supply limitation of drivetrains, refueling inconveniences, perception of risk, and concern of cargo limitation [8], [20], [21], [152], [277]. Both refueling inconvenience and supply limitation of drivetrains were set exogenously since these factors are beyond the control of freight operators in the study region of BC. Eq. (4-6) was used to estimate the total intangible cost of each alternative drivetrain.

$$i_j(t) = i_{F_j} + i_{Ex_j}(t) + i_{En_j}(t) \quad \text{4-6}$$

i_{F_j} is the fixed intangible cost related to the cargo limitation, $i_{Ex_j}(t)$ is the sum of refueling inconveniences and the supply limitation of drivetrains. Eq. (4-7) from [21], [277] was used to calculate these costs:

$$i_{Ex_j}(t) = \left(\frac{1}{2}\right)\frac{TD}{R_j} \times w \times RT_j \times SA_j(t) - C_1 \times log\left(\frac{n_j(t)}{N}\right) \quad \text{4-7}$$

TD is the annual travel distance, *R* is the range, *w* is the hourly wage of a truck driver, *RT* is the refueling time multiplier, *SA* is the station availability multiplier, $n_j(t)/N$ is the model availability multiplier, and C_1 is a constant. In Eq. (4-7) the first and second terms, respectively, represent the refueling inconveniences and the supply limitation of drivetrains. We assumed 40 $/hour for driver wage from [21] with 40% uncertainty range. Table 4-7 presents the station availability and model availability multipliers applied to each refueling infrastructure and drivetrain option during the simulation period. The "Slow" and "Rapid" labels in this table refer to the infrastructure roll-out scenarios that will be defined in section 2.3.1. We assumed 100% uncertainty range for the model availability multipliers.

Table 4-7: Assumed station (SA) and model availability (nj/N) multipliers for alternative drivetrain HDTs in short and long haul markets.

Multipliers	Fuel option/Drivetrains		2020		2025		2030		2035		2040		2045		2050	
			Slow	Rapid	Slow	Rapid	Slow	Rapid	Slow	Rapid	Slow	Rapid	Slow	Rapid	Slow	Rapid
Station availability multipliers	CNG	Short	2.5	2.5	2.5	2.5	2.5	2.5	2.5	2.5	2.5	2.5	2.5	2.5	2.5	2.5
		Long	5	5	5	5	5	5	5	5	5	5	5	5	5	5
	H_2	Short	11	11	11	11	11	11	11	6	11	1	11	1	11	1
		Long	22	22	22	22	22	22	22	11.5	22	1	22	1	22	1
	Electric charger	Short	3	3	3	3	3	3	3	2	3	1	3	1	3	1
		Long	5	5	5	5	5	5	5	3	5	1	5	1	5	1
	Catenary		8	8	8	8	8	8	8	4.5	8	1	8	1	8	1
Model availability multipliers	CNG	Short	0.4		0.5		0.6		0.7		0.8		0.9		1	
		Long	0.25		0.35		0.45		0.55		0.65		0.75		0.85	
	Plug-in hybrid diesel	Short	0.15		0.2		0.25		0.30		0.35		0.40		0.45	
		Long	0.15		0.25		0.35		0.45		0.55		0.65		0.75	
	Plug-in hybrid CNG	Short	0.1		0.15		0.2		0.25		0.3		0.35		0.4	
		Long	0.15		0.25		0.35		0.45		0.55		0.65		0.75	
	Battery electric	Short	0.4		0.5		0.6		0.7		0.8		0.9		1	
		Long	0.22		0.34		0.46		0.58		0.7		0.82		0.94	
	Plug-in hybrid fuel cell	Short	0.2		0.3		0.4		0.5		0.6		0.7		0.8	
		Long	0.22		0.34		0.46		0.58		0.70		0.82		0.94	
	Fuel cell	Short	0.2		0.3		0.4		0.5		0.6		0.7		0.8	
		Long	0.22		0.34		0.46		0.58		0.70		0.82		0.94	
	Plug-in hybrid diesel catenary (short haul)		0.1		0.15		0.2		0.25		0.3		0.35		0.4	
	Plug-in hybrid CNG catenary (short haul)		0.1		0.15		0.2		0.25		0.3		0.35		0.4	
	Battery electric catenary (short haul)		0.15		0.2		0.25		0.30		0.35		0.40		0.45	
	Plug-in hybrid Gas Turbine (long haul)		0.13		0.21		0.29		0.37		0.45		0.53		0.61	

For a drivetrain with more than one station usage (e.g., CNG and charger stations in the case of plug-in hybrid CNG) the station availability multiplier was assumed to be the average of station availability multipliers related to each drivetrain power source. We assumed 3.5-4.5 times higher SA availability for hydrogen station comparing to the charging station since we assumed transmitting and distributing of hydrogen is much more challenging than electricity. Furthermore, electricity networks currently are available almost everywhere, which could lead to the roll-out of charging infrastructure with fewer barriers. We used Eq. (4-8) to make the cost associated with the perception of risk endogenous to model. This cost declines over time with increases in market share of technology *j* (i.e., as freight operators gain familiarity with new technologies).

$$i_{En_j}(t) = \frac{i_{R_j}(t_0)}{1 + Ae^{B \times MS_j(t-1)}} \quad \text{4-8}$$

$i_{R_j}(t_0)$ indicates the initial intangible cost at the base year, A (equal to 0.0065) and B (equal to 40) are fixed parameters that determine the shape of intangible cost function [214], [259], and $MS_j(t-1)$ is market share of technology at previous simulation step.

We used Eq. (4-9) to account for the cost associated with the concern of cargo limitation, which was estimated by profit loss due to the reduction in cargo capacity:

$$i_{F_j} = C_2 \times TD \times M \times \left(1 - CL_j\right) \quad \text{4-9}$$

C_2 is the average of freight company profit in $/tkm, TD is the annual travel distance, CL_j is the relative cargo capacity of alternative drivetrain j compared to the baseline diesel, and M is the cargo mass (tonne). The average freight revenue per truck is around USD$0.11/tkm according to the US DOT and we assumed 30% of the revenue is the net profit [278]. We estimated the CL_j factor for each drivetrain option from [260]. Table 4-8 presents the cargo capacity (CLj) and refueling time multipliers relative to diesel as well as the cost related to the perception of risk. We assumed 100% uncertainty range for the risk-related costs. Whenever possible, we selected the magnitude of parameters for estimating the intangible costs consistent and proportionate with the relevant literature [21], [277]. Otherwise, we used our best judgment in assuming the intangible cost parameters and their uncertainty ranges.

Table 4-8: Assumed cargo capacity (CLj) and refueling time (RTj) multipliers for alternative drivetrain HDTs in short and long haul markets.

Drivetrains		Cargo capacity relative to diesel (CLj)	Refueling time relative to diesel (RTj)	Perception of risk in 2020 ($) ($i_{R_j}(t_0)$)
CNG	Short	1	1-1.2	0
	Long	0.99	1-1.2	10,000
Plug-in hybrid diesel	Short	0.99	1-2.5	10,000
	Long	0.99	1-3	30,000
Plug-in hybrid CNG	Short	0.99	1-3	20,000
	Long	0.98	1.5-3.5	40,000
Battery electric	Short	0.93	3-10	40,000
	Long	0.67	3-10	50,000
Plug-in hybrid fuel cell	Short	0.97	1.5-5	50,000
	Long	0.84	1.5-5	60,000
Fuel cell	Short	1	1-1.5	30,000
	Long	0.96	1-1.5	40,000
Plug-in hybrid diesel catenary		0.99	1-2.5	20,000
Plug-in hybrid CNG catenary		0.99	1-3	40,000
Battery electric catenary		0.98	1.5-5	60,000
Plug-in hybrid Gas Turbine		0.79	1.5-5	40,000

4.3.3.4 Well-to-wheel GHG emissions

The well-to-wheel (WTW) GHG emissions refers to the emissions produced through vehicle operation stage and fuel production [137]. In each time frame, the net GHG emissions ($GHG_{Net}(t)$) in Mt CO_{2e} was calculated using Eq. (4-10):

$$GHG_{Net}(t) = 10^{-12} \times TD(t) \times \left[GHG_D(t) \times \left[\left(St_{old-D}(t) \times FC_D(t_0) \right) + \left(St_{new-D}(t) \times FC_D(t) \right) \right] + \sum_{k=1}^{n} GHG_k(t) \times \left(\sum_{j=1}^{m} FC_j(t) \times St_j(t) \right) \right] \quad 4\text{-}10$$

$TD(t)$ is the annual travel distance in km, $GHG_D(t)$ is the diesel WTW GHG emission factor in g CO_2/MJ in each time frame, $FC_D(t_0)$ is the fuel consumption of diesel drivetrain in MJ/km unit in the base year of 2020, $St_{old-D}(t)$ is the remaining stock of diesel HDTs, $St_{old-D}(t)$ is the stock of new diesel HDTs, $GHG_k(t)$ is WTW emissions of various fuels including electricity, diesel, hydrogen, and CNG in g CO_2e/MJ. Table 4-9 presents the assumed range of WTW GHG emissions factors for various fuel supplies.

Table 4-9: Considered range of well to wheel GHG emissions by various fuels

Drivetrain	equivalent CO_2e (g/MJ)	Sources
Diesel	91-8-94.76	[16], [279]
Renewable diesel (HDRD)	16.39-53.7	[16]
Conventional natural gas (CNG)	63.04-79.6	[16], [279], [280]
Renewable natural gas (RNG)	7.33-30.8	[280]
BC electricity mix: 95% Hydroelectricity and 5% natural gas	7.2-19.73	[16], [279]
Hydrogen (Reformer natural gas)	96.82-106.1	[16], [279]
Hydrogen (Hydroelectricity)	11.2-37.43	[16], [279]

Currently, renewable diesel is a key fuel in compliance with BC's Low-carbon Fuel Standard (LCFS) [281] as its application does not require any change in the current fuel system, drivetrains, or any additional infrastructure. Therefore, we assumed that renewable diesel is blended with diesel to comply with BC's LCFS. In addition to the blending percentage that was set exogenously, the blended diesel was assumed to compete with pure renewable diesel endogenously. Eq. (4-11) from [16] was used to determine the market share of blended diesel and pure renewable diesel:

$$MS_{RD}(t) = \frac{(EC_{RD}(t) + i_{RD}(t))^{-v}}{\sum(EC_K(t) + i_K(t))^{-v}} \qquad 4\text{-}11$$

$MS_{RD}(t)$ is the market share of renewable diesel in time t, EC_{RD} is the cost of renewable diesel, and i_{RD} is the intangible cost of renewable diesel. The market heterogeneity parameter (v) reflects the preferences of a freight operator for supporting the environment by using renewable diesel. The intangible cost of renewable diesel was selected to have a mean of 70% market share of renewable diesel by 2050. The renewable content for natural gas and hydrogen was set exogenously as they are gaseous fuels and the choice of using renewable or conventional appears to be beyond the control of a freight operator.

Renewable natural gas (RNG) is biomethane, which in the short term can be produced via anaerobic digestion of organic waste and landfill gas. The long term RNG potential in BC was estimated to be 93.6 PJ (i.e. 27% of the current BC natural gas demand) mainly from gasification of woody biomass [242], [282]. Therefore, we assumed renewable natural gas (RNG) is blending at an increasing percentage over time starting at 1% in 2020 and reaches the maximum blending percentage of 27% by 2050. Although, the majority of the long term potential sourced from

gasification of woody biomass, we assumed its GHG emissions intensity to be identical with the short term anaerobic digestion and landfill gas sources.

For 2020, it was assumed hydrogen is only available via the reforming process since the majority of current US demand is supplied through the reforming of natural gas [283]. We assumed the reforming process is gradually substituted by the electrolysis process until 2050 in which the entire hydrogen demand is renewable.

4.3.4 Scenarios

4.3.4.1 Infrastructure roll-out scenarios

Infrastructure is the fundamental factor determining the diffusion of alternative drivetrains vehicles [252]. It is most likely that refueling infrastructure that supports alternative drivetrains for HDTs will be rolled out in multiple development stages [284]. We assumed three stages of development. Figure 4-3 presents a conceptual framework for each infrastructure development stage.

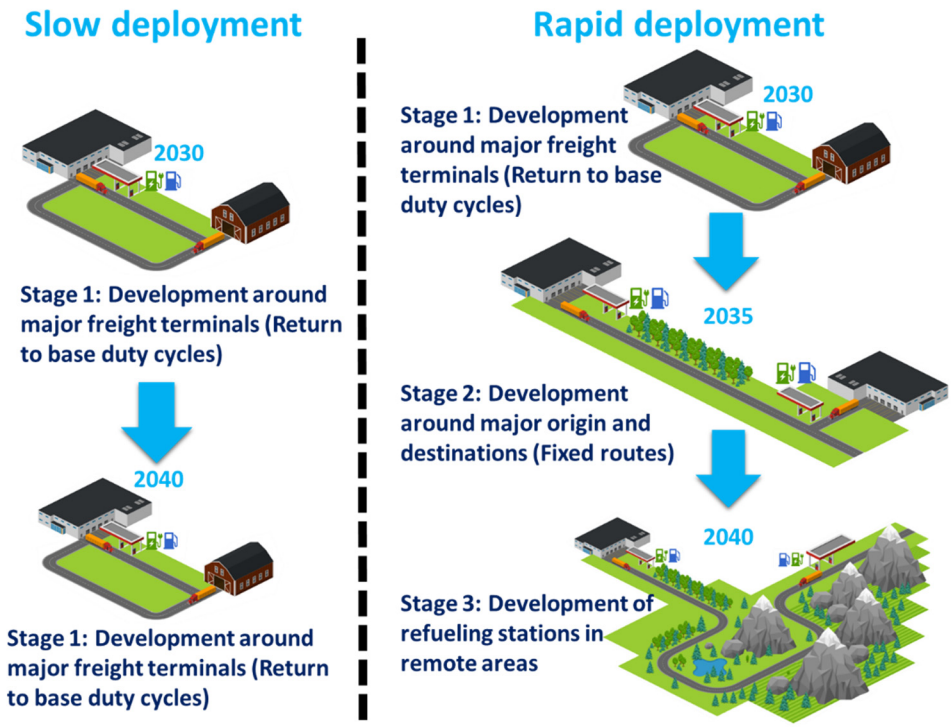

Figure 4-3: Conceptual framework of slow and rapid infrastructure deployment pathways (the picture was produced via https://icograms.com).

We assumed the first stage is a sporadic development around a few major freight terminals of BC. The low density of refueling infrastructure in the first stage means that they can only serve a limited number of alternative drivetrains HDTs such as those with “return to base”

duty cycles. We assumed that the second phase of development is associated with development around major origin and destinations. The second phase of development could be more suitable for those HDTs with fixed routes. We assumed the third phase of development involves the availability of refueling stations to be on par with diesel. Currently, diesel is available in 50 different locations across BC for commercial HDTs [285]. We assume all roll-out scenarios initiate in stage one of development by 2030. We consider several roll-out scenarios during 2030 to 2040 as follows:

1. **Slow deployment of all stations** in both short and long haul markets, meaning that all alternative refueling options remain in stage one during the simulation period. We assume battery chargers, hydrogen, and CNG are available in only 1-2 locations for both short and long haul markets. Additionally, we assumed the catenary installation is only available for 8 km.
2. **Rapid deployment of all stations** (except for CNG station) in both short and long haul markets, meaning by 2040, the stage of infrastructure development is changing from stage one to three for charger, hydrogen, and catenary infrastructure. The catenary in the third stage is available for 265 km across major freight routes in Metro Vancouver obtained from [101].
3. **Rapid deployment of charging stations** in both short and long haul markets, meaning by 2040 coverage of chargers increases to be on par with diesel while the development of other refueling options remains in stage one.
4. **Rapid deployment of H_2 stations** in both short and long haul markets, meaning by 2040, coverage of H_2 stations is in par with diesel, while the development of other refueling options remains in stage one.
5. **Rapid deployment of charging stations and catenary** infrastructure in short haul market, meaning by 2040 coverage of chargers is on par with diesel and catenary installation is available for 265 km, while the development of other refueling options remains in stage one.

We translated each of these scenarios into different intangible costs and specific energy consumptions. The translation of intangible cost was implemented via variable refueling inconveniences costs related to the “Slow” and “Rapid” deployment scenarios (see station availability (SA) multipliers in Table 4-7). Second, the fuel consumptions of drivetrains have improved in “Rapid” scenarios for plug-in hybrids as the result of more catenary line coverage

and considering two charging events per day (see Table 4-3). For example, in "Rapid deployment of H_2 stations" we implemented the SA of fuel cell from the "Rapid" column of Table 4-7, while for other drivetrains the SAs were considered from the "Slow" column.

4.3.4.2 Ambitious ZEV mandate scenarios

We considered ZEV drivetrains to be all plug-in electric, catenary, and hydrogen-powered options. Therefore, in short and long haul there are 8 and 6 ZEV drivetrains, respectively. The assumed ZEV requirement starts at 25% in 2025 and increases by 25% for every 5 years until reaches 100% of sale by 2040, and then remains constant until 2050. We assumed two ambitious ZEV scenarios: one that constrains plug-in hybrid electric vehicles (PHEVs) that emit tailpipe CO_2 and the other without any limitation. These scenarios are as follows:

1. **Constraining the PHEVs** scenario in which we assumed (consistent with California ZEV mandate) at least 45% of ZEV sales in each time frame should be non-PHEV ZEVs [286]. The non-PHEV ZEVs for both short and long haul were battery electric, plug-in hybrid fuel cell, and fuel cell. Battery electric catenary is other non-PHEV ZEV that was only applicable to short haul.
2. **Without constraining PHEVs** with tailpipe emissions.

We combined the ambitious ZEV policy with a weak complementary policy including a carbon tax, a LCFS, and a fuel economy standard. We assumed a constant carbon price of $50 /tonne CO_2e during the simulation period. We considered a 10% reduction in the carbon intensity of diesel for 2020-2030 and then increasing to 15% for the 2030-2050 period. As stated earlier we assumed meeting the LCFS is obtained via blending with renewable diesel. For the fuel efficiency standard, we assumed the specific energy consumption of all drivetrains relative to their initial magnitudes improved by 16%, 20%, and 24% corresponding to 2020-2025, 2025-2030, and 2030-2050 periods.

4.4 Results

The section presents the study results including: 1) the emerging ZEV drivetrains in the short and long haul market corresponding to the infrastructure roll-out scenarios; 2) the probability of meeting the 80% GHG emissions reduction target for 2050 in the short and long

haul HDT markets; and 3) the projection of energy demand from various sources corresponding to the roll-out scenarios.

4.4.1 Dominant drivetrains in short haul

Figure 4-4 presents the mean of 20,000 Monte Carlo simulations for new market shares calculation in the short haul market, in combination with various infrastructure roll-out and ZEV sale scenarios during 2015 to 2050. Considering those drivetrains that are capturing 80% market share in 2050 as the winning criteria, fuel cell is among winning drivetrains in 6 scenarios. These scenarios are slow and rapid deployment of all stations as well as rapid deployment of hydrogen stations, all of them with and without PHEVs sales constraint. When fuel cell is winning, it captures 15-89% market share in 2050, which the highest occurs in rapid hydrogen stations deployment with the PHEVs sales constraint. The lowest value of 15% is related to slow deployment of all stations scenario when there is not any constraint on PHEVs sales. Plug-in hybrid fuel cell with around 18% mean market share appears as the third winning option in 2050 under rapid deployment of all stations scenarios (with and without PHEVs sale constraint).

Battery electric emerges as winner in all scenarios except in rapid hydrogen deployment scenarios. The range of mean market share for battery electric in winning scenarios is %19-87%. Similar to fuel cell, the lowest market share value is related to the scenario with slow deployment of all stations and without any constraint on PHEVs sales. Plug-in hybrid diesel emerges as winner in 4 scenarios including slow deployment of all station with and without constraint, rapid deployment of charging stations without constraint, and rapid deployment of charging stations and catenary installations without constraint. In these scenarios by 2050 plug-in hybrid diesel as a winner captures 20-41% market share. Plug-in parallel hybrid CNG only in one scenario of slow deployment of all stations and without PHEVs sales constraint appears as winner with 12% market share.

In all deployment scenarios, catenary drivetrains do not emerge as a winner. Even when there is support for catenary and charging stations, catenary drivetrains market share does not exceed 5.5%. The plug-in parallel hybrid diesel catenary captures this highest market share under slow deployment of all station scenario when there is not any constraint.

Overall, the last three scenarios at the bottom of the figure seem rather intuitive. This means when the deployment push is toward charging stations, more battery electric drivetrains

could be expected. Additionally, more hydrogen powered drivetrains is expected to be among winners with favorable hydrogen stations deployment conditions. In the slow and rapid deployment of all stations scenarios, there is an uneven split between market share of battery electric, fuel cell, plug-in hybrid fuel cell, and plug-in hybrid diesel.

Figure 4-5 presents the breakdown of annualized life cycle cost for all considered drivetrains in the short haul market under rapid deployment of all stations scenarios in 2030 and 2050 timeframes. This figure could help to interpret the market share results demonstrated in Figure 4-4. For example, fuel cell is leading the market with 54-52% of sales compared to battery electric with 24-25% of sales under rapid deployment of all stations. The reason is mostly related to a substantial reduction in refueling inconveniences cost for hydrogen stations in 2050. Charging time is an important factor contributing to that cost and even in 2050, the charging time is still assumed much higher for battery electric, which makes it less competitive than fuel cell.

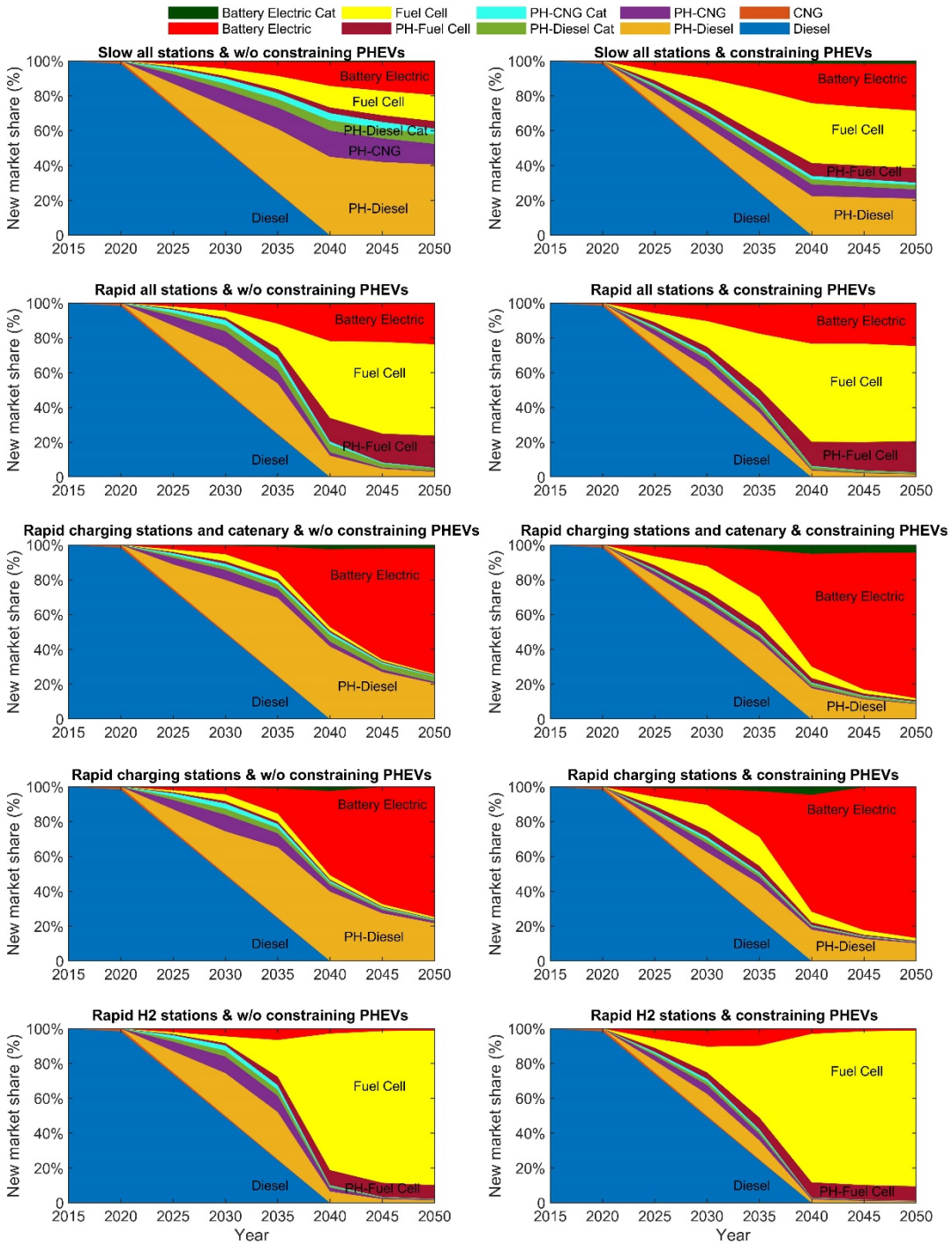

Figure 4-4: The mean of new market share for short haul market under ambitious ZEV mandates and various infrastructure roll out scenarios.

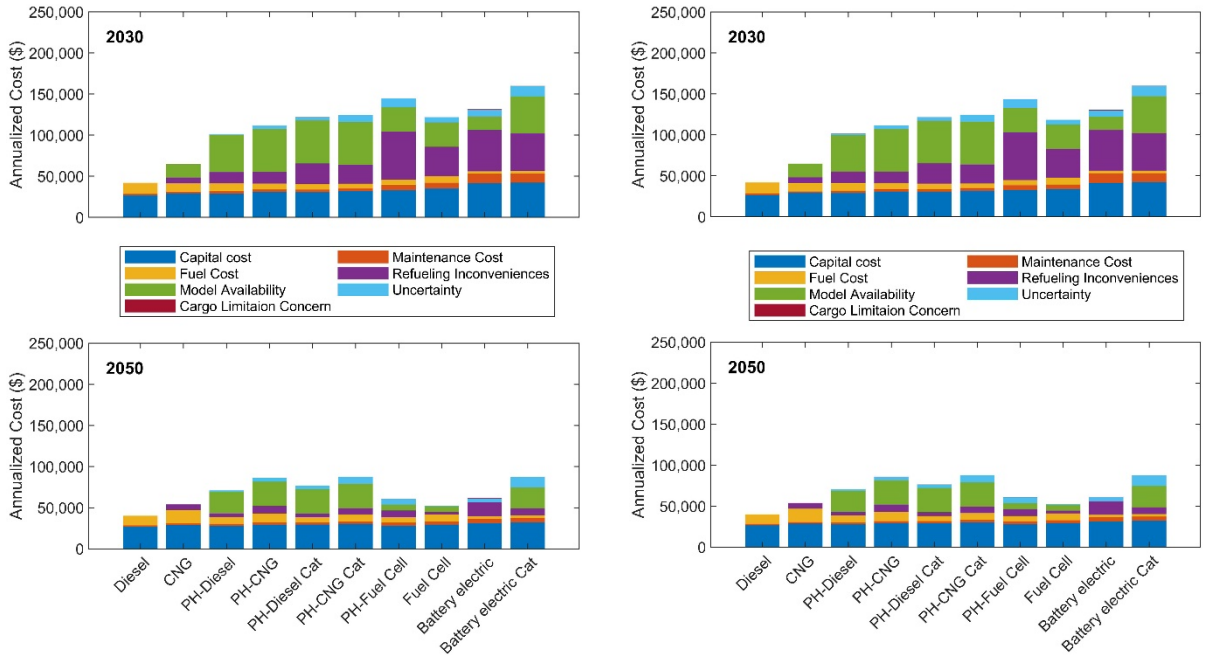

A) Without constraining PHEVs **B)** With constraining PHEVs

Figure 4-5: The breakdown of costs in short haul market under rapid deployment of all stations in 2030 and 2050 timeframes.

Figure 4-6 presents the uncertainty ranges in the market share of the ZEV drivetrains in the short haul market for 2050 with respect to various infrastructure roll-out and ZEV sale scenarios. These drivetrains are sorted by their median values, based on the slow deployment of all stations scenario when there is a constraint on PHEVs sales. For each drivetrain, the box represents the range between 25% and 75% of simulated new market shares. Furthermore, the whiskers indicate 5% and 95% of simulated new market shares. The square marker and the notch on each box plot represent the mean and median values, respectively.

Fuel cell appears to be dominant for close to 100% of simulations under the rapid deployment of hydrogen stations scenarios (with and without PHEVs sales constraint). Fuel cell also dominates in 5-8% of simulations in rapid deployment of all station scenarios (with and without PHEVs sales constraint). In comparison battery electric is 100% dominant in rapid charging and rapid charging and catenary scenarios when there is the PHEVs sales constraint. It is interesting that while battery electric 100% domination is depending to the PHEVs sales constraint, fuel cell (under rapid hydrogen deployment) is 100% dominated regardless of the constraint. This is again related to the lower refueling inconveniences cost of fuel cell. In the rapid charging and rapid charging and catenary scenarios when there is no constraint, battery

electric dominates for around 50% of simulations. Battery electric also is slightly dominant for around 1-10% of simulations in slow deployment of all station scenarios.

In all scenarios (except for the rapid H_2 station deployment), battery electric seems to a have higher uncertainty range than other drivetrains. It seems when constraining PHEVs sale, the range of uncertainties for winning drivetrains are decreasing. Among winning drivetrains, the highest uncertainty range is for battery electric with 95.4% related to the rapid deployment of charging and catenary infrastructure without constraining PHEVs sale. Although fuel cell is leading in the rapid all stations scenarios, it has a very high uncertainty range of 5-94% compared to the fuel cell in the rapid H_2 stations scenario with a 58-99% uncertainty range.

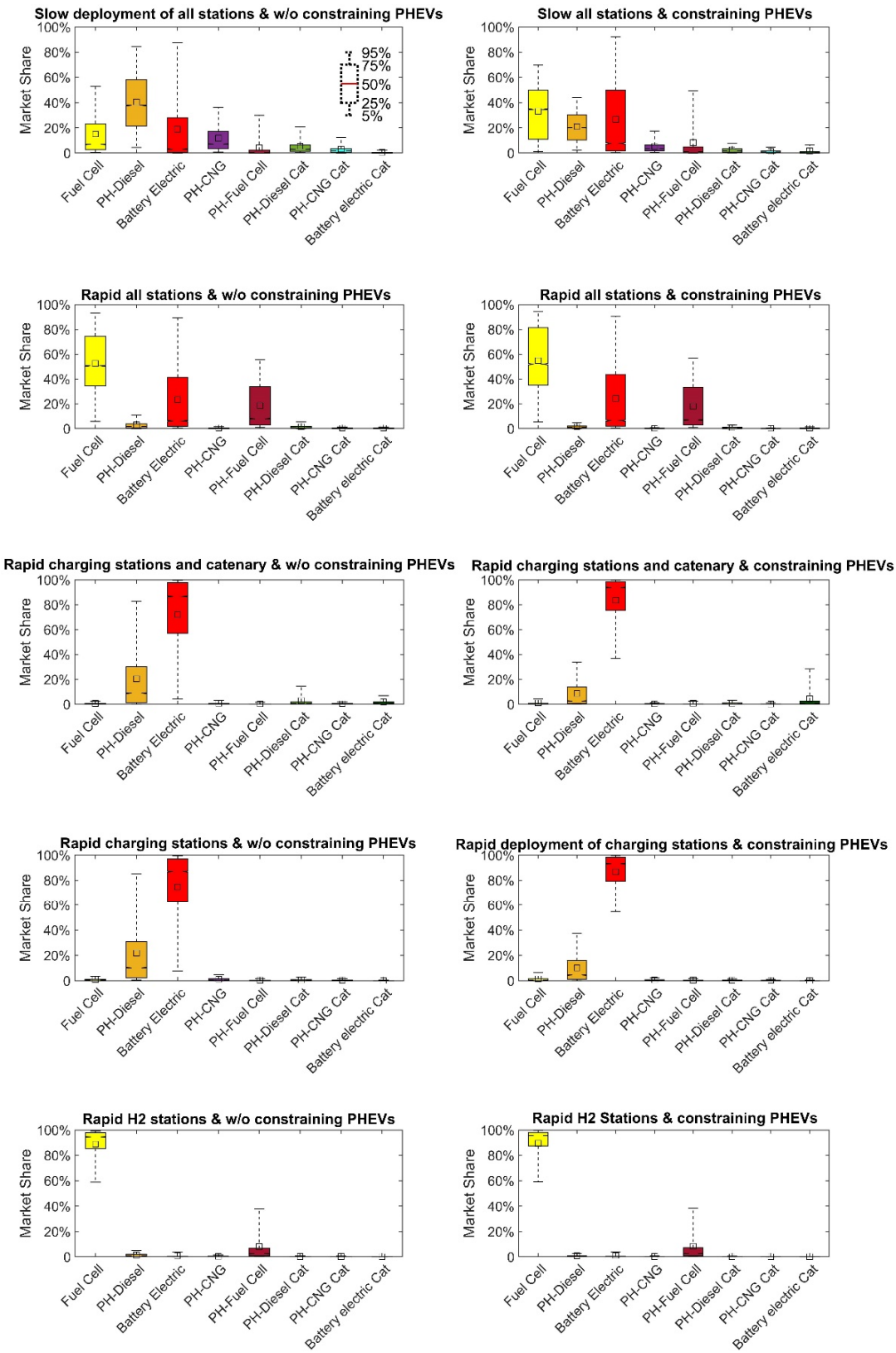

Figure 4-6: The uncertainty range of winning ZEV drivetrains for short haul HDTs in 2050 under ambitious ZEV mandate and infrastructure roll out scenarios.

4.4.2 Dominant drivetrains in long haul

Figure 4-7 presents the mean values of new market shares of drivetrains based on 20,000 Monte Carlo simulations in the long-haul market with the ambitious ZEV sale requirements in combination with various infrastructure roll-out scenarios during 2015 to 2050. Considering those drivetrains capturing 80% market share in 2050 as the wining criteria, the plug-in hybrid diesel drivetrain emerge as a winner in all scenarios with 2050 mean market share of 18-94%. The lowest market share value of 18% is related to the rapid deployment of hydrogen station when there is a constraint on PHEVs sales.

Battery electric is winner with 43% mean market share in only one scenario of rapid deployment of charging stations when there is a constraint of PHEVs sales. Furthermore, in the slow roll-out of all stations when there is a constraint on PHEVs sales, battery electric drivetrains obtain slightly more market share than in rapid roll-out of all stations scenario. This means, when stations are at slow pace of development, more plug-in hybrids and battery electric can be seen and when more stations are available the share is substituted by fuel cell drivetrains with fewer refueling inconveniences costs.

Fuel cell appears as winner in 5 scenarios with 2050 mean market share of 27-78%. These scenarios include: slow deployment of all stations with PHEVs sales constraint, rapid deployment of all stations with and without constraint, and rapid deployment of hydrogen stations with and without constraint. The lowest market share of 27% is associated with scenario of rapid deployment of all stations without constraint on PHEVs sales. In all scenarios, plug-in hybrid fuel cell does not emerge as winner. The highest captured mean market share for plug-in hybrid fuel cell is 8.7%, which is under rapid deployment of all stations with constraint on PHEVs sales. Similar to short haul for 2050 in the rapid all station scenario with constraint on PHEVs sales, fuel cell drivetrain is leading with 57% sale compared to plug-in hybrid diesel with around 30% sales. However, the fuel cell loses its competitiveness when there is not a constraint on PHEVs sales.

In all scenarios, the gas turbine does not emerge as a winning drivetrain and its 2050 market share does not exceed 0.9%. Plug-in hybrid CNG also never appears as winner. However, it captures up to 11% mean market share by 2050, which the highest is under slow deployment of all stations without constraint on PHEVs scenario.

Figure 4-8 presents the breakdown of life cycle cost for all long haul drivetrains in 2030 and 2050 timeframes, which could be helpful to interpret the obtained mean market share results in long haul. For example, the interpretation for very low market share of gas turbine drivetrain in all scenarios is mainly due to the intangible and the capital cost assumptions. The intangible costs are related to the costs of model availability, refueling inconveniences, and concern of cargo limitations assumptions that significantly reduces the competitiveness of this drivetrain. The high cost of refueling inconvenience in 2050 for this drivetrain is due to the fact that we assumed the deployment of CNG stations remains unchanged during the simulation period.

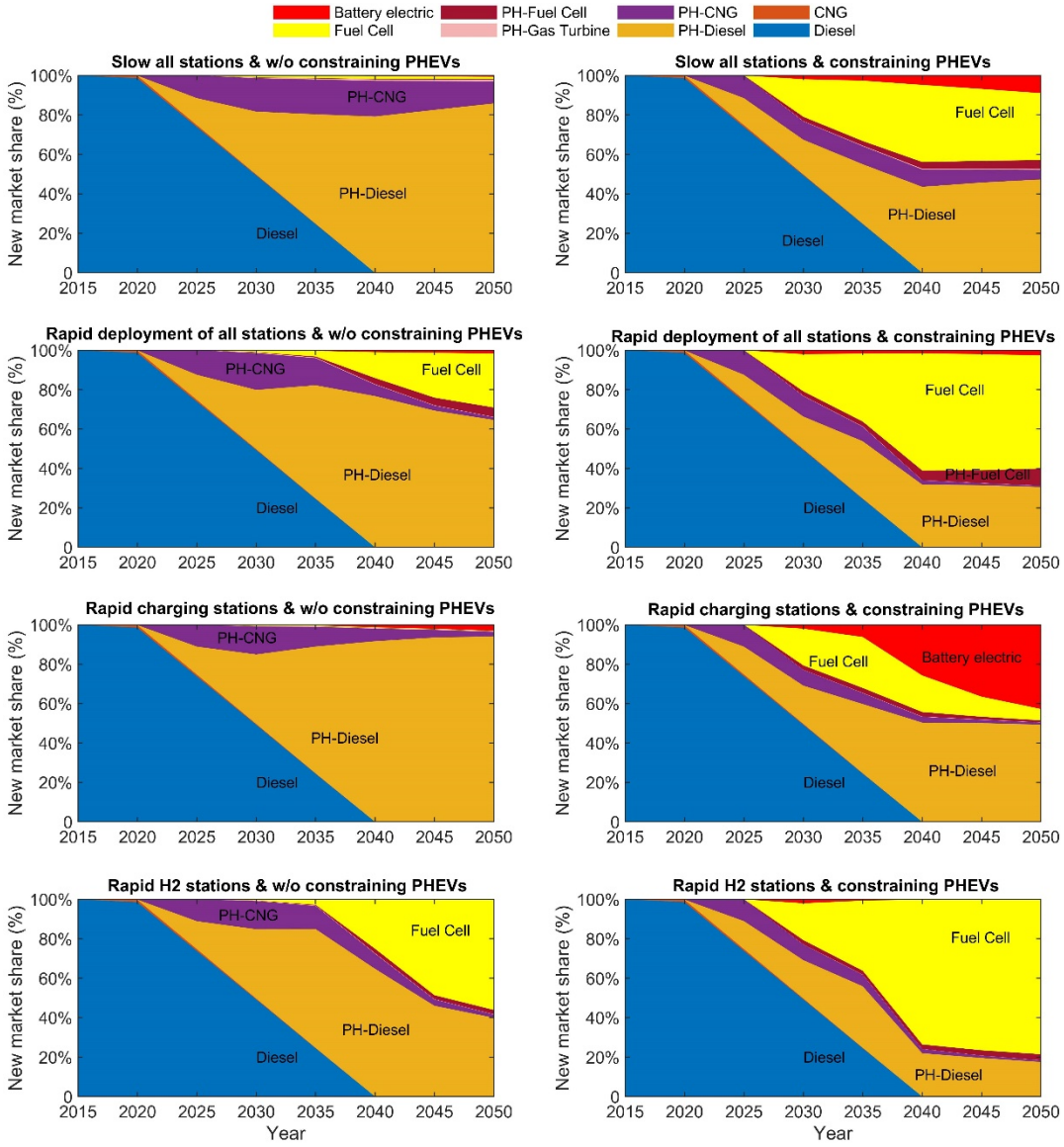

Figure 4-7: The mean of new market share for long haul HDTs under ambitious ZEV mandate and various infrastructure roll out scenarios.

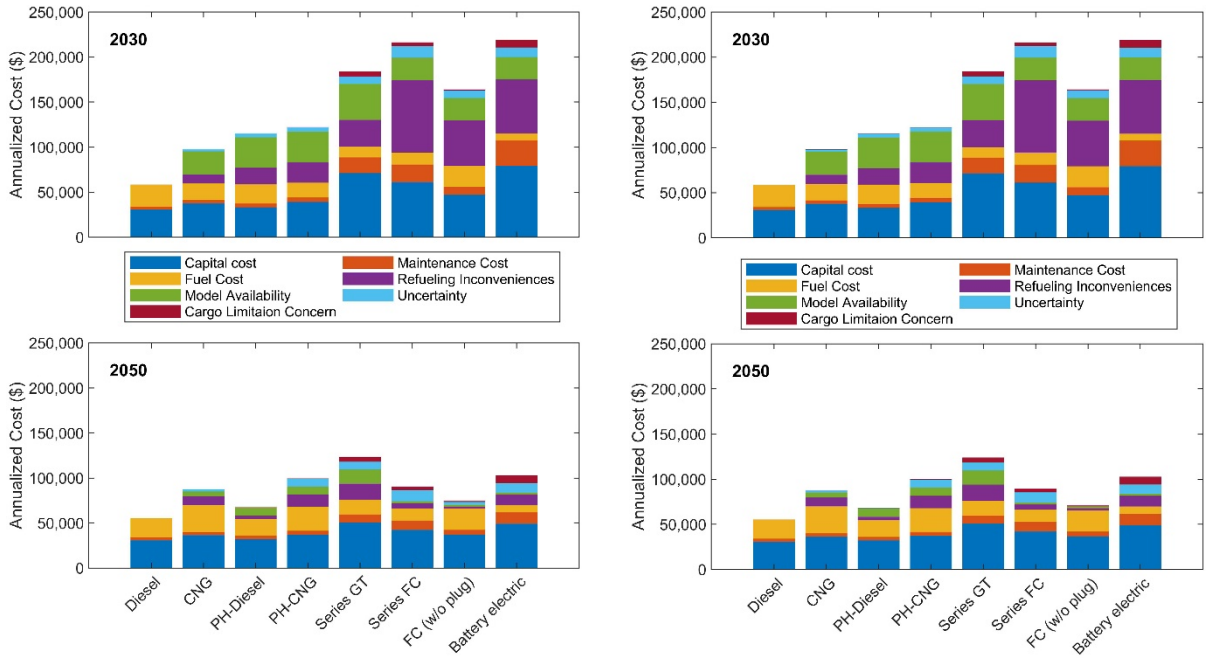

A) Without constraining PHEVs **B)** With constraining PHEVs

Figure 4-8: The breakdown of costs in long haul market under rapid deployment of all stations.

Figure 4-9 presents the uncertainty range of the ZEV drivetrains in the long-haul market for 2050 with respect to various infrastructure roll-out and ZEV sales scenarios. Similar to short haul they are sorted by their median values, based on the slow infrastructure roll-out scenario when there is a constraint on PHEVs sales. Furthermore, for each drivetrain, the box and whiskers represents the range of 25-75% and 5- 95% of simulated new market shares respectively. The square marker and the notch on each box plot represent the mean and median values, respectively.

Plug-in hybrid diesel in most of the scenarios obtains the highest chance to become a winning drivetrain. Plug-in hybrid diesel also appears to be around 100% dominated in two scenarios without PHEVs sales constraint including slow deployment of all stations and rapid deployment of charging stations. Plug-in hybrid diesel also captures partial domination in 54% and 61% of results under rapid deployment of all stations without PHEVs sale constraint and slow deployment of all stations with PHEVs sale constraint respectively.

Fuel cell captures around 100% domination in only one scenario of rapid deployment of hydrogen stations with constraint on PHEVs sales. Fuel cell also dominates in 77% and 3% of

simulations under rapid deployment of all stations with the PHEVs sales constraint and rapid hydrogen deployment without constraint scenarios respectively.

Comparing this figure with the short haul results, lower uncertainty ranges for the long haul scenarios are noticeable. Unlike short haul fuel cell that is 100% dominated under the favorable rapid hydrogen deployment scenarios regardless of the PHEVs sales constraint, the long haul fuel cell is only dominated when there is a constraint on the PHEVs sales. Among winning drivetrains, the highest uncertainty range is for plug-in hybrid diesel with 64% related to the rapid all stations deployment without constraining PHEVs sale.

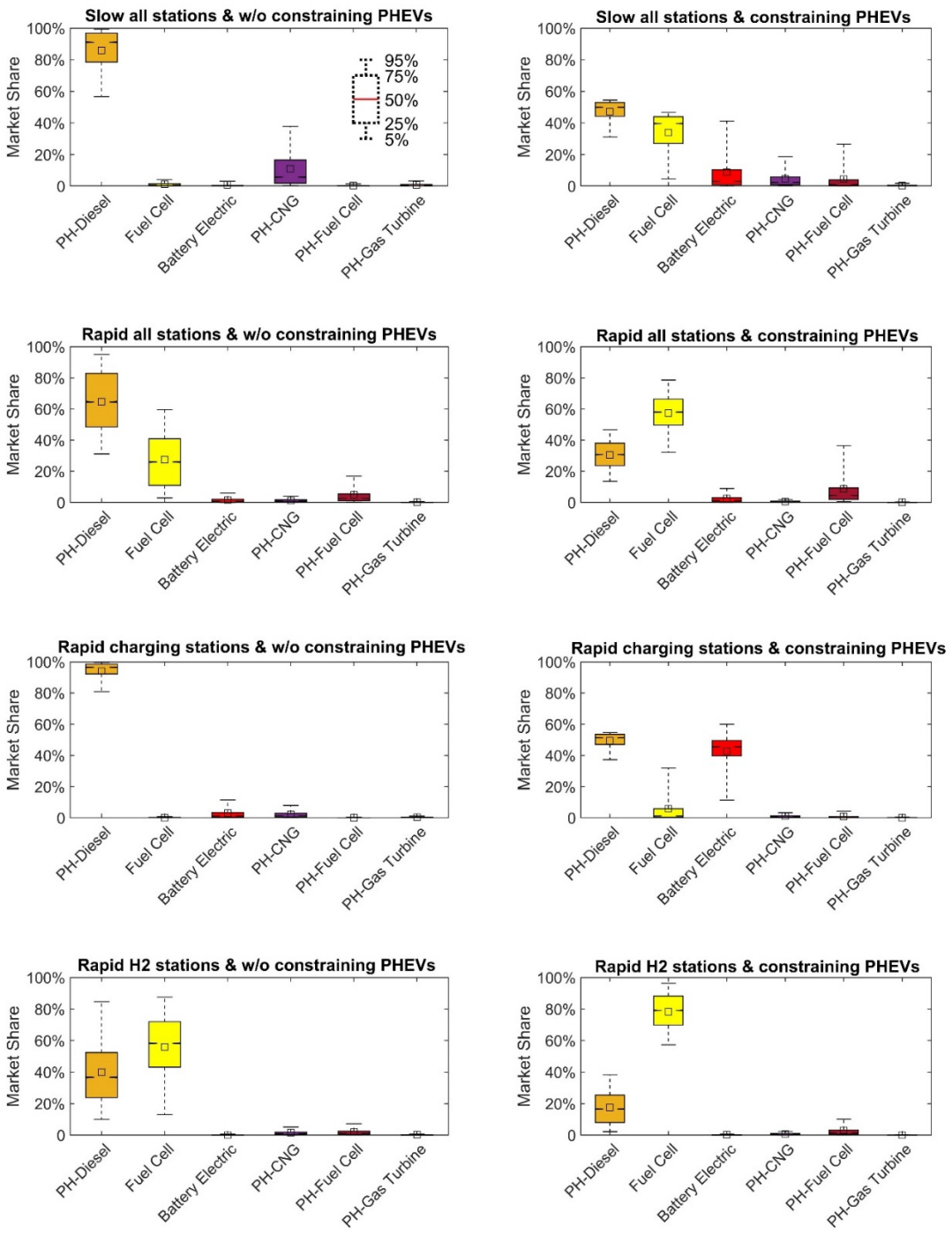

Figure 4-9: The uncertainty range of winner ZEV drivetrains for long haul HDTs in 2050 under ambitious ZEV mandate and various infrastructure roll out scenarios.

4.4.3 Short and long haul GHG emissions

Figure 4-10 displays the probability of meeting the 2050 target for an 80% reduction in GHG emissions in short and long haul markets under the ambitious ZEV mandates combined with various infrastructure roll-out scenarios. The probability of meeting the 2050 target is

higher for the short haul market compared to the long haul. Even when there is no constraint on PHEVs sales, the probability of meeting the 2050 target for various roll-out scenarios ranges from 38.9-99.7% in short haul. However, in the long haul market there is a limited chance (0.4-2.7%) of meeting the 2050 target without constraining PHEVs sales. When constraining PHEVs sales for the long haul market, the probability of meeting the 2050 target increases to 7.3-20% for various roll-out scenarios. The main reason for the low chance of meeting the 2050 target in long haul is because of the lower difference in fuel consumption of diesel and ZEV drivetrains on long haul routes compared to the short haul. This means the ZEV mandate for short haul could substantially reduce GHG emissions while there is less room for improvement in GHG emissions reduction for long haul. The median GHG emissions reductions of 2050 in long haul are 35-51% and 26-30.5% respectively corresponding to without PHEVs sales constraint and with constraint scenarios. This could help to understand how far is the long-haul sector from achieving 2050 targets, which is 6-31% across all long haul scenarios to meet the target for at least 50% of results.

The highest probability of meeting the GHG emissions target in short haul is achieved in the scenarios with the rapid deployment of H_2 stations as well as rapid deployment of all stations when there is a constraint on PHEVs sales. Similarly, in long haul the highest probability is in the scenarios with the rapid deployment of hydrogen-refueling stations. Overall for both short and long haul markets, constraining PHEVs sales and rapid infrastructure deployment increase the chance of meeting the 2050 target, though the improvement percentage is varied across scenarios. The highest variation is around 46% in short haul when comparing slow deployment scenarios with and without constraining PHEVs sales. When comparing the role of infrastructure in the adoption of ZEV drivetrains compared to the slow deployment scenario without constraint on PHEV sales, the highest improvement in short haul is for rapid deployment of H_2 station scenario with 60.8 % improvement. Similarly, in the long haul the highest improvement is related to rapid H_2 station deployment with 12.7% further reduction in GHG emission when comparing scenarios with the constraint of PHEVs sales.

Figure 4-11 displays the GHG emissions reduction trajectory in entire BC HDT market under the various considered scenarios. For each graph of this figure the blue and pink solid lines represent the median of simulated GHGs with PHEVs sales constraint and without constraint respectively. We created this Figure by combining the 5%, 50%, and 95% of GHG emissions

reduction results from short and long haul sector in each simulation period. Overall, it is evident that more GHG emissions reduction could be expected in rapid deployment of hydrogen stations scenarios.

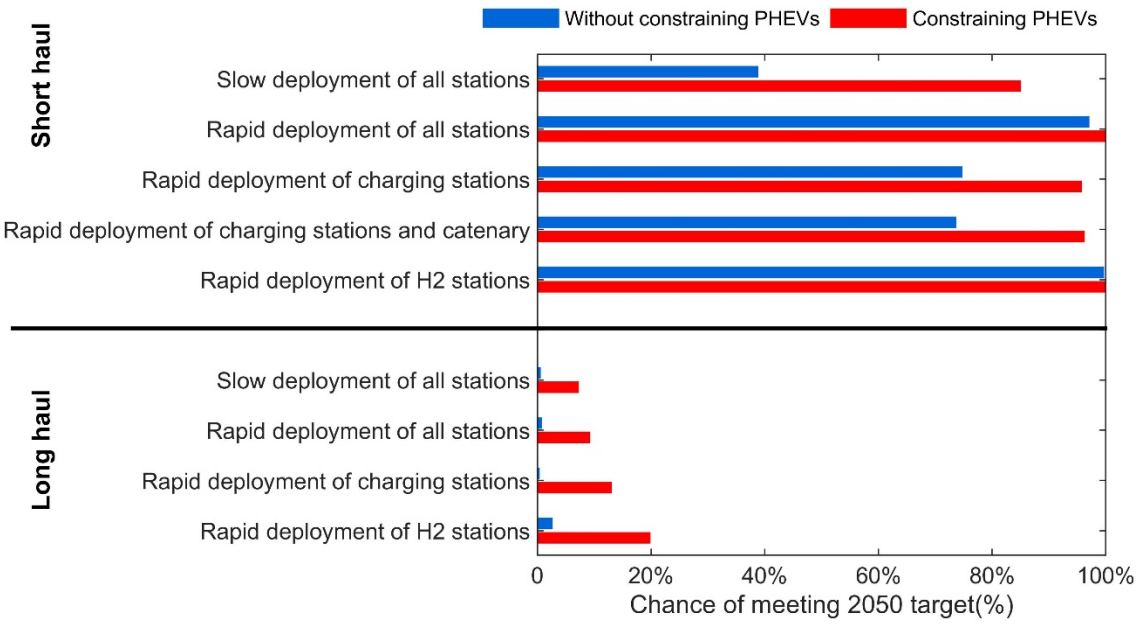

Figure 4-10: The probability of meeting 2050 target for short and long haul HDT markets under the ambitious ZEV mandates and various infrastructure roll out scenarios.

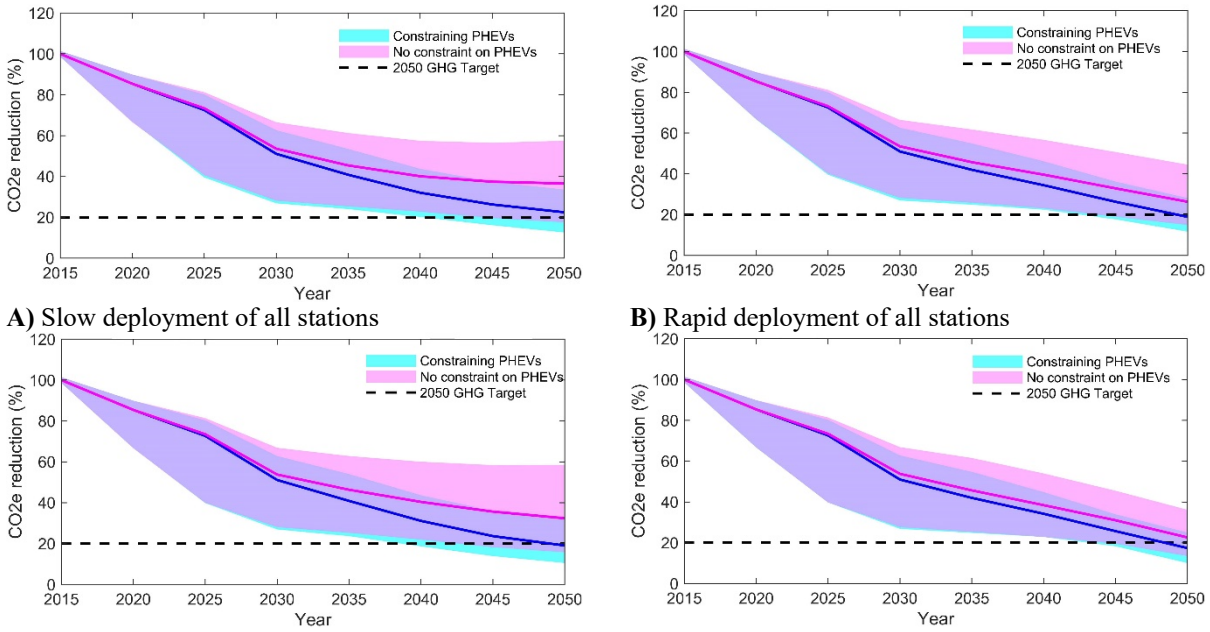

Figure 4-11: The GHG emissions reduction trajectory in entire BC HDT market (including their uncertainty ranges) under the various considered scenarios during 2015-2050.

4.4.4 Energy demand in short and long haul HDT markets

Figure 4-12 shows the sum of mean values of energy demand from various sources in the short and long haul markets under various infrastructure roll-out during 2015 to 2050. It can be seen that in all scenarios, energy demand declines between 2015 and 2050 despite the increasing trend in transport demand. This trend occurs mainly due to the adoption of more efficient drivetrains. By 2050, when comparing the highest demand for alternative fuels among scenarios, H_2 has the highest demand of almost 17.2 PJ in the rapid hydrogen deployment scenario when there is a constraint on PHEV sales.

Figure 4-13 and Figure 4-14 represent the uncertainty of 2050 energy demands from each fuel type for short and long haul BC HDTs respectively, under the ambitious ZEV mandates and various infrastructures roll out scenarios. The highest uncertainty range among all fuel types when combining whiskers magnitudes across short and long haul sectors is related to renewable diesel with 5.9 -24.6 PJ. This range is related to rapid deployment of charging station without PHEVs sale constraint scenario. The hydrogen demand from electrolysis is around 13.8-20.2 PJ for rapid deployment of hydrogen stations with PHEVs sale constraint scenario, when combining the whiskers magnitudes of short and long haul results for hydrogen from electrolysis source. The combined electricity demand under this scenario is 0-1.6 PJ.

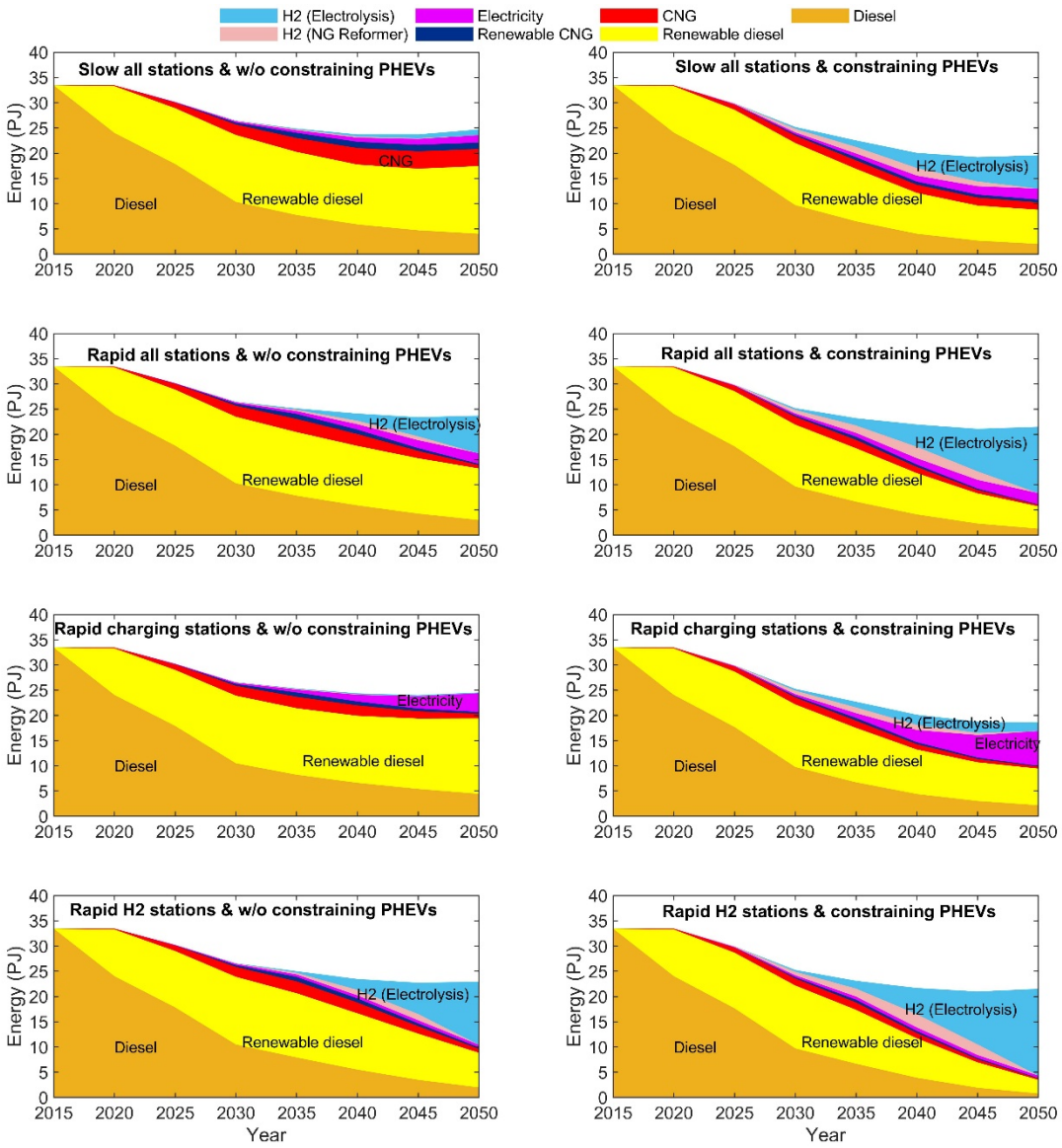

Figure 4-12: The sum of mean energy demands for short and long haul HDTs under the ambitious ZEV mandate and various infrastructures roll out scenarios during 2015-2050.

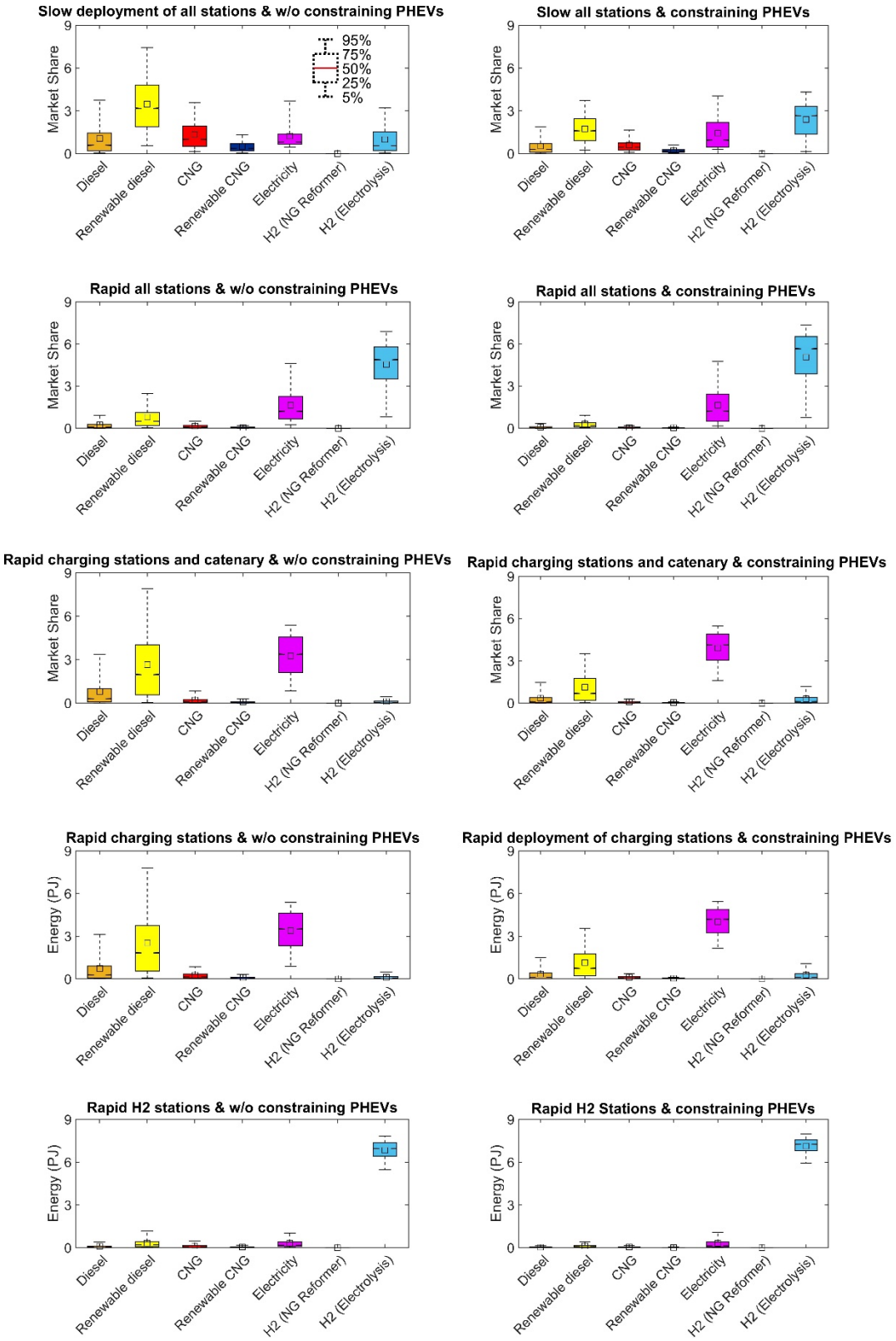

Figure 4-13: The uncertainty of 2050 energy demands from various sources for short haul BC HDTs under the ambitious ZEV mandates and various infrastructures roll out scenarios

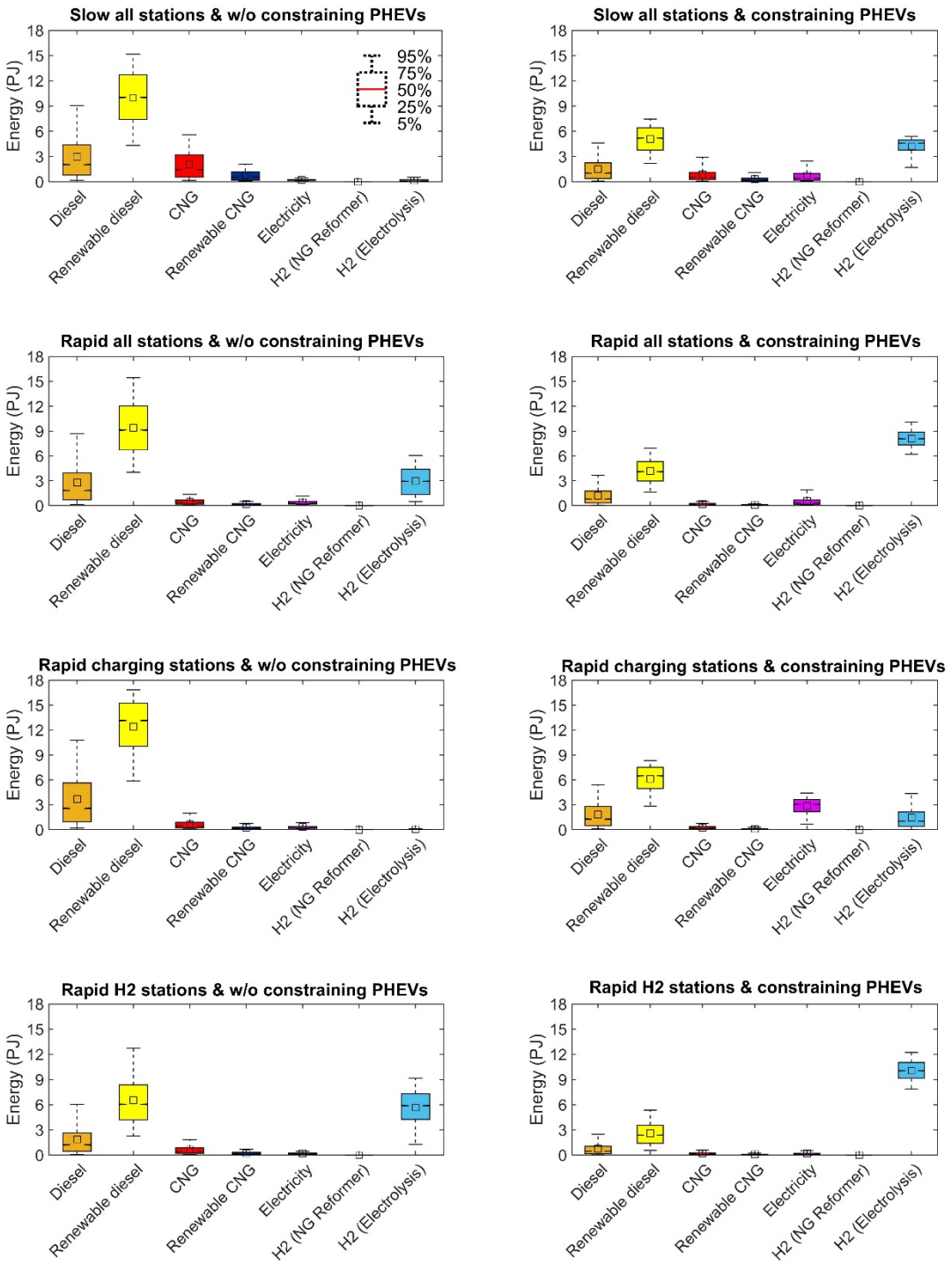

Figure 4-14: The uncertainty of 2050 energy demands from various sources for long haul BC HDTs under the ambitious ZEV mandates and various infrastructures roll out scenarios

4.5 Discussion and conclusions

This section summarizes the main findings, presents the insights of the study, highlights the limitations, and proposes several directions for future studies.

4.5.1 Main findings related to the winning drivetrains and GHG emissions

Since we have not found a comparable study in the reviewed literature, it is quite difficult to compare the results of this study with the literature. Still, in some cases, we found similarities and discrepancies in findings. Considering the mean market share result and the winning criteria (those that capture more than 80% mean market share by 2050), in the short haul market, both battery electric and fuel cell drivetrains emerged as potential winners, depending on the roll-out scenario. Considering the market share distribution results, we found close to 100% dominance percentage for battery electric in rapid charging and rapid charging and catenary scenarios when there is the PHEVs sales constraint. In comparison, we found dominance of fuel cell for close to 100% of simulations in rapid deployment of hydrogen stations with and without PHEVs sales requirement.

Unlike Fulton and Miller [21] who found infrastructure deployment impacts both fuel cell and battery electric equally, we found by 2050 fuel cell is leading in rapid deployment of all stations scenarios both in terms of mean of market share and domination percentage. This was mostly due to its much lower refueling inconveniences cost of the fuel cell compared to the battery electric. Our finding is in agreement with Shafiei et al. [41] who found a larger impact from hydrogen infrastructure on the adoption of fuel cell cars compared to charging infrastructure for battery drivetrain options. This finding is also in agreement with Hammond et al. [20], Siskos and Moysoglou [22], and Yeh et al. [3] studies that found domination of fuel cell drivetrain over battery electric for HDTs.

In the long haul market, plug-in hybrid diesels obtained 18-94% new market shares (mean magnitudes) across all scenarios and always emerged as winning drivetrains in all of the long haul scenarios. Plug-in hybrid diesel also dominated for almost 100% of simulations in two scenarios of rapid and slow deployment of all stations both without PHEVs sale constraint. Plug-in hybrid diesel also found with 61% and 54% domination in scenarios of rapid deployment of all stations without constraint and slow deployment of all stations with constraint. The success of plug-in hybrid diesel owes to its much smaller battery pack, efficient drivetrain, and lower refueling time. In comparison with the literature, Gambhir et al. [258] assumed a 60% market

share of hybrid HDTs in China for 2050. Shafiei et al. [41] showed that plug-in hybrid diesel and fuel cell can equally win the freight market in New Zealand when there is a ban on internal combustion drivetrains. Furthermore, Carrara and Longden [40] did not include fuel cell and found by 2100 in the 2 ºC climate scenario one could expect battery electric and plug-in hybrid diesels to emerge as winner in the market.

We found fuel cell as the second winner of the long haul market. We also found by 2050 in the 5 wining scenarios fuel cell captures 27-78% mean market share. The result indicated 100% superiority for fuel cell under rapid deployment of hydrogen stations only if PHEVs sale is constraint, which is unlike short haul fuel cell that is 100% superior under both rapid deployment of hydrogen stations scenario regardless of constraint. This finding is relatively comparable with Fulton and Miller [203] and Miller et al. [21] that considered fuel cell as only realist ZEV option for long haul HDTs operation.

Based on all considered scenarios, we found any catenary option cannot gain more than a 5.5% market share due to their higher intangible costs (including the perception of risk and lack of model availability). This finding is in contrast with Mulholland et al., International Energy Agency, and Plötz et al. [9], [18], [245] who viewed catenary as a winning drivetrain option. For example, Plötz et al. [18] used an optimization model (without behavioral parameters) and forecasted 40-50% penetration of catenary trucks in Europe for 2040 if one-third of European highways be electrified with overhead lines.

In terms of meeting 80% GHGs emissions reduction for 2050, the probability of meeting the target was found to be much higher in short haul than the long haul. The probability of meeting the target is increased by 11-60.8% in short haul and 0-12.7% in long haul when comparing slow and rapid roll-out scenarios. The highest impact for both short and long haul was related to the rapid hydrogen station deployment. In this scenario, the chance of meeting the 2050 target for short and long haul increases from 39% to 99.7% (without constraining PHEVs sales) and from 7.3% to 20% (with a constraint on PHEVs sale) respectively. This finding is comparable with Shafiei et al. [41], who found 2050 GHG emissions reduction improves by 15% when there is a push toward infrastructure development of ZEV options.

4.5.2 Implications of the study

This study implies the necessity for strategies to encourage the rapid deployment of infrastructure to further increase the adoption rate of ZEV drivetrains in the freight sector and

increase the chance of meeting the 2050 target for transportation. Although the hydrogen pathway could produce a higher adoption rate and GHG emissions reduction, plug-in hybrid diesels win the market in all of the long haul scenarios (considering the mean of market-share results). We found more certainty in domination of plug-in hybrid diesel than fuel cell. Therefore, it seems to be a more realistic option for widespread adoption in the long haul sector since they rely on conventional diesels with much reduced electricity requirements, as well as less expensive capital costs compared to the pure electric drivetrains. The deployment of plug-in hybrid diesel could also pave the way toward the deployment of pure electric drivetrains. Therefore, we recommend that the long haul market focuses at least in the near term on plug-in hybrid diesel drivetrain deployment.

Although we found slightly more domination of fuel cell than battery electric in terms of simulation percentage and mean of market share, in the short haul market, both battery electric and fuel cell drivetrains seem realistic. Therefore, both charging and hydrogen refueling infrastructure could be equally supported. To rapidly eliminate the intangible costs government could pick either one of fuel cell or battery electric option for short haul and plug-in hybrid diesel or fuel cell as the second choice for long haul and support the development of their associated infrastructure.

Government also could fund to initiate the incorporation of ZEV HDTs (e.g. battery electric and fuel cell) and their infrastructure around major freight terminals as a first step to more accurately validate the financial and non-financial cost assumptions of each option in the real-world environment. An example of such ZEV HDTs demonstration project for heavy-duty trucks have initiated by California state authorities [287], [288]. Comprehensive and detailed data collection is recommended to more accurately distinguish the short and long haul HDTs, and then identify suitable low carbon options based on duty cycles, which also requires government support.

This study indicated the lowest GHG emissions achieved in rapid deployment of hydrogen stations (with limitation on PHEVs sales). This scenario implies a mean of 17 PJ hydrogen via electrolysis process demand with 13.8-20.2 PJ uncertainty range. Hydro or low carbon electricity seems to be highly critical to produce hydrogen, which requires significant expansion. Considering 70% energy conversion efficiency for the water electrolysis process [289], up to 20-29 PJ of hydroelectricity is required corresponding to the rapid hydrogen

deployment scenario. Considering the electricity demand in this scenario, the total required hydroelectricity is 20-30.6 PJ. This energy is equivalent to 55-85% of the annual production capacity of the in-construction Site C dam in Northeastern BC, which is 36 PJ (5,100 GWh) [290].

4.5.3 Limitations and directions for future research

We summarize the limitations of this study as follows, each limitation potentially could be a directions for future research:

- We allocated GHG emission intensities of fuel supplies and their costs exogenously. Future studies could make this endogenous to the CIMS-HDT by considering a market model of various fuel supplies by implementing the cost and GHG emissions of their feedstock and production pathways.
- In the present study, we only considered four endogenous features. A future study could be improved by including more endogenous feedback from other freight sectors and energy systems. Additionally, future studies can further extend the region to capture the Canada-wide market, as well as adding competition of rail and medium-duty trucks technologies.
- Due to the lack of disaggregated data for the short and long haul HDT markets, we applied a number of assumptions to split transport demand and HDT population in the short and long haul markets, which could impact the results.
- In each short and long haul market, the energy consumption of drivetrains was the average of simulations on three routes that only represent a subset of the entire freight routes of BC. Future studies could be improved by including further routes and drive cycles.
- Fully and partially autonomous HDTs have recently emerged with potential operational cost saving that could be the subject of future studies to examine their probability of being a dominant drivetrain [291].
- There is uncertainty with regards to assumptions especially related to behavior parameters. Given the uncertainty of assumptions, surveying and conducting interviews with freight operators would be recommended to more accurately quantify the non-financial costs.

- The impact of battery swaps on electrification potential was evaluated by Çabukoglu et al. [256], which can reduce refueling inconveniences. A future study could be improved by including battery swap technology to further evaluate the competitiveness of battery electric and hydrogen powered drivetrains.

Chapter 5

5 Conclusions and future work

Quantifying the characteristics of alternative HDTs in terms of energy consumption, well to wheel GHG emissions, total ownership costs, and intangible costs is key for effective climate policy design. This dissertation proposed a novel and comprehensive framework based on the physical energy consumption model of alternative drivetrains to determine the role of infrastructure, drivetrain options, and fuel choice in meeting GHG emissions reduction target in BC. The analysis framework was presented in chapter 2, 3, and 4. The vehicle adoption model based on infrastructure scenario and ZEV mandates (chapter 4) and the technology evaluation methods (chapter 2 and 3) in the HDT sector of BC can provide useful insights for industry, researchers, and decision makers.

Although this dissertation was focused on the Canadian province of BC, as a case study, the applied methods and obtained results could be insightful for other regions around the world. It can be helpful for truck manufacturers to design an appropriately sized energy storage system compatible with intended freight routes. Additionally, utility companies can apply the framework for estimating the implication of ZEV policy in term of total energy consumption. Government sectors could apply the insights of this study when planning for future infrastructure

development. The following sections summarize the main conclusions and implications of the work and proposed areas for future research.

5.1 Key insights

In the second chapter a physical energy consumption model was formulated to simulate six realistic drive cycles based on the grade profile of BC routes to compare CNG and diesel for on-road performance. In the third chapter, 16 drivetrains technology were quantified in terms of their energy consumption, well-to-wheel GHG emissions, total ownership cost, GHG abatement cost, and cargo capacity. The fourth chapter presented a dynamic vehicle adoption model to determine the role of ambitious ZEV mandates together with various pathways for infrastructure roll outs. The high resolution drivetrain models that developed in chapter 2 and 3 created a detail presentation of alternative drivetrains HDTs for short and long haul markets that enabled a long term vehicle adoption projection in chapter 4. The main insights of this body of work are summarized as follows:

- On-road CO_2 emissions reductions from CNG HDTs were found to be 12.6- 15.3% depending on the drive cycle and vehicle gross mass. The loss in CO_2 reduction potential was due to an efficiency gap between CNG and diesel engines and the heavier mass of CNG versus diesel vehicles. An assessment of advanced CNG and diesel trucks showed achievable CO_2 reductions of 41–51% and 31–42% over the longer term, compared to baseline current diesel technology.
- A technique was proposed to include grade profile into drive cycle definition and showed including grade simulation can increase fuel consumption by as much as 24%.
- The sensitivity analysis of diesel and CNG drivetrains showed that weight improvement is more critical for cycles with higher kinetic intensities. Cycles with more idling conditions are more suitable for applying engine friction (e.g. synthetic oil) and accessory load (e.g. solar PV system) reduction technologies. Finally, technology that improves aerodynamic drag coefficient, rolling resistance coefficient, and indicated thermal efficiency was found highly effective for all high-speed highway cycles.
- Comparing 16 drivetrain technologies, battery electric catenary and pure battery electric were found to have the lowest WTW GHG emissions using hydroelectricity (2-3.9 g/tkm) on short haul and long haul respectively, 95-99% lower than a baseline diesel.

- In term of the total ownership cost (TOC), parallel hybrid diesel was found to have the lowest TOCs on both short and long haul routes (0.5-1.2 $/km), 2-15% lower than conventional diesel counterparts. Similarly, the plug-in parallel hybrid diesel was found to have the lowest abatement cost that was negative on most drive cycles either using diesel or bio-diesel. In respect to cargo capacity, plug-in parallel hybrid fuel cell and conventional diesel were found to have highest cargo capacity for short and long haul routes respectively.
- A Monte Carlo simulation was performed to evaluate the uncertainty of WTW GHGs and TOC for 15 drivetrains on the longest and most demand routes. Results indicated the parallel hybrid diesel has the lowest TOC while battery electric has the lowest well to wheel GHG emissions when comparing median magnitudes of WTW GHGs and TOCs.
- Overall, results of comparing 16 drivetrains were found variable depending on key assumptions. The upstream fuel emissions and rolling friction coefficients were found as critical factors in well-to-wheel GHG emissions. Discount rate, fuel price, battery cost, and rolling friction coefficient were found as main contributors of the total ownership cost.
- This study showed how to optimize the size of energy storage systems for alternative drivetrains on the intended cycles. In reality, due to low energy density of battery and hydrogen systems it is costly and inefficient to operate a long haul alternative drivetrain HDT on a short-haul route.
- This study developed six 1-Hz drive cycles with grades from the sparse raw activity data of 1,616 heavy-duty trucks operating in BC during November 2016 [153], which represent realistic freight routes. The study highlighted the utility of the activity data for evaluating energy consumption, GHG emissions, and energy storage sizing of alternative drivetrains HDTs, which is insightful for freight operators, HDT manufactures, and decision makers.
- In this study, the evaluated winner drivetrains in the short and long haul HDT market of BC subject to various scenario of infrastructure roll outs and ZEV mandates was explored. Winner drivetrains are defined as those that capture 80% of mean market share by 2050. The probability of meeting the GHG emissions target for 2050 associated with each scenario were evaluated. Overall 10 and 8 drivetrains were simulated for short haul

and long haul respectively. Winner drivetrains varied across different scenarios depending on constrains on the adoption of plug-in hybrids and infrastructure roll-out scenarios. Battery electric and fuel cell drivetrains were found as top two winners of short haul market, which could play large role in this market. In the long haul, plug-in hybrid diesel was found to be among winner drivetrains in all scenarios. The second winning option in long haul was fuel cell, which was winning in 5 scenarios.

- Considering the distribution of 2050 new market share results, battery electric, fuel cell, plug-in hybrid diesel were found with absolute domination under a number of short and long haul market scenarios. In short haul, battery electric capture 100% domination in market share for 2050 under rapid deployment of charging as well as charging and catenary scenarios when there is a constraint on plug-in hybrids sales. However, fuel cell in short haul obtained 100% domination under both scenarios of rapid deployment of hydrogen stations regardless of plug-in hybrids sales constraint. In long haul, plug-in hybrid diesel captured 100% domination under slow deployment of all stations and rapid charging stations scenarios both without plug-in hybrids sales constraint. Fuel cell in the long haul captured 100% domination under rapid deployment of hydrogen stations scenario with plug-in hybrids sales constraint.
- It was found that the probability of meeting the 2050 target increased by 11-60.8% in short haul and 0-12.7% in long haul, depending on the infrastructure deployment scenarios. Rapid deployment of hydrogen stations was found to have the highest impact on increasing the adoption rate of fuel cell drivetrains and probability of meeting the GHG emissions target. Across different scenarios, the probability of meeting the 2050 target for short haul and long haul BC HDT market were found to be 38.5-100% and 0-20% respectively. The lower probability of long haul is due to a lower fuel efficiency gap between ZEV drivetrains and the baseline diesel in the long haul compared to the short haul.

5.2 Implications and recommendations

This study has highlighted the following technical and policy implications regarding the implementation of low carbon HDTs in the BC freight sector:

- The relative bulk and weight of the battery electric and fuel cell HDT drivetrains leads to a much lower operational flexibility of usage between short and long haul routes when

considering overall efficiency of vehicle drivetrain capacity utilization, compared to conventional diesel HDTs. Daily operation data of a larger set of BC HDT fleet could help examine the possibility of using battery electric and fuel cell HDTs with a fixed storage size for mixed usage, and then determine refueling frequency requirements. Additional data collection therefore seems a worthwhile and necessary for more accurately capturing BC HDT characteristics and targeting incentive and regulatory policy.

- Deploying BC fossil-derived natural gas resources in the HDT sector with conventional CNG drivetrains will not lead to much climate benefit considering well to wheel GHG emissions. To obtain a climate benefit using BC natural gas resources, HDTs should be equipped with either hybrid or advanced drivetrain technologies to provide a meaningful GHG emissions reduction.
- Hydroelectricity was found highly critical in obtaining the lowest GHG emissions for battery electric and fuel cell drivetrains. Considering 70% energy conversion efficiency for the water electrolysis process [289], up to 20-30.6 PJ of hydroelectricity is required corresponding to the rapid hydrogen fuel cell deployment scenario. This energy is equivalent to 55-85% of the annual production capacity of the in-construction Site C dam in Northeastern BC, which is 36 PJ (5,100 GWh) [290].
- Relying only on a stringent ZEV mandate as a silver bullet cannot achieve the 2050 target for BC HDTs. A stringent ZEV mandate should be combined with a stringent low carbon fuel standard, as well as a strategy to enable rapid deployment of the infrastructure required to support alternative drivetrain HDTs.
- Observing the deployment scenarios, battery electric and fuel cell were found as the main dominant drivetrain of short haul and plug-in hybrid diesel and fuel cell as the main dominant drivetrain options in the short and long haul markets respectively, dependent on the infrastructure scenario. Government could send a strong signal to the market by picking one drivetrain option in the short and long haul and supporting the development of its associated infrastructure accordingly.
- Demonstration projects aided by government funding could help adoption of ZEV drivetrains for HDTs and help better quantifying financial and non-financial costs by nullifying the first-mover initial tangible and intangible costs. California State, for

example, has initiated several ZEV drivetrains demonstration projects for short haul HDT operations in several locations around the state [287], [288].

5.3 Future studies

Although the current analysis framework was sufficient in analyzing various alternative drivetrain technologies and ZEV policy scenarios, the following extensions are recommended for future studies to further extend the current analysis framework and its utility:

- In the energy consumption model, the impact of road gradient was captured for both diesel and CNG engines in a similar way. However, performance data indicated rather different CO_2 emissions behavior for hill climbing highway routes when CNG and diesel engines operate close to their nominal capacities. A future study could further calibrate the parametric model of diesel and CNG engines using engine maps enhanced with the field experimental data.
- The physical energy consumption model of alternative drivetrains developed in this study could be used toward the creation of an economic route selection online application. For example, a smart phone application could provide the optimized route with respect to energy consumption considering road congestions, topography, operation assignments, and drivetrain technology.
- This study only simulated CO_2 emissions of CNG and diesel engines and assumed the CH_4 and N_2O emissions proportionate to CO_2 emissions. Future studies could improve this by considering CH_4 and N_2O emissions as well as criteria pollutions (e.g. NOx, CO, and HC) of alternative drivetrains under various drive cycle using methodology presented in [98]. Local air quality benefit could then be quantified.
- This study proposed a consistent methodology to compare 16 drivetrains technology based on their physical fuel consumption model. However, in the future, energy consumption calculations could be refined with the availability of experimental data for parallel and series hybrid drivetrains. Furthermore, the sizing of energy storage systems for intended routes could be extended to optimize other drivetrain sub-systems such as electric motor power and torque.

- The impact of extreme weather conditions (e.g. cold climate) and battery degradation over time [231], [244] are other battery sizing factors that can be varied by operating routes and could be the subject of future studies.
- In chapter 3, the Monte Carlo simulation was applied to the longest freight routes between Vancouver to Calgary, which for the future studies could be extended to other routes.
- The cost of infrastructure (e.g. fast charging station) in chapter 3 were assumed identical for all routes, which could be adjusted for the future studies based on traffic volume and infrastructure nearby (e.g. substation) along an intended route.
- This study showed the importance of renewable natural gas (RNG), biodiesel, and renewable diesel in reducing GHG emissions. Further studies could examine the role of bio and synthetic fuels including feedstock options, their availability, technology pathways (e.g. methanation of CO_2 with renewable power [79]), and their GHG emissions intensities.
- Combining the physical energy consumption models and the vehicle adoption model (CIMS-HDT) could be a new approach to examine the interaction of policy with technology that computationally could be time-consuming. This approach could be the subject of future studies that would allow capturing more technological parameters (e.g. aerodynamic drag) of HDTs in the vehicle adoption model.
- This study evaluated the fleet of 1,616 container trucks operating around BC [153] to determine the main characteristic of HDTs in terms of daily travel distance, elevation change, and average speed and then selected 6 representative cycles. Future studies could examine the remaining fleets in BC to better categorize the daily travel distances that directly impact the size of the energy storage system on-board HDTs.
- Future studies could conduct surveys of freight operators to better quantify the non-financial cost of drivetrain.
- The CIMS-HDT in this study only considered short and long haul market in BC. These freight sectors could be extended to medium-duty trucks and rail transportation for future studies. Furthermore, the domain of policy simulation could be extended to Canada wide.

- Autonomous technologies have emerged recently that will likely be first adoptable by HDT and could reduce the operational cost [291]. In future, the CIMS-HDT could be improved by implementing the financial and non-financial cost of this technology option and explore impact on drivetrain choice.

Bibliography

[1] Jos G.J. Olivier; et al, “Trends in global co 2 emissions 2016,” 2016.

[2] M. Moultak, N. Lutsey, and D. Hall, “Transitioning to zero-emission heavy-duty freight vehicles,” *Int. Counc. Clean Transp.*, no. September, 2017.

[3] S. Yeh *et al.*, “Detailed assessment of global transport-energy models’ structures and projections,” *Transp. Res. Part D Transp. Environ.*, vol. 55, pp. 294–309, 2017.

[4] J. M. Wang *et al.*, “Near-Road Air Pollutant Measurements: Accounting for Inter-Site Variability Using Emission Factors,” *Environ. Sci. Technol.*, vol. 52, no. 16, pp. 9495–9504, 2018.

[5] B. Plumptre, E. Angen, and D. Zimmerman, “The State of Freight (Understanding greenhouse gas emissions from goods movement in Canada),” The Pembina Foundation, Calgary, 2017.

[6] P. Kluschke, T. Gnann, P. Plötz, and M. Wietschel, “Market diffusion of alternative fuels and powertrains in heavy-duty vehicles : A literature review,” *Energy Reports*, vol. 5, pp. 1010–1025, 2019.

[7] S. Tongur and M. Engwall, “The business model dilemma of technology shifts,” *Technovation*, vol. 34, no. 9, pp. 525–535, Sep. 2014.

[8] H. Zhao, W. Qian, L. Fulton, M. Jaller, and A. Burke, “A Comparison of Zero-Emission Highway Trucking Technologies,” p. 58, 2018.

[9] International Energy Agency, “Energy Technology Perspectives 2017,” 2017.

[10] Environment and Climate Change Canada, “CANADA’S MID-CENTURY LONG-TERM LOW-GREENHOUSE GAS DEVELOPMENT STRATEGY,” 2019.

[11] British Columbia government, “Climate Action Legislation - Province of British Columbia,” 2008. [Online]. Available: https://www2.gov.bc.ca/gov/content/environment/climate-change/planning-and-action/legislation. [Accessed: 12-Feb-2019].

[12] Natural Resources Canada, “Comprehensive Energy Use Database | Natural Resources Canada,” 2018. [Online]. Available: http://oee.nrcan.gc.ca/corporate/statistics/neud/dpa/menus/trends/comprehensive_tables/list.cfm. [Accessed: 18-Aug-2018].

[13] British Columbia government, “New act ensures B.C. remains leader on clean energy vehicles | BC Gov News,” 2019. [Online]. Available: https://news.gov.bc.ca/releases/2019EMPR0018-001077. [Accessed: 27-Dec-2019].

[14] British Columbia government, “Renewable & Low Carbon Fuel Requirements Regulation - Province of British Columbia,” 2018. [Online]. Available: https://www2.gov.bc.ca/gov/content/industry/electricity-alternative-energy/transportation-energies/renewable-low-carbon-fuels. [Accessed: 17-Oct-2018].

[15] British Columbia government, “British Columbia’s Carbon Tax - Province of British Columbia,” 2019. [Online]. Available:

https://www2.gov.bc.ca/gov/content/environment/climate-change/planning-and-action/carbon-tax. [Accessed: 27-Dec-2019].

[16] J. Lepitzki and J. Axsen, “The role of a low carbon fuel standard in achieving long-term GHG reduction targets,” *Energy Policy*, vol. 119, no. May, pp. 423–440, 2018.

[17] V. Keller *et al.*, “Electricity system and emission impact of direct and indirect electri fi cation of heavy-duty transportation,” *Energy*, vol. 172, pp. 740–751, 2019.

[18] P. Plötz, T. Gnann, P. Jochem, H. Ümitcan, and T. Kaschub, “Impact of electric trucks powered by overhead lines on the European electricity system and CO 2 emissions,” *Energy Policy*, vol. 130, no. April, pp. 32–40, 2019.

[19] T. Mai *et al.*, “Electrification Futures Study : Scenarios of Electric Technology Adoption and Power Consumption for the United States Electrification Futures Study : Scenarios of Electric Technology Adoption and Power Consumption for the United States,” 2018.

[20] W. Hammond, J. Axsen, and E. Kjeang, “How to slash GHG emissions in the freight sector? Policy insights from a technology adoption model of Canada,” *Energy Policy*, no. November, pp. 1–14, 2019.

[21] M. Miller, Q. Wang, and L. Fulton, “Truck Choice Modeling: Understanding California’s Transition to Zero-Emission Vehicle Trucks Taking into Account Truck Technologies, Costs, and Fleet Decision Behavior,” 2017.

[22] P. Siskos and Y. Moysoglou, “Assessing the impacts of setting CO2 emission targets on truck manufacturers: A model implementation and application for the EU,” *Transp. Res. Part A Policy Pract.*, vol. 125, no. February, pp. 123–138, 2019.

[23] Canada Oil & Natural Gas Producers, “British columbia’s oil and natural gas industry,” 2019.

[24] CE-CERT-UCR, “Comprehensive Modal Emission Model (CMEM).” [Online]. Available: https://www.cert.ucr.edu/cmem/. [Accessed: 12-Feb-2019].

[25] O. US EPA, “MOVES and Other Mobile Source Emissions Models.”

[26] Argonne National Laboratory, “Welcome To Autonomie,” 2015. [Online]. Available: https://www.autonomie.net/. [Accessed: 12-Feb-2019].

[27] T. Markel *et al.*, “ADVISOR: a systems analysis tool for advanced vehicle modeling,” *J. Power Sources*, vol. 110, no. 2, pp. 255–266, Aug. 2002.

[28] P. J. Sturm and S. Hausberger, *Energy and fuel consumption from heavy duty vehicles. COST 346 -Final Report*. 2005.

[29] G. Scora, K. Boriboonsomsin, and M. Barth, “Value of eco-friendly route choice for heavy-duty trucks,” *Res. Transp. Econ.*, vol. 52, pp. 3–14, 2015.

[30] G. Fontaras *et al.*, “An experimental evaluation of the methodology proposed for the monitoring and certification of CO2 emissions from heavy-duty vehicles in Europe,” *Energy*, vol. 102, pp. 354–364, 2016.

[31] Z. Gao *et al.*, “Fuel Consumption and Cost Savings of Class 8 Heavy- Duty Trucks Powered By Natural Gas,” *92th Transp. Res. Board Annu. Meet.*, vol. 543, p. 18, 2012.

[32] D. Y. Lee, A. Elgowainy, A. Kotz, R. Vijayagopal, and J. Marcinkoski, “Life-cycle implications of hydrogen fuel cell electric vehicle technology for medium- and heavy-duty trucks,” *J. Power Sources*, vol. 393, no. January, pp. 217–229, 2018.

[33] G. S. Sandhu, H. Christopher Frey, S. Bartelt-Hunt, and E. Jones, “In-use activity, fuel use, and emissions of heavy-duty diesel roll-off refuse trucks,” *J. Air Waste Manag. Assoc.*, vol. 65, no. 3, pp. 306–323, 2015.

[34] J. Kast, R. Vijayagopal, J. J. Gangloff, and J. Marcinkoski, “Clean commercial transportation: Medium and heavy duty fuel cell electric trucks,” *Int. J. Hydrogen Energy*, vol. 42, no. 7, pp. 4508–4517, 2017.

[35] M. L. M. Oliveira, C. M. Silva, R. Moreno-Tost, T. L. Farias, A. Jiménez-López, and E. Rodríguez-Castellón, “Modelling of NOx emission factors from heavy and light-duty vehicles equipped with advanced aftertreatment systems,” *Energy Convers. Manag.*, vol. 52, no. 8–9, pp. 2945–2951, 2011.

[36] B. Sen, T. Ercan, and O. Tatari, “Does a battery-electric truck make a difference? – Life cycle emissions, costs, and externality analysis of alternative fuel-powered Class 8 heavy-duty trucks in the United States,” *J. Clean. Prod.*, vol. 141, pp. 110–121, 2017.

[37] A. Alamia, I. Magnusson, F. Johnsson, and H. Thunman, “Well-to-wheel analysis of bio-methane via gasification, in heavy duty engines within the transport sector of the European Union,” *Appl. Energy*, vol. 170, no. 2016, pp. 445–454, 2016.

[38] H. Zhao, A. Burke, and L. Zhu, “Analysis of Class 8 hybrid-electric truck technologies using diesel, LNG, electricity, and hydrogen, as the fuel for various applications,” in *EVS27 International Battery, Hybrid and Fuel Cell Electric Vehicle Symposium*, 2013, no. Epa 2010, pp. 1–16.

[39] W. Hammond, “How to slash GHG emissions in the freight sector? Policy insights from a technology adoption model of Canada,” Simon Fraser University, 2019.

[40] S. Carrara and T. Longden, “Freight futures: The potential impact of road freight on climate policy,” *Transp. Res. Part D Transp. Environ.*, vol. 55, no. 308329, pp. 359–372, 2017.

[41] E. Shafiei, J. Leaver, and B. Davidsdottir, “Cost-effectiveness analysis of inducing green vehicles to achieve deep reductions in greenhouse gas emissions in New Zealand,” *J. Clean. Prod.*, vol. 150, pp. 339–351, 2017.

[42] Tesla, “Semi | Tesla,” 2018. [Online]. Available: https://www.tesla.com/semi. [Accessed: 27-Feb-2018].

[43] B. Choe, “Zero Emission Heavy Duty Drayage Truck Demonstration,” 2016.

[44] D. Oxford, “Cummins Update for The Go With Natural Gas Workshop,” 2014.

[45] Volvogroup, “New trucks from Volvo running on LNG offer the same performance as diesel, but with 20-100% lower CO_2 emissions,” 2017. [Online]. Available: https://www.volvotrucks.com/en-en/news/press-release.html?pubid=22389. [Accessed: 25-Aug-2018].

[46] Scania, “World’s first electric road opens in Sweden | Scania Group,” 2016. [Online].

Available: https://www.scania.com/group/en/worlds-first-electric-road-opens-in-sweden/. [Accessed: 27-Feb-2018].

[47] Green Car Congress, “Walmart showcases WAVE tractor-trailer at MATS; micro-turbine range extended electric vehicle with 45.5 kWh Li-ion pack - Green Car Congress,” 2014. [Online]. Available: http://www.greencarcongress.com/2014/03/20140328-wave.html. [Accessed: 27-Feb-2018].

[48] BYD, “TRUCK - BYD USA,” 2019. [Online]. Available: http://en.byd.com/usa/truck/. [Accessed: 19-Jan-2019].

[49] US Hybrid, “US Hybrid Corporation,” 2018. [Online]. Available: https://ushybrid.com/powertrain/. [Accessed: 27-Jun-2018].

[50] Green Car Congress, “Daimler Trucks North America unveils two Freightliner electric vehicle models and Electric Innovation Fleet - Green Car Congress,” 2018. [Online]. Available: https://www.greencarcongress.com/2018/06/20180607-dtna.html. [Accessed: 25-Oct-2018].

[51] ThorTrucks, “Thor Trucks - A Fleet-Focused Transportation Lab Based in California,” 2019. [Online]. Available: https://www.thortrucks.com/. [Accessed: 24-Jan-2019].

[52] Nikola Motor, “Nikola Corp,” 2018. [Online]. Available: https://nikolamotor.com/. [Accessed: 27-Feb-2018].

[53] Toyota, “Toyota Doubles-Down on Zero Emissions Heavy-Duty Trucks | CORPORATE | TOYOTA Global Newsroom,” 2018. [Online]. Available: https://newsroom.toyota.co.jp/en/corporate/23722307.html. [Accessed: 15-Oct-2018].

[54] Argonne National Laboratory, “The Greenhouse gases, Regulated Emissions, and Energy use in Transportation (GREET) Model,” 2017. [Online]. Available: https://greet.es.anl.gov/. [Accessed: 02-Oct-2018].

[55] S&T2 Consultants Inc, “GHGenius, Model Version 4.03a,” 2013. [Online]. Available: https://www.ghgenius.ca/. [Accessed: 02-Mar-2018].

[56] J. Kast, G. Morrison, J. J. Gangloff, R. Vijayagopal, and J. Marcinkoski, “Designing hydrogen fuel cell electric trucks in a diverse medium and heavy duty market,” *Res. Transp. Econ.*, pp. 1–10, 2017.

[57] H. Zhao, A. Burke, and M. Miller, “Analysis of Class 8 truck technologies for their fuel savings and economics,” *Transp. Res. Part D Transp. Environ.*, vol. 23, pp. 55–63, 2013.

[58] B.C. Ministry of Transportation and Infrastructure, “Elevations of Major Summits & Passes on B.C. Highways - Province of British Columbia,” *B.C. Ministry of Transportation and Infrastructure*, 2015. [Online]. Available: https://www2.gov.bc.ca/gov/content/transportation/driving-and-cycling/traveller-information/routes-and-driving-conditions/elevations. [Accessed: 12-Feb-2019].

[59] NRC and Transportation Research Board- National Research Council, *Technologies and Approaches to Reducing the Fuel Consumption of Medium- and Heavy-Duty Vehicles*. Washington, D.C., D.C.: National Academies Press, 2010.

[60] Transportation Research Board- National Research Council, *Reducing the Fuel*

Consumption and Greenhouse Gas Emissions of Medium- and Heavy-Duty Vehicles, Phase Two. D.C.: National Academies Press, 2014.

[61] Transportation Research Board- National Research Council, *Review of the 21st Century Truck Partnership, Second Report*. D.C.: National Academies Press, 2012.

[62] U.S. Environmental Protection Agency, "Final Rulemaking to Establish Greenhouse Gas Emissions Standards and Fuel Efficiency Standards for Medium- and Heavy-Duty Engines and Vehicles," 2011.

[63] U.S. Environmental Protection Agency, "Greenhouse Gas Emissions and Fuel Efficiency Standards for Medium-and Heavy-Duty Engines and Vehicles -Phase 2," 2016.

[64] O. Delgado and N. Lutsey, "Advanced tractor-trailer efficiency technology potential in the 2020–2030 timeframe," 2015.

[65] F. Tong, P. Jaramillo, and I. M. L. Azevedo, "Comparison of Life Cycle Greenhouse Gases from Natural Gas Pathways for Medium and Heavy-Duty Vehicles," *Environ. Sci. Technol.*, vol. 49, no. 12, pp. 7123–7133, 2015.

[66] S. J. Hammond, *Political Theory : An Encyclopedia of Contemporary and Classic Terms*. 2008.

[67] K. Ribeiro *et al.*, *Transport and its infrastructure*. 2007.

[68] A. M. Jaffe *et al.*, "STEPS White Paper : Exploring the Role of Natural Gas in U . S . Trucking (Revised Version)," pp. 1–69, 2015.

[69] Transport Canada, "TRANSPORTATION IN CANADA 2015 Overview Report," 2015.

[70] R. Muncrief and B. Sharpe, "overview of the heavy-duty vehicle market and CO2 emissions in the european Union," *Int. Counc. Clean Transp.*, no. December, pp. 1–14, 2015.

[71] Environment and Climate Change Canada., "Greenhouse gas emissions by Canadian economic sector - Canada.ca," 2018.

[72] G. Baldwin, "Truck Use 2002—A Canada-United States Comparison," 2002.

[73] BC Climate Action Secretariat, "Provincial Greenhouse Gas Inventory - Province of British Columbia," 2015. [Online]. Available: https://www2.gov.bc.ca/gov/content/environment/climate-change/data/provincial-inventory. [Accessed: 17-Oct-2018].

[74] BC Ministry of Transportation and Infrastructure, "B.C. on the Move: B.C.s 10-year Transportation Plan," no. March, 2015.

[75] O. Delgado and R. Muncrief, "Assessment of Heavy-Duty Natural Gas Vehicle Emissions: Implications and Policy Recommendations," *ICCT White Pap.*, no. July, 2015.

[76] S. A. Park and H. Tak, "The environmental effects of the CNG bus program on metropolitan air quality in Korea," *Ann. Reg. Sci.*, vol. 49, no. 1, pp. 261–287, 2012.

[77] FortisBC, "FortisBC launches incentive program for heavy-duty natural gas vehicles," 2012. [Online]. Available: https://www.fortisbc.com/MediaCentre/NewsReleases/2012/Pages/FortisBC-launches-

incentive-program-for-heavy-duty-natural-gas-vehicles.aspx. [Accessed: 12-Feb-2019].

[78] B. J. S. Cannon, “Natural Gas : an Essential Bridge To Hydrogen Fuel Cell Vehicles,” 2012.

[79] J. Ogden, A. M. Jaffe, D. Scheitrum, Z. McDonald, and M. Miller, “Natural gas as a bridge to hydrogen transportation fuel: Insights from the literature,” *Energy Policy*, vol. 115, no. January, pp. 317–329, 2018.

[80] J. R. Camuzeaux, R. A. Alvarez, S. A. Brooks, J. B. Browne, and T. Sterner, “Influence of methane emissions and vehicle efficiency on the climate implications of heavy-duty natural gas trucks,” *Environ. Sci. Technol.*, vol. 49, no. 11, pp. 6402–6410, 2015.

[81] L. Rose, M. Hussain, S. Ahmed, K. Malek, R. Costanzo, and E. Kjeang, “A comparative life cycle assessment of diesel and compressed natural gas powered refuse collection vehicles in a Canadian city,” *Energy Policy*, vol. 52, pp. 453–461, 2013.

[82] M. Shahraeeni, S. Ahmed, K. Malek, B. Van Drimmelen, and E. Kjeang, “Life cycle emissions and cost of transportation systems: Case study on diesel and natural gas for light duty trucks in municipal fleet operations,” *J. Nat. Gas Sci. Eng.*, vol. 24, pp. 26–34, 2015.

[83] Argonne National Laboratory, “The greenhouse gases regulated emissions and energy use in transportation model,” 2015. [Online]. Available: https://greet.es.anl.gov/. [Accessed: 12-Feb-2019].

[84] D. C. Quiros *et al.*, “Real-World Emissions from Modern Heavy-Duty Diesel, Natural Gas, and Hybrid Diesel Trucks Operating Along Major California Freight Corridors,” *Emiss. Control Sci. Technol.*, vol. 2, no. 3, pp. 156–172, 2016.

[85] Westport Fuel Systems, “Company Overview,” *Westport Fuel Syst.*, no. May, pp. 132–134, 2017.

[86] Graz University of Technology, “HDV-CO2-Lot4-SR7 - VECTO tool development: completion of methodology to simulate Heavy Duty Vehicles, fuel consumption and CO2 emissions; upgrades to the existing version of VECTO, and completion of certification methodology to be incorporated into a Comi.” [Online]. Available: https://www.tugraz.at/en/institutes/iti/research/projects/vecto/. [Accessed: 12-Feb-2019].

[87] U.S. EPA., “Regulations for Greenhouse Gas Emissions from Commercial Trucks & Buses,” 2016. [Online]. Available: https://www.epa.gov/regulations-emissions-vehicles-and-engines/regulations-greenhouse-gas-emissions-commercial-trucks. [Accessed: 27-Feb-2018].

[88] AVL Company, “AVL CRUISE™ - avl.com,” 2015. [Online]. Available: https://www.avl.com/cruise/. [Accessed: 12-Feb-2019].

[89] G. Zamboni, M. André, A. Roveda, and M. Capobianco, “Experimental evaluation of Heavy Duty Vehicle speed patterns in urban and port areas and estimation of their fuel consumption and exhaust emissions,” *Transp. Res. Part D Transp. Environ.*, vol. 35, pp. 1–10, 2015.

[90] D. W. Wyatt, H. Li, and J. E. Tate, “The impact of road grade on carbon dioxide (CO2) emission of a passenger vehicle in real-world driving,” *Transp. Res. Part D Transp. Environ.*, vol. 32, pp. 160–170, 2014.

[91] V. Franco, O. Delgado, and R. Muncrief, “HEAVY-DUTY VEHICLE FUEL-EFFICIENCY SIMULATION: A COMPARISON OF US AND EU TOOLS,” 2015.

[92] A. Lajunen, “Fuel economy analysis of conventional and hybrid heavy vehicle combinations over real-world operating routes,” *Transp. Res. Part D Transp. Environ.*, vol. 31, pp. 70–84, 2014.

[93] N. Lutsey, C. J. Brodrick, and T. Lipman, “Analysis of potential fuel consumption and emissions reductions from fuel cell auxiliary power units (APUs) in long-haul trucks,” *Energy*, vol. 32, no. 12, pp. 2428–2438, 2007.

[94] K. Liu, T. Yamamoto, and T. Morikawa, “Impact of road gradient on energy consumption of electric vehicles,” *Transp. Res. Part D Transp. Environ.*, vol. 54, pp. 74–81, 2017.

[95] J. Wang, K. Liu, and T. Yamamoto, “Improving electricity consumption estimation for electric vehicles based on sparse GPS observations,” *Energies*, vol. 10, no. 1, pp. 19–22, 2017.

[96] A. Soofastaei, S. M. Aminossadati, M. M. Arefi, and M. S. Kizil, “Development of a multi-layer perceptron artificial neural network model to determine haul trucks energy consumption,” *Int. J. Min. Sci. Technol.*, vol. 26, no. 2, pp. 285–293, 2016.

[97] Google Inc, “Google Earth.” [Online]. Available: https://www.google.com/earth/. [Accessed: 12-Feb-2019].

[98] M. Barth, G. Scora, and T. Younglove, “Modal Emissions Model for Heavy-Duty Diesel Vehicles,” *Transp. Res. Rec. J. Transp. Res. Board*, vol. 1880, no. 1, pp. 10–20, 2004.

[99] U.S. Environmental Protection Agency, “Dynamometer Drive Schedules,” *U.S. Environmental Protection Agency*. [Online]. Available: https://www.epa.gov/vehicle-and-fuel-emissions-testing/dynamometer-drive-schedules. [Accessed: 12-Feb-2019].

[100] U.S. Environmental Protection Agency, “HDUDDS - Urban Dynamometer Driving Schedule for Heavy Duty Vehicles.” [Online]. Available: https://www.epa.gov/sites/production/files/2015-10/huddscol.txt. [Accessed: 12-Feb-2019].

[101] S. Pittman and A. Stanevicius, “WHERE ARE THE TRUCKS ? USING GPS DATA TO DRIVE PORT DECISION-MAKING.” .

[102] “TCX Converter - The multiconverter tool,” *http://www.tcxconverter.com*. [Online]. Available: http://www.tcxconverter.com/TCX_Converter/TCX_Converter_ENG.html. [Accessed: 12-Feb-2019].

[103] E. Wood *et al.*, “Appending high-resolution elevation data to GPS speed traces for vehicle energy modeling and simulation appending high-resolution elevation data to GPS speed traces for vehicle energy modeling and simulation,” *Tech. report, NREL/TP-5400-61109*, no. June, 2014.

[104] M. P. O ’keefe, A. Simpson, K. J. Kelly, and D. S. Pedersen, “Duty Cycle Characterization and Evaluation Towards Heavy Hybrid Vehicle Applications,” in *SAE World Congress and Exhibition*, 2007, pp. 1–12.

[105] R. Prohaska, A. Duran, A. Ragatz, and K. Kelly, “Statistical Characterization of Medium -

Duty Electric Vehicle Drive Cycles," *EVS28 Int. Electr. Veh. Symp. Exhib.*, no. Md, pp. 1–10, 2015.

[106] R. A. Giannelli, E. K. Nam, K. Helmer, T. Younglove, G. Scora, and M. Barth, "Heavy-Duty Diesel Vehicle Fuel Consumption Modeling Based on Road Load and Power Train Parameters," *SAE Int. J. Commer. Veh.*, 2005.

[107] J. L. Jiménez-Palacios, "Understanding and Quantifying Motor Vehicle Emissions with Vehicle Specific Power and TILDAS Remote Sensing," *Massachusetts Inst. Technol. Cambridge*, no. 1993, p. 361, 1999.

[108] E. K. Nam and R. Giannelli, "Fuel Consumption Modeling of Conventional and Advanced Technology Vehicles in the Physical Emission Rate Estimator (PERE) - Draft," *U.S. Environ. Prot. Agency*, no. February, p. 124, 2005.

[109] M. Ross and F. An, "The Use of Fuel by Spark Ignition Engines," *SAE Int. J. Commer. Veh.*, 1993.

[110] Eaton, "The FR Se - (' B' ratio , 'C' ratio and High Torque Models)," Galesburg, 2015.

[111] U.S. EIA, "Carbon Dioxide Emissions Coefficients," *U.S. EIA*, 2016. [Online]. Available: https://www.eia.gov/environment/emissions/co2_vol_mass.php. [Accessed: 12-Feb-2019].

[112] R. G. Boundy, S. W. Diegel, L. L. Wright, and S. C. Davis, "Biomass Energy Data Book-Appendix A: Lower and Higher Heating Values of Gas, Liquid and Solid Fuels," *Oak Ridge Natl. Lab.*, 2011.

[113] U.S. EIA, "Energy Conversion Calculators," *U.S. Energy Information Administration (EIA)*. [Online]. Available: https://www.eia.gov/energyexplained/index.php?page=about_energy_conversion_calculator. [Accessed: 12-Feb-2019].

[114] Cummins Westport Inc, "ISX12 G, Heavy-Duty Natural Gas Truck Engine," Vancouver, 2015.

[115] Mack Trucks Inc., "MP7 Engine Performance," 2013.

[116] M. Ross and F. An, "Model of Fuel Economy with Application to Driving Cycles and Traffic Management," *Transp. Res. Rec.*, vol. 1416, 1993.

[117] Randall Guensler, S. Yoon, C. Feng, H. Li, and J. Jun, "Heavy-duty diesel vehicle modal emission model (HDDV-MEM) volume i: Modal emission modeling framework," 2005.

[118] J. Patten, B. Mcauliffe, W. Mayda, and B. Tanguay, "Technical Report Review of Aerodynamic Drag Reduction Devices for Heavy Trucks and Buses," 2012.

[119] T. Muster, "Fuel savings potential and costs considerations for US class 8 heavy duty trucks throught resistance reductions and improved propulsions technologies until 2020," Cambridge, Massachusetts, 2000.

[120] O. Delgado and N. Lutsey, "The U.S. SuperTruck Program, Expediting The Development of Advanced Heavy-Duty Vehicle Efficiency Technologies," 2014.

[121] U.S. Environmental Protection Agency, "Low-Viscosity Lubricants-A Glance at Clean Freight Strategies," 2016.

[122] U.S. Environmental Protection Agency, “A Glance at Clean Freight Strategies: Weight Reduction,” 2016.

[123] M. Barth *et al.*, “Development of a Comprehensive Modal Emissions Model, Final Report, NCHRP Project 25-11,” 2000.

[124] U.S. DOE-Energy Efficiency and Renewable Energy), “Workshop Report: Trucks and Heavy-Duty Vehicles Technical Requirements and Gaps for Lightweight and Propulsion Materials,” 2013.

[125] T. Nems *et al.*, “Chapter 7 . Transportation Demand Module By submodules and their components , key assumptions on transportation demand and energy consumption,” no. January, pp. 79–103, 2017.

[126] D. C. Quiros, J. Smith, A. Thiruvengadam, T. Huai, and S. Hu, “Greenhouse gas emissions from heavy-duty natural gas, hybrid, and conventional diesel on-road trucks during freight transport,” *Atmos. Environ.*, vol. 168, pp. 36–45, 2017.

[127] BTS, “Table 1-11: Number of U.S. Aircraft, Vehicles, Vessels, and Other Conveyances | Bureau of Transportation Statistics,” 2018. [Online]. Available: https://www.bts.gov/archive/publications/national_transportation_statistics/table_01_11. [Accessed: 09-Sep-2018].

[128] R. M. Ben Sharpe, Nic Lutsey, Oscar Delgado, “U.S. efficiency and greenhouse gas emission regulations for model year 2018-2027 heavy-duty vehicles, engines, and trailers | International Council on Clean Transportation,” *ICCT*, 2016. [Online]. Available: https://www.theicct.org/publications/us-efficiency-and-greenhouse-gas-emission-regulations-model-year-2018-2027-heavy-duty. [Accessed: 08-Sep-2018].

[129] H. H. Liuhanzi Yang, “China’s Stage VI emissions standard for heavy-duty vehicles (final rule) | International Council on Clean Transportation,” *ICCT*, 2018. [Online]. Available: https://www.theicct.org/publications/china’s-stage-vi-emissions-standard-heavy-duty-vehicles-final-rule. [Accessed: 09-Sep-2018].

[130] R. Muncrief and F. Rodriguez, “Briefing: A roadmap for heavy-duty engine CO2 standards within the European Union framework,” no. September, 2017.

[131] G. Giuliano, L. White, and S. Dexter, “Developing Markets for Zero-Emission Vehicles in Goods Movement,” no. March, 2018.

[132] Technology Advancement Office of SCAQMD, “Clean Fuels Program -2017 Annual Report and 2018 Plan Update,” 2018.

[133] Forbes, “Toyota’s Hydrogen Fuel Cell Kenworth Can Revolutionize Heavy Transport,” 2017. [Online]. Available: https://www.forbes.com/sites/markewing/2017/08/09/toyotas-hydrogen-fuel-cell-kenworth-can-revolutionize-heavy-transport/#5859dba56e48. [Accessed: 27-Feb-2018].

[134] Siemens, “eHighway – Solutions for electrified road freight transport,” 2017. [Online]. Available: https://www.siemens.com/press/en/feature/2015/mobility/2015-06-ehighway.php. [Accessed: 27-Feb-2018].

[135] Scania, “Hybrid truck for city use | Scania Group,” 2018. [Online]. Available: https://www.scania.com/group/en/take-control-hybrid-truck-for-city-use/. [Accessed: 27-

Jun-2018].

[136] Volvo Group, “Volvo Truck tests a hybrid vehicle for long haul,” 2017. [Online]. Available: http://www.volvogroup.com/en-en/news/2017/feb/news-2476234.html. [Accessed: 27-Feb-2018].

[137] US DOE, “GREET - Free and maintained,” 2018. [Online]. Available: https://greet.es.anl.gov/greet/gettingstarted/wtw.html. [Accessed: 27-Jun-2018].

[138] S. J. Curran, R. M. Wagner, R. L. Graves, M. Keller, and J. B. Green, “Well-to-wheel analysis of direct and indirect use of natural gas in passenger vehicles,” *Energy*, vol. 75, pp. 194–203, 2014.

[139] Y. Bicer and I. Dincer, “Comparative life cycle assessment of hydrogen, methanol and electric vehicles from well to wheel,” *Int. J. Hydrogen Energy*, vol. 42, no. 6, pp. 3767–3777, 2017.

[140] C. Bauer, J. Hofer, H. J. Althaus, A. Del Duce, and A. Simons, “The environmental performance of current and future passenger vehicles: Life Cycle Assessment based on a novel scenario analysis framework,” *Appl. Energy*, vol. 157, pp. 871–883, 2015.

[141] R. Danielis, M. Giansoldati, and L. Rotaris, “A probabilistic total cost of ownership model to evaluate the current and future prospects of electric cars uptake in Italy,” *Energy Policy*, vol. 119, no. April, pp. 268–281, 2018.

[142] Q. De Clerck, T. van Lier, M. Messagie, C. Macharis, J. Van Mierlo, and L. Vanhaverbeke, “Total Cost for Society: A persona-based analysis of electric and conventional vehicles,” *Transp. Res. Part D Transp. Environ.*, no. February, pp. 1–21, 2018.

[143] O. Van Vliet, A. S. Brouwer, T. Kuramochi, M. Van Den Broek, and A. Faaij, “Energy use, cost and CO2emissions of electric cars,” *J. Power Sources*, vol. 196, no. 4, pp. 2298–2310, 2011.

[144] M. Yazdanie, F. Noembrini, S. Heinen, A. Espinel, and K. Boulouchos, “Well-to-wheel costs, primary energy demand, and greenhouse gas emissions for the production and operation of conventional and alternative vehicles,” *Transp. Res. Part D Transp. Environ.*, vol. 48, pp. 63–84, 2016.

[145] L. Nurhadi, S. Borén, and H. Ny, “A sensitivity analysis of total cost of ownership for electric public bus transport systems in swedish medium sized cities,” *Transp. Res. Procedia*, vol. 3, no. July, pp. 818–827, 2014.

[146] G. Correa, P. Muñoz, T. Falaguerra, and C. R. Rodriguez, “Performance comparison of conventional, hybrid, hydrogen and electric urban buses using well to wheel analysis,” *Energy*, vol. 141, pp. 537–549, 2017.

[147] D. Dreier, S. Silveira, D. Khatiwada, K. V. O. Fonseca, R. Nieweglowski, and R. Schepanski, “Well-to-Wheel analysis of fossil energy use and greenhouse gas emissions for conventional, hybrid-electric and plug-in hybrid-electric city buses in the BRT system in Curitiba, Brazil,” *Transp. Res. Part D Transp. Environ.*, vol. 58, no. December 2017, pp. 122–138, 2018.

[148] Z. Gao *et al.*, “The evaluation of developing vehicle technologies on the fuel economy of

long-haul trucks," *Energy Convers. Manag.*, vol. 106, pp. 766–781, 2015.

[149] T. Zhou, M. J. Roorda, H. L. MacLean, and J. Luk, "Life cycle GHG emissions and lifetime costs of medium-duty diesel and battery electric trucks in Toronto, Canada," *Transp. Res. Part D Transp. Environ.*, vol. 55, pp. 91–98, 2017.

[150] D.-Y. Lee, V. M. Thomas, and M. A. Brown, "Electric Urban Delivery Trucks: Energy Use, Greenhouse Gas Emissions, and Cost-Effectiveness," *Environ. Sci. Technol.*, vol. 47, no. 14, pp. 8022–8030, 2013.

[151] O. Zirn, S. Krauth, and M. Ahlborn, "Hybridisation Potentials for Heavy Trucks Considering Route Topography," *IFAC-PapersOnLine*, vol. 49, no. 21, pp. 316–321, 2016.

[152] S. Sripad and V. Viswanathan, "Performance Metrics Required of Next-Generation Batteries to Make a Practical Electric Semi Truck," *ACS Energy Lett.*, vol. 2, no. 7, pp. 1669–1673, 2017.

[153] Vancouver Fraser Port Authority, "Container Truck GPS Data of November 2016," 2016. .

[154] Natural Resources Canada, "Transportation Sector British Columbia and Territories Table 12: Road Transportation Secondary Energy Use and GHG Emissions by Transportation Mode | Natural Resources Canada," 2018. [Online]. Available: http://oee.nrcan.gc.ca/corporate/statistics/neud/dpa/showTable.cfm?type=CP&sector=tran&juris=bct&rn=12&page=0. [Accessed: 18-Jul-2018].

[155] H. Talebian, O. E. Herrera, M. Tran, and W. Mérida, "Electrification of road freight transport: Policy implications in British Columbia," *Energy Policy*, vol. 115, no. September 2017, pp. 109–118, 2018.

[156] S. M. Lajevardi, J. Axsen, and C. Crawford, "Examining the role of natural gas and advanced vehicle technologies in mitigating CO2 emissions of heavy-duty trucks: Modeling prototypical British Columbia routes with road grades," *Transp. Res. Part D Transp. Environ.*, vol. 62, pp. 186–211, Jul. 2018.

[157] Mack Trucks, "MP8 445C Engine," 2014.

[158] UQM Technologies Inc, "UQM Datasheet, UQM PowerPhase® HD 220 System," Longmont, 2013.

[159] Ford Motor Company, "Truck Powertrain Summary," 2014.

[160] Engine Distributors Inc, "Engine Distributors Inc. » Ford CSG-637 Engine," *Engine Distributors Inc.*, 2019. [Online]. Available: http://www.edi-dist.com/ford-csg-637-engine/. [Accessed: 21-Mar-2019].

[161] Loop Energy, "LOOP Energy, More power to move you.," 2017.

[162] M. Mintz, J. Han, and A. Burnham, "Alternative and renewable gaseous fuels to improve vehicle environmental performance," in *Alternative Fuels and Advanced Vehicle Technologies for Improved Environmental Performance: Towards Zero Carbon Transportation*, Elsevier, 2014, pp. 90–116.

[163] T. Korakianitis, A. M. Namasivayam, and R. J. Crookes, "Natural-gas fueled spark-

ignition (SI) and compression-ignition (CI) engine performance and emissions," *Prog. Energy Combust. Sci.*, vol. 37, no. 1, pp. 89–112, Feb. 2011.

[164] M. F. Ezzat and I. Dincer, "Development and exergetic assessment of a new hybrid vehicle incorporating gas turbine as powering option," *Energy*, vol. 170, pp. 112–119, 2019.

[165] E. Faghani, "Effect of Injection Strategies on Particulate Matter Emissions From HPDI Natural-Gas Engines," no. November, p. 262, 2015.

[166] NREL, "Development of the High-Pressure Direct-Injection ISX G Natural Gas Engine," 2004.

[167] Truckinginfo, "Westport Dropping 15-Liter LNG Engine for North America - Fuel Smarts - Trucking Info," 2013. [Online]. Available: https://www.truckinginfo.com/114651/westport-dropping-15-liter-lng-engine-for-north-america. [Accessed: 16-Jun-2018].

[168] Panasonic, "Panasonic NCR18650B," *Data sheet*, no. 469, p. 2, 2012.

[169] EMvalley, "The Cells in Tesla's 90 kWh Model S that 'Partially Use Silicon' – What Can They Be? – Electromobility News," 2015. [Online]. Available: http://www.emvalley.com/news/the-cells-in-teslas-90-kwh-model-s-that-partially-use-silicon-what-can-they-be/. [Accessed: 28-Feb-2018].

[170] A. Mahmoudzadeh Andwari, A. Pesiridis, S. Rajoo, R. Martinez-Botas, and V. Esfahanian, "A review of Battery Electric Vehicle technology and readiness levels," *Renew. Sustain. Energy Rev.*, vol. 78, pp. 414–430, Oct. 2017.

[171] BYD, "LONG-RANGE BATTERY ELECTRIC," 2016. [Online]. Available: http://www.byd.com/usa/wp-content/uploads/2016/08/T9-final.pdf. [Accessed: 27-Feb-2018].

[172] J. Goldman, "Electric Class 8 Truck Product Description Electric," Poway, CA, 2014.

[173] State of California Air Resources Board, "Draft Technology Assessment: Heavy-Duty Hybrid Vehicles," 2015.

[174] D. Connolly, "Economic viability of electric roads compared to oil and batteries for all forms of road transport," *Energy Strateg. Rev.*, vol. 18, pp. 235–249, 2017.

[175] Wrightspeed, "Wrightspeed Range-Extended Electric Powertrains," 2018. [Online]. Available: https://www.wrightspeed.com/. [Accessed: 27-Feb-2018].

[176] J. Chen, J. B. Siegel, A. G. Stefanopoulou, and J. R. Waldecker, "Optimization of purge cycle for dead-ended anode fuel cell operation," *Int. J. Hydrogen Energy*, vol. 38, no. 12, pp. 5092–5105, 2013.

[177] N. Armaroli and V. Balzani, "The hydrogen issue," *ChemSusChem*, vol. 4, no. 1, pp. 21–36, 2011.

[178] K. Walkowicz, A. Duran, and E. Burton, "Fleet DNA Project Data Summary Report," 2016.

[179] D. Surowski, "Distance between Points on the Earth's Surface Abstract," 2011.

[180] U.S. Geological Survey, “Global 30 Arc-Second Elevation (GTOPO30) | The Long Term Archive,” 1996. [Online]. Available: https://lta.cr.usgs.gov/GTOPO30. [Accessed: 04-Mar-2018].

[181] Canadian Task Force on Vehicle Weights and Dimensions Policy, “Heavy Truck Weight and Dimension Limits for Interprovincial Operations in Canada,” 2019.

[182] M. Saxe, “Bringing fuel cells to reality and reality to fuel cells - A systems perspective on the use of fuel cells,” KTH - Royal Institute of Technology, 2008.

[183] US DOE, “Technology Assessment of a Fuel Cell Vehicle: 2017 Toyota Mirai Energy Systems Division,” *US DOE -Energy Syst. Div.*, 2017.

[184] NRC, *Technologies and Approaches to Reducing the Fuel Consumption of Medium- and Heavy-Duty Vehicles*. Washington, D.C.: National Academies Press, 2010.

[185] M. A. R. Do Nascimento, L. D. O. Rodrigues, E. E. B. G. E. C. Dos Santos, F. L. G. Dias, E. I. G. Velásques, and R. a. M. Carrillo, “Micro Gas Turbine Engine: A Review,” in *Progress in Gas Turbine Performance*, E. Benini, Ed. 2014, pp. 107–142.

[186] N. Murgovski, L. Johannesson, and J. Sjöberg, “Convex modeling of energy buffers in power control applications,” *IFAC Proc. Vol.*, vol. 45, no. 30, pp. 92–99, 2012.

[187] EPCPower, “EPC Power Corporation | RS-11,” *EPCPower*, 2019. [Online]. Available: https://www.epcpower.com/products/specs/rs-11/. [Accessed: 21-Mar-2019].

[188] US Hybrid, “Heavy Duty Integrated Electric Drive Unit ‘ EDU240 ,’” 2019.

[189] Kinetics Drive Solutions Inc, “3-Speed Electric Drive System,” Langley, 2013.

[190] UQM Technologies Inc, “POWERPHASE ® HD 220,” 2019.

[191] US Hybrid, “Medium Duty Integrated Electric Drive Unit ‘ EDU200 ,’” *US Hybrid*, 2019.

[192] J. Kurtz, S. Sprik, C. Ainscough, G. Saur, and S. Onorato, “Fuel Cell Electric Vehicle Evaluation,” *DOE Hydrog. Fuel Cells Progr. 2018 Annu. Merit Rev. Peer Eval. Meet.*, p. 18, 2018.

[193] Green Car Congress, “Wrightspeed unveils new turbine range extender for medium- and heavy-duty electric powertrains, 30% more efficient than current microturbine generators,” *Green Car Congress*, 2015. [Online]. Available: https://www.greencarcongress.com/2015/05/wrightspeed.html. [Accessed: 19-Mar-2019].

[194] U.S. EPA, “Class 8 CNG / Diesel System Cost Analysis,” U.S. EPA, 2015.

[195] US DOE, “Target Explanation Document: Onboard Hydrogen Storage for Light-Duty Fuel Cell Vehicles,” *U.S Drive*, no. May, pp. 1–29, 2017.

[196] A. J. Simon, “Cryo-Compressed Pathway Analysis,” 2016.

[197] T. Navidi, Y. Cao, and P. T. Krein, “Analysis of wireless and catenary power transfer systems for electric vehicle range extension on rural highways,” *2016 IEEE Power Energy Conf. Illinois, PECI 2016*, 2016.

[198] A. Maitra, “Utility Direct Technology Boosts Efficiency Of Fast Charging For Electric Vehicle,” *How2Power Today*, no. March, pp. 1–5, 2012.

[199] A. Franca, Y. Zhao, G. Duffy, A. Jami, and J. Petrunic, “Techno-economic modelling of an electric bus demonstration project in London Ontario,” 2018.

[200] B. Nykvist and M. Nilsson, “Rapidly falling costs of battery packs for electric vehicles,” *Nat. Clim. Chang.*, vol. 5, no. 4, pp. 329–332, 2015.

[201] B. Nykvist, F. Sprei, and M. Nilsson, “Assessing the progress toward lower priced long range battery electric vehicles,” *Energy Policy*, vol. 124, no. October 2018, pp. 144–155, 2019.

[202] U.S. Department of Energy, “Overview of the DOE Advanced Battery R&D Program,” 2015.

[203] L. Fulton and M. Miller, “Strategies for Low-Carbon Emission Trucks in the United States,” 2015.

[204] N. T. Stetson, “Hydrogen Storage Program Area,” 2017.

[205] A. Wilson *et al.*, “DOE Hydrogen and Fuel Cells Program Record,” 2016.

[206] J. M. Miller, “Electric Motor R&D Oak Ridge National Laboratory,” *2013 U.S. DOE Hydrog. Fuel Cells Progr. Veh. Technol. Progr. Annu. Merit*, 2013.

[207] D. Scheitrum, A. Myers Jaffe, R. Dominguez-Faus, and N. Parker, “California low carbon fuel policies and natural gas fueling infrastructure: Synergies and challenges to expanding the use of RNG in transportation,” *Energy Policy*, vol. 110, pp. 355–364, Nov. 2017.

[208] BC-Hydro, “General Service Business Rates,” 2019. [Online]. Available: https://app.bchydro.com/accounts-billing/rates-energy-use/electricity-rates/business-rates.html. [Accessed: 12-Mar-2019].

[209] Natural Resources Canada, “Average Retail Prices in Canada | Energy Sources | Natural Resources Canada,” *Natural Resources Canada*, 2019. [Online]. Available: http://www2.nrcan.gc.ca/eneene/sources/pripri/prices_bycity_e.cfm?productID=5&locationID=66&locationID=39&locationID=2&frequency=M&priceYear=2019&Redisplay=. [Accessed: 15-Mar-2019].

[210] California Air Resource Board, “Advanced Clean Transit Meetings and Workshops, Cost Assumptions and Data Sources,” 2016. [Online]. Available: https://www.arb.ca.gov/msprog/bus/actmeetings.htm. [Accessed: 02-Mar-2018].

[211] California Air Resources Board, “Draft Technology Assessment: Medium- And Heavy-Duty Fuel Cell Electric Vehicles,” no. November, 2015.

[212] B. Hyman, “Engineering Economics,” in *Fundamentals of Engineering Design*, 2nd Editio., Pearson, 2002.

[213] D. A. Castelo Branco, A. Szklo, G. Gomes, B. S. M. C. Borba, and R. Schaeffer, “Abatement costs of CO2emissions in the Brazilian oil refining sector,” *Appl. Energy*, vol. 88, no. 11, pp. 3782–3790, 2011.

[214] M. Sykes and J. Axsen, “No free ride to zero-emissions: Simulating a region’s need to implement its own zero-emissions vehicle (ZEV) mandate to achieve 2050 GHG targets,” *Energy Policy*, vol. 110, pp. 447–460, Nov. 2017.

[215] Steve Josephs, “The per-mile Costs of Operating Compressed Natural Gas Trucks:

Experience from 16 Million Miles with the Cummins ISX12G," 2015.

[216] M. Lammert and K. Walkowicz, "Thirty-Six Month Evaluation of UPS Diesel Hybrid-Electric Delivery Vans," 2012.

[217] E. Neandross, P. Couch, and T. Grimes, "Zero-Emission Catenary Hybrid Truck Market Study," 2012.

[218] California Air Resource Board, "Innovative Clean Transit Meetings and Workshops," 2018. [Online]. Available: https://arb.ca.gov/msprog/ict/meeting.htm. [Accessed: 18-Apr-2018].

[219] National Biodiesel Board, "Automakers' and Engine Manufacturers' Positions of Support for Biodiesel Blends," 2012. [Online]. Available: http://biodiesel.org/using-biodiesel/oem-information/oem-statement-summary-chart. [Accessed: 28-Feb-2018].

[220] US DOE, "Alternative Fuels Data Center: Renewable Hydrocarbon Biofuels," 2018. [Online]. Available: https://www.afdc.energy.gov/fuels/emerging_hydrocarbon.html. [Accessed: 10-Oct-2018].

[221] The Canadian Energy and Emissions Data Centre, "Liquid Biofuels Data-Provincial Diesel and Biodiesel/Renewable Diesel Consumption," Mar-. [Online]. Available: https://www.sfu.ca/ceedc/databases/Biofuels.html. [Accessed: 17-Mar-2018].

[222] A. Burnham, "Updated fugitive greenhouse gas emissions for natural gas pathways in the GREET model," 2016.

[223] N. N. Clark *et al.*, "Pump-to-wheels methane emissions from the heavy-duty transportation sector," *Environ. Sci. Technol.*, vol. 51, no. 2, pp. 968–976, 2017.

[224] G. Myhre *et al.*, "Anthropogenic and Natural Radiative Forcing," *Clim. Chang. 2013 Phys. Sci. Basis. Contrib. Work. Gr. I to Fifth Assess. Rep. Intergov. Panel Clim. Chang.*, pp. 659–740, 2013.

[225] and A. K. K. Kelly, R. Prohaska, A. Ragatz, "NREL DriveCAT - Chassis Dynamometer Test Cycles. National Renewable Energy Laboratory," 2016. [Online]. Available: www.nrel.gov/transportation/drive-cycle-tool. [Accessed: 14-Jul-2018].

[226] S. Yun, K. Lee, and K. Yi, "Development of a power management strategy to minimize the fuel consumption of a heavy-duty series hybrid electric vehicle," *J. Mech. Sci. Technol.*, vol. 29, no. 10, pp. 4399–4406, 2015.

[227] A. Karvountzis-Kontakiotis, A. M. Andwari, A. Pesyridis, S. Russo, R. Tuccillo, and V. Esfahanian, "Application of Micro Gas Turbine in Range-Extended Electric Vehicles," *Energy*, vol. 147, pp. 351–361, 2018.

[228] M. Ben Chaim, E. Shmerling, and A. Kuperman, "A fuel efficiency evaluation of gas-turbine-engine-based hybrid vehicles," *Int. J. Green Energy*, vol. 12, no. 4, pp. 328–332, 2015.

[229] O. P. R. van Vliet, T. Kruithof, W. C. Turkenburg, and A. P. C. Faaij, "Techno-economic comparison of series hybrid, plug-in hybrid, fuel cell and regular cars," *J. Power Sources*, vol. 195, no. 19, pp. 6570–6585, 2010.

[230] J. Li *et al.*, "Towards Low-Cost, High Energy Density, and High Power Density Lithium-

Ion Batteries," *Oak Ridge Natl. Lab.*, pp. 1–27, 2017.

[231] Z. Lei, Y. Zhang, and X. Lei, "Improving temperature uniformity of a lithium-ion battery by intermittent heating method in cold climate," *Int. J. Heat Mass Transf.*, vol. 121, pp. 275–281, 2018.

[232] J. Jaguemont, L. Boulon, and Y. Dubé, "A comprehensive review of lithium-ion batteries used in hybrid and electric vehicles at cold temperatures," *Appl. Energy*, vol. 164, pp. 99–114, 2016.

[233] A. Burnham *et al.*, "Enabling fast charging – Infrastructure and economic considerations," *J. Power Sources*, vol. 367, pp. 237–249, 2017.

[234] Capstone Microturbine, "Capstone MicroTurbine User ' s Manual," 2005.

[235] B. Zohuri, *Hydrogen Energy Challenges and Solutions for a Cleaner Future*. Springer International Publishing AG, 2019.

[236] NewsWire, "Transport Canada mandates new technologies for trucks and buses to improve safety," 2017. [Online]. Available: https://www.newswire.ca/news-releases/transport-canada-mandates-new-technologies-for-trucks-and-buses-to-improve-safety-664962593.html. [Accessed: 24-Mar-2018].

[237] Federal Motor Carrier Safety Administration, "Electronic Logging Devices to be Required Across Commercial Truck and Bus Industries | Federal Motor Carrier Safety Administration," 2015. [Online]. Available: https://www.fmcsa.dot.gov/newsroom/electronic-logging-devices-be-required-across-commercial-truck-and-bus-industries. [Accessed: 24-Mar-2018].

[238] TheHindu, "GPS to be mandatory for all commercial vehicles by year-end - The Hindu," 2017. [Online]. Available: http://www.thehindu.com/news/national/karnataka/GPS-to-be-mandatory-for-all-commercial-vehicles-by-year-end/article17079038.ece. [Accessed: 24-Mar-2018].

[239] B. Dale, "A sober view of the difficulties in scaling cellulosic biofuels," *Biofuels, Bioprod. Biorefining*, vol. 11, no. 1, pp. 5–7, Jan. 2017.

[240] L. Bauer and W. Quapp, "Scale-Up of Emerging Biofuel Technologies : Biofuels Digest," *BiofuelsDigest*, 2016.

[241] Canadian Gas Association, "Renewable Natural Gas Technology Roadmap for Canada," no. December. p. 24, 2014.

[242] Hallbar Consulting, Research Institute of Sweden, and BC Ministry of Energy and Mines, "Resource Supply Potential for Renewable Natural Gas in B . C .," no. March. 2017.

[243] Natural Resources Canada, "Electric Charging and Alternative Fuelling Stations Locator | Natural Resources Canada," 2018. [Online]. Available: https://www.nrcan.gc.ca/energy/transportation/personal/20487#/analyze?region=CA-BC&fuel=CNG&fuel=LNG&cng_fill_type=Q&cng_vehicle_class=HD&show_map=true&lng_vehicle_class=HD. [Accessed: 19-Oct-2018].

[244] T. S. Bryden, A. Holland, G. Hilton, B. Dimitrov, C. P. de León Albarrán, and A. Cruden, "Lithium-ion degradation at varying discharge rates," *Energy Procedia*, vol. 151, pp. 194–

198, 2018.

[245] E. Mulholland, J. Teter, P. Cazzola, Z. McDonald, and B. P. Ó Gallachóir, “The long haul towards decarbonising road freight – A global assessment to 2050,” *Appl. Energy*, vol. 216, no. November 2017, pp. 678–693, 2018.

[246] Pembina Institute, “Fuel savings and emissions reductions in heavy-duty trucking A blueprint for further action in Canada,” 2019.

[247] T. Earl, L. Mathieu, S. Cornelis, S. Kenny, C. C. Ambel, and J. Nix, “Analysis of long haul battery electric trucks in EU,” *8th Commer. Veh. Work.*, no. May, pp. 17–18, 2018.

[248] R. G. Cong, D. Caro, and M. Thomsen, “Is it beneficial to use biogas in the Danish transport sector? – An environmental-economic analysis,” *J. Clean. Prod.*, vol. 165, no. 2017, pp. 1025–1035, 2017.

[249] A. Arteconi, M. Spitoni, F. Polonara, and F. Spigarelli, “The feasibility of liquefied biomethane as alternative fuel: a comparison between European and Chinese markets,” *Int. J. Ambient Energy*, vol. 38, no. 5, pp. 481–488, 2017.

[250] Stephanie Searle, “Renewable gas is a distraction for Europe | International Council on Clean Transportation,” *International Council on Clean Transportation*, 2018. [Online]. Available: https://theicct.org/blog/staff/renewable-gas-distraction-europe. [Accessed: 30-Jul-2019].

[251] BC government, “Greenhouse Gas Reduction Targets Act of British Columbia.” [Online]. Available: http://www.bclaws.ca/civix/document/id/lc/statreg/07042_01. [Accessed: 18-Aug-2018].

[252] S. Tongur and M. Engwall, “Environmental Innovation and Societal Transitions Exploring window of opportunity dynamics in infrastructure transformation,” *Environ. Innov. Soc. Transitions*, vol. 25, pp. 82–93, 2017.

[253] U.S. EPA, “Options for Simplifying MOVES Onroad Source Types and Ramps-FCA MOVES Review Work Group -,” 2016.

[254] J. C. González Palencia, M. Araki, and S. Shiga, “Energy consumption and CO2 emissions reduction potential of electric-drive vehicle diffusion in a road freight vehicle fleet,” *Energy Procedia*, vol. 142, pp. 2936–2941, 2017.

[255] A. C. Askin, G. E. Barter, T. H. West, and D. K. Manley, “The heavy-duty vehicle future in the United States: A parametric analysis of technology and policy tradeoffs,” *Energy Policy*, vol. 81, no. 2015, pp. 1–13, 2015.

[256] E. Çabukoglu, G. Georges, L. Küng, and G. Pareschi, “Battery electric propulsion : An option for heavy-duty vehicles ? Results from a Swiss case-study,” *Transp. Res. Part C*, vol. 88, no. January, pp. 107–123, 2018.

[257] H. Liimatainen, O. Van Vliet, and D. Aplyn, “The potential of electric trucks – An international commodity-level analysis,” *Appl. Energy*, vol. 236, no. December 2018, pp. 804–814, 2019.

[258] A. Gambhir, L. K. C. Tse, D. Tong, and R. Martinez-botas, “Reducing China ’ s road transport sector CO 2 emissions to 2050 : Technologies , costs and decomposition analysis

q," *Appl. Energy*, vol. 157, pp. 905–917, 2015.

[259] J. Axsen, D. C. Mountain, and M. Jaccard, "Combining stated and revealed choice research to simulate the neighbor effect: The case of hybrid-electric vehicles," *Resour. Energy Econ.*, vol. 31, no. 3, pp. 221–238, 2009.

[260] S. M. Lajevardi, J. Axsen, and C. Crawford, "Comparing Alternative Heavy-duty Drivetrains based on GHG Emissions, Ownership and Abatement costs: Simulations of Freight Routes in British Columbia," *Transp. Res. Part D Transp. Environ.*, vol. 76, pp. 19–55, 2019.

[261] A. Nikas, H. Doukas, and A. Papandreou, "A Detailed Overview and Consistent Classification of Climate-Economy Models," in *Understanding Risks and Uncertainties in Energy and Climate Policy*, Cham: Springer International Publishing, 2018, pp. 1–54.

[262] O. Bahn, M. Marcy, K. Vaillancourt, and J. Waaub, "Electri fi cation of the Canadian road transportation sector : A 2050 outlook with TIMES-Canada," vol. 62, pp. 593–606, 2013.

[263] M. Jaccard, "International Handbook on the Economics of Energy," in *Combining top down and bottom up in energy economy models*, J. Evans and L. Hunt, Eds. 2009.

[264] G. Kamiya, J. Axsen, and C. Crawford, "Modeling the GHG emissions intensity of plug-in electric vehicles using short-term and long-term perspectives," *Transp. Res. Part D Transp. Environ.*, vol. 69, pp. 209–223, 2019.

[265] R. Murphy and M. Jaccard, "Energy efficiency and the cost of GHG abatement: A comparison of bottom-up and hybrid models for the US," *Energy Policy*, vol. 39, no. 11, pp. 7146–7155, 2011.

[266] T. A. Litman, "Understanding transport demands and elasticities: how prices and other factors affect travel behavior," 2018.

[267] Statistics Canada, "Canadian Freight Analysis Framework," *Statistics Canada*, 2019. [Online]. Available: https://www150.statcan.gc.ca/n1/en/catalogue/50-503-X. [Accessed: 25-Jul-2019].

[268] J. Norris and G. Escher, "Heavy Duty Vehicles Technology Potential and Cost Study," 2017.

[269] U.S. EIA, "Annual Energy Outlook 2018 with projections to 2050," *Annu. Energy Outlook 2018 with Proj. to 2050*, vol. 44, no. 8, pp. 1–64, 2018.

[270] J. Fox, J. Axsen, and M. Jaccard, "Picking Winners: Modelling the Costs of Technology-specific Climate Policy in the U.S. Passenger Vehicle Sector," *Ecol. Econ.*, vol. 137, pp. 133–147, Jul. 2017.

[271] U.S. DOE, "Technology Fact Sheet Series: Microturbines.', DOE/EE-1329 July 2016.," 2016.

[272] Darrell Proctor, "Microturbine Market Ready to Expand," *POWER Magazine*, 2017. [Online]. Available: https://www.powermag.com/microturbine-market-ready-to-expand/. [Accessed: 21-Jan-2019].

[273] CAFCP, "By The Numbers | California Fuel Cell Partnership," *California Fuel Cell Partnership*, 2019. [Online]. Available: https://cafcp.org/by_the_numbers. [Accessed: 03-

Feb-2019].

[274] NGV Global, “Current Natural Gas Vehicle Statistics | NGV Global Knowledgebase,” 2018. [Online]. Available: http://www.iangv.org/current-ngv-stats/. [Accessed: 26-Oct-2018].

[275] National Energy Board, “Canada’s Energy Future 2018: An Energy Market Assessment,” 2018.

[276] A. M. Jaffe, R. Dominguez-Faus, N. C. Parker, D. P. Scheitrum, J. Wilcock, and M. Miller, “The Feasibility of Renewable Natural Gas as a Large-Scale, Low Carbon Substitute,” 2016.

[277] D. L. Greene, “TAFV Alternative Fuels and Vehicles Choice Model Documentation,” U.S. Department of Energy (DOE), 2001.

[278] United States Department of Transportation, “Average Freight Revenue per Ton-Mile | National Transportation Statistics Table 3-21,” *National Transportation Statistics*, 2018. [Online]. Available: https://www.bts.gov/content/average-freight-revenue-ton-mile. [Accessed: 23-Jul-2019].

[279] Argonne National Laboratory, “A fresh design for GREET life cycle analysis tool,” *Argonne National Laboratory*, 2018. [Online]. Available: https://greet.es.anl.gov/index.php?content=greetdotnet. [Accessed: 04-Feb-2019].

[280] BC Ministry of Energy and Mines, “Renewable and Low Carbon Fuel Requirements Regulation, Approved Carbon Intensities,” 2019.

[281] BC EMPR, “2017/18 Review of BC-LCFS Compliance Pathways,” 2018.

[282] NEB, “NEB - Provincial and Territorial Energy Profiles - British Columbia,” *National Energy Board*, 2019. [Online]. Available: https://www.neb-one.gc.ca/nrg/ntgrtd/mrkt/nrgsstmprfls/bc-eng.html. [Accessed: 03-Feb-2019].

[283] US DOE, “Hydrogen Production: Natural Gas Reforming | Department of Energy,” *US DOE*, 2019. [Online]. Available: https://www.energy.gov/eere/fuelcells/hydrogen-production-natural-gas-reforming. [Accessed: 25-Jan-2019].

[284] North American Council for Freight Efficiency, “AMPING UP : CHARGING INFRASTRUCTURE,” 2019.

[285] Trucker Path Inc., “Diesel Stations Nearby | Truck Fuel | Trucker Path,” 2019. [Online]. Available: https://truckerpath.com/trucker-path-app/diesel-station-near-me/. [Accessed: 27-Jul-2019].

[286] Union of Concerned Scientists, “What is ZEV? | Union of Concerned Scientists,” *Union of Concerned Scientists*, 2016. [Online]. Available: https://www.ucsusa.org/clean-vehicles/california-and-western-states/what-is-zev. [Accessed: 25-Apr-2019].

[287] SCAQMD, “SCAQMD Approves $90.7 Million Zero-Emission Truck Demonstration.” SCAQMD, 2018.

[288] California Air Resources Board, “Advanced Technology Demonstration Projects | California Air Resources Board,” 2019. [Online]. Available: https://ww2.arb.ca.gov/our-work/programs/low-carbon-transportation-investments-and-air-quality-improvement-

program-0. [Accessed: 26-Dec-2019].

[289] International Energy Agency, “The Future of Hydrogen, Seizing today’s opportunities Report,” 2019.

[290] BC Hydro, “Project Overview | Site C.” [Online]. Available: https://www.sitecproject.com/about-site-c/project-overview. [Accessed: 20-Aug-2018].

[291] R. Stern, “Autonomous Trucks Creating New Freight Landscape,” *Res. Manag.*, vol. 62, no. 3, 2019.

[292] J. Kendall, “Electric power to revolutionize heavy-duty distribution trucks - SAE International,” *SAE*, 2016. [Online]. Available: https://www.sae.org/news/2016/07/electric-power-to-revolutionize-heavy-duty-distribution-trucks. [Accessed: 27-Feb-2018].

[293] Jalopnik, “Toyota’s Secret Project To Make A Hydrogen Fuel Cell-Powered Big Rig,” 2017. [Online]. Available: https://jalopnik.com/toyotas-secret-project-to-make-a-hydrogen-fuel-cell-pow-1794458195. [Accessed: 27-Feb-2018].

[294] ArsTechnica, “Toyota is testing heavy-duty hydrogen trucks at the Port of Long Beach | Ars Technica,” 2017. [Online]. Available: https://arstechnica.com/cars/2017/04/toyota-starts-project-portal-the-first-hydrogen-fuel-cell-tractor-trailer/. [Accessed: 27-Feb-2018].

[295] US Hybrid, “US Hybrid Announces China Fuel Cell Joint Venture and Unveils Class 8 Fuel Cell Port Drayage Truck for San Pedro Ports | US Hybrid,” 2017. [Online]. Available: http://ushybrid.com/us-hybrid-announces-china-fuel-cell-joint-venture-and-unveils-class-8-fuel-cell-port-drayage-truck-for-san-pedro-ports/. [Accessed: 27-Feb-2018].

[296] Q. Dai, A. Elgowainy, J. Kelly, J. Han, and M. Wang, “Life Cycle Analysis of Hydrogen Production from Non-Fossil Sources,” 2016.

[297] Powerstrokehub, “3.2L Power Stroke Diesel,” *Powerstrokehub.com*, 2019. [Online]. Available: http://www.powerstrokehub.com/3.2-power-stroke.html. [Accessed: 21-Mar-2019].

[298] J. Howell and J. Harger, “CNG and LNG : What ’ s Best for Your Fleet ?,” 2013.

[299] BC Government, “Interpretation Guidelines Manual British Columbia Employment Standards Act and Regulations - Province of British Columbia ESR Section 1 – Definitions – Long Haul Truck Driver,” 2019. [Online]. Available: https://www2.gov.bc.ca/gov/content/employment-business/employment-standards-advice/employment-standards/igm/esr-definitions/esr-def-long-haul-truck-driver. [Accessed: 14-Jan-2019].

[300] Wikipedia, “Drayage,” *Dedola Global Logistics*, 2019. [Online]. Available: https://en.wikipedia.org/wiki/Drayage. [Accessed: 12-Feb-2019].

Appendix A

Table A1: Summary of the main characteristic of proposed alternative drivetrains for HDTs. In this list only CNG is commercially available

Technology	Manufacturer	Propulsion system	Transmission	Range (km)	Vehicle gross weight (kg)	Energy storage system	Recharge time	Source
Conventional natural gas	Mack-Volvo	298 kW (Cummins 11.9 L)	10 speed-Eaton Fuller	-	-	CNG & LNG tanks	15 minutes	[44]
Plug-in parallel hybrid diesel	Mack-Volvo	295 kW (Mack MP7 11 L) + 150 kW electric motor	Automated Manual	500	-	340 L Diesel tank + 20 kWh battery	2 hr with 11 kw Charger	[43]
Parallel hybrid diesel with Catenary	Scania	268 kW (Scania 9 Liters)+ 130kW electric motor	12 speed with integrated electric motor	500	-	340 L Diesel tank +5 kWh battery	-	[46]
Plug-in LNG parallel hybrid	US Hybrid - Peterbilt 384	239kW (Cummins 8.9L)+ 223 kW electric motor	Automated Manual	450	-	272 DLE LNG tank + 80 kWh battery	4 hrs with 20 kw Charger	[43]
Plug-in CNG series hybrid	BAE/Kenworth	2×200kW electric motor + 239kW (Cummins 8.9L)	Automated Manual	-	-	189 DLE CNG tank + 100 kWh battery	2 hrs Off-board 90 kW charger	[43]
Series hybrid with gas-turbine	Peterbilt &Wal-Mart	electric motor in-series with 65 kW gas-turbine	-	-	36,000	CNG or diesel tank + 45.5 kWh battery	-	[47]
Plug-in CNG series hybrid with catenary	TransPower - International Prostar	300 kW electric motor in-series with 205 kW Ford engine (3.7 L CNG)	Automated Manual	-	36,000	227 DLE CNG tank + 155 kWh battery	2-3 hrs	[43]
Battery electric	BYD	2×180 kW electric motor	Automated Manual	148	54,000	188 kWh battery	2.5 hr	[171]
	Transpower	300 kW electric motor	Automated Manual	193 -241	36,000	311 kWh battery	3-4 hrs	[43]
	US Hybrid	320 kW electric motor	Direct Drive	112-161	36,000	240 kWh battery	4 hrs with 60kW	[43], [49]
	Daimler	2×125 kW electric motor	2 stages reduction gear	200	26,000	212 kWh battery	10 hrs	[292]
	Tesla Motors	4×186kW electric motor	Direct Drive	400-800	36,000	1000 kWh battery	0.5 hr	[42]
H_2 fuel cell	Kenworth-Toyota	500 kW electric motor+ 2×114 kW PEM fuel cell	-	241-386	36,000	40 kg H_2 +12 kWh battery	-	[293], [294]
	US Hybrid	320kW electric motor+ 80 kW PEM fuel cell FCe 80	-	322	36,000	25 kg H_2 +30 kWh battery	9 minutes	[43], [295]
	Nikola Motor	4×186kW electric motor	-	1,287-1,930	37,000-39,000	100 kg +320 kWh battery	15 minutes	[52]

Table A2: Additional parameters for modeling alternative drivetrain HDT

Component	Unit	Quantity	Source
Air density	kg/m3	1.225	
Diesel (lower heating value)	MJ/kg	42.6	Lajevardi et al. , [156]
Natural gas (lower heating value)	MJ/kg	47.14	Lajevardi et al. , [156]
Hydrogen (lower heating value)	MJ/kg	120	[296]
Carbon content of CNG	kgC/kgfuel	64.7%	Lajevardi et al. , [156]
Carbon content of diesel	kgC/kgfuel	86.4%	Lajevardi et al. , [156]
Conventional engine rpm to speed ratio in top gear, SR	rpm/kph	15.5	
3 speed transmission for electric motor based on BYD	-	3.58-1	[189]
Final gear ratio for electric motor	-	5	
UQM 220 HD electric motor without transmission	kg	125	[190]
UQM 220 HD electric motor with transmission	kg	217	[189]
CNG engine: 3.7 L Ford engine (82 kW @ 3200 rpm)	kg	161	[160]
Diesel engine: 3.2 L Ford engine (138 kW @ 3000 rpm)	kg	233	[297]
CNG emission control mass for 11.9 L Cummins engine	kg	70	[194]
Diesel emission control	kg	250	[298]

Table A3: Incremental mass of alternative drivetrains to comparable diesel on each cycle

Drivetrains		SDD (kg)	LDD (kg)	RH (kg)	FH (kg)	HCH1 (kg)	HCH2 (kg)
Gross vehicle mass of diesel drivetrain		**30,224**	**30,299**	**30,313**	**31,066**	**31,253**	**31,271**
Incremental mass	CNG	-9	127	152	252	587	622
	Battery electric	941	4,339	4,856	9,356	18,574	18,607
	Plug-in series hybrid fuel cell	239	1,819	1,719	3,578	9,567	8,954
	Plug-in parallel hybrid fuel cell	-160	2	65	824	2,940	1,839
	Parallel hybrid fuel cell (w/o plug-in)	99	234	281	596	1,373	1,278
	Plug-in parallel hybrid Diesel	723	723	716	733	488	257
	Plug-in series hybrid diesel	344	1,780	1,624	4,022	9,020	8,364
	Plug-in parallel hybrid diesel Catenary	404	380	458	943	453	491
	Plug-in series hybrid diesel Catenary	357	652	1,840	5,103	7,040	7,047
	Plug-in series hybrid gas turbine	606	2,754	2,728	5,875	12,001	11,720
	Plug-in parallel hybrid CNG	590	724	739	879	1,072	849
	Plug-in parallel hybrid CNG Catenary	228	262	409	1,081	1,246	995
	Plug-in series hybrid CNG	739	3,097	3,263	6,606	13,866	13,168
	Plug-in series hybrid CNG Catenary	369	645	2094	6925	11573	11848

Table A4: On-road and upstream GHG emissions for all simulated drivetrains on various considered routes (g/tkm)

Drivetrains	GHG emissions		SDD	LDD	RH	FH	HCH1	HCH2
Diesel	On-road CO_2		125.7	74.0	70.6	70.9	75.1	67.9
	On-road CH_4		0.1	0.1	0.1	0.1	0.1	0.1
	On-road N_2O		0.1	0.0	0.0	0.0	0.0	0.0
	Upstream CO_2 (Low)		18.2	10.7	10.2	10.3	10.9	9.8
	Upstream CH_4 (Low)		7.2	4.2	4.0	4.1	4.3	3.9
	Upstream N_2O (Low)		1.3	0.7	0.7	0.7	0.8	0.7
	Upstream CO_2 (High)		21.4	12.6	12.0	12.1	12.8	11.6
	Upstream CH_4 (High)		8.2	4.8	4.6	4.6	4.9	4.4
	Upstream N_2O (High)		0.5	0.3	0.3	0.3	0.3	0.2
	Well to Wheel (Low)		152.6	89.8	85.7	86.1	91.1	82.4
	Well to Wheel (High)		156.0	91.8	87.6	88.0	93.2	84.3
	GHG reduction percentage relative to a comparable high carbon diesel		2.2%	2.2%	2.2%	2.2%	2.2%	2.2%
CNG	On-road CO_2		101.1	59.7	57.0	57.5	61.2	55.4
	On-road CH_4		6.1	3.6	3.5	3.5	3.7	3.4
	On-road N_2O		0.0	0.0	0.0	0.0	0.0	0.0
	Methane leakage		12.9	7.6	7.3	7.4	7.8	7.1
	Upstream CO_2 (Low)		-101.5	-60.0	-57.2	-57.7	-61.4	-55.7
	Upstream CH_4 (Low)		22.5	13.3	12.7	12.8	13.6	12.4
	Upstream N_2O (Low)		0.6	0.3	0.3	0.3	0.4	0.3
	Upstream CO_2 (High)		18.0	10.6	10.1	10.2	10.9	9.9
	Upstream CH_4 (High)		15.2	9.0	8.6	8.7	9.2	8.4
	Upstream N_2O (High)		0.8	0.5	0.5	0.5	0.5	0.4
	Well to Wheel (Low)		41.8	24.7	23.6	23.8	25.3	22.9
	Well to Wheel (High)		154.1	91.1	87.0	87.7	93.3	84.6
	GHG reduction percentage relative to a comparable high carbon diesel	(Low carbon)	73.2%	73.1%	73.1%	73.0%	72.9%	72.8%
		(High carbon)	1.2%	0.7%	0.8%	0.4%	-0.2%	-0.3%
Battery electric	On-road CO_2		0.0	0.0	0.0	0.0	0.0	0.0
	On-road CH_4		0.0	0.0	0.0	0.0	0.0	0.0
	On-road N_2O		2.4	2.3	2.3	2.8	3.6	3.1
	Upstream CO_2 (Low)		0.2	0.2	0.2	0.3	0.3	0.3
	Upstream CH_4 (Low)		0.0	0.0	0.0	0.0	0.0	0.0
	Upstream N_2O (Low)		39.0	38.4	37.6	46.5	58.3	51.5
	Upstream CO_2 (High)		2.3	2.3	2.3	2.8	3.5	3.1
	Upstream CH_4 (High)		0.0	0.0	0.0	0.0	0.0	0.0
	Upstream N_2O (High)		2.6	2.6	2.5	3.1	3.9	3.4
	Well to Wheel (Low)		41.3	40.7	39.8	49.3	61.8	54.6
	Well to Wheel (High)		0.0	0.0	0.0	0.0	0.0	0.0
	GHG reduction percentage relative to a comparable high carbon diesel	(Low carbon)	98.3%	97.2%	97.1%	96.5%	95.8%	95.9%
		(High carbon)	73.5%	55.6%	54.5%	44.0%	33.7%	35.3%

(Continued)

Table A4 (Continued): On-road and upstream GHG emissions for all simulated drivetrains on various considered routes (g/tkm)

Drivetrains	GHG emissions		SDD	LDD	RH	FH	HCH1	HCH2
Battery electric catenary	On-road CO_2		0.0	0.0	0.0	-	-	-
	On-road CH_4		0.0	0.0	0.0	-	-	-
	On-road N_2O		0.0	0.0	0.0	-	-	-
	Upstream CO_2 (Low)		2.1	1.8	1.9	-	-	-
	Upstream CH_4 (Low)		0.2	0.2	0.2	-	-	-
	Upstream N_2O (Low)		0.0	0.0	0.0	-	-	-
	Upstream CO_2 (High)		34.3	29.8	31.1	-	-	-
	Upstream CH_4 (High)		2.1	1.8	1.9	-	-	-
	Upstream N_2O (High)		0.0	0.0	0.0	-	-	-
	Well to Wheel (Low)		2.3	2.0	2.1	-	-	-
	Well to Wheel (High)		36.3	31.6	33.0	-	-	-
	GHG reduction percentage relative to a comparable high carbon diesel	(Low carbon)	99%	98%	98%	-	-	-
		(High carbon)	77%	66%	62%	-	-	-
Plug-in series hybrid fuel cell	On-road CO_2		0.0	0.0	0.0	0.0	0.0	0.0
	On-road CH_4		0.0	0.0	0.0	0.0	0.0	0.0
	On-road N_2O		0.0	0.0	0.0	0.0	0.0	0.0
	Upstream CO_2 (Low)		4.2	4.2	4.3	4.9	5.6	5.1
	Upstream CH_4 (Low)		0.4	0.4	0.4	0.4	0.5	0.5
	Upstream N_2O (Low)		0.0	0.0	0.0	0.0	0.0	0.0
	Upstream CO_2 (High)		49.5	48.2	48.1	56.5	66.5	59.3
	Upstream CH_4 (High)		4.3	4.3	4.4	5.0	5.7	5.2
	Upstream N_2O (High)		0.3	0.3	0.3	0.3	0.4	0.3
	Well to Wheel (Low)		4.6	4.6	4.7	5.4	6.1	5.6
	Well to Wheel (High)		54.0	52.8	52.7	61.8	72.5	64.8
	GHG reduction percentage relative to a comparable high carbon diesel	(Low carbon)	97.0%	95.0%	94.6%	93.9%	93.4%	93.4%
		(High carbon)	65.4%	42.5%	39.8%	29.8%	22.2%	23.2%
Plug-in parallel hybrid fuel cell	On-road CO_2		0.0	0.0	0.0	0.0	0.0	0.0
	On-road CH_4		0.0	0.0	0.0	0.0	0.0	0.0
	On-road N_2O		0.0	0.0	0.0	0.0	0.0	0.0
	Upstream CO_2 (Low)		7.5	7.0	6.8	7.6	7.9	7.4
	Upstream CH_4 (Low)		0.7	0.6	0.6	0.7	0.7	0.7
	Upstream N_2O (Low)		0.0	0.0	0.0	0.0	0.0	0.0
	Upstream CO_2 (High)		75.6	68.1	66.3	74.4	79.7	72.7
	Upstream CH_4 (High)		7.7	7.1	6.9	7.7	8.1	7.6
	Upstream N_2O (High)		0.5	0.4	0.4	0.5	0.5	0.4
	Well to Wheel (Low)		8.2	7.6	7.4	8.3	8.7	8.1
	Well to Wheel (High)		83.7	75.7	73.7	82.6	88.2	80.7
	GHG reduction percentage relative to a comparable high carbon diesel	(Low carbon)	94.7%	91.7%	91.5%	90.6%	90.7%	90.4%
		(High carbon)	46.3%	17.6%	15.9%	6.1%	5.3%	4.2%

(Continued)

Table A4 (Continued): On-road and upstream GHG emissions for all simulated drivetrains on various considered routes (g/tkm)

Drivetrains	GHG emissions		SDD	LDD	RH	FH	HCH1	HCH2
Parallel hybrid fuel cell (no plug)	On-road CO_2		0.0	0.0	0.0	0.0	0.0	0.0
	On-road CH_4		0.0	0.0	0.0	0.0	0.0	0.0
	On-road N_2O		0.0	0.0	0.0	0.0	0.0	0.0
	Upstream CO_2 (Low)		10.1	7.5	7.4	8.0	8.9	8.1
	Upstream CH_4 (Low)		0.9	0.7	0.7	0.7	0.8	0.7
	Upstream N_2O (Low)		0.0	0.0	0.0	0.0	0.0	0.0
	Upstream CO_2 (High)		98.7	72.9	72.5	78.3	86.4	79.0
	Upstream CH_4 (High)		10.4	7.7	7.6	8.2	9.1	8.3
	Upstream N_2O (High)		0.6	0.4	0.4	0.5	0.5	0.5
	Well to Wheel (Low)		11.1	8.2	8.1	8.8	9.7	8.9
	Well to Wheel (High)		109.6	81.0	80.5	87.0	96.0	87.8
	GHG reduction percentage relative to a comparable high carbon diesel	(Low carbon)	92.9%	91.1%	90.7%	90.0%	89.6%	89.5%
		(High carbon)	29.7%	11.8%	8.1%	1.1%	-3.0%	-4.2%
Plug-in parallel hybrid diesel	On-road CO_2		60.2	50.5	45.6	56.5	68.2	61.3
	On-road CH_4		0.1	0.1	0.1	0.1	0.1	0.1
	On-road N_2O		0.0	0.0	0.0	0.0	0.0	0.0
	Methane leakage		9.5	7.5	6.8	8.3	9.9	8.9
	Upstream CO_2 (Low)		3.5	2.9	2.6	3.2	3.9	3.5
	Upstream CH_4 (Low)		0.6	0.5	0.5	0.6	0.7	0.6
	Upstream N_2O (Low)		21.7	12.5	11.2	12.3	12.0	10.7
	Upstream CO_2 (High)		4.6	3.5	3.2	3.8	4.5	4.0
	Upstream CH_4 (High)		0.3	0.2	0.2	0.2	0.2	0.2
	Upstream N_2O (High)		73.9	61.5	55.6	68.8	82.8	74.4
	Well to Wheel (Low)		86.8	66.7	60.3	73.0	85.0	76.3
	Well to Wheel (High)		60.2	50.5	45.6	56.5	68.2	61.3
	GHG reduction percentage relative to a comparable high carbon diesel	(Low carbon)	52.6%	33.0%	36.5%	21.9%	11.2%	11.7%
		(High carbon)	44.4%	27.3%	31.2%	17.0%	8.8%	9.4%
Plug-in series hybrid diesel	On-road CO_2		36.3	37.8	41.3	44.5	45.8	44.3
	On-road CH_4		0.04	0.04	0.05	0.05	0.05	0.05
	On-road N_2O		0.02	0.02	0.02	0.02	0.02	0.02
	Upstream CO_2 (Low)		6.5	6.5	6.9	7.7	8.4	7.8
	Upstream CH_4 (Low)		2.2	2.3	2.4	2.7	2.8	2.6
	Upstream N_2O (Low)		0.4	0.4	0.4	0.5	0.5	0.5
	Upstream CO_2 (High)		26.0	23.7	21.3	27.9	36.5	30.3
	Upstream CH_4 (High)		3.6	3.5	3.5	4.1	4.7	4.2
	Upstream N_2O (High)		0.2	0.2	0.2	0.2	0.3	0.3
	Well to Wheel (Low)		45.40	47.05	51.08	55.41	57.47	55.22
	Well to Wheel (High)		66.21	65.33	66.42	76.91	87.34	79.14
	GHG reduction percentage relative to a comparable high carbon diesel	(Low carbon)	70.9%	48.7%	41.7%	37.1%	38.3%	34.5%
		(High carbon)	57.6%	28.8%	24.2%	12.6%	6.3%	6.1%

(Continued)

Table A4 (Continued): On-road and upstream GHG emissions for all simulated drivetrains on various considered routes (g/tkm)

Drivetrains	GHG emissions		SDD	LDD	RH	FH	HCH1	HCH2
Plug-in parallel hybrid diesel Catenary	On-road CO_2		34.79	17.36	26.47	53.22	63.98	59.13
	On-road CH_4		0.04	0.02	0.03	0.06	0.08	0.07
	On-road N_2O		0.01	0.01	0.01	0.02	0.03	0.03
	Upstream CO_2 (Low)		6.82	3.83	4.75	7.99	9.45	8.66
	Upstream CH_4 (Low)		2.14	1.11	1.59	3.06	3.67	3.38
	Upstream N_2O (Low)		0.36	0.18	0.27	0.54	0.65	0.60
	Upstream CO_2 (High)		35.20	24.48	19.69	13.88	14.10	11.73
	Upstream CH_4 (High)		4.02	2.42	2.63	3.75	4.36	3.95
	Upstream N_2O (High)		0.25	0.16	0.16	0.21	0.25	0.22
	Well to Wheel (Low)		44.17	22.51	33.13	64.90	77.85	71.87
	Well to Wheel (High)		74.32	44.45	49.00	71.16	82.78	75.13
	GHG reduction percentage relative to a comparable high carbon diesel	(Low carbon)	71.7%	75.5%	62.2%	26.3%	16.5%	14.7%
		(High carbon)	52.4%	51.6%	44.1%	19.2%	11.2%	10.9%
Plug-in series hybrid diesel Catenary	On-road CO_2		5.47	2.49	9.18	23.91	45.47	44.59
	On-road CH_4		0.01	0.00	0.01	0.03	0.05	0.05
	On-road N_2O		0.00	0.00	0.00	0.01	0.02	0.02
	Upstream CO_2 (Low)		2.68	2.16	3.04	5.42	8.21	7.77
	Upstream CH_4 (Low)		0.48	0.30	0.68	1.54	2.74	2.66
	Upstream N_2O (Low)		0.06	0.03	0.10	0.25	0.47	0.46
	Upstream CO_2 (High)		31.97	30.01	29.70	36.18	34.53	29.10
	Upstream CH_4 (High)		2.22	1.94	2.29	3.48	4.57	4.19
	Upstream N_2O (High)		0.15	0.14	0.15	0.22	0.28	0.25
	Well to Wheel (Low)		8.71	4.99	13.01	31.16	56.96	55.55
	Well to Wheel (High)		39.82	34.58	41.33	63.84	84.92	78.21
	GHG reduction percentage relative to a comparable high carbon diesel	(Low carbon)	94.4%	94.6%	85.1%	64.6%	38.9%	34.1%
		(High carbon)	74.5%	62.3%	52.8%	27.5%	8.9%	7.2%
Plug-in series hybrid gas turbine	On-road CO_2		19.02	19.81	21.63	23.32	23.97	23.15
	On-road CH_4		1.16	1.20	1.31	1.42	1.46	1.41
	On-road N_2O		0.00	0.00	0.00	0.00	0.00	0.00
	Methane leakage		2.43	2.53	2.76	2.98	3.06	2.96
	Upstream CO_2 (Low)		-19.09	-19.88	-21.70	-23.41	-24.04	-21.33
	Upstream CH_4 (Low)		4.37	4.54	4.94	5.35	5.54	5.33
	Upstream N_2O (Low)		0.11	0.12	0.13	0.14	0.15	0.14
	Upstream CO_2 (High)		27.79	27.16	25.76	32.34	41.39	35.50
	Upstream CH_4 (High)		4.33	0.03	0.03	0.04	0.04	0.04
	Upstream N_2O (High)		0.26	0.26	0.27	0.31	0.35	0.32
	Well to Wheel (Low)		8.01	8.32	9.08	9.80	10.14	11.66
	Well to Wheel (High)		54.98	50.99	51.77	60.41	70.27	63.38
	GHG reduction percentage relative to a comparable high carbon diesel	(Low carbon)	94.9%	90.9%	89.6%	88.9%	89.1%	86.2%
		(High carbon)	64.8%	44.4%	40.9%	31.4%	24.6%	24.8%

(Continued)

Table A4 (Continued): On-road and upstream GHG emissions for all simulated drivetrains on various considered routes (g/tkm)

Drivetrains	GHG emissions		SDD	LDD	RH	FH	HCH1	HCH2
Plug-in parallel hybrid CNG	On-road CO_2		46.24	40.54	37.40	46.17	56.21	50.13
	On-road CH_4		2.81	2.46	2.27	2.80	3.41	3.04
	On-road N_2O		0.01	0.01	0.00	0.01	0.01	0.01
	Methane leakage		5.96	5.19	4.79	5.88	7.19	6.40
	Upstream CO_2 (Low)		-46.17	-40.58	-37.44	-46.07	-56.48	-50.28
	Upstream CH_4 (Low)		10.46	9.08	8.37	10.28	12.54	11.17
	Upstream N_2O (Low)		0.27	0.23	0.22	0.27	0.32	0.29
	Upstream CO_2 (High)		19.60	11.12	9.99	10.92	10.32	9.09
	Upstream CH_4 (High)		7.71	0.04	0.04	0.04	0.05	0.05
	Upstream N_2O (High)		0.43	0.35	0.32	0.38	0.46	0.41
	Well to Wheel (Low)		19.58	16.94	15.62	19.35	23.21	20.76
	Well to Wheel (High)		82.75	59.70	54.81	66.22	77.65	69.12
	GHG reduction percentage relative to a comparable high carbon diesel	(Low carbon)	87.4%	81.5%	82.2%	78.0%	75.1%	75.4%
		(High carbon)	47.0%	34.9%	37.5%	24.8%	16.7%	18.0%
Plug-in parallel hybrid CNG Catenary	On-road CO_2		25.18	14.42	22.57	43.31	52.79	48.67
	On-road CH_4		1.53	0.88	1.37	2.63	3.21	2.96
	On-road N_2O		0.00	0.00	0.00	0.01	0.01	0.01
	Methane leakage		3.22	1.85	2.88	5.54	6.75	6.22
	Upstream CO_2 (Low)		-23.52	-13.20	-21.77	-43.22	-52.83	-48.77
	Upstream CH_4 (Low)		5.77	3.34	5.11	9.68	11.78	10.86
	Upstream N_2O (Low)		0.15	0.09	0.13	0.25	0.30	0.28
	Upstream CO_2 (High)		33.25	23.81	18.60	12.16	12.35	10.28
	Upstream CH_4 (High)		5.52	0.02	0.03	0.04	0.05	0.05
	Upstream N_2O (High)		0.33	0.21	0.25	0.37	0.44	0.40
	Well to Wheel (Low)		12.33	7.37	10.30	18.20	22.01	20.22
	Well to Wheel (High)		69.03	41.19	45.70	64.06	75.58	68.58
	GHG reduction percentage relative to a comparable high carbon diesel	(Low carbon)	92.1%	92.0%	88.2%	79.3%	76.4%	76.0%
		(High carbon)	55.7%	55.1%	47.8%	27.2%	18.9%	18.6%
Plug-in series hybrid CNG	On-road CO_2		20.22	21.05	22.99	24.79	25.48	24.66
	On-road CH_4		1.23	1.28	1.40	1.51	1.55	1.50
	On-road N_2O		0.00	0.00	0.00	0.00	0.00	0.00
	Methane leakage		2.59	2.70	2.95	3.18	3.27	3.16
	Upstream CO_2 (Low)		-18.65	-19.84	-21.67	-23.04	-23.12	-22.70
	Upstream CH_4 (Low)		4.67	4.83	5.27	5.71	5.93	5.71
	Upstream N_2O (Low)		0.12	0.13	0.14	0.15	0.16	0.15
	Upstream CO_2 (High)		31.62	26.11	28.34	35.96	46.19	39.54
	Upstream CH_4 (High)		4.73	0.03	0.03	0.04	0.04	0.04
	Upstream N_2O (High)		0.28	0.27	0.29	0.34	0.39	0.35
	Well to Wheel (Low)		10.19	10.15	11.07	12.30	13.26	12.48
	Well to Wheel (High)		60.68	51.44	56.00	65.81	76.92	69.26
	GHG reduction percentage relative to a comparable high carbon diesel	(Low carbon)	93.5%	88.9%	87.4%	86.0%	85.8%	85.2%
		(High carbon)	61.1%	44.0%	36.1%	25.2%	17.5%	17.8%

(Continued)

Table A4 (Continued): On-road and upstream GHG emissions for all simulated drivetrains on various considered routes (g/tkm)

Drivetrains	GHG emissions		SDD	LDD	RH	FH	HCH1	HCH2
Plug-in series hybrid CNG catenary	On-road CO_2		3.05	1.38	5.11	13.31	25.91	24.83
	On-road CH_4		0.19	0.08	0.31	0.81	1.57	1.51
	On-road N_2O		0.00	0.00	0.00	0.00	0.00	0.00
	Methane leakage		0.39	0.18	0.65	1.71	3.26	3.18
	Upstream CO_2 (Low)		-1.45	0.29	-3.59	-11.67	-23.80	-23.46
	Upstream CH_4 (Low)		0.85	0.47	1.31	3.18	5.91	5.74
	Upstream N_2O (Low)		0.02	0.01	0.04	0.09	0.16	0.15
	Upstream CO_2 (High)		32.03	30.24	30.80	39.61	43.52	37.97
	Upstream CH_4 (High)		2.35	0.02	0.02	0.03	0.04	0.04
	Upstream N_2O (High)		0.16	0.14	0.17	0.27	0.37	0.35
	Well to Wheel (Low)		3.05	2.43	3.83	7.42	13.00	11.95
	Well to Wheel (High)		38.16	32.04	37.06	55.73	74.69	67.87
	GHG reduction percentage relative to a comparable high carbon diesel	(Low carbon)	98.0%	97.4%	95.6%	91.6%	86.0%	85.8%
		(High carbon)	75.5%	65.1%	57.7%	36.7%	19.9%	19.5%

(Continued)

Table A5: The lower and upper limit of the total ownership cost for all drivetrains at each cycle when the infrastructure cost is included

Total ownership cost of Drivetrains with and without infrastructure cost		Average ($/km)		SDD ($/km)		LDD ($/km)		RH ($/km)		FH ($/km)		HCH1 ($/km)		HCH2 ($/km)	
		Low	High	Low	High	Low	High	Low	High	Low	High	Low	High	Low	High
Diesel	Without infrastructure cost	0.73	0.77	1.35	1.41	0.67	0.71	0.63	0.67	0.61	0.65	0.57	0.61	0.52	0.56
	With infrastructure cost	0.73	0.77	1.35	1.41	0.67	0.71	0.63	0.67	0.61	0.65	0.57	0.61	0.52	0.56
CNG	Without infrastructure cost	0.61	1.02	1.16	1.80	0.57	0.95	0.53	0.89	0.51	0.87	0.47	0.86	0.43	0.78
	With infrastructure cost	0.75	1.16	1.55	2.19	0.70	1.08	0.65	1.01	0.61	0.97	0.53	0.92	0.48	0.83
Battery electric	Without infrastructure cost	0.80	0.80	1.05	1.05	0.68	0.68	0.65	0.65	0.86	0.86	0.83	0.83	0.73	0.73
	With infrastructure cost	1.03	1.03	1.70	1.70	0.90	0.90	0.84	0.84	1.02	1.02	0.92	0.92	0.81	0.81
Battery electric catenary	Without infrastructure cost	0.63	0.63	0.92	0.92	0.45	0.45	0.51	0.51	-	-	-	-	-	-
	With infrastructure cost	1.21	1.21	1.97	1.97	0.82	0.82	0.83	0.83	-	-	-	-	-	-
Plug-in series hybrid fuel cell	Without infrastructure cost	0.75	0.91	1.08	1.23	0.67	0.82	0.63	0.80	0.70	0.87	0.75	0.93	0.66	0.84
	With infrastructure cost	0.97	1.13	1.69	1.83	0.88	1.03	0.82	0.98	0.84	1.02	0.84	1.02	0.74	0.91
Plug-in parallel hybrid fuel cell	Without infrastructure cost	0.79	1.13	1.23	1.57	0.73	1.06	0.69	1.01	0.73	1.09	0.72	1.08	0.64	0.98
	With infrastructure cost	1.06	1.40	1.98	2.33	0.99	1.32	0.92	1.24	0.91	1.27	0.83	1.19	0.73	1.08
Parallel hybrid fuel cell	Without infrastructure cost	0.85	1.25	1.44	1.92	0.78	1.13	0.74	1.10	0.75	1.14	0.74	1.16	0.67	1.05
	With infrastructure cost	1.14	1.53	2.22	2.70	1.05	1.40	0.98	1.34	0.94	1.33	0.85	1.27	0.77	1.15
Plug-in parallel hybrid diesel	Without infrastructure cost	0.65	0.67	1.13	1.16	0.59	0.62	0.54	0.56	0.57	0.60	0.55	0.58	0.49	0.52
	With infrastructure cost	0.66	0.69	1.17	1.20	0.61	0.63	0.55	0.57	0.58	0.60	0.55	0.59	0.50	0.53
Plug-in series hybrid diesel	Without infrastructure cost	0.73	0.75	1.04	1.05	0.65	0.67	0.61	0.63	0.70	0.72	0.74	0.76	0.65	0.67
	With infrastructure cost	0.82	0.85	1.30	1.31	0.74	0.76	0.69	0.71	0.76	0.79	0.78	0.80	0.68	0.70

(Continued)

Table A5 (Continued): The lower and upper limit of the total ownership cost for all drivetrains at each cycle when the infrastructure cost is included

Total ownership cost of Drivetrains with and without infrastructure cost		Average ($/km)		SDD ($/km)		LDD ($/km)		RH ($/km)		FH ($/km)		HCH1 ($/km)		HCH2 ($/km)	
		Low	High	Low	High	Low	High	Low	High	Low	High	Low	High	Low	High
Plug-in parallel hybrid diesel catenary	Without infrastructure cost	0.61	0.65	1.05	1.07	0.50	0.53	0.49	0.53	0.57	0.64	0.55	0.60	0.50	0.53
	With infrastructure cost	0.94	0.98	1.97	1.99	0.81	0.84	0.77	0.81	0.80	0.86	0.69	0.74	0.61	0.65
Plug-in series hybrid diesel catenary	Without infrastructure cost	0.62	0.72	0.95	0.98	0.48	0.49	0.51	0.55	0.66	0.77	0.60	0.81	0.53	0.74
	With infrastructure cost	1.03	1.13	2.09	2.12	0.87	0.88	0.86	0.90	0.93	1.04	0.77	0.98	0.68	0.89
Plug-in series hybrid gas turbine	Without infrastructure cost	0.76	0.89	1.13	1.25	0.67	0.80	0.63	0.77	0.71	0.86	0.73	0.89	0.65	0.79
	With infrastructure cost	0.94	1.08	1.65	1.77	0.85	0.98	0.79	0.93	0.84	0.99	0.81	0.96	0.71	0.86
Plug-in parallel hybrid CNG	Without infrastructure cost	0.57	0.86	1.03	1.32	0.53	0.78	0.48	0.71	0.49	0.78	0.46	0.82	0.41	0.73
	With infrastructure cost	0.70	0.99	1.39	1.68	0.65	0.90	0.59	0.82	0.58	0.87	0.52	0.87	0.46	0.77
Plug-in parallel hybrid CNG catenary	Without infrastructure cost	0.55	0.77	0.98	1.14	0.48	0.57	0.46	0.60	0.50	0.77	0.47	0.80	0.42	0.73
	With infrastructure cost	0.98	1.20	2.17	2.32	0.89	0.98	0.82	0.96	0.79	1.06	0.64	0.98	0.57	0.88
Plug-in series hybrid CNG	Without infrastructure cost	0.75	0.89	1.04	1.17	0.64	0.77	0.62	0.77	0.72	0.88	0.78	0.94	0.67	0.83
	With infrastructure cost	0.96	1.11	1.63	1.76	0.84	0.97	0.80	0.95	0.87	1.02	0.86	1.02	0.75	0.91
Plug-in series hybrid CNG catenary	Without infrastructure cost	0.67	0.74	0.93	0.95	0.47	0.48	0.52	0.55	0.71	0.80	0.72	0.88	0.65	0.80
	With infrastructure cost	1.15	1.23	2.27	2.29	0.93	0.94	0.93	0.96	1.04	1.12	0.92	1.08	0.82	0.97

Table A6: The abatement costs of GHG emissions on various short and long haul cycles using low and high carbon intensity fuels ($/tonne CO_2e)

Drivetrains	SDD		LDD		RH		FH		HCH1		HCH2	
	High	Low	High	Low	High	Low	High	Low	High	Low	High	Low
Plug-in parallel hybrid diesel	-160.6	-111.9	-163.7	-82.8	-187.1	-114.8	-141.5	-17.8	-153.5	86.2	-195.6	38.4
Plug-in series hybrid diesel	-36.8	-19.6	157.1	119.5	176.8	138.3	866.2	338.3	2146.7	392.0	1935.4	390.7
Battery electric	189.3	141.5	279.5	159.9	276.7	155.3	651.9	297.3	693.9	244.2	610.2	224.3
Battery electric catenary	326.1	253.9	150.6	100.9	224.8	143.5	-	-	-	-	-	-
Plug-in parallel hybrid CNG	31.3	150.9	-48.8	192.0	-82.8	166.3	-88.2	234.8	-237.4	262.4	-260.3	246.8
Plug-in series hybrid gas turbine	186.8	177.9	273.1	226.5	274.6	233.3	516.5	299.2	640.1	289.7	568.2	288.5
Plug-in series hybrid CNG	186.0	176.1	256.5	228.1	335.6	256.7	721.9	340.4	1106.5	350.5	949.1	333.7
Plug-in series hybrid diesel catenary	398.7	325.2	213.9	149.3	306.9	226.2	825.3	473.1	1446.3	694.8	1624.0	793.7
Plug-in parallel hybrid diesel catenary	473.2	358.5	183.7	154.2	225.0	201.3	685.5	677.4	664.3	664.7	625.8	639.7
Plug-in series fuel cell	207.0	198.6	331.3	255.1	329.4	261.4	548.3	307.0	801.9	320.2	692.3	310.2
Plug-in series hybrid CNG catenary	489.2	384.7	272.9	188.6	367.5	245.7	824.6	395.2	1150.3	390.3	1126.8	390.6
Plug-in parallel hybrid CNG catenary	542.0	396.8	205.7	190.3	238.1	243.5	437.4	393.2	220.0	345.1	189.3	344.1
CNG	6722.2	456.8	2879.4	377.2	1841.7	368.1	-796.6	347.0	19230.9	312.4	9292.1	312.6
Plug-in parallel fuel cell	547.4	412.1	1219.1	477.7	1296.7	475.4	3512.5	514.8	3194.8	452.3	3711.8	455.2
Parallel hybrid fuel cell (no plug)	1172.6	582.2	2148.9	543.0	3084.5	552.9	20832.2	562.3	-	520.0	-	523.0
Diesel	-	1155.8	-	1155.8	-	1155.8	-	1155.8	-	1155.8	-	1155.8

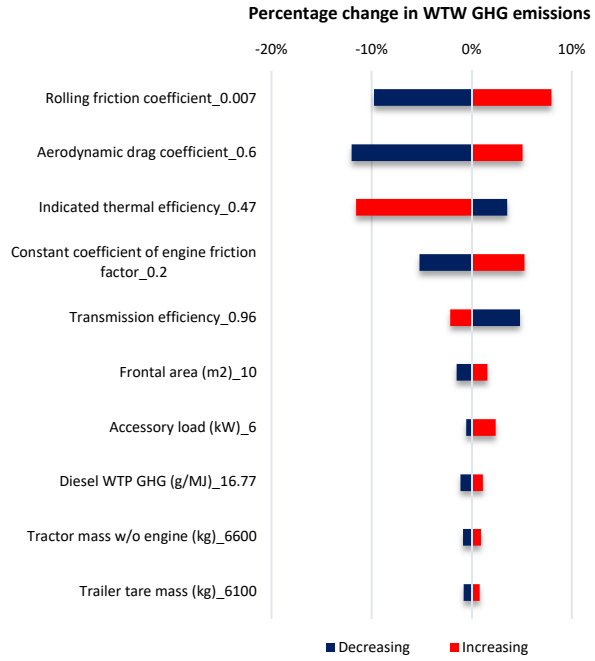

a. Conventional diesel. The sensitivity was presented in percentage change from baseline value of 83.3 g CO2e/MJ.

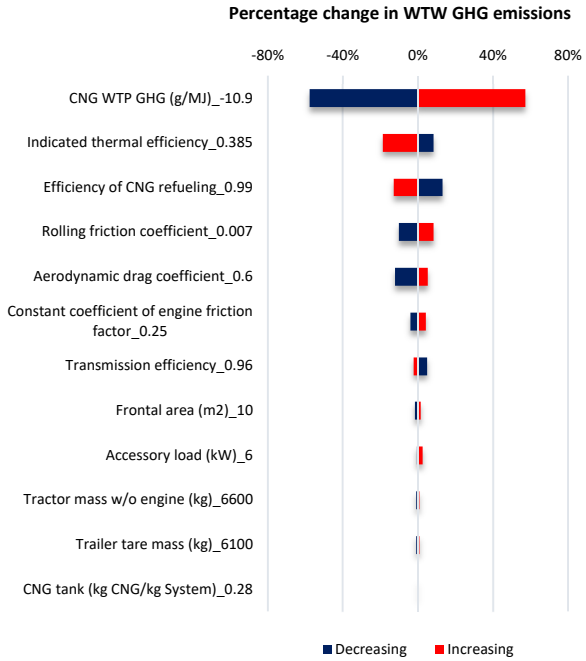

b. Conventional CNG. The sensitivity was presented in percentage change from baseline value of 53.7 g CO2e/MJ.

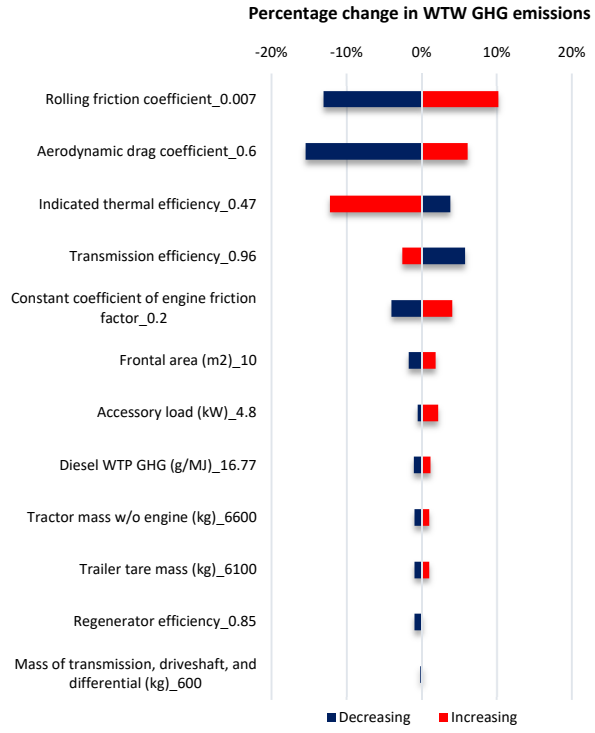

c. Plug-in parallel hybrid diesel. The sensitivity was presented in percentage change from baseline value of 75.3 g CO2e/MJ.

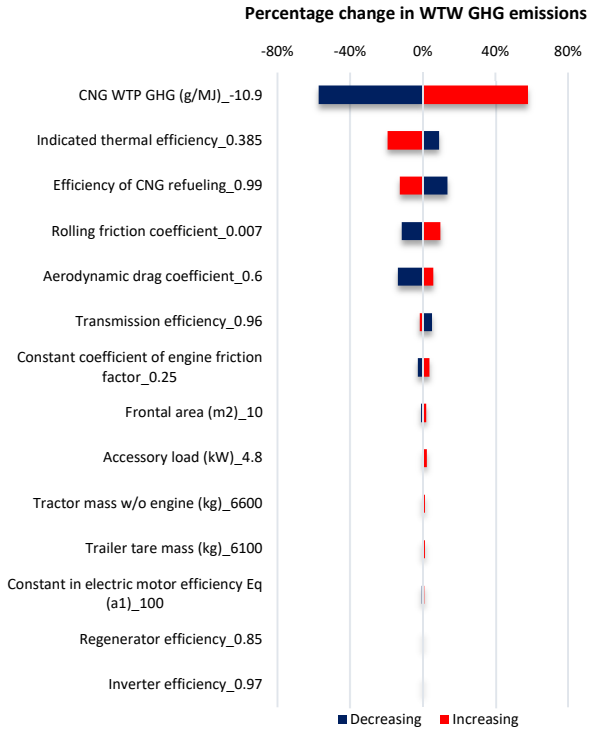

d. Plug-in parallel hybrid CNG. The sensitivity was presented in percentage change from baseline value of 48.7 g CO2e/MJ.

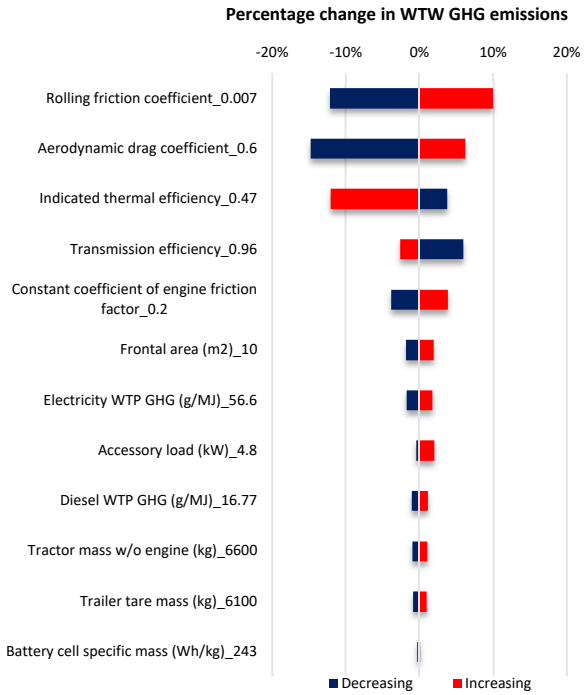

e. Plug-in parallel hybrid diesel catenary. The sensitivity was presented in percentage change from baseline value of 73.2 g CO2e/MJ.

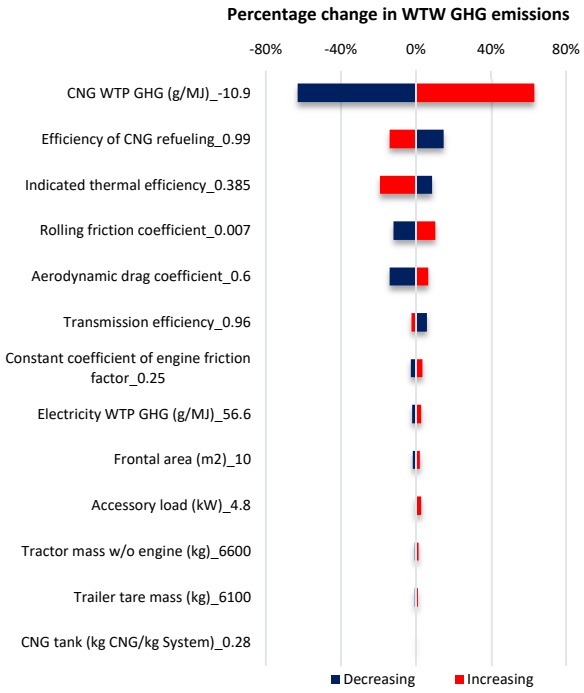

f. Plug-in parallel hybrid CNG catenary. The sensitivity was presented in percentage change from baseline value of 44.9 g CO2e/MJ.

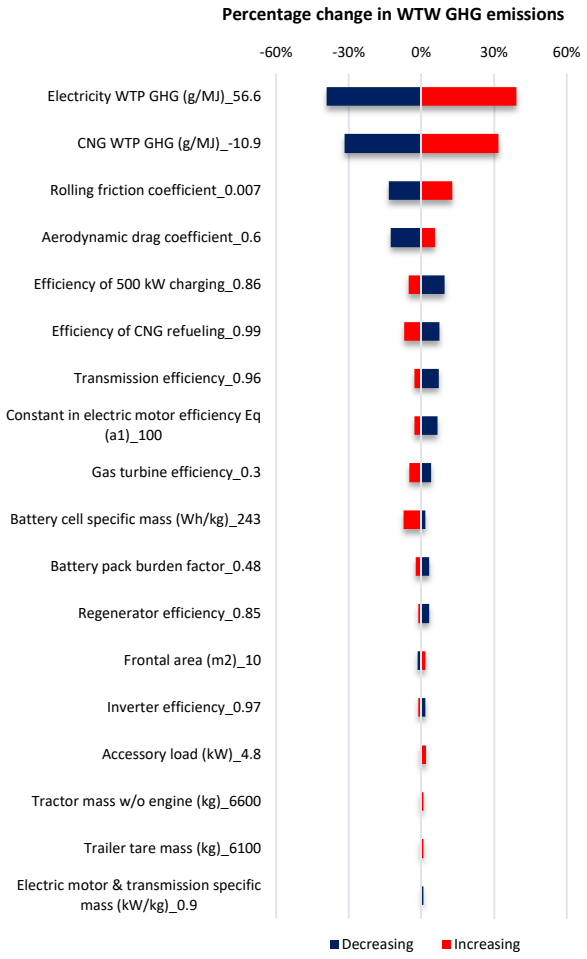

g. Plug-in series hybrid gas turbine. The sensitivity was presented in percentage change from baseline value of 40.5 g CO2e/MJ.

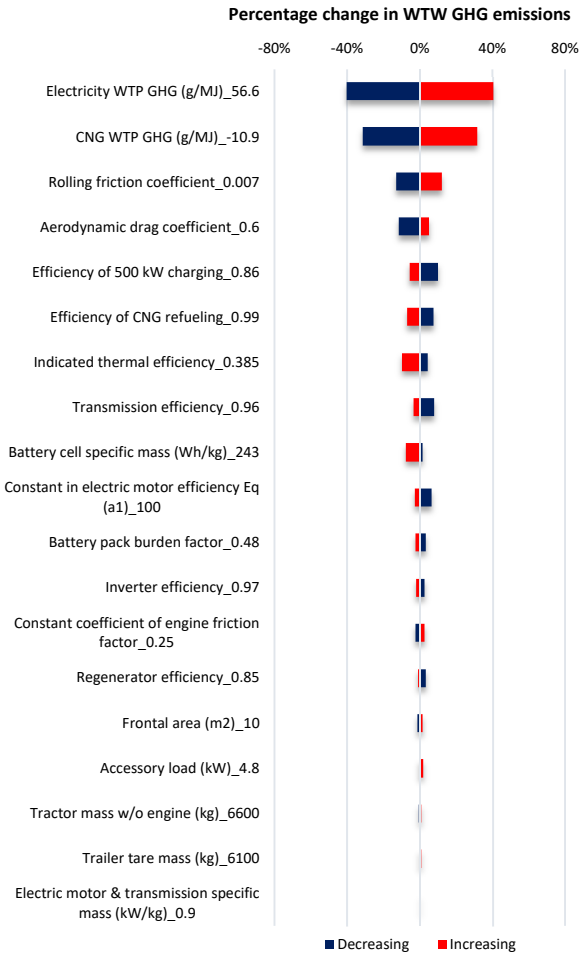

h. Plug-in series hybrid CNG. The sensitivity was presented in percentage change from baseline value of 44 g CO2e/MJ.

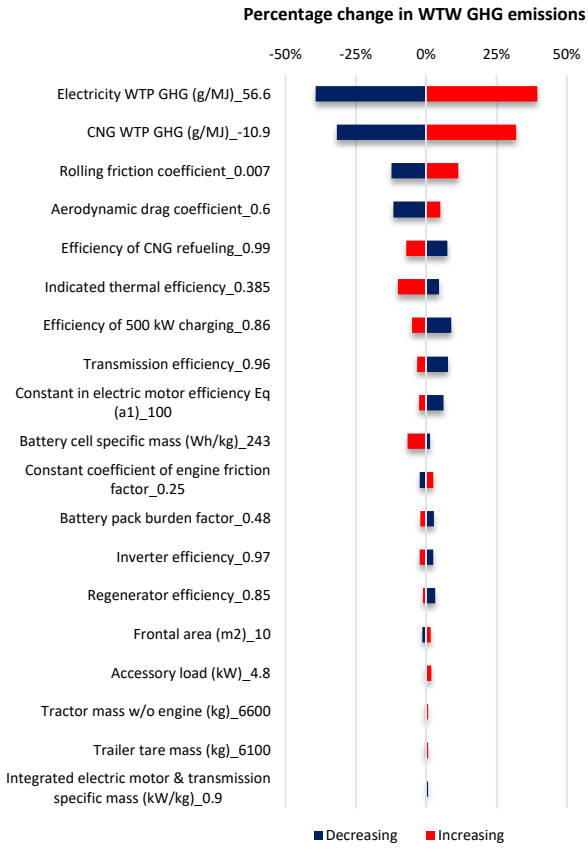

i. Plug-in series hybrid CNG catenary. The sensitivity was presented in percentage change from baseline value of 43.6 g CO2e/MJ.

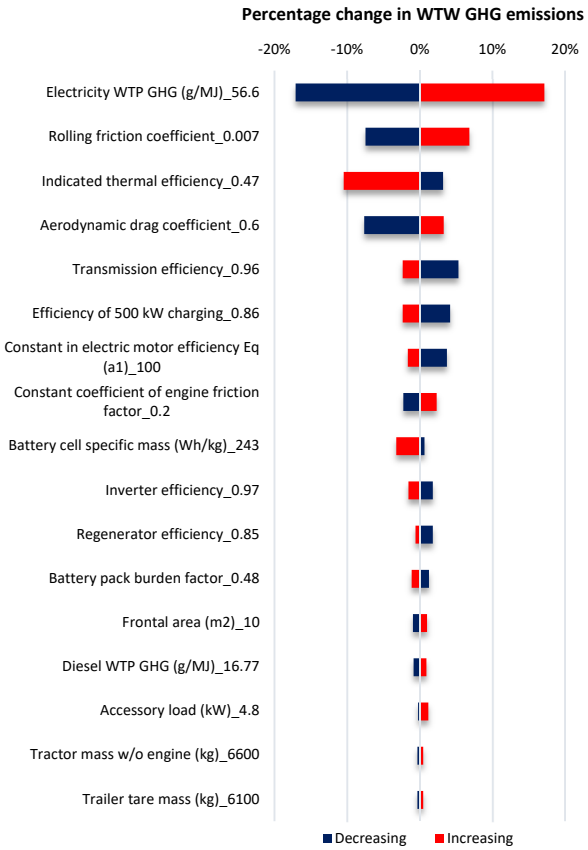

j. Plug-in series hybrid diesel. The sensitivity was presented in percentage change from baseline value of 67.3 g CO2e/MJ.

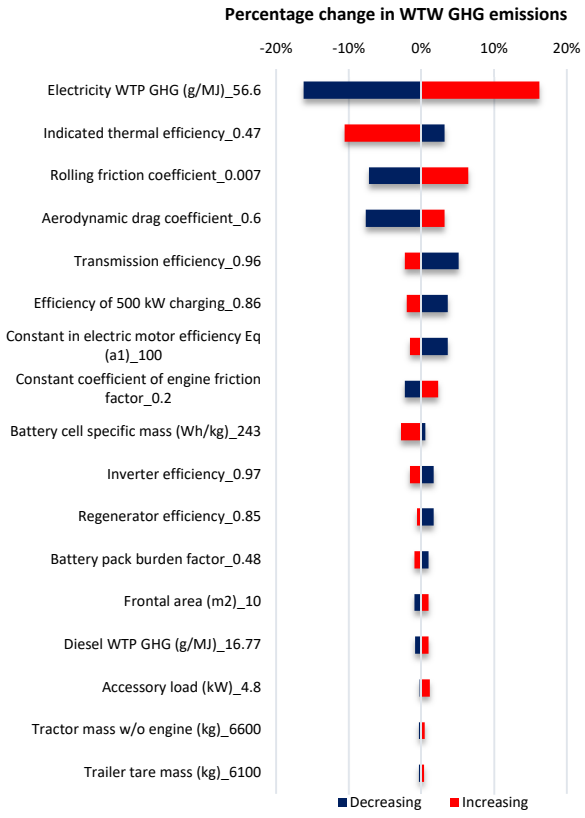

k. Plug-in series hybrid diesel catenary. The sensitivity was presented in percentage change from baseline of 67.1 g CO2e/MJ.

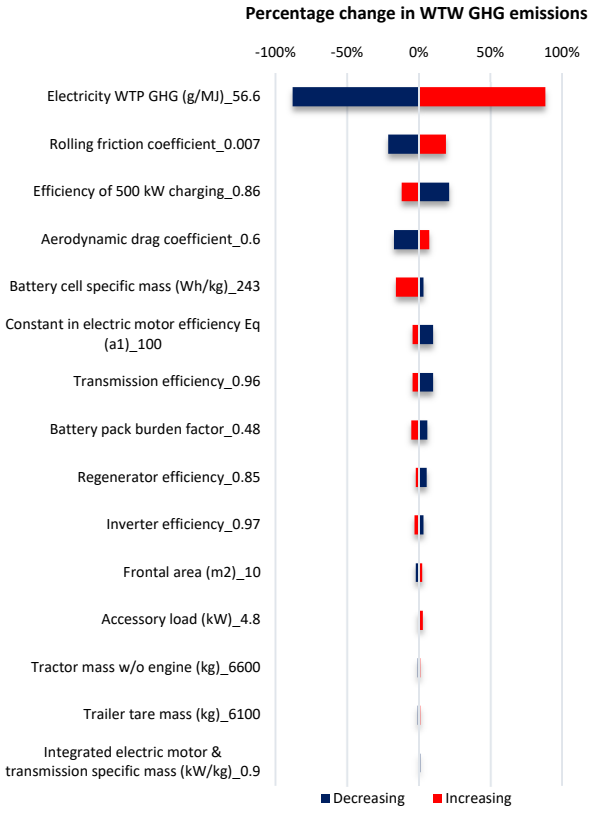

l. Battery electric. The sensitivity was presented in percentage change from baseline value 29.3 g CO2e/MJ.

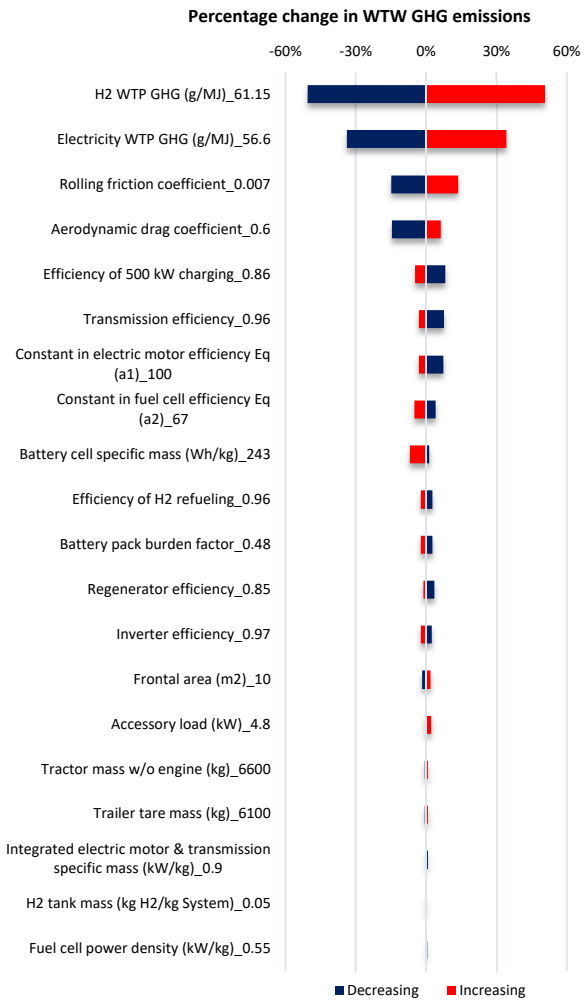

m. Plug-in series hybrid fuel cell. The sensitivity was presented in percentage change from baseline value of 35.6 g CO2e/MJ.

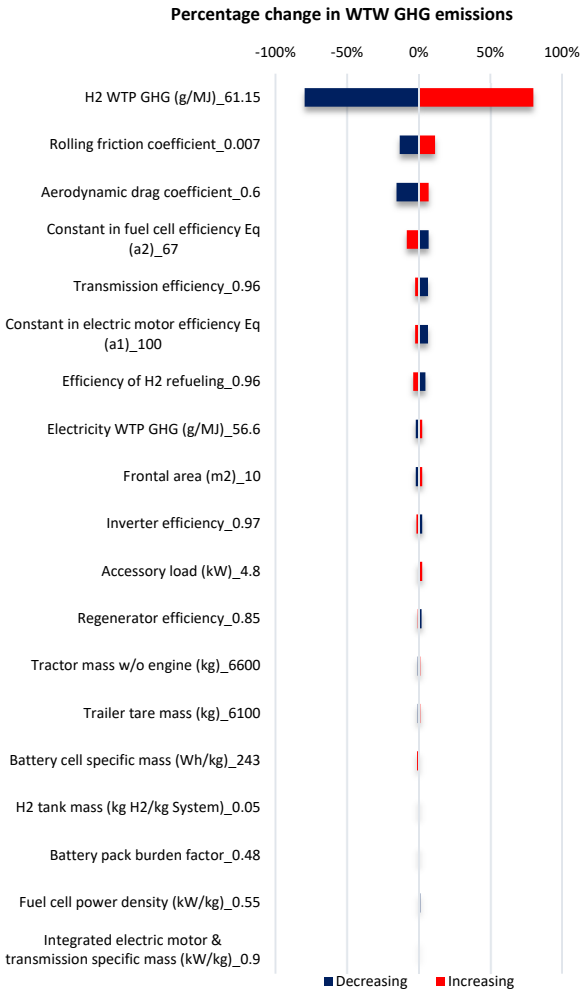

n. Plug-in parallel hybrid fuel cell. The sensitivity was presented in percentage change from baseline value of 44.7 g CO2e/MJ.

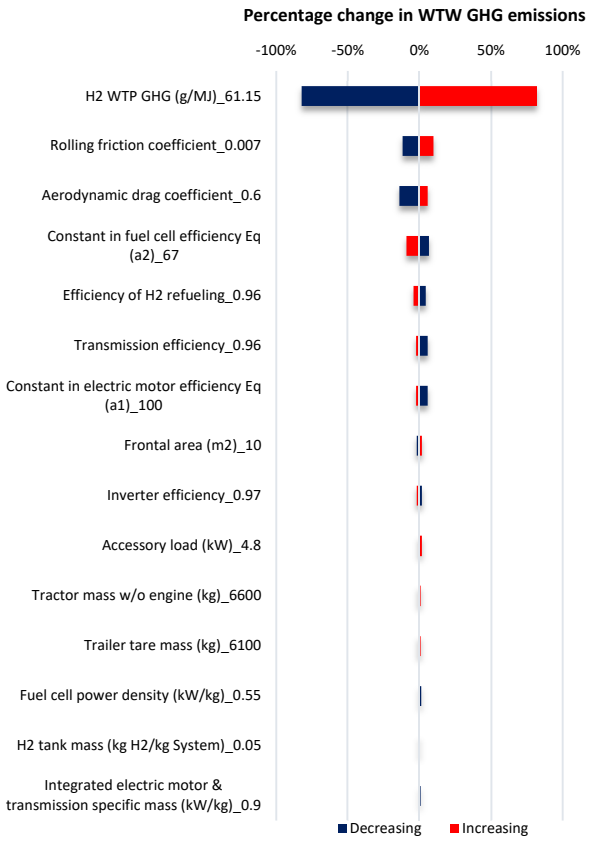

o. Parallel hybrid fuel cell (w/o plug-in). The sensitivity was presented in percentage change from baseline value of 48.4 g CO2e/MJ.

Figure A1: Sensitivity of well to wheel GHG emissions to input parameters for all drivetrains on HCH2 cycle. For each parameter the sensitivity was demonstrated in percentage change from the simulated WTW GHG emissions with baseline parameters. The baseline value of each parameter was also provided at the end of each label in the vertical axis. Additionally, the lower and upper values for each parameter were implemented from Table 5 to 10. It is worthwhile to mention that only parameters with more 0.5% change between their low and high are shown in these plots.

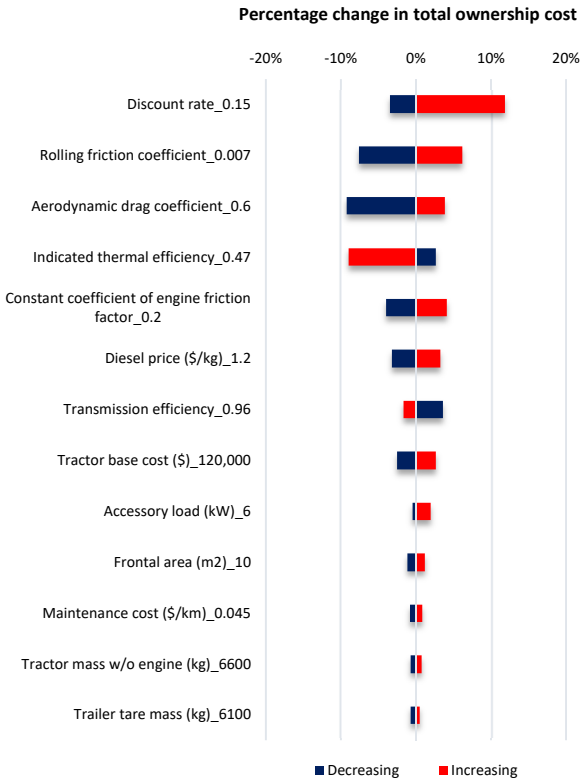

a. Conventional diesel. The sensitivity was presented in percentage change from baseline value of 0.53 $/km.

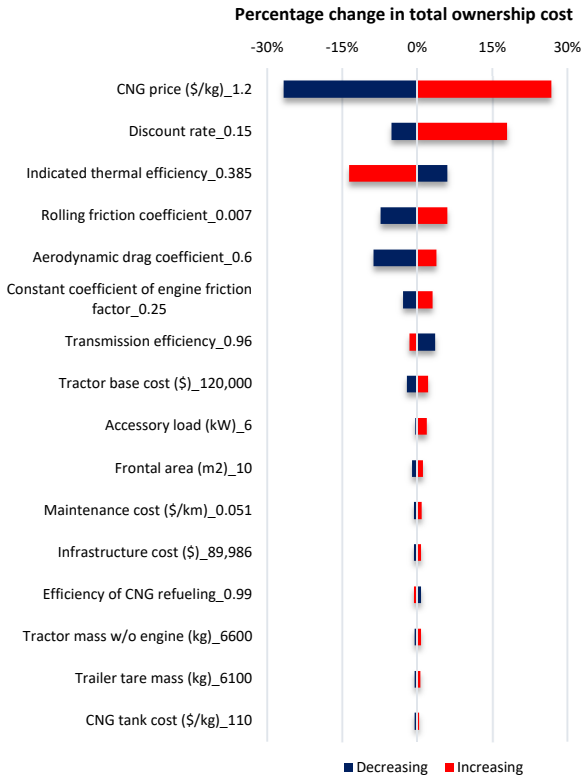

b. Conventional CNG. The sensitivity was presented in percentage change from baseline value of 0.65 $/km.

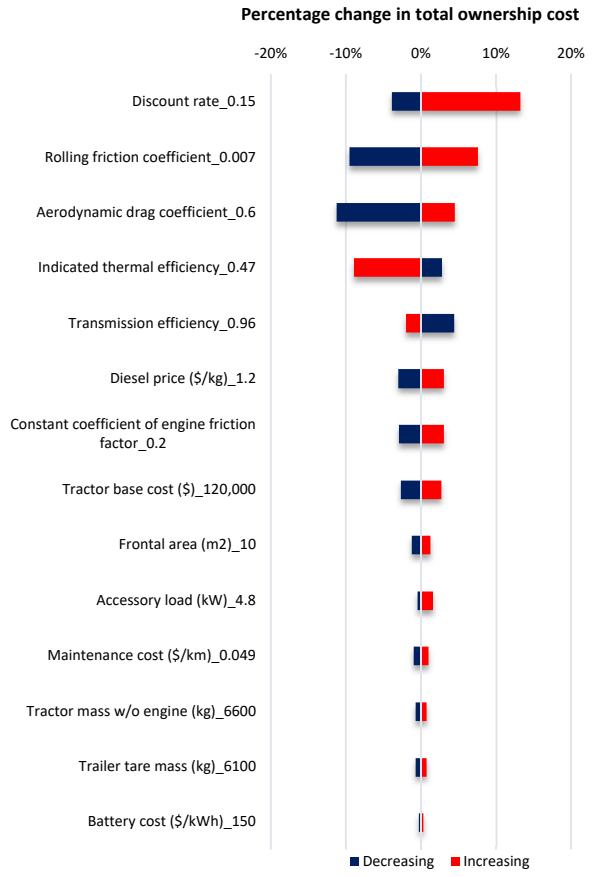

c. Plug-in parallel hybrid diesel. The sensitivity was presented in percentage change from baseline value of 0.51 $/km.

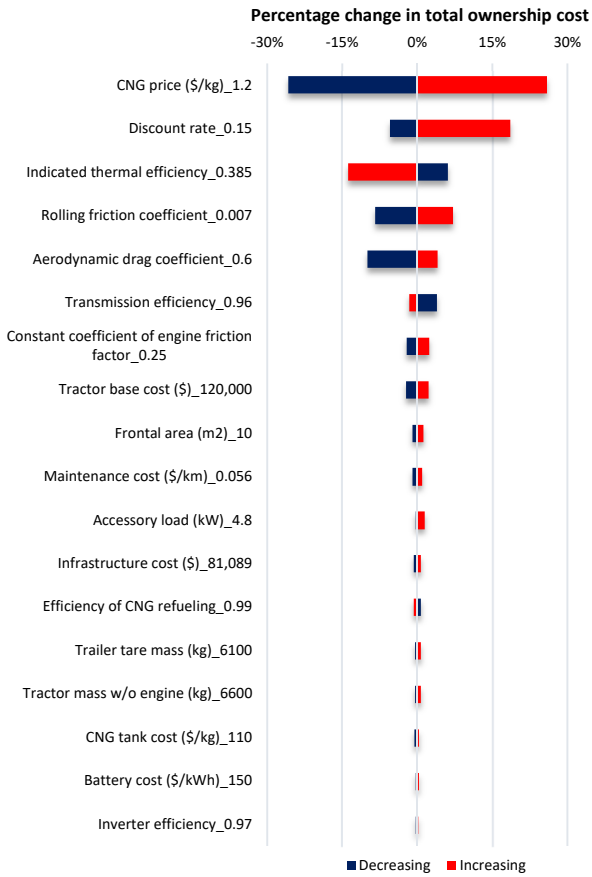

d. Plug-in parallel hybrid CNG. The sensitivity was presented in percentage change from baseline value of 0.61 $/km.

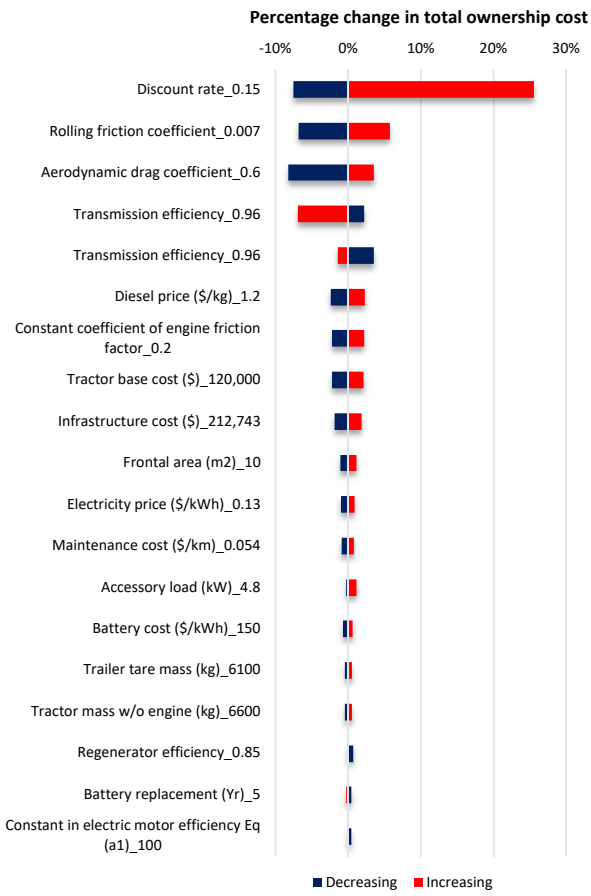

e. Plug-in parallel hybrid diesel catenary. The sensitivity was presented in percentage change from baseline value of 0.63 $/km.

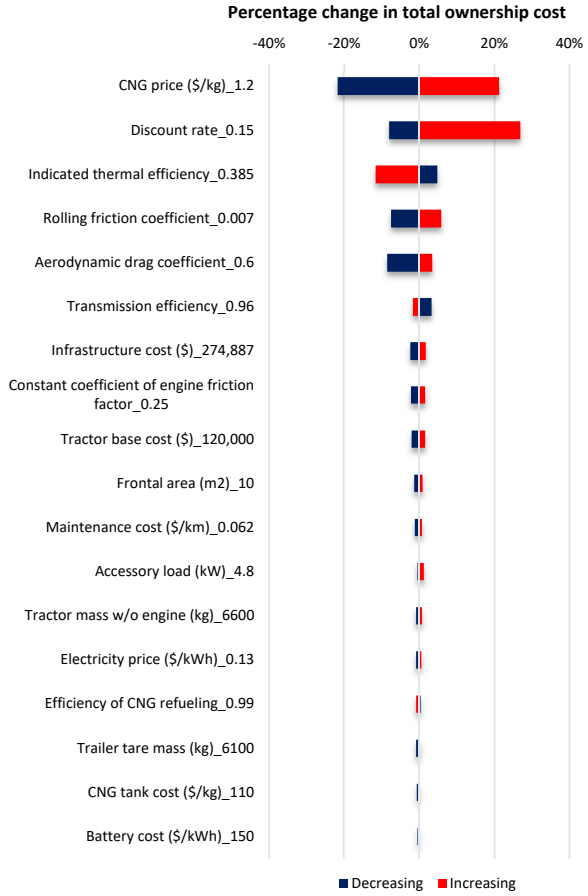

f. Plug-in parallel hybrid CNG catenary. The sensitivity was presented in percentage change from baseline value of 0.75 $/km.

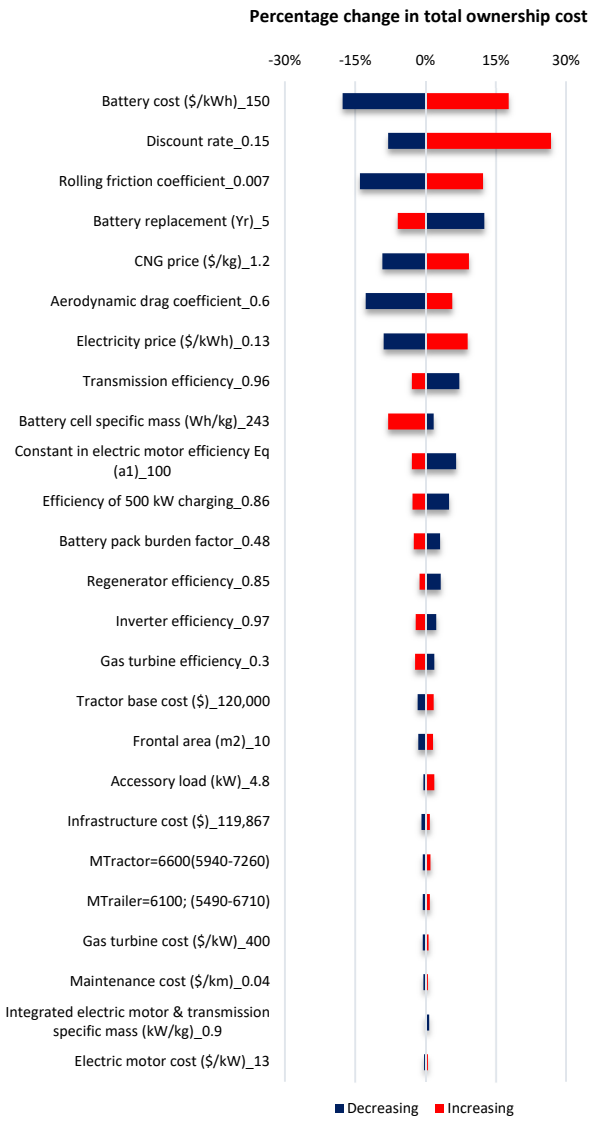

g. Plug-in series hybrid gas turbine. The sensitivity was presented in percentage change from baseline value of 0.79 $/km.

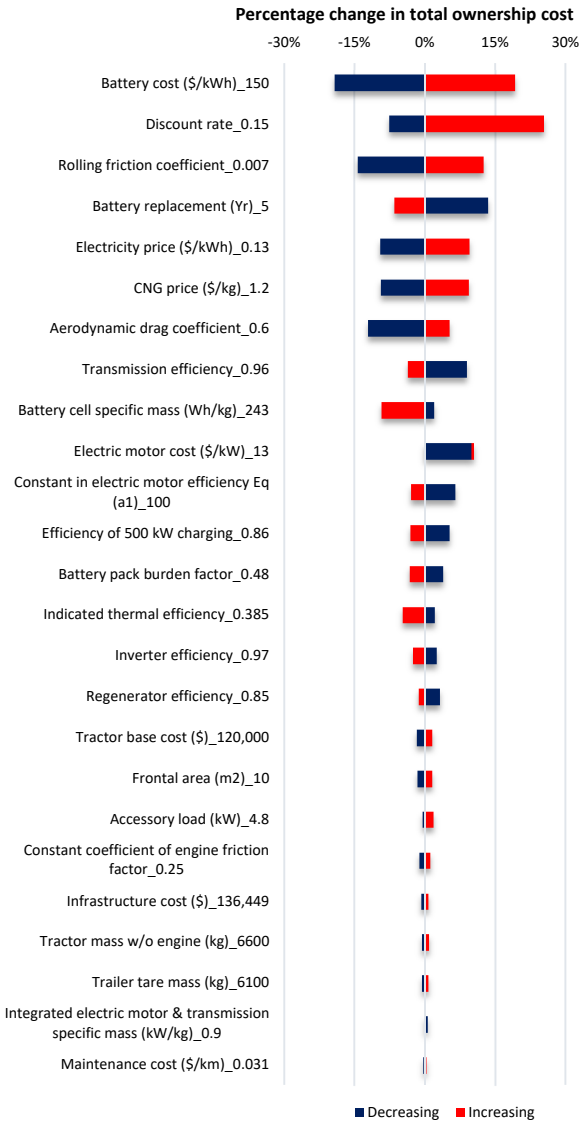

h. Plug-in series hybrid CNG. The sensitivity was presented in percentage change from baseline value of 0.83 $/km.

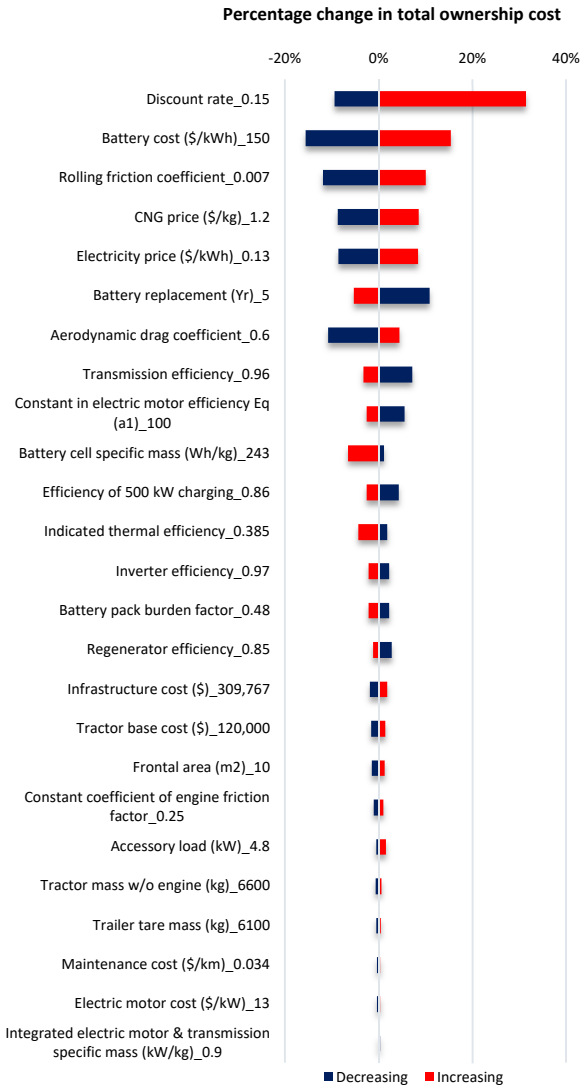

i. Plug-in series hybrid CNG catenary. The sensitivity was presented in percentage change from baseline value of 0.91 $/km.

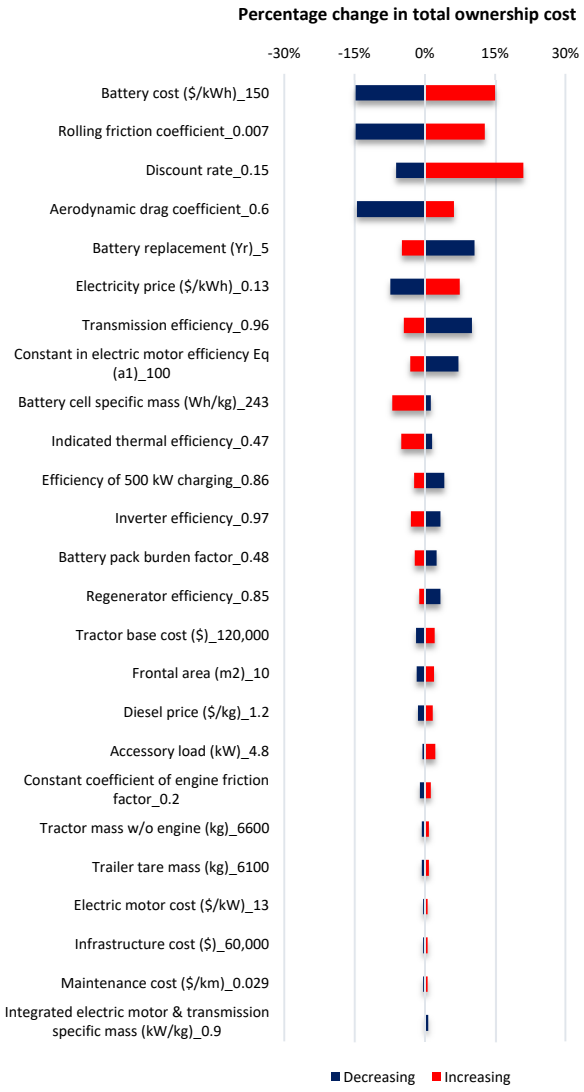

j. Plug-in series hybrid diesel. The sensitivity was presented in percentage change from baseline value of 0.7 $/km.

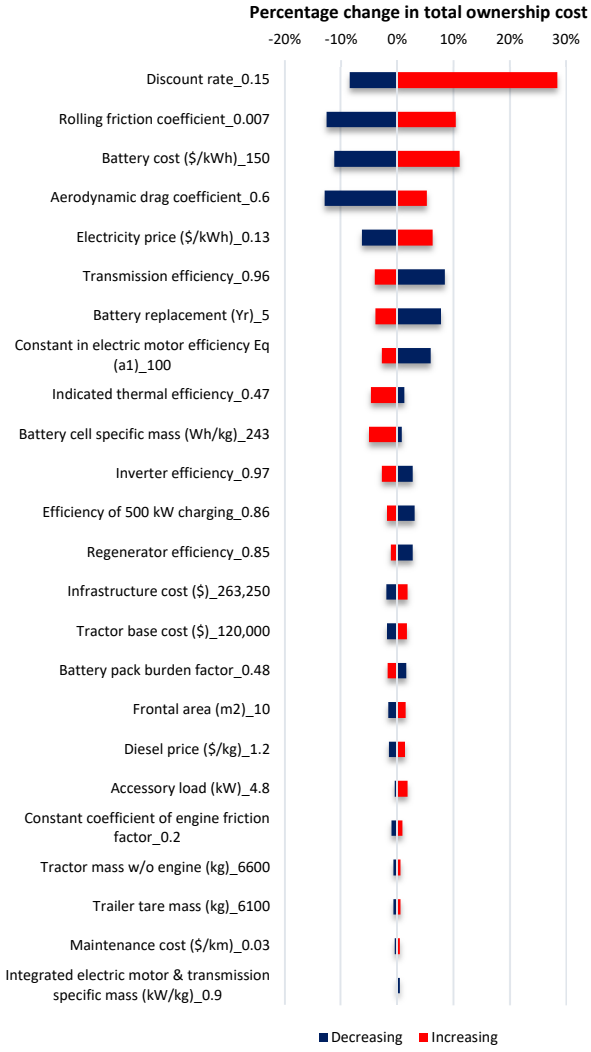

k. Plug-in series hybrid diesel catenary. The sensitivity was presented in percentage change from baseline value of 0.78 $/km.

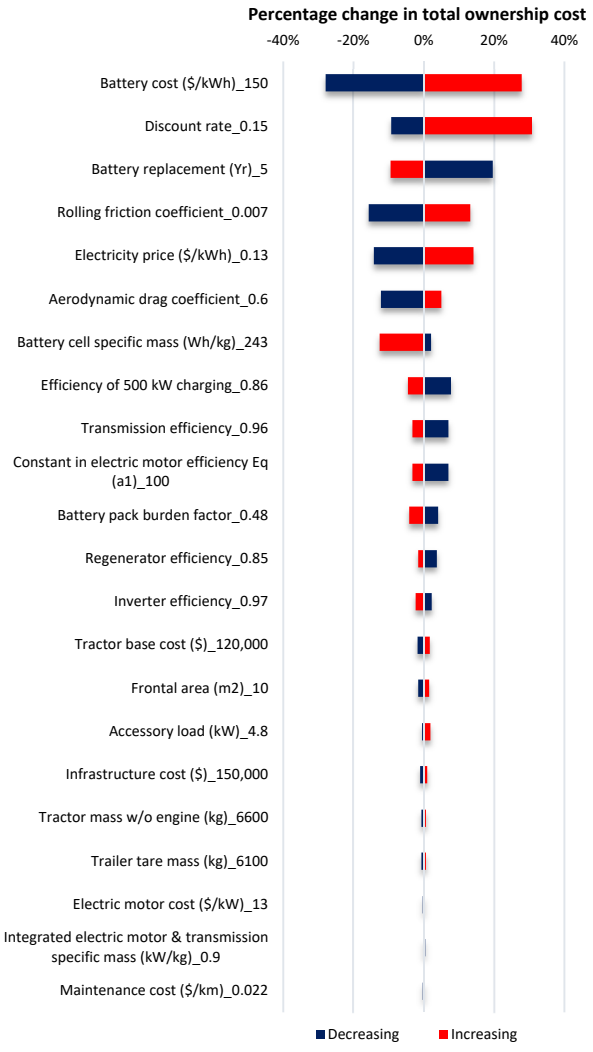

l. Battery electric. The sensitivity was presented in percentage change from baseline value of 0.82 $/km.

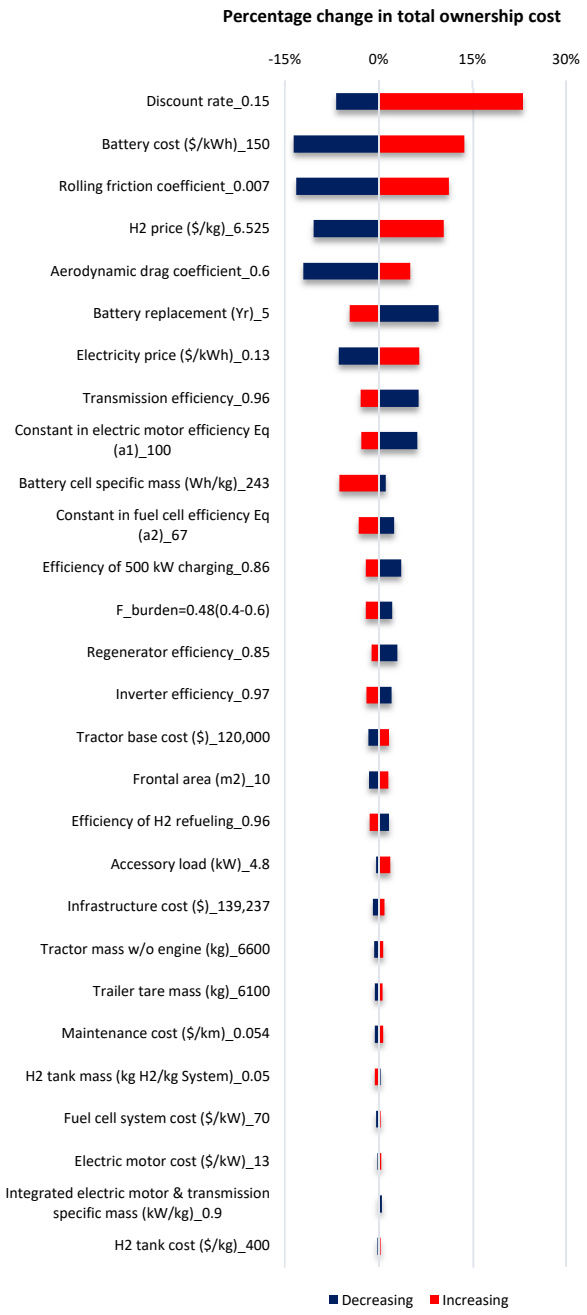

m. Plug-in series hybrid fuel cell. The sensitivity was presented in percentage change from baseline value of 0.84 $/km.

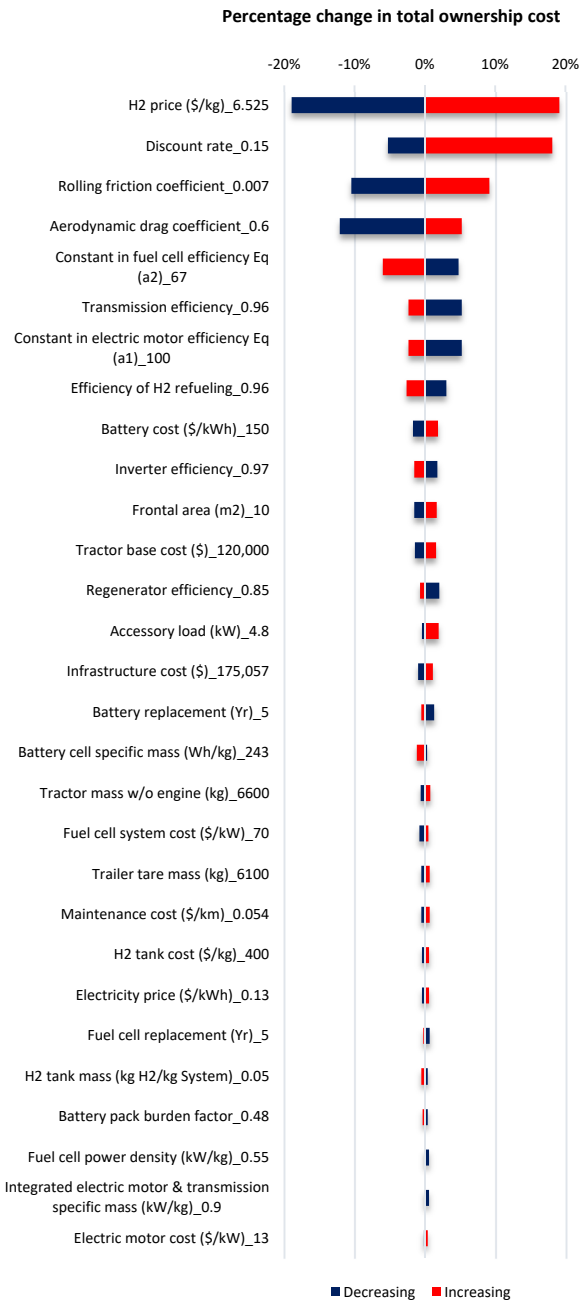

n. Plug-in parallel hybrid fuel cell. The sensitivity was presented in percentage change from baseline value of 0.91 $/km.

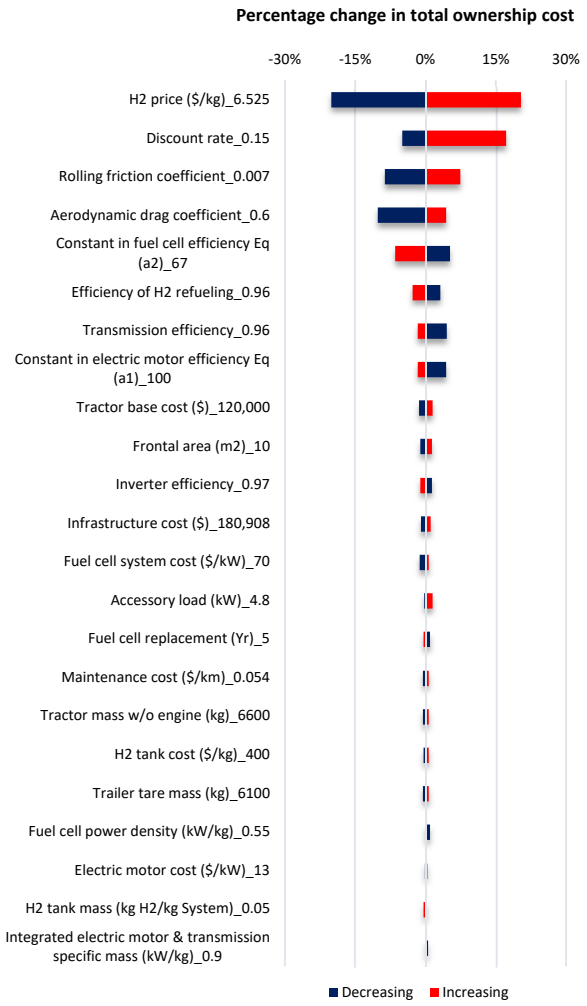

o. Parallel hybrid fuel cell (w/o plug-in). The sensitivity was presented in percentage change from baseline value of 0.96 $/km.

Figure A2: Sensitivity of total ownership cost estimation to input parameters for all drivetrains on HCH2 cycle. For each parameter the sensitivity was demonstrated in percentage change from the simulated total ownership cost with baseline parameters. The baseline value of each parameter was also provided at the end of each label in the vertical axis. The lower and upper values for each parameter were provided in Table 5 to 10.